UNIVERSITAT DE BARCELONA

Synthesis and optimization of new sphingolipid sensors for metabolism and trafficking studies

Ana Pou Cabello

UNIVERSITAT DE BARCELONA

FACULTAT DE FARMÀCIA

PROGRAMA DE DOCTORAT DE QUÍMICA ORGÀNICA

SYNTHESIS AND OPTIMIZATION OF NEW SPHINGOLIPID SENSORS FOR METABOLISM AND TRAFFICKING STUDIES

Memòria presentada per **Ana Pou Cabello**
per optar al Grau de Doctora per la Universitat de Barcelona

Directors:

Dr. Antonio Delgado Cirilo

Dr. José Luís Abad Saiz

Tutor:

Dr. Antonio Delgado Cirilo

Doctorand:

Ana Pou Cabello

ANA POU CABELLO
2017

The present doctoral thesis has been carried out at the Institute of Advanced Chemistry of Catalonia (IQAC), which belongs to the Spanish National Research Council (CSIC).

This work was supported by grants from the Spanish Ministry of Economy and Competitiveness (Project CTQ2014-54743-R). A predoctoral fellowship contract to A.P.(BES-2012-056019) is also acknowledged.

Als meus estimats pares

AGRAÏMENTS

Tot i que ja estava avisada des del primer moment de que fer una Tesi Doctoral no seria el camí fàcil a escollir, no vaig tenir cap dubte en que seria una experiència única i molt gratificant durant la meva evolució tant professional com personal. Durant aquests quatre anys he pogut gaudir com una nena petita dels moments àlgids de la ciència, però també he patit el que significa el fet d'investigar en un camp de recerca tant complex com és el de la Química Biomèdica. El suport i ajut obtinguts durant aquesta etapa han sigut incondicionals, per tant m'agradaria fer referència a certes persones que han influït en el desenvolupament d'aquest treball.

En primer lloc, agrair als meus directors de Tesi, Dr. Antonio Delgado i Dr. José Luís Abad, pel seu suport acadèmic, la seva proximitat en el moment de resoldre problemes de qualsevol tipus, i la confiança dipositada en mi. Gràcies per haver-me donat la oportunitat de realitzar aquest projecte en el vostre grup de recerca. Paral·lelament, també vull donar les gràcies a la Dres. Gemma Fabriàs i Josefina Casas, per la seva paciència i interès en la realització dels experiments biològics duts a terme en aquest treball, i en el recolzament tant acadèmic com emocional obtinguts. Al Dr. J.Pablo Salvador, per la seva gran ajuda rebuda durant la col·laboració en el vostre grup, i la santa paciència que has tingut amb mi. Gràcies per haver-me introduït en el món dels "microarrays", és interessantíssim!

A tots els companys de laboratori amb els que he coincidit, tant del laboratori de Química com el de Biologia; als doctorands, tècnics, estudiants...per les xerrades de cada migdia amb els nostres tuppers, els cafès, els pastissos d'aniversari, els sopars, i sobretot el recolzament del dia a dia al laboratori, ja que m'heu fet sentir com a casa. Però en especial, volia mencionar a la Raquel, l'Ana i la Mireia, on amb elles he viscut experiències inoblidables, viatges i molts riures.

Vull agrair també als amics de la Universitat, per haver seguit formant part de la meva vida i de manera molt especial. Sobretot a la Maria i la Mireia, els meus amors incondicionals.

Als amics del meu estimat Masnou, d'on no hi ha manera de fer-me'n sortir, vosaltres sou la meva "vàlvula d'escape" i els moments viscuts durant aquest temps han sigut infinits. En especial a les nenes, que sempre han estat allà quan ho he necessitat, i el meu dia a dia no té sentit sense vosaltres. Us adoro!

Als meus companys de pis, Gerard i Abbou, per haver creat aquesta petita família tant bonica i haver-me aguantat els meus alt-i-baixos emocionals durant la realització d'aquesta tesi.

Als meus pares, pels valors transmesos, per l'educació rebuda, i perquè els hi dec tot a ells. A la meva germana Laura, la meva mitja taronja, la meva bessona d'ànima, ja que tot i estar lluny en molts moments sempre et sento molt a prop. I que no falti el meu gos, en Daff, aquest sí que m'ha aguantat matí, tarda i nit, i mai s'ha queixat de res!

Per últim a tu, Pau, pel recolzament durant l'últim any del procés, i per fer-me increïblement feliç en el camí tant bonic que hem emprès junts.

A tots vosaltres, gràcies!

ABBREVIATIONS

ADIBO	Azadibenzocyclooctyne
BuLi	Butyllithium
CDase	Ceramidase
CDI	Carbonyldiimidazole
Cer	Ceramide
CerS	Ceramide synthase
C1P	Ceramide-1-phosphate
DA	Diels Alder
DABCO-Br	1,4-diazabicyclo[2.2.2]octane and bromine
DBCO	Dibenzocyclooctyne
Des1	Dihydroceramide desaturase
DhCer	Dihydroceramide
DhSph	Dihydrosphingosine
DMAP	*N,N*-Dimethylpyridin-4-amine
DMF	Dimethylformamide
DMSO	Dimetilsulphoxide
EDC	*N*-(3-Dimethylaminopropyl)-*N*'-ethylcarbodiimide
Et_2O	Diethyl ether
EtOH	Ethanol
Et_3N	Triethylamine
EtOAc	Ethyl acetate
FG	Functionalized group
Fmoc	Fluorenylmethyloxycarbonyl
GC-MS	Gas chromatography–mass spectrometry
GlcCer	Glucosylceramide
GPTMS	(3-Glycidyloxypropyl)trimethoxysilane

h	hours
HMPA	Hexamethylphosphoramide
HOBt	Hydroxybenzotriazole
HPLC	High pressure liquid chromatography
HPLC-FD	High pressure liquid chromatography coupled to a fluorescence detector
HRMS	High Resolution Mass Spectrometry
HSQC	Heteronuclear Single-Quantum Correlation
HTS	High throughput screening
KHDMS	Potassium bis(trimethylsilyl)amide
MeOH	Methanol
min	minutes
(*R*)-MPA	(*R*)-α-methoxy-α-phenylacetic
MTT	3-(4,5-Dimethylthiazol-2-yl)-2,5-diphenyltetrazolium bromide
MS	Mass spectrometry
NBD	Nitrobenzo-2-oxa-1,3-diazole
NBS	*N*-bromosuccinimide
NMR	Nuclear magnetic resonance
NSB	Non-Specific Binding
PTAD	4-Phenyl-1,2,4-triazoline-3,5-dione
rt	Room temperature
R_t	Retention time
Sa	sphinganine
SK	sphingosine kinase
SKI II	Sphingosine kinase inhibitor
SLs	Sphingolipids
SM	Sphingomyelin
SMase	Sphingolyelinase

SMS	Sphingomyelin synthase
SMMs	Small Molecule Microarrays
So	Sphingosine
SPT	Serine palmitoyl transferase
S1P	Sphingosine-1-phosphate
S1PL	Sphingosine-1-phosphate lyase
TAD	1,2,4-triazoline-3,5-dione
TAMRA	Tetramethyl rhodamine
TBS	Tert-butyldimethylsilyl
THF	Tetrahydrofurane
THTPA	Tris(3-hydroxypropyltriazolylmethyl)amine
TLC	Thin-layer chromatography
*p*TsOH	*p*-Toluenesulphonic acid
UPLC	Ultra-Performance Liquid Chromatography
UPLC-TOF MS	Ultra-Performance Liquid Chromatography Time-of-flight mass spectrometry

TABLE OF CONTENTS

1. GENERAL INTRODUCTION AND OBJECTIVES

1. GENERAL INTRODUCTION AND OBJECTIVES

1.1. Sphingolipids

Sphingolipids (SLs) are ubiquitous structural components of eukaryotic cell membranes. Since their discovery in 1884 by J. L. W. Thudichum and until very recently, SLs have been considered inert components of membranes with merely structural roles.[1] However, during the last decades, several studies revealed their major role as bioactive molecules comprising various bioactive signalling processes that regulate a diversity of cellular activities, including regulation of cell growth, death, senescence, adhesion, migration, inflammation, angiogenesis and intracellular trafficking.[2,3]

SLs are generally composed of a polar head group and two nonpolar tails: a 18-carbon chain amino alcohol, also known as sphingoid base, and a fatty acid moiety attached via a *N*-acyl linkage. Functionalization at the C1–OH with different polar groups gives rise to complex SLs. Depending on the nature of the *O*–linked moiety, this large family of metabolites may range from simple phosphate or phosphocholine derivatives to complex glycoconjugated ceramide species (Fig. 1.1).[4]

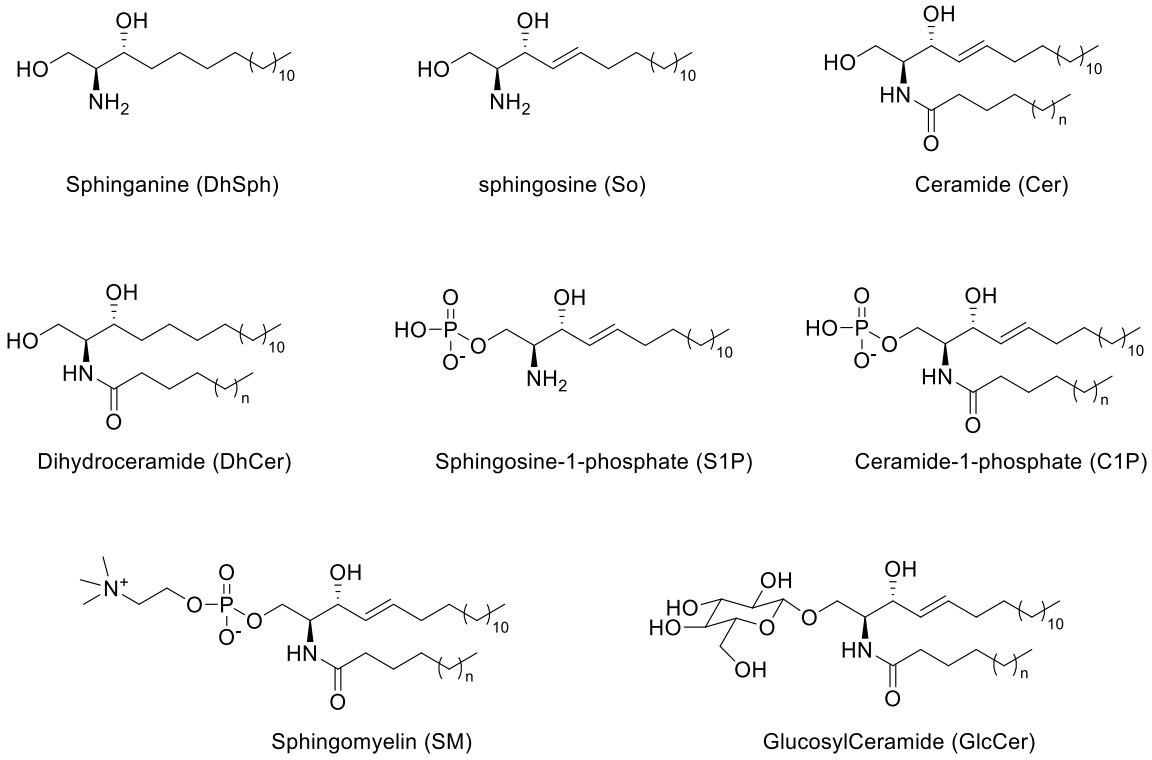

Figure 1.1. *Structure of representative SLs.*

The sphingoid bases are long-chain aliphatic compounds and include a wide array of 2-amino-1,3-dihydroxyalkanes or 2-amino-1,3-dihydroxyalkenes with (2*S*,3*R*)-*erythro* configuration.[5] The most frequent in mammal tissues are sphingosine (So), sphinganine (Sa), and phytosphingosine, also found abundantly in yeast and plants. These species can be found

in their free amino form or *N*-acylated with fatty acids of variable length and degrees of insaturation, generating a diversity of ceramide species.

The head groups define the different sphingolipid classes, with a hydroxyl group found in ceramides and a phosphate group in the phosphorylated derivatives. Complex SLs hold a phosphorylcholine moiety in sphingomyelin (SM), and one or several carbohydrate units in the various known glycosphingolipids (GLs).

1.1.1. Metabolism and compartmentalization

SLs metabolism includes a series of biosynthetic and catabolic reactions in which Cer plays a significant role. (Fig. 1.2).[6] Thus, the so called *de novo* biosynthesis (blue) takes place in the endoplasmic reticulum (ER) and starts with the condensation of serine with palmitoyl–CoA, catalysed by serine palmitoyl transferase (SPT) to give 3–keto-sphinganine. This molecule is subsequently reduced to sphinganine (Sa) and then *N*-acylated by several ceramide synthases (CerS) to give dihydroceramides (dhCer). CerS exhibit strict specificity for the fatty acid added to the sphingoid base and determine the fatty acid composition of the SLs in the cell. Most dhCers are immediately desaturated to ceramides (Cer) by dihydroceramide desaturase (Des1).[7,8]

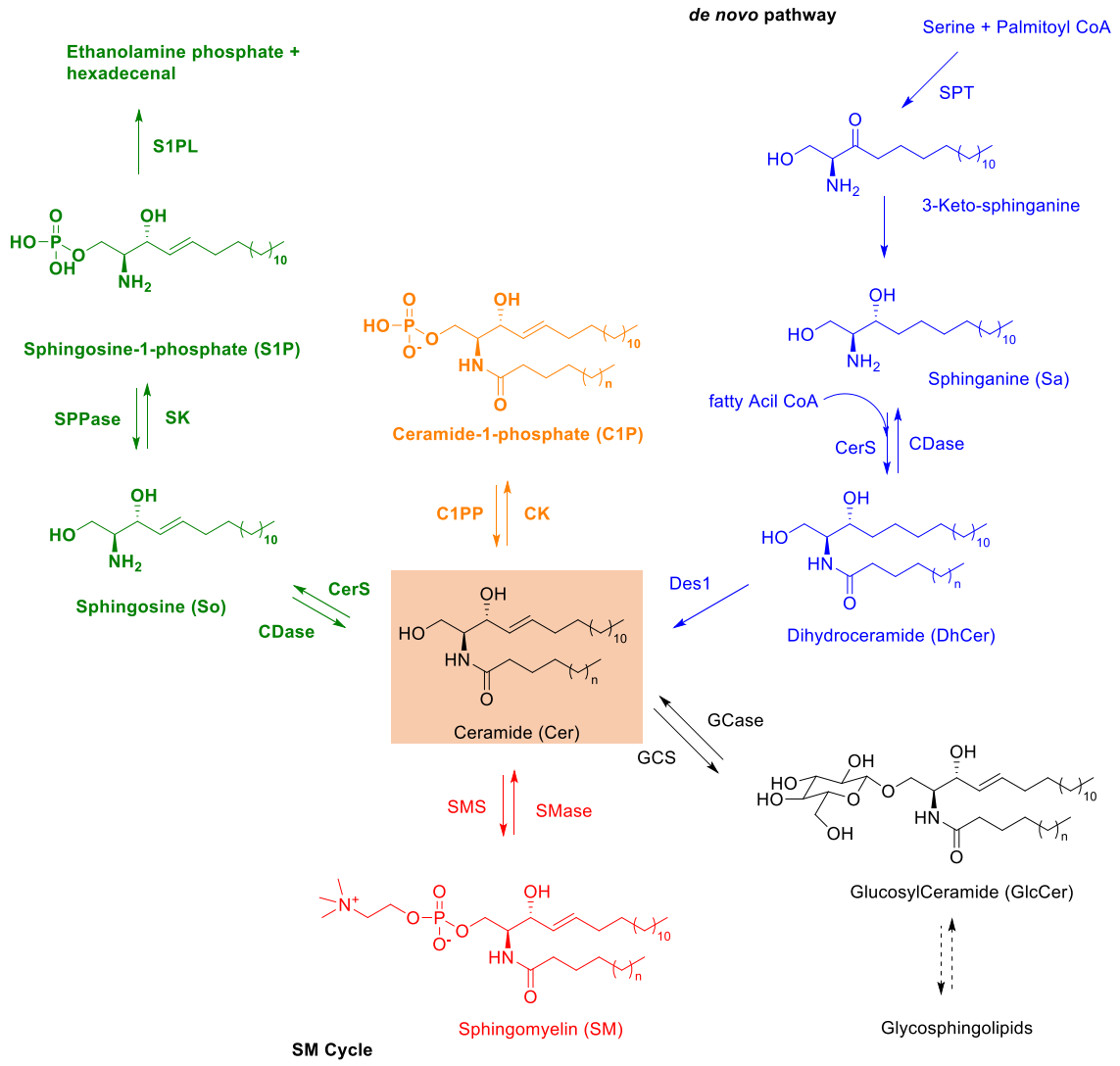

Figure 1.2. *Sphingolipid metabolic pathways: de novo pathway (blue), SM cycle (red), glycosphingolipids (black), irreversible step of the SLs metabolism (green) and phosphorylation of ceramide by CK (orange).*

Cer can also be metabolized by ceramidases (CDases), which remove the amide-linked fatty acid to form sphingosine (So, green), which is available for recycling into SLs pathway through acylation by CerS, or phosphorylation to S1P by sphingosine kinase (SK).[9] The last and irreversible step of the SLs metabolism is represented by sphingosine-1-phosphate lyase (S1PL), an enzyme that cleaves S1P into ethanolamine phosphate and hexadecenal.[10] Alternatively, S1P can be degraded by specific phosphatases (SPPase) to sphingosine. Moreover, Cer can have many other destinations; it can be transformed into SM (red) by the action of sphingomyelin synthase (SMS), converted into glucosylceramide (GlcCer, black) by glucosylceramide synthase (GCS), or phosphorylated by ceramide kinase (CK, orange).

SLs levels are regulated by the balance between the synthesis and degradation that occurs in multiple cellular compartments.[8] The advances in understanding the metabolism of SLs have generated evidences that prove the existence of multiple enzymes which, although distinctly localized, catalyse the same reaction.[11]

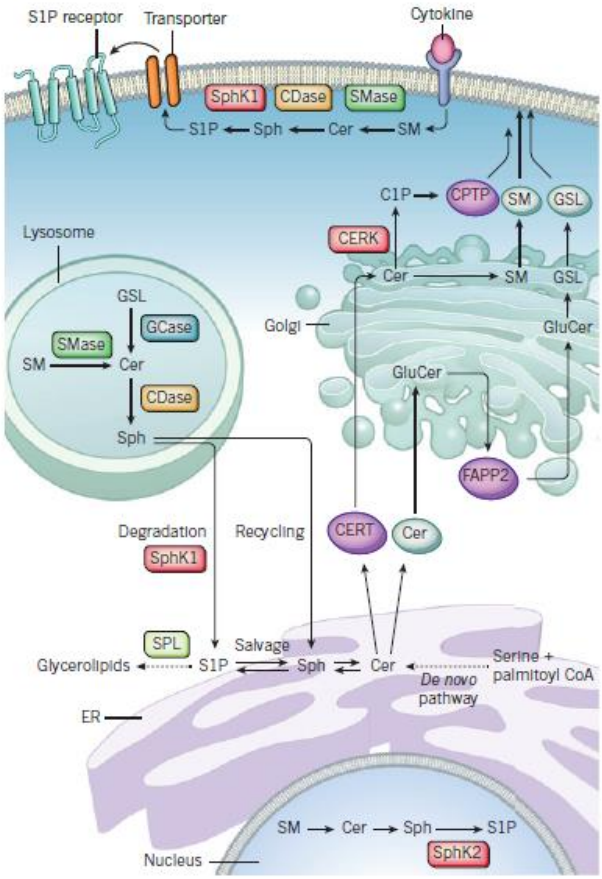

Figure 1.3. *Subcellular compartmentalization of SLs metabolism. Image taken from Maceyka et al.*[12]

SLs are mainly synthesized in the endoplasmic reticulum (ER) and in the Golgi apparatus and are then transported to the plasma membrane and other organelles (Fig. 1.3). Cer, which is formed in the endoplasmic reticulum, is transported to the Golgi apparatus for its further transformation into SM, the major SL constituent of the cell membranes, and glucosyl ceramide (GlcCer). The transport of Cer to the Golgi occurs either through the action of the transfer protein CERT, which specifically delivers Cer for SM synthesis, or through vesicular transport, which delivers Cer for the synthesis of GlcCer. In turn, the transfer of GlcCer for glycosphingolipids (GSL) synthesis requires the action of the recently identified transport protein FAPP2.

SM is an important structural element of the biological membrane. Together with cholesterol, it forms ordered domains that constitute important signalling platforms for proteins. As a result, the plasma membrane contains a substantial proportion of the total cellular SM content. Plasma membrane SM can be metabolized to Cer by SMases. Internalization of membrane SLs proceeds through the endosomal pathway and, once inside the cells, SM and GSL can travel to the lysosomal compartment where they will be metabolized to Cer by SMase and glucosidases (GCase). The resulting Cer is then hydrolysed by acid ceramidase (CDase) to form sphingosine (So), which after leaving the cytosol can be recycled again in the ER to form Cer.[8,13,14]

1.1.2. Sphingolipids in disease

Bioactive SLs are involved in the regulation of important signalling pathways. Thus, alteration of SLs metabolism may cause pathologic conditions and contribute to fatal diseases, such as different types of cancer, Alzheimer or type 2 diabetes.[15,16]

Cer has been implicated in the pathogenesis of several cellular states, including cancer. Apoptosis and autophagy are two essential cellular functions in which Cer is involved. Apoptosis is a programmed cell death, which is essential for the proper development and the maintenance of cell homeostasis. Autophagy is a catabolic process in which the cytoplasmic components are engulfed in autophagosomes, and delivered to lysosomes for their degradation and recycling. Autophagy promotes cell survival during periods of stress, including hypoxia or nutrient deprivation, although it can also mediate cell death.[15,17]

In general, cancer cells present a reduction in Cer levels producing a decrease in apoptosis. The origin of the decrease in Cer levels is diverse. In hepatocellular carcinoma and in breast, colon, lung, ovary, stomach, uterus, kidney and rectum cancers, there is an overexpression of the enzymes involved in the synthesis of complex SLs and CERT protein, giving rise to reduced levels of proapoptotic Cer. In addition, sphingomyelinase (SMase) and sphingosine-1-phosphatase (S1PP) genes are down regulated, causing low Cer levels, whereas gene expression involved in *de novo* biosynthesis becomes unaltered.

Furthermore, the use of Cer analogues has been shown to promote apoptotic/autophagic pathways in cancer cells. For this reason, the use of modified sphingolipids as anti-cancer therapeutics represents a promising option for treating cancer in the future. Nowadays, several strategies based on this approach have been developed,[15]as the liposome-mediated delivery of C_6-Cer.[18]

It is known that Alzheimer's disease is implicated in changes in the sphingolipid metabolism [16,19] affecting levels of genes involved in the *de novo* synthesis during the early stages of the disease.[20] The key role of SMases in this disease is to promote apoptosis in neuronal cells through the generation of proapoptotic Cer.[21]

Type 2 diabetes is characterized by insulin resistance in skeletal muscle cells, adipose tissue and liver. Cer is an attractive candidate to be a primary culprit involved in mediating the skeletal muscle insulin resistance observed in this disease, as it is elevated by both inflammation and nutrient overload.[22] Numerous studies demonstrate that increasing Cer levels inhibit insulin signalling and cause insulin resistance.[23] Moreover, Holland *et al.* showed that inhibition of the *de novo* synthesis of Cer by blocking serine palmitoyl transferase (SPT) can prevent the insulin resistance caused by corticosteroids, saturated fats, and genetic models of obesity.[24]

1.1.3. Chemical probes of sphingolipid metabolizing enzymes

The use of specific probes to monitor the enzyme activity of specific SLs metabolizing enzymes, as well as their intracellular localization and trafficking, is gaining importance in contemporary chemical biology and drug design approaches.[14] The biological relevance and the growing interest around some SLs metabolizing enzymes as drug targets highlights the need for potent and selective inhibitors that efficiently modulate their activities. In this regard, the rapid and efficient identification of sphingolipid metabolism enzyme inhibitors may be achieved by massive screening of chemical libraries. However, this requires the availability of high throughput screening (HTS) methods, which are currently very scarce in the sphingolipid arena.

Before the implementation of assays based on the use of non-natural substrates, many enzyme determinations were performed with radioactive substrates. Examples include radiolabelled Cer for CerK,[25] CDases,[26] and SMS,[27] radiolabelled dhCer for Des1,[28] radiolabelled SM and GlcCer for SMases[29] and glucocerebrosidases (GBA),[30] respectively, and [4,5-^{3}H]S1P for sphingosine-1-phosphate lyase (S1PL).[31]

The disadvantages of working with radioactive materials have stimulated the development of non-natural substrates to monitor SL metabolizing enzymes. The sphingoid aliphatic chain shortening is the simplest natural substrate modification so far reported. Spassieva *et al*.[32] described the use of non-natural C(17) sphingoid bases (Sa(C17) and So(C17), Fig. 1.4), in combination with mass spectrometry, for the assay of CerS and SK. In a contribution of our group,[33] a series of stereochemically defined 1-deoxysphinganine and 1-deoxysphingosine were evaluated as probes to unravel CerS activity in intact cells by UPLC-TOF methods. Among the different analogues tested, compounds **ES285**, **RBM1-77** and **RBM1-73** (Fig. 1.4) turned out to be suitable probes for CerS profiling. These probes are metabolically stable at both C1 and at the amide linkage, after CerS acylation, and thus the resulting amide composition reflects the overall CerS activities under a given set of conditions. In particular, compound **ES285** (spisulosine) led to the highest acylation rates, thus being the compound of choice as chemical probe to evaluate CerS activity and the distribution of *N*-acylated metabolites under given biological conditions.

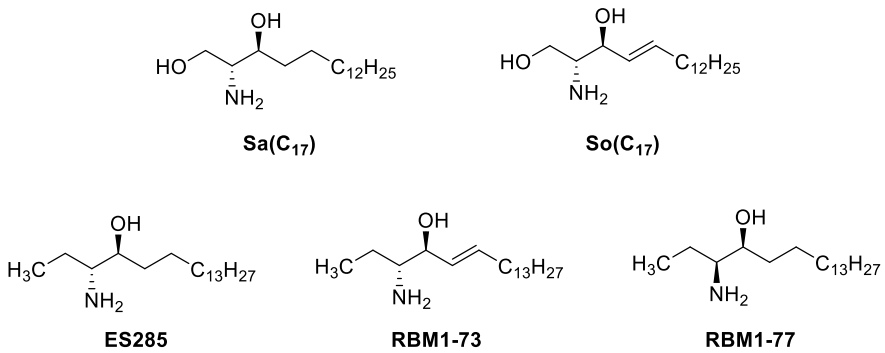

Figure 1.4. *Minimally modified substrates for the determination of SK or CerS activity.*

Nevertheless, fluorescent substrates are amongst the non-natural substrates more extensively used. For example, a fluorescent assay based on the use of commercially available NBD-labelled sphinganine (Sa(NBD), Fig. 1.5) as CerS substrate has been described.[34] According to the authors, the assay is suitable for the detection of endogenous CerS activity, both in cells or tissue homogenate protein and is more sensitive than the previously reported radioactive assay. Interestingly, Sa(NBD) behaves similarly as the natural substrate in terms of enzyme affinity. The detection and quantification of the resulting dhCer(NBD) is carried out directly on the TLC plate, and the reported detection limit has been estimated in 0.5 pmol.

Another fluorometric assay to quantify SK activity is based on the use of a labelled C_{15}NBDSo as substrate (SoC_{15}(NBD), Fig. 1.5).[35] The method is suitable to measure the activity of SK, both from purified preparations and from lysate extracts of mammalian cells. In addition to NBD,[36] BODIPY derivatives have also been tested as SK substrates (Fig. 1.5).

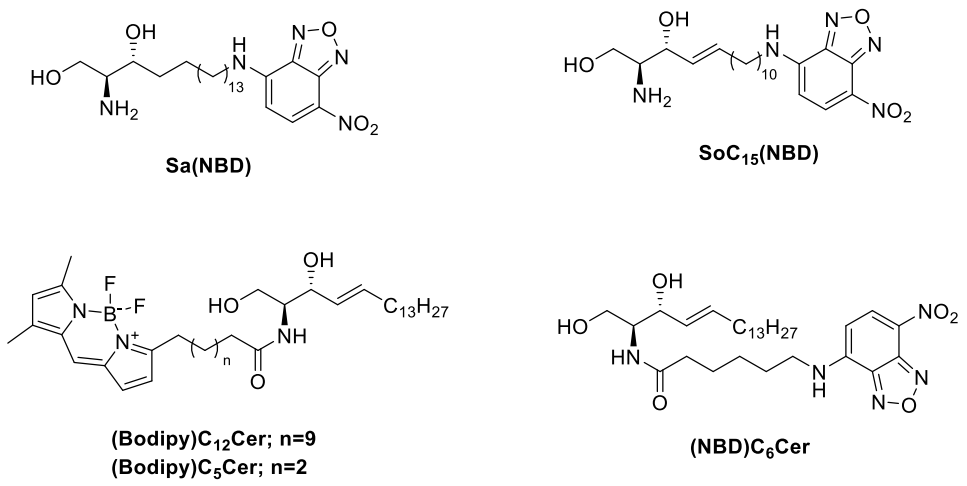

Figure 1.5. *Fluorescent non-natural probes*

Regarding CDase activity, the use of fluorescent (NBD)C_6Cer as CDase substrate (Fig. 1.5) was already reported by Merrill *and col.* in assays carried out *in vitro* and in intact hepatocytes.[37] Furthermore, Bhabak *et al*. reported on two FRET probes, (NBD)C_{12}Cer$_7$(NR) and (NR)C_{12}CerC_7(NBD) (Fig. 1.6), for the real-time determination of CDase activity.[38] The probes were designed by combination of NBD and NR as donor and acceptor FRET pairs, respectively, located as part of the acyl chain and/or the sphingoid base of the Cer substrate. Probe (NBD)C_{12}CerC_7(NR) turned out to be a better substrate than (NR)C_{12}CerC_7(NBD) for CDases, with K_m values of 142 µM and 182 µM for recombinant neutral and acid CDase, respectively. Finally, similarly as discussed above, fluorescent substrates, incorporating a fluorescent reporter as part of the sphingoid base chain, have been developed for SPL and Des1 (*see* Section 1.1.4.3).[14]

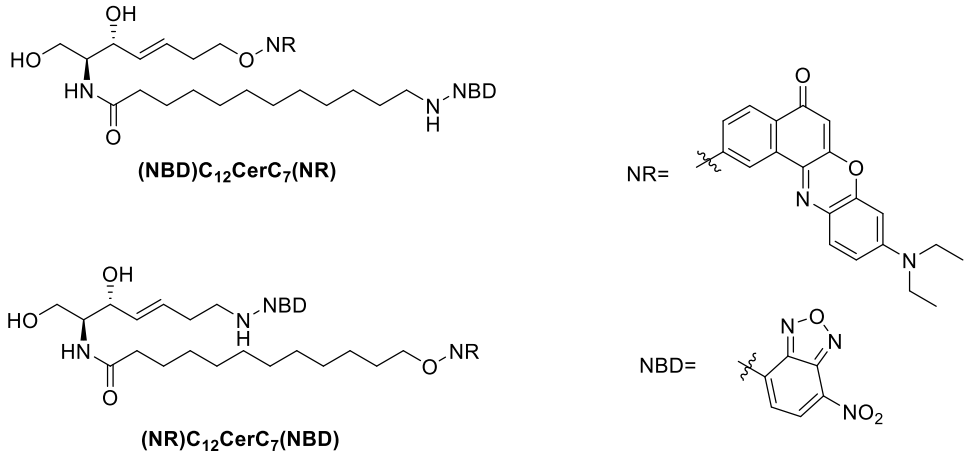

***Figure 1.6**. FRET-based probes for real time determination of CDase activity.*

1.1.4. Dihydroceramide and Dihydroceramide desaturase (Des1)

Des1 catalyses the last step of the *de novo* biosynthesis of SLs,[39] which requires the introduction of a *trans* Δ^4-double bond in the carbon chain of dhCer to generate Cer.[40] As a result, this enzyme is crucial for the balance between sphingolipids and dihydrosphingolipids.

Based on *in vitro* experiments, dhCers were initially considered as inert Cer intermediates. Apparently, short length cell permeable dhCers failed to reproduce the effects of other Cer analogues.[41] In fact, dhCers were often used as controls in experimental settings to study cell growth inhibition, apoptosis and cell death in a variety of cell types.[42] However, recent reports [43-44] indicate that dhCers are, in fact, bioactive lipids, although their effect may differ from those elicited by Cers. The use of biophysical models,[45] as well as genetic[43] and pharmacological[43,44] tools to decrease Des1 activity has proven crucial to reveal the biological activity of dhCer derivatives.

1.1.4.1. Identification and characterization of Des1

The Des1 gene was first cloned in 1996 in *Drosophila melanogaster* as *DEGS1* (Drosophila degenerative spermatocyte 1), while investigating the role of the gene in the initiation of meiosis during spermatogenesis.[41] Soon after, Cadena *et al.* demonstrated that Degs1 was a membrane desaturase, localized to the ER membrane, where it has access to newly synthesized dhCer species.[46]

Two genes (Des1 and Des2) have been described, being Des2 a bifunctional enzyme which exhibits Δ^4-desaturase and Δ^4-hydroxylase activities. This enzyme is responsible for the biosynthesis of glycosphingolipids containing 4-hydroxysphinganine in the small intestine.[47] However, Des1 exhibits high dhCer Δ^4-desaturase activity and very low Δ^4-hydroxylase activity. The tissue distribution profile of both enzymes is considerably different. Des1 is ubiquitously distributed, whereas Des2 is preferentially expressed in small intestine, skin and kidney where the production of phytoceramides is essential.[40,48]

From the biochemical point of view, studies carried out in the late 90s demonstrated that Des1 requires NADPH[49] or NADH[50] as electron donor and oxygen as electron acceptor. The electron provided by NAD(P)H is sequentially transported from the cofactor to NADH-cytochrome b5 reductase, cytochrome b5, and the terminal desaturase, which reduces oxygen to water and oxidizes dhCer to Cer (Fig. 1.7).[51]

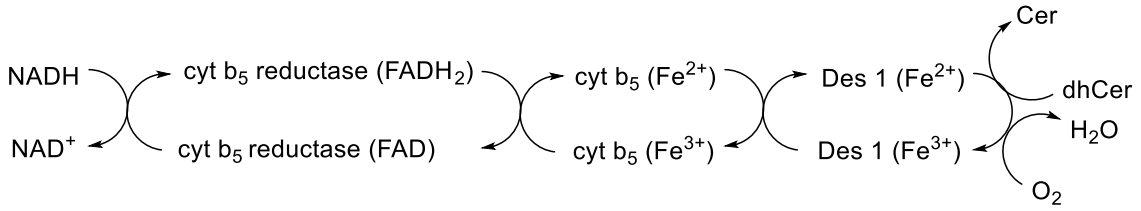

Figure 1.7. *Des1 enzymatic complex.*[47]

Des1 activity is largely affected by the configuration of the substrate sphingoid base . Desaturation of the D-*erythro*-isomer is much abundant than that of the L or D-*threo*-isomers. Other factors that influence the enzymatic activity are the length of the alkyl chains of the amide-linked fatty acid; for instance, *in vitro* activity in rat liver microsomes decreases when the length of the chain is increased.[28,50] However, in foetal rat skin and liver homogenates, C18/C14-Cer is a better substrate for desaturation than dhCer analogues containing fatty acids with 18, 10, 6, or 2 carbon atoms.[48] The enzyme is active over a broad pH range (6.5-9), being around 8.5 the optimal.[49]

1.1.4.2. Des1 inhibitors

The availability of Des1 inhibitors and their use as pharmacological tools has helped to refute the biological innocuousness of dhCer. Most of the evidences come from studies where inhibition of Des1 causes an accumulation of dhCer. Several drugs have been described to inhibit Des1 activity, including GT11[39] o XM462,[52] reported by our group in years 2001 and 2012, respectively. In addition, a series of drugs and natural products also show inhibitory effect on Des1 activity. The outcome of this inhibition is varied, depending on the cell line, the degree of inhibition (and, thus, the resulting amounts of accumulated dhCer) and the experimental conditions.[40]

The first reported synthetic Des1 inhibitor was compound GT11 (Fig. 1.8).[53] This cyclopropane-containing sphingolipid carries out a competitive inhibition against the substrate with a K_i=6 µM and it is active both *in vitro* and in intact cells.[54] As mentioned above, XM462 is another Des1 inhibitor reported by our group, whose effect occurs both *in vitro* and in cultured cells with IC_{50} values of 8.2 and 0.78 µM, respectively.[39]

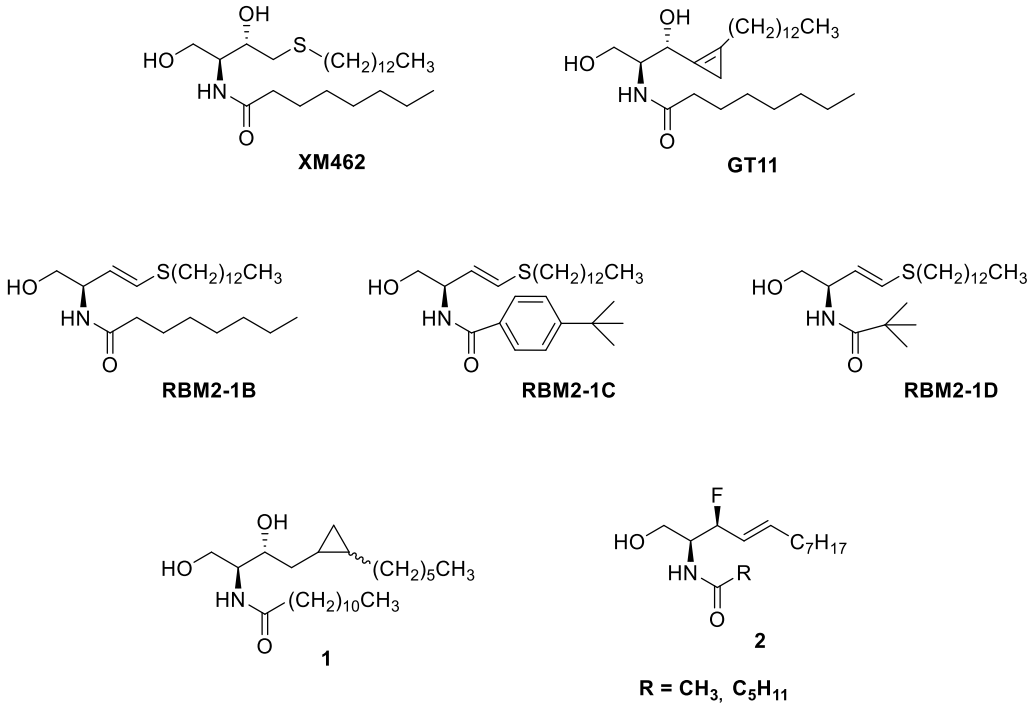

Figure 1.8. *Cer analogues reported as Des1 inhibitors.*

Other analogues have been described to inhibit Des1 activity. For example, two dhCer analogues with an allylic fluoride replacing the 3-hydroxyl group (**2**, Fig. 1.8) have been reported.[55] These compounds have been evaluated as potential Des1 inhibitors by an *in vitro* assay using rat liver microsomes, showing a slight inhibition of the desaturase activity (9% when equimolar concentrations of the substrate and inhibitors were used). A C12-dhCer analogue with a cyclopropane ring at C-5 and C-6 has been described (**1**, Fig. 1.8) and shown to inhibit Des1 activity, although to a much lesser extent that GT11, in cultured keratinocytes.[56]

In addition to these Cer analogues, a series of drugs and natural products have been reported to inhibit Des1 (Fig. 1.9), including fenretinide, resveratrol, celecoxib, tetrahydrocannabinol, curcumin and some vitamin E components. For example, fenretinide is a synthetic derivative of all-*trans*-retinoic acid, a vitamin A analogue, which has been widely investigated for the prevention and treatment of cancer. [57] It has been reported to induce apoptotic cell death and to repress cell proliferation, thereby being useful to halt tumour growth.[44]

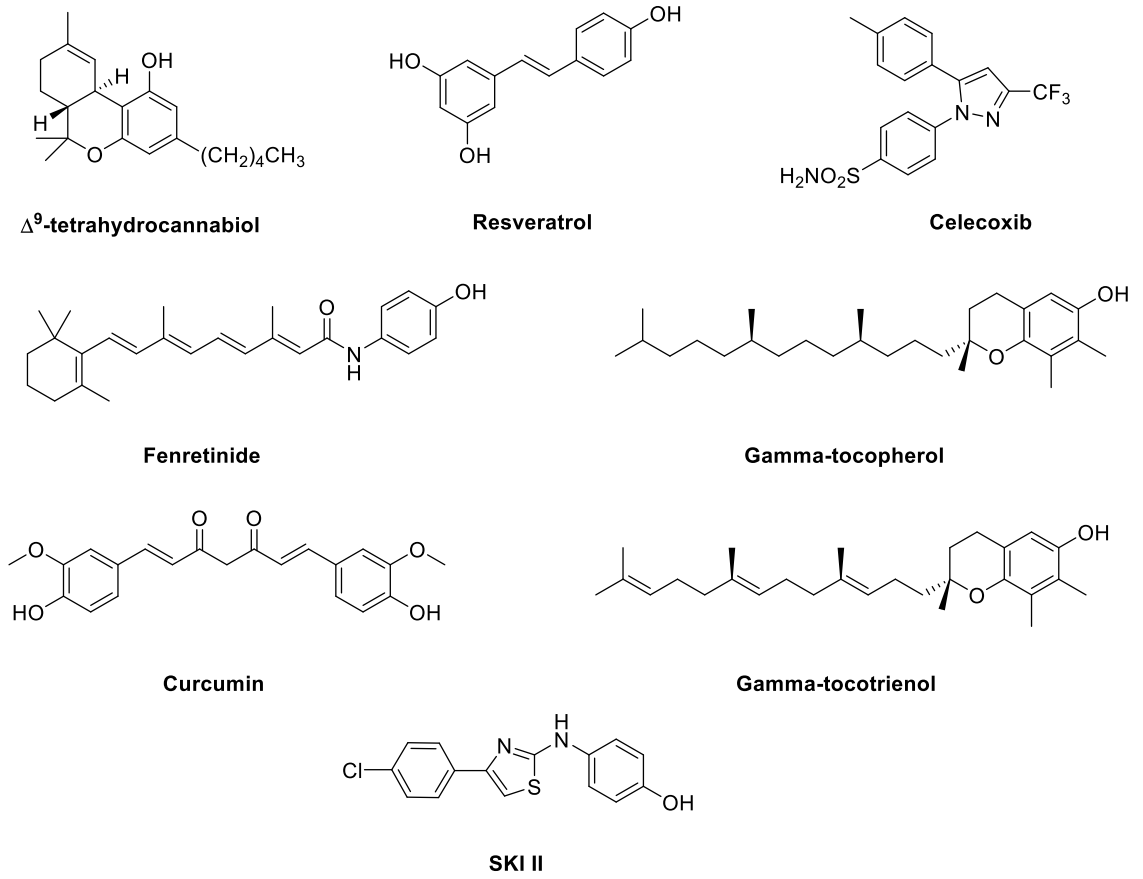

Figure 1.9. *Compounds structurally unrelated to Cer reported as Des1 inhibitors.*

Resveratrol (Fig. 1.9) is a dietary polyphenol with well recognized antioxidant and health beneficial properties.[58] In addition to thousands of research papers related to resveratrol, approximately 300 review articles have been published. In relation to SLs, it has been reported that resveratrol might kill chronic myelogenous leukaemia cells [59] and promyelocytic leukaemia cells[60] through increasing intracellular generation and accumulation of apoptotic Cer. In most of the cancer cell lines tested, resveratrol arrests cell cycle in G1/S phase, blocks proliferation[61] and, under prolonged treatment, it is able to induce apoptotic cell death by Cer accumulation.[60]

Also the dual sphingosine kinase 1-2 inhibitor SKI II (4-[[4-(4-chlorophenyl)-2-thiazolyl]amino] phenol) has been recently reported by our group [62] as a non-competitive Des1 inhibitor (Ki= 0.3 mM). Molecular modelling studies supported that the SKI II-induced decrease in Des1 activity could result from inhibition of NADH-cytochrome b5 reductase. Treatment of HGC 27 cells with SKI II resulted in decreased S1P levels and increased amounts of dhCer.[63]

1.1.4.3. Chemical probes to monitor Des1 activity

In Section 1.1.3 we have been discussed some chemical probes of sphingolipid metabolizing enzymes. In this section, we will focus our attention in the development of chemical tools to study Des1 functions. As a result, some non-natural dhCer derivatives have been reported over

the past decades as chemical probes to determine the activity of this enzyme. However, none of them have been used to develop HTS–amenable assays for library screening.

In 1997, Michael *et al*. described a radioactivity labelled dhCer analogue (*N*-[1- ^{14}C]octanoyl-*D*-*erythro*-sphinganine, Fig. 1.10) as Des1 substrate and NADH or NADPH as co-substrate to monitor the activity of the protein from the intact rat liver microsomes.[64] Cer formed by desaturation of this substrate was detected by autoradiography after extraction with organic solvents and separation by thin-layer chromatography (TLC).[28]

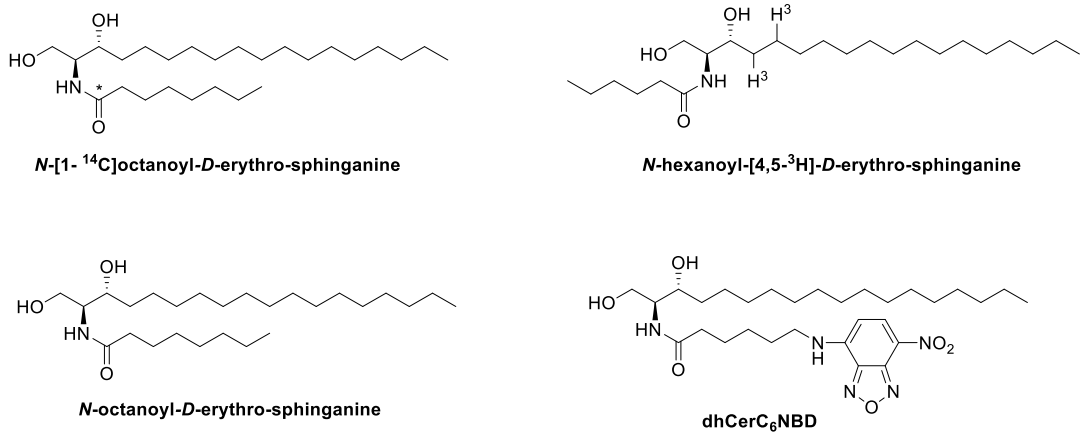

Figure 1.10. *Des1 substrates used in the different assays for Des1 activity reported to date.*

An alternative way to determine Des1 activity was reported by Geeraert *et al.* In this method, the truncated dhCer analogue *N*-hexanoyl-[4,5-^{3}H]-D-*erythro*-sphinganine (Fig. 1.10) was used to study the conversion of dhCer into Cer by rat hepatocytes. The formation of tritiated water after the addition of the tritiated substrate to intact and permeabilized rat hepatocytes was followed to measure the enzyme activity.[49]

The disadvantages of working with radioactive materials stimulated the development of non-natural substrates to monitor SL metabolizing enzymes.[14] Thus, Des1 activity can be also determined by using *N*-octanoyl-*D*-*erythro*-sphinganine as substrate, and monitoring the formation of Cer by GC-MS of the volatile trimethylsilyl derivatives.[65]

The simplicity and the sensitivity of fluorometric analytical techniques have boosted the development of substrates that incorporate a generally bulky, fluorescent reporter as part of the sphingoid structure. In this case, the fluorescent analogue dhCerC$_6$NBD (Fig. 1.10) has been used as Des1 substrate, allowing the measurement of Des1 activity by HPLC-FD.[66] The kinetic parameters of dhCerC$_6$NBD desaturation have been determined in rat liver microsomes after incubation with different substrate concentrations and lipid analysis by HPLC coupled to a fluorescence detector. Under these conditions, a K_m of 7.7 µM for the fluorescent substrate was determined.[67]

1.2. Triazolinediones as Highly Enabling Synthetic Tools

The 1,2,4-triazoline-3,5-diones (TADs) are heterocyclic systems with an azo moiety connected to two carbonyl functionalities.[68] This electronic conjugation stabilizes the azo function, but the electron-withdrawing carbonyl groups and the symmetry of the electronic system is responsible for a very particular orbital-controlled electrophilic reactivity, similar to that of carbenes or singlet oxygen,[69] which are highly reactive, but unstable reagents with very short lifetimes.[70] Indeed, TADs have a reactivity profile very similar to that of singlet oxygen, and favour ultrafast Diels Alder, Alder-ene (Fig. 1.11) and [2+2]-cycloaddition reactions for a similar range of substrates (electron-rich or nonpolarized olefins). This similarity in reactivity can also be related to a correspondence in the particular arrangement and energies of the frontier orbitals (HOMO and LUMO), with a filled and an empty π-type orbital of very similar energy.[69]

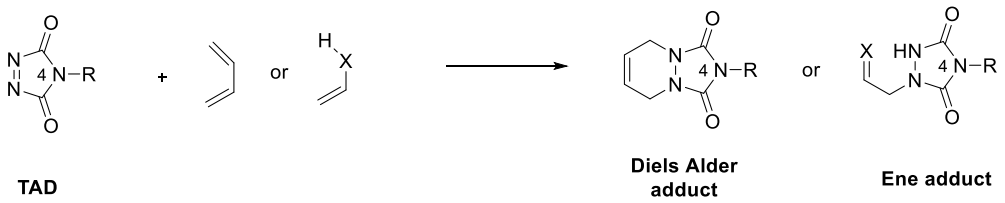

Figure 1.11. *General Diels Alder and Ene adducts formed with TAD reagents.*

Although only Diels Alder and Alder-ene reactions will be discussed in this Thesis, it is known that TADs participate in a large number of reactions and they have become a well-established class of synthetic tools for a wide range of applications,[71] including click chemistry.[72]

1.2.1. Reactivity of TADs in Diels Alder Reaction

Diels Alder or hetero Diels Alder reactions are recognized as one of the most efficient and widely applicable organic bond-forming reactions. These reactions consist in a [4+2]-cycloaddition between a conjugated diene and a dienophile, which involve 4 π-electrons of the diene and 2π-electrons of the dienophile (Fig. 1.12). Moreover, Diels Alder and hetero Diels Alder reactions allow the introduction of two new carbon−carbon or carbon-heteroatom σ-bonds, respectively, and up to four new stereocenters,[73] with very pronounced and predictable levels of chemo-, stereo-, and regioselectivity.

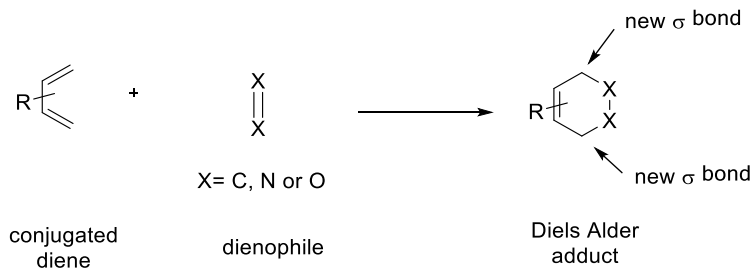

Figure 1.12*. General scheme of Diels Alder and hetero Diels Alder reactions.*

The Diels Alder reaction has an enormous substrate scope, but the use of TADs as dienophiles in the Diels Alder reaction was not established before the 1960s, when Cookson *et al.* described pure crystalline 4-phenyl-1,2,4-triazoline-3,5-dione (PTAD).[68] Since then, the reactivity of TADs in Diels Alder reactions has been extensively studied with components of low molecular weight in organic synthesis,[68,74,75,76] in pharmaceutical applications [77] and in orthogonal peptide labelling. [78,79]

TADs have become an intensively studied class of Diels Alder substrates, acquiring the reputation of being the fastest dienophiles that can be isolated.[70] The exceptional reactivity of TADs can be appreciated by the fact that their reaction is claimed to be almost instantaneous and quantitative, even at low temperatures with dienes of low reactivity. Moreover, as their reactivity depends, to a certain extent, on the nature of the 4-substituent (Fig. 1.11), electron-poor 4-aryl substituents can even further increase the electrophilicity up to the point that TAD reagents, for example, 4-(4-nitrophenyl)-TAD, become too reactive to be isolated.[80]

1.2.2. Reactivity of TADs in Alder-ene Reactions

Although the Ene reaction is one of the most simple and versatile reaction of organic chemistry, it is scarcely studied and virtually ignored in nearly all text books.[81] The Alder-ene reaction, described by Alder *et al.* in 1943,[82] can be defined as the reaction between an alkene bearing an allylic hydrogen (the "ene") and a double bond (the "enophile"). It is a type of pericyclic reaction that comprises a [1,5] hydrogen shift of a σ-bonded hydrogen atom and the formation of a new C−C σ-bond at the expense of a C−C π-bond (Fig. 1.13). [83]

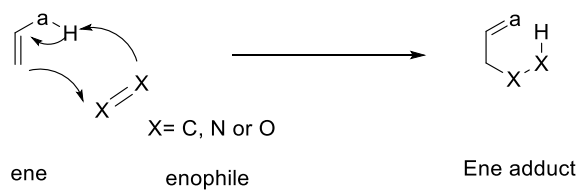

***Figure 1.13**. General scheme representing Ene reactions.*

The ene component is an alkene (or enol), which can react with a quite broad range of enophiles. These include alkenes, alkynes, allenes, carbonyls, imines and main-group double bonds.[83] The ene component can be considered to act either as a nucleophile or as a 4-electron-coupling partner in the concerted process, akin to the diene component in a Diels Alder reaction. Consequently, electron-rich alkenes are more reactive than electron-deficient ones by several orders of magnitude. The enophile component is preferably an electron deficient species.

Despite the great potential in organic synthesis of the ene reaction,[81] the applications of the Alder-ene reaction have been rather limited, as compared to the Diels Alder reaction. One reason is the unfavourable activation entropy and enthalpy, related to the highly-ordered transition state with relatively poor orbital overlap, which results in much slower reaction

rates. The introduction of highly reactive enophiles, such as TADs, however, has opened the door to quite reliable and even selective intermolecular ene reactions.

From a mechanistic perspective, ene reactions often proceed in a concerted manner through a cyclic transition state, although they can also proceed through stepwise mechanisms involving carbocation intermediates (Fig. 1.14).[83] For many ene reactions, the exact mechanism is either not defined or has been shown to proceed by both concerted and ionic pathways, depending on the reaction conditions. If Lewis acid catalysts are employed, both mechanisms can coexist, with an earlier transition state representing an increased carbocation character during the C–C bond-forming reaction.

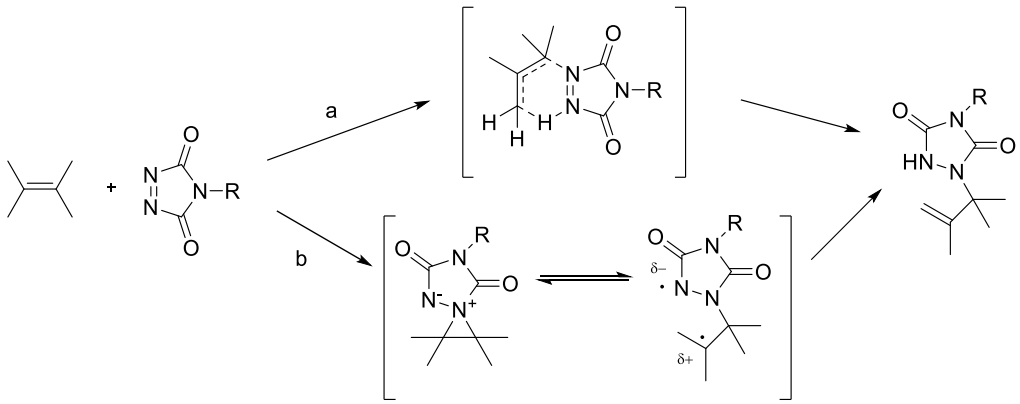

Figure 1.14. *The two mechanisms considered for an Alder-ene reaction between a mono-olefin and a TAD compound. a) Concerted pericyclic process, via six-membered ring transition state; b) Stepwise mechanism, via an open zwitterion.*

These two mechanisms have been a matter of some debate in the literature, where a six-electron concerted pericyclic process has been disregarded in favour of a stepwise route involving the formation of the zwitterion aziridinium imide.[84]

1.2.3. Use of Triazolinediones in "click"reactions

Click reactions are considered as one of the most efficient strategies to introduce covalent links between two moieties. In this context, Barbas *et al.* developed a series of azide-containing urazoles, using different synthetic approaches.[79,85] These azido urazoles (Fig. 1.15) were successfully reacted, after a previous oxidation to the corresponding TAD reagent, with an alkyne system in a copper-catalyzed 1,3-dipolar cycloaddition reaction.

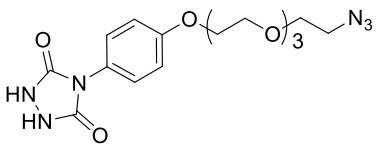

Figure 1.15. *Azide containing urazole, described by Barbas et al.*[79]

Although hetero-Diels Alder reactions have been considered by Sharpless and Finn as "beautiful representatives of click chemistry ideals", TAD-based chemistry has not been discussed in the context of click chemistry until almost a decade after its initial report.[79] Indeed, besides having the reputation of the "most reactive" dienophiles, TADs also have a reputation of being "exotic" reagents and have been generally regarded as highly unstable species. Nevertheless, the synthesis of TADs can be straightforward and it generally involves high-yielding steps. Moreover, no purification steps are usually required, at least when chemoselectivity issues are carefully considered in the choice of starting materials and reagents. It is believed that this "lag" for TADs to emerge as versatile click chemistry tools is reminiscent of the similar lag in its initial adoption as useful dienophiles and enophiles in organic synthesis.

As far as we know, TADs have been used for some other analytical applications, such as bioconjugation of peptides and proteins,[85] derivatization of lipid metabolites in biological samples,[86] and also as tools in modular chemical library synthesis,[87] among others.[71]

1.3. Objectives

The seminal idea and the leading motivation of the present doctoral thesis was the development of a HTS assay to monitor Des1 , one of the enzymes of the *de novo* SL biosynthesis. The expansion of new methods for the quantification of SL enzymes and the use of specific probes to monitor their intracellular localization and trafficking is gaining importance in contemporary chemical biology and drug design approaches. In addition, the discovery of new Des1 inhibitors with improved potency and selectivity would be greatly accelerated with the use of efficient HTS assays.

Based on the above considerations, the main objective of this thesis is the design of new chemical probes for their implementation into a fluorescent HTS assay to monitor Des1 activity. Ideally, this assay should be adaptable to a microarray format by using a solid-supported substrate, followed by derivatization of the Des1 reaction product with a fluorescent reporter. For this purpose, two options will be considered:

1) In a first approach, the use of a supported dhCer derivative, as a surrogate of the natural Des1 substrate, will be evaluated (Fig. 1.16A). In this case, the resulting natural Δ^4-Cer arising from the enzymatic reaction should be trapped with a suitable enophile through an Alder-ene reaction.
2) On the other hand, the use of a supported non-natural Δ^6-dhCer (Fig. 1.16B) as Des1 substrate will also be considered. After the enzymatic reaction, the resulting $\Delta^{4,6}$-Cer should be reacted with a fluorescent dienophile, through a Diels-Alder reaction, for its subsequent detection and quantification.

Interestingly, the reactivity of a triazolinedione (TAD) is compatible with both types of reactions.[69,88,89] For this reason, the first objective will be addressed to evaluate the ability of TAD to react with a natural Δ^4-Cer as an Alder-ene partner (according to approach 1, Fig. 1.16A) or with a $\Delta^{4,6}$-Cer in a Diels-Alder reaction, according to approach 2 (Fig. 1.16B).

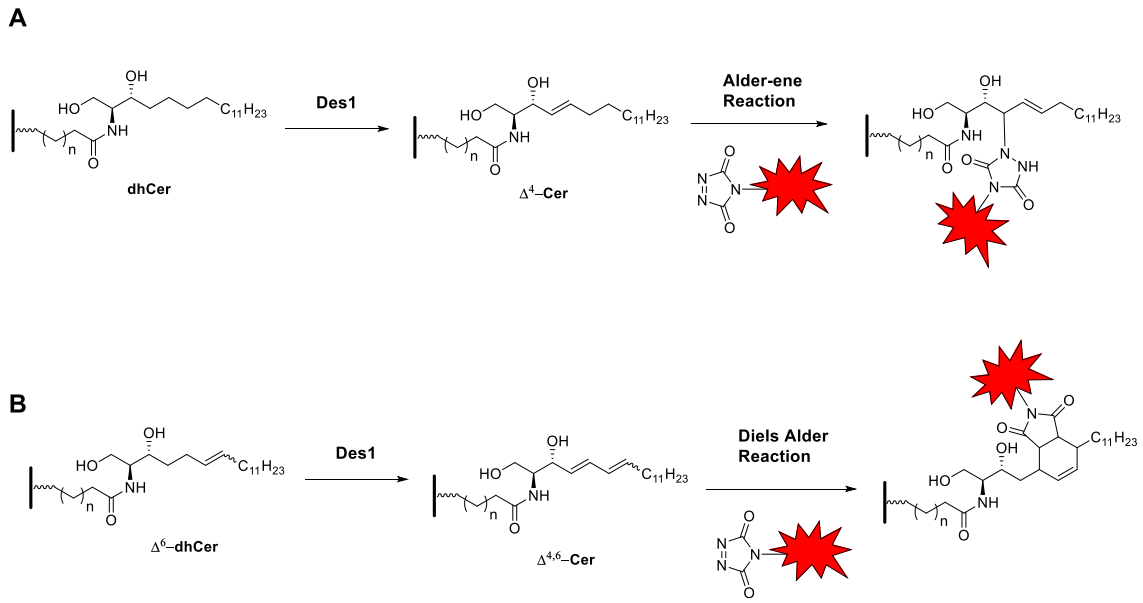

Figure 1.16. A. *Design of a HTS assay using an immobilized natural dhCer as substrate. The reaction product can react with a fluorescent enophile through an Alder-ene reaction.* ***B.*** *Design of a HTS assay using immobilized Δ^6-dhCer analogue. The reaction product can react with a fluorescent dienophile (such as TAD reagent) through a Diels Alder reaction.*

In both cases (Fig. 1.16), a suitable fluorescent TAD derivative will be designed and synthesized as labelling reagent. Preliminary experiments will be carried out with a simple TAD model compound in solution to explore the ability of sphingoid bases, bearing a natural Δ^4-Cer or a non-natural $\Delta^{4,6}$-Cer, as Alder-ene or Diels Alder substrates, respectively.

As it will be discussed in Section 2.1, the preliminary results obtained with Δ^4-Cer and TAD prompted us to consider approach 2 (Fig 1.16B) as the most reliable one. This required the study of both *E*- and *Z*-Δ^6-dhCers as Des1 substrates in *in vitro* experiments, as it will be reported in Section 2.3.1.

With the optimized reaction conditions in hand, the design of a Des1 HTS assay, amenable to microarray formats, will require:

- The synthesis of microarray supported Δ^6-dhCer and $\Delta^{4,6}$-Cer derivatives for assay optimization.

- The development of a protocol to monitor Des1 activity in cell lysates using the supported Δ^6-dhCer substrate in a microarray format.

- The optimization of the HTS assay on a microarray format for the subsequent detection of the enzymatic reaction product with a suitable fluorescent TAD reagent.

2. CHEMICAL TOOLS FOR THE DEVELOPMENT OF A HTS ASSAY IN AN ARRAY SYSTEM

2. CHEMICAL TOOLS FOR THE DEVELOPMENT OF A HTS ASSAY IN AN ARRAY SYSTEM

2.1. Preliminary assays

As mentioned in Section 1.1.4, Des1 is the enzyme involved in the conversion of dhCer into Cer by inserting a *trans*-4,5-double bound into the sphingoid backbone of dhCer. The typical dhCer analogue that is used to study the conversion of dhCer into Cer is *N*-octanoyldhCer (C_8-dhCer).[90] The conversion of this substrate into *N*-octanoylSo is followed by GC-MS and currently used to monitor Des1 activity.[91,92] However, this method is not amenable for HTS formats.

As indicated in Section 1.3, two approaches can be foreseen to design a Des1 assay amenable for HTS formats. On one hand (approach A), the use of a suitable *N*-acyldhCer as substrate would produce the corresponding *trans*-Δ^4-Cer, which could be trapped by a fluorescent TAD-reporter through an Alder-ene reaction. Alternatively, (approach B), the use of a non-natural Δ^6-dhCer as substrate would give rise, by the action of Des1, to a $\Delta^{4,6}$-diene system susceptible of reaction with a TAD derivative through a Diels-Alder reaction. Preliminary tests to evaluate the scope of each the two approaches were undertaken and the results are reported in this section.

Approach A

The reactivity of a Cer derivative in an Alder-ene type reaction with a TAD reagent as enophile was tested in solution using Δ^4-C_8Cer **RBM8-349** and PTAD[70] as reaction partners (Fig. 2.1). The reaction was carried out in CH_2Cl_2 using 10 equiv. of PTAD and kept at room temperature for 24 h. Unfortunately, no trace of the expected ene-type adduct was observed under these conditions, even after the successive additions of TAD at several time intervals along the reaction course. Given the nature of the enzymatic assay for which this process had to be developed, we disregarded the use of harsher reaction conditions, since they probably would have not been compatible with the assay conditions. These experiments led us to disregard the use of an Alder-ene reaction between a TAD reagent and a monoene Cer for the monitorization of Des1 activity.

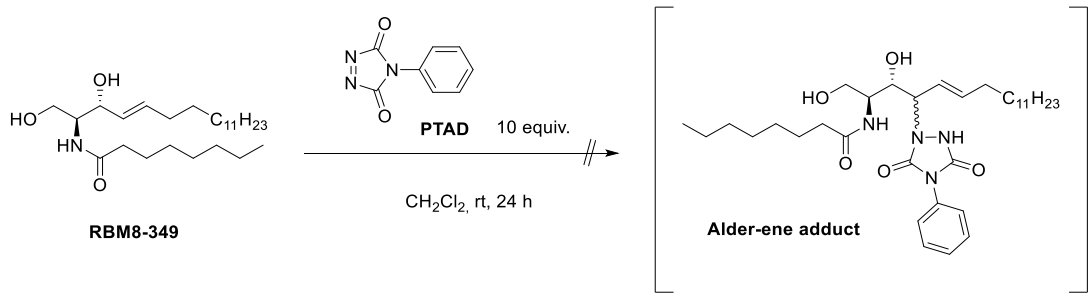

Figure 2.1. *Expected reactivity of Δ^4-C_8Cer **RBM8-349** and PTAD through an Alder-ene reaction.*

Approach B

As indicated above, the use of a Δ^6-dhCer as Des1 substrate would be a reasonable alternative to monitor the enzyme activity if the resulting $\Delta^{4,6}$-diene were reactive in a Diels Alder type reaction with a suitable dienophile.

The optimization of the Diels Alder reaction was carried out with model diene **RBM8-216** (Fig. 2.2). This diene presents the $\Delta^{4,6}$-(*E,Z*) configuration of the expected Des1 reaction product (*see* Section 2.3 for a complete discussion about the required configuration for this diene).

Concerning the dienophile, it is known that maleimides are suitable partners for Diels Alder reaction.[93,94] In addition, some of them, bearing a fluorescent tag, are commercially available and suitable for "click chemistry" processes,[95] despite they are not as reactive as TADs against dienes.[71]

The results of the Diels Alder reaction between **RBM8-216** and two model dienophiles are collected in Table 2.21. Initially, the reaction was carried out with *N*-phenylmaleimide (entry 1) as dienophile, but no coupling adduct was observed, unreacted starting materials being isolated instead. This result is in agreement with the sluggish reactivity of internal dienes in Diels Alder reactions under non-forcing conditions.

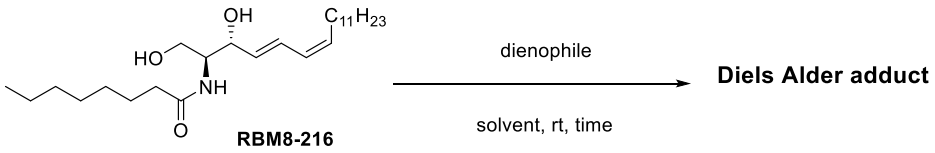

Figure 2.2. *General scheme of the evaluation of Diels Alder reaction with PTAD and maleimide derivatives. Results are summarized in Table 2.21.*

Table 2.21. Reactivity of RBM8-216 with some comercially dienophiles.

Entry	Dienophile	Solvent	Time (h)	Yield (%)	Diels Alder adduct
1	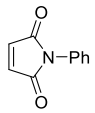	DMSO	3	–	–
2	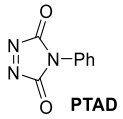 **PTAD**	THF/CH_2Cl_2	16	50	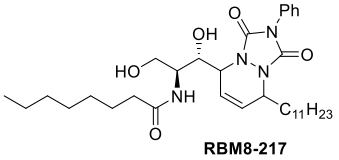 **RBM8-217**

Reaction of the (*E,Z*)-$\Delta^{4,6}$-diene **RBM8-216** with the commercially available PTAD was also considered (entry 2). The reaction was carried out in solution using 5 equiv. of PTAD in CH_2Cl_2/THF (1:1). Gratifyingly, a single Diels Alder adduct was isolated in quantitative yield after 16 hours at room temperature.

In light on these preliminary results, we considered the Diels Alder reaction between a $\Delta^{4,6}$-Cer and a TADs as the strategy of choice for the development of a Des1 assay.

2.2. Synthesis of chemical probes to monitor Des1 activity

Stimulated by the above results, we next focused our attention on the synthesis of Δ^{6}-dhCer analogues to determine their suitability as Des1 substrates able to give rise to the corresponding $\Delta^{4,6}$-Cer products. Although our main goal was to perform the enzymatic reaction on a solid-supported substrate, we first carried out the enzymatic assay in solution to verify the suitability of the Δ^{6}-dhCer as Des1 substrate.

Among the available Des1 assays, the use of dhCerC_6NBD as a fluorescent Des1 substrate[39,67] has been routinely used in our group. The assay is based on the conversion of dhCerC_6NBD into CerC_6NBD (Fig. 2.3), which can be quantified by HPLC coupled to a fluorescence detector (HPLC-FD).

Examples showing that both *Z* [96–98] and *E*-monoenoic fatty acids[99–101] are accepted by acyl-CoA desaturases to produce conjugated dienes by introduction of an additional double bond at the vicinal position have been reported in the literature. To assess the stereoselectivity of Des1 in the desaturation of our required non-natural Δ^{6}-dhCer monoenes, compounds **RBM8-029** and **RBM8-126** were synthesized, together with the isomeric dienes **RBM8-053** and **RBM8-138**, the expected Des1 reaction products, which were used as analytical standards (Fig. 2.3). These compounds bear the C_6NBD moiety essential to monitor Des1 activity from cell lysates by HPLC-FD. In addition, the *N*-octanoyl isomeric *E*- and *Z*-monoene Δ^{6}-dhCer (**RBM2-085** and **RBM8-202**, respectively) were also synthesized to study their activity as Des1 substrates in intact cells (Fig. 2.3). This also required the synthesis of the expected (*E,E*)-$\Delta^{4,6}$-Cer and (*E,Z*)-$\Delta^{4,6}$-Cer diene products (**RBM2-076** and **RBM8-216**, respectively) as analytical standards for UPLC-TOF analysis of the lipid extracts (*see* Section 2.3.3).

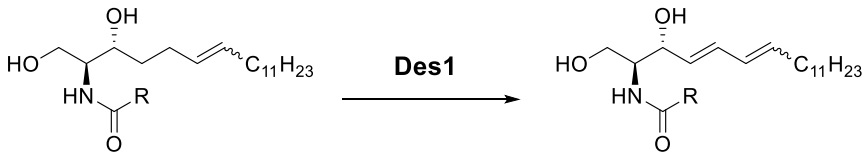

6,7-dehydro- **dhCerC$_6$NBD**	R=R$_1$	(*4E*, 6,7-dehydro)-**CerC$_6$NBD**	R=R$_1$
6*E*- **RBM8-029**	R=R$_1$	4*E*,6*E*- **RBM8-053**	R=R$_1$
6*Z*- **RBM8-126**	R=R$_1$	4*E*,6*Z*- **RBM8-138**	R=R$_1$
6*E*- **RBM2-085**	R=R$_2$	4*E*,6*E*- **RBM2-076**	R=R$_2$
6*Z*- **RBM8-202**	R=R$_2$	4*E*,6*Z*- **RBM8-216**	R=R$_2$

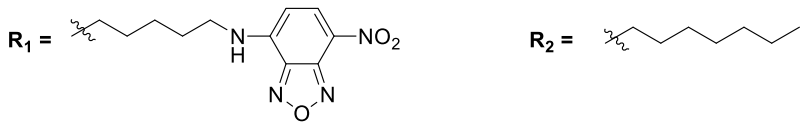

Figure 2.3. *DhCer analogues and Cer analogues to perform the enzymatic reaction in solution by HPLC-FD or as analytical standards for UPLC-TOF analysis.*

2.2.1. Synthesis of Δ^6-monoenes

2.2.1.1. Synthesis of (*E*)-Δ^6-Cer RBM8-029 and RBM2-085

The synthesis of the (*E*)-Δ^6-monoenes was carried out by acylation of the corresponding unsaturated sphingoid base, which was synthesized from Garner's aldehyde,[102,103] as described in Figure 2.4. The preparation of **RBM2-085** was first reported by Bittman *et al*. in 2002.[104] Unlike the reported procedure, we were interested in a more convenient and direct route for the preparation of the required Δ^6-Cer. Towards this end, we used a stereoselective cross-metathesis[105] between olefin **RBM8-009** and 1-tridecene in the presence of Grubbs catalyst, 2nd generation, as the key step (see below).

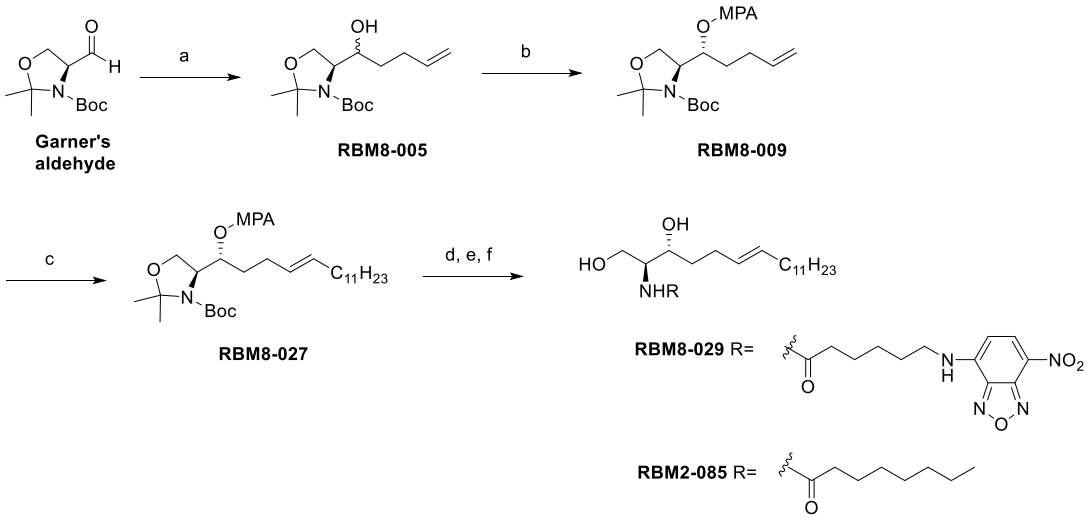

Figure 2.4. *Reagents and conditions. (a) 3-butenylmagnesium bromide, THF, 76%. (b) (R)-MPA, EDC, DMAP, CH_2Cl_2, d.r (S,S,R:S,R,R): 4/1, 57%. (c) n-tridecene, Grubbs II, d.r (E,Z): 6/1, 53%. (d) K_2CO_3, MeOH, 75%, (e) AcCl, MeOH. (f) C_6NBD acid for* ***RBM8-029*** *or n-octanoic acid for* ***RBM2-085****, HOBt, EDC, CH_2Cl_2, 32% yield in steps (e) and (f) for* ***RBM8-029*** *and 36% yield for* ***RBM2-085****.*

The synthetic route started with the addition of 4-butenylmagnesium bromide to Garner's aldehyde in THF at -78 ºC, giving an inseparable 4:1 *erythro/threo* mixture of alkenols, which could be separated after derivatization as (*R*)-MPA esters. Interestingly, this derivatization turned out to be useful not only for the configurational assignment of the new stereocenter in **RBM8-009**, following the methodology of Riguera,[106] but also to allow the chromatographic separation of the initially formed mixture of diastereomers.

The method described by Riguera and coworkers[106] relies on the derivatization of a mixture of two diastereomers, in our case (*S,R*) and (*S,S*) **RBM8-005**, with (*R*)-MPA to obtain the diastereomeric pairs (*S,R,R*) and (*S,S,R*), which could be separated by flash chromatography. Once isolated, the proton NMR signals of the two diastereomers (named F1 and F2, arbitrarily) were assigned (Table 2.5). The remarkable chemical shift differences for some key protons around C_3 are expressed as $\Delta\delta^{F1F2}$ in Table 2.5.

Table 2.5. $\Delta\delta^{RS}$ values from ^{1}H-NMR spectra for RBM8-009 diastereomers (F1 and F2)

	δH_A	δH_B	δH_C	δH_D	δH_E	δH_F	δH_G
F1	1.64	2.0	5.72	4.96	4.92	3.85	3.57
F2	1.58	1.54	5.51	4.63	4.80	3.96	3.84
$\Delta\delta^{F1F2}$	0.06	0.46	0.21	0.33	0.12	-0.11	-0.27

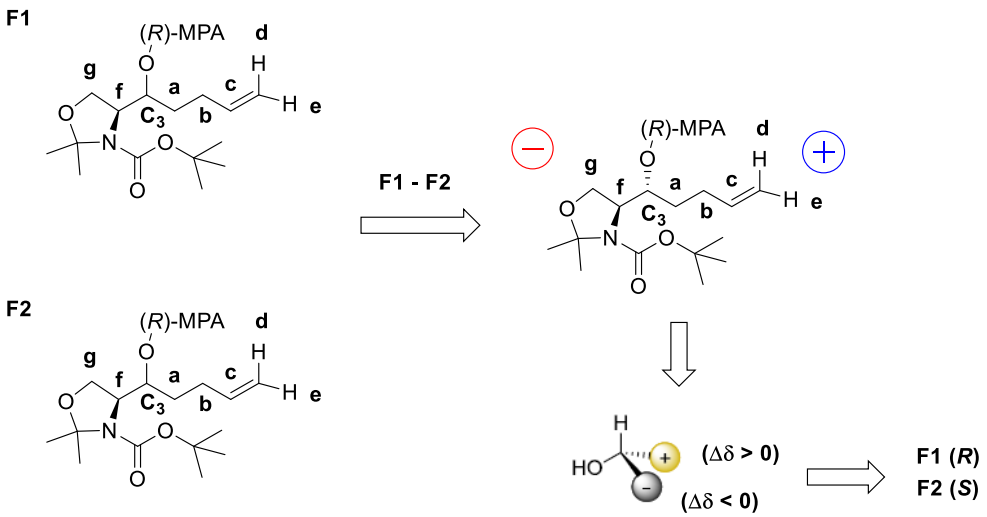

Figure 2.6. *Procedure for the assignment of the configuration of* ***RBM8-009*** *by derivatization with (R)-MPA.*

Note that $\Delta\delta^{F1F2}$ obtained were positive (+) on the right of the C_3 center and negative (-) on the left. This is the basis for the empirical rule described by Riguera for the configurational assignment of the C_3 centre of F1 as (*R*) and that of F2 as (*S*), as indicated in Figure 2.6.

Following the above reaction sequence (Fig. 2.4), the cross-metathesis of **RBM8-009** with 1-tridecene afforded **RBM8-027** as a (*E*)/(*Z*) 6:1 isomeric mixture in 53% yield. The pure (*E*) isomer could be separated in the course of the MPA removal and deprotection steps. Thus, MPA removal, followed by the simultaneous oxazolidine and *N*-Boc deprotection under acidic conditions, and *N*-acylation of the intermediate sphingoid base with octanoic acid or with C_6NBD-acid in the presence of EDC and HOBt as coupling reagents, led to Δ^6-Cer **RBM2-085** and **RBM8-029** in acceptable overall yields.

2.2.1.2. Synthesis of (*Z*)-Δ^6-Cer RBM8-126 and RBM8-202

The synthesis of the isomeric (*Z*)-Δ^6-monoene **RBM8-126** relied on a stereocontrolled Wittig reaction as the key step. The synthesis started with the diastereoselective addition[107] of the lithiated OTBS-protected propargyl alcohol **RBM8-090** to the Garner's aldehyde (Fig. 2.7), giving a *erythro*/*threo* diastereomeric ratio of 36:1. This outstanding diastereoselection can be explained by operation of the well-accepted Felkin-Anh transition state.[103] The best reaction conditions required the use of THF as solvent at low temperature (-78 ˚C) to favour the observed diastereoselectivity.[108] In a subsequent step, compound **RBM8-095** was obtained quantitatively by the complete hydrogenation of the triple bond using a Rh catalyst.

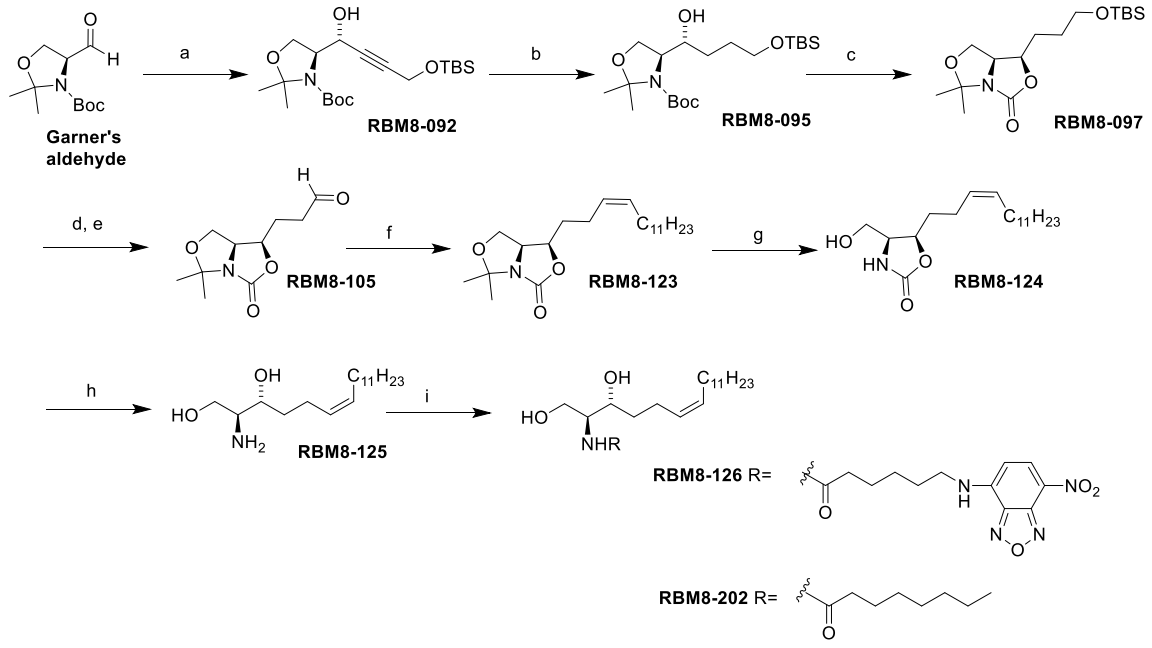

Figure 2.7. *Reagents and conditions. (a) TBS propargyl alcohol* ***RBM8-090****, BuLi, THF, -78 ˚C, d.r. (erythro/threo): 36/1, 89%. (b)* H_2*, Rh cat, MeOH, 99% (c) NaH, THF, 50 ˚C, 85%. (d) TBAF, THF, 0 ˚C to rt, 86%. (e) IBX, EtOAc, 85 ˚C, 87%. (f)* $BrPh_3PC_{12}H_{25}$*, BuLi, HMPA, THF, d.r.(E/Z):1/30, 64%. (g) pTsOH,* H_2O*, MeOH, 84%. (h) NaOH, EtOH, 103 ˚C, 70%. (i)* C_6*NBD acid for* ***RBM8-126*** *and n-octanoic acid for* ***RBM8-202****, HOBt, EDC,* CH_2Cl_2*, 80% and 87%, respectively.*

The protection of the secondary alcohol of **RBM8-095** was carried out by formation of the bicyclic oxazolo[3,4-*c*]oxazolone **RBM8-097**, arising from the intramolecular displacement of the Boc group by the transient alkoxide resulting from treatment of **RBM8-095** with NaH. Deprotection of the primary alcohol with TBAF,[109] followed by oxidation with IBX[110] led to aldehyde **RBM8-105**. A stereocontrolled Wittig reaction with a phosphonium ylide derived from *n*-dodecylphosphonium bromide afforded the (*Z*)-olefin **RBM8-123** in 64% yield in a 30:1 (*Z*)/(*E*) diastereoselectivity. The sequential hydrolysis of the isopropylidene and the oxazolidinone moieties, followed by *N*-acylation of the resulting sphingoid base **RBM8-125** with C_6NBD acid, afforded the corresponding (*Z*)-Δ^6-dhCer **RBM8-126** in good yield. Similarly, the *N*-octanoyl derivative **RBM8-202** was obtained by *N*-acylation of **RBM8-125** with *n*-octanoic acid under identical reaction conditions.

The unambiguous configuration of the (*E*) and (*Z*)-Δ^6-dhCer **RBM2-085** and **RBM8-202** will be discussed in the next section.

2.2.1.3. An integrated route for (*E*) and (*Z*)-Δ^6-monoenes

Despite both (*E*)- and (*Z*)-Δ^6-monoenes could be obtained as described in the previous sections, we tried to optimize their preparation by designing a common synthetic route to improve the overall synthetic efficiency and the diastereoselectivity of some of the key steps.

Regarding the synthesis of the (*E*)-Δ^6-dhCer's **RBM8-029** and **RBM2-085** (Fig. 2.4), the addition of 4-butenylmagnesium bromide to Garner's aldehyde took place with a modest 4:1 *erythro/threo* diastereoselectivity and the subsequent cross-metathesis with 1-tridecene led to a moderate 6:1 ratio of *E/Z* olefins **RBM8-027**. On the contrary, the synthesis of (*Z*)-Δ^6-dhCer's **RBM8-126** and **RBM8-022** (Fig. 2.7) started with the highly diastereocontrolled addition of a lithium acetylide to Garner's aldehyde to give alcohol **RBM8-092** with a remarkable 36:1 *erythro/threo* diastereoselectivity. In a subsequent step, the Wittig reaction from aldehyde **RBM8-105** was also highly diastereoselective, leading to a mixture of *Z/E* olefins in a 30/1 ratio. Last, but not least, the deprotection of the oxazolo[3,4-*c*]oxazolone system in **RBM8-123** to give the (*Z*)-Δ^6 free sphingoid base proved superior to the deprotection of the *N*-Boc oxazoline system present in **RBM8-027**, leading to the (*E*)-Δ^6 sphingoid free base (Fig. 2.4). Overall, the route designed to the (*Z*) isomers was superior in terms of diastereoselectivity to the route leading to the (*E*) isomers. This prompted us to consider aldehyde **RBM8-105** as a pivotal precursor for both (*Z*)-Δ^6 and (*E*)-Δ^6 sphingoid bases. To this end, aldehyde **RBM8-105** was first transformed into olefin **RBM8-139** by methylenation with triphenylphosphonium methylide (Fig. 2.8) in order to explore the potential of this terminal olefin in cross-metathesis reactions using (*E*) or (*Z*)-selective olefin metathesis catalysts.

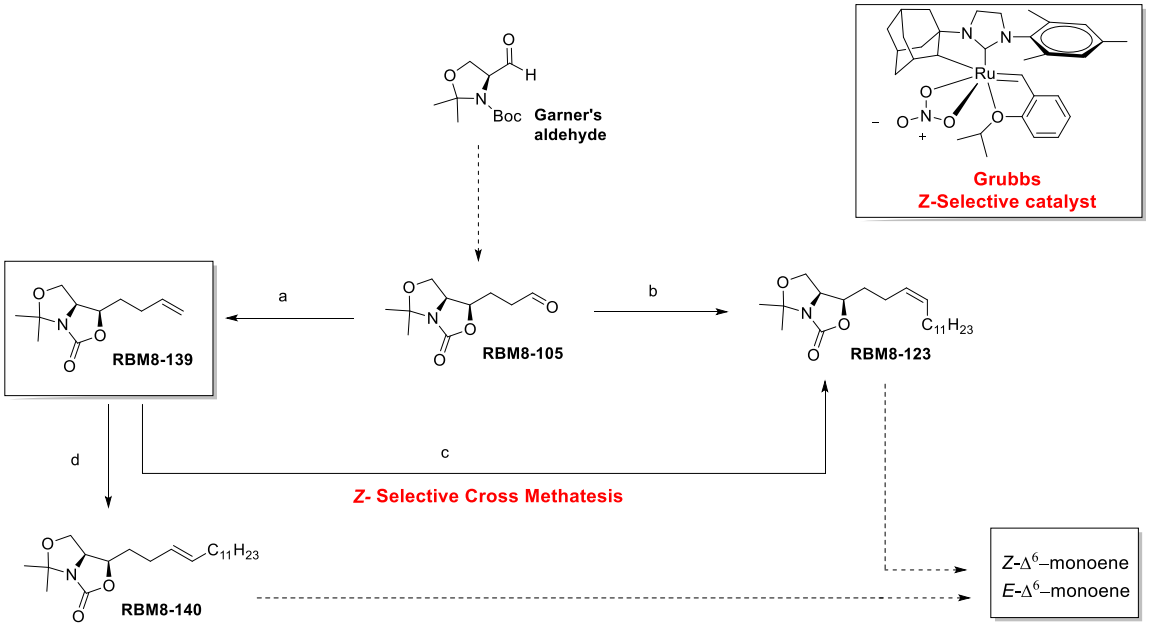

Figure 2.8. *Integrated route for (E) and (Z)-Δ^6-monoenes. Reagents and conditions. (a) $BrPh_3PCH_3$, KHDMS, THF, 0˚C to rt, 56%. (b) $BrPh_3PC_{12}H_{25}$, BuLi, HMPA, THF, d.r.(E/Z):1/30. (c) 1-tridecene, Grubbs Z-selective (Ru), CH_2Cl_2, reflux, d.r. (E/Z):1/8, 60%. (d) 1-tridecene, Grubbs II, CH_2Cl_2, reflux, d.r.(E/Z):6/1, 63%.*

First, in order to attempt a higher (*E*)-selectivity, 1-tridecene was reacted with alkene **RBM8-139** in the presence of Grubbs 2nd generation catalyst.[105] Nonetheless, despite the yield improved slightly (from 53% to 63%) in comparison with the formation of the cross metathesis adduct leading to **RBM8-027** (Fig. 2.4, Section 2.2.1.1), the (*E*:Z) ratio was similar in both cases.

On the other hand, a cross metathesis reaction with the Grubb's Z-selective ruthenium catalyst[111–113] shown in Fig. 2.8 was considered. This catalyst has been reported to give enhanced *Z*-selectivity due to its unique chelating *N*-heterocyclic carbene arquitecture.[114] The reaction proceeded at high temperature affording **RBM8-123**, albeit in a poor stereoisomeric ratio ((*E/Z*):1/8) (Fig. 2.6). This stereoselectivity is sensibly lower that that resulting from the Wittig reaction from aldehyde **RBM8-105** (*E/Z* : 1/30) leading to the same product (Fig. 2.7).

Nonetheless, although this alternative "integrated sequence" was not superior to the initially designed in terms of diastereselectivity, it was useful for the unambiguous assignment of the double bond configuration in olefins **RBM8-123** and **RBM8-140**. Thus, as indicated in Figure 2.9A, significant differences for the olefin carbons in the *E* or *Z* isomers were observed in the ^{13}C NMR spectra of the corresponding olefins. In addition, the higher *Z*-stereoselectivity of the Wittig reaction from aldehyde **RBM8-105**, in comparison with the Z-selective cross metathesis from **RBM8-139**, can be easily inferred by inspection of the corresponding ^{13}C NMR spectra (Fig. 2.9B).

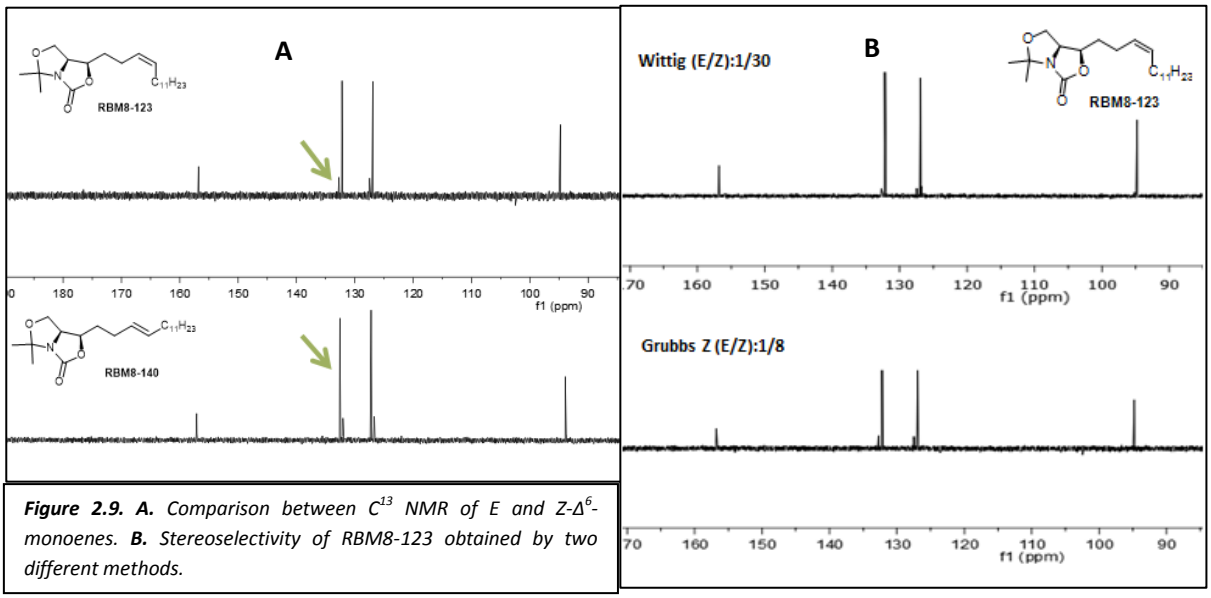

Figure 2.9. A. *Comparison between C^{13} NMR of E and Z-Δ^6-monoenes.* ***B.*** *Stereoselectivity of RBM8-123 obtained by two different methods.*

2.2.2. Synthesis of $\Delta^{4,6}$- dienes

2.2.2.1. Retrosynthetic analysis

The synthesis of Cer containing a $\Delta^{4,6}$-diene framework was initially envisaged by a convergent route leading to a 6,4-enyne in which the generation of the (*E*)-Δ^{4}-stereochemistry relied on the diastereoselective reduction of a the C4-triple bond, as depicted in Figure 2.10.

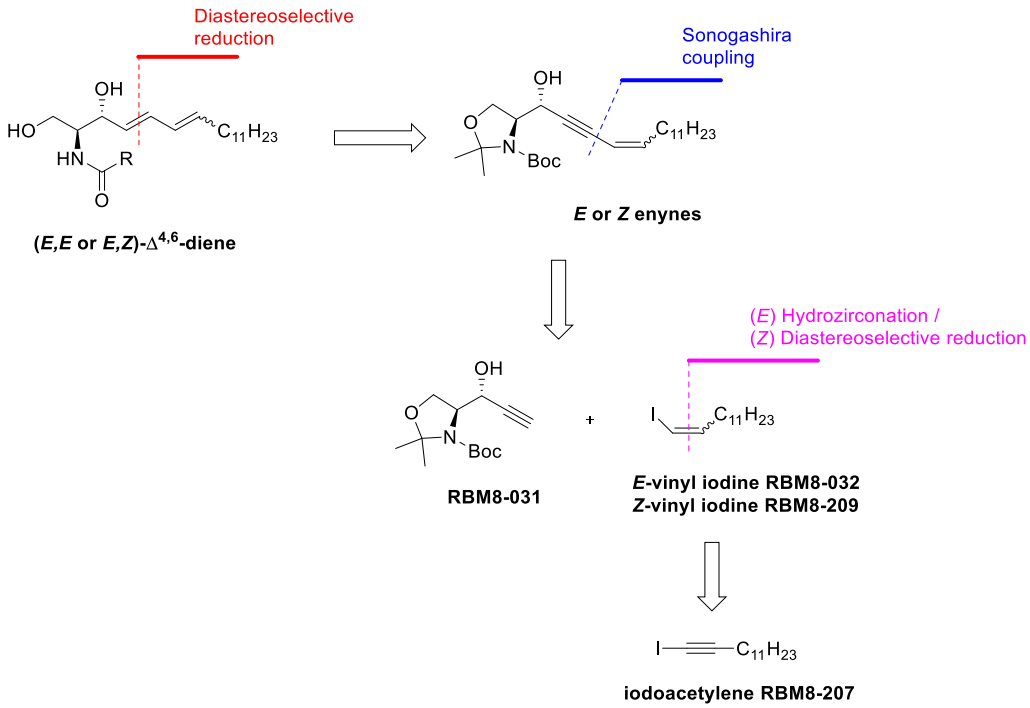

Figure 2.10. *Retrosynthetic analysis for the synthesis of $\Delta^{4,6}$-Cer.*

For the construction of the sp-sp^2 C_5-C_6 bond we considered the assembly of the acetylide **RBM8-031** with a suitable (*E*) or (*Z*)-1-vinyl iodide by a Sonogashira cross coupling.[115–117] The configuration of the Δ^{6}-double bond would be given by that of the starting vinyl iodide. Thus, the required (*E*)-vinyl iodide **RBM8-032** was obtained by hydrozirconation of the starting iodoacetylene **RBM8-207** using Schwartz's reagent,[118] whereas diimide reduction[119] of the same iodoacetylene led to the (*Z*)-vinyl iodide **RBM8-209**.

2.2.3.1. Synthesis of (*E,E*) and (*E,Z*)-$\Delta^{4,6}$-Cer RBM8-053 and RBM8-138

According to the above retrosynthetic analysis (Fig. 2.10), the acetylide **RBM8-031** was the common building block for the Sonogashira couplings required for the construction of the (*E,E*) and (*E,Z*)-$\Delta^{4,6}$-Cer skeletons. The preparation of this building block has been reported in the literature.[120] Thus, lithiated ethynyltrimethylsilane was added to Garner's aldehyde at -78 ºC in THF and HMPA as co-solvent (Fig. 2.11). The addition of cation-complexing agents, such as HMPA, resulted in an increased *erythro* selectivity by preventing an alternative chelating transition state leading to a *threo* adduct.[103,121] The subsequent desilylation of the resulting alkynol in methanolic K_2CO_3 gave the deprotected terminal alkyne **RBM8-031** in 73% yield in two steps and high diastereoselectivity.

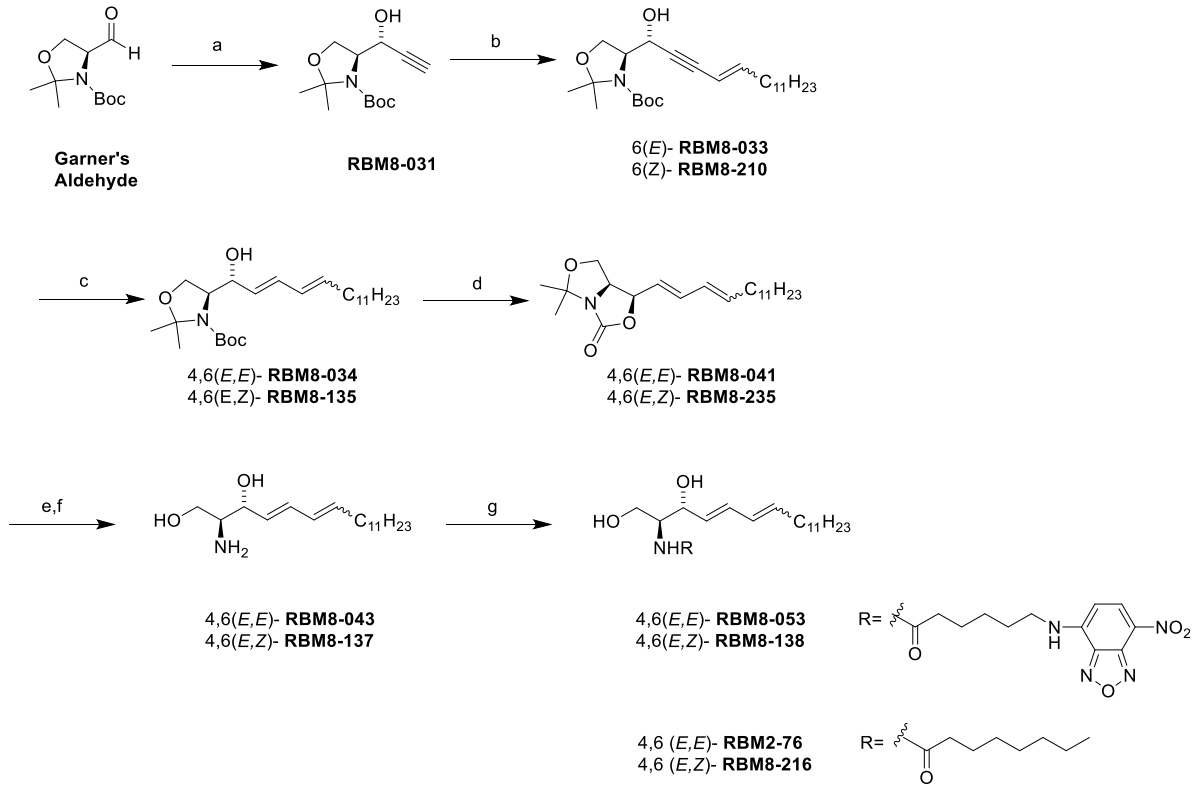

Figure 2.11. *Reagents and conditions. (a) 1. ethynyl-TMS, BuLi, HMPA, THF, 2. K_2CO_3, MeOH, 73% in two steps. (b) (E) or (Z)-iodotridecene (**RBM8-032** or **RBM8-209**), Pd(PPh$_3$)$_4$, CuI, piperidine, (E) 42% and (Z) 72%. (c) Red-Al, THF, 0˚C, (E,E) 85% and (E,Z) 95% (d) NaH, THF, 50˚C, (E,E) 70% and (E,Z) 80% (e) pTsOH, MeOH, (E,E) 82% and (E,Z) 85%. (f) NaOH, EtOH, reflux, (E,E) 82% and (E,Z) 98%. (g) C_6NBD acid for **RBM8-053** and **RBM8-138**, n-octanoic acid for **RBM2-076** and **RBM8-216**, HOBt, EDC, CH_2Cl_2.*

The synthesis of the enynes **RBM8-033** and **RBM8-210** by Sonogashira cross coupling,[115] required the long-chain (*E*) and (*Z*)-vinyl iodides **RBM8-032** and **RBM8-209**, respectively (Figs. 2.10 and 2.12). Hydrozirconation of the commercially available 1-tridecyne using Schwartz's reagent,[118] followed by iodination, afforded the (*E*)-vinyl iodide **RBM8-032** in high yield and total stereoselectivity. On the other hand, the synthesis of the (*Z*)-vinyl iodide **RBM8-209** was carried out by reduction of iodotridecyne[122,123] with potassium azodicarboxylate[119,122,124] and acetic acid. The treatment of potassium azodicarboxylate with a carboxylic acid in protic or

aprotic organic solvent results in the ultimate formation of diimide, which is a very useful reagent for the mild reduction of C–C π-systems.[125] The use of potassium azodicarboxylate as a source of diimide is particularly useful for the *syn* reduction of alkynyl halides, as it is required in our case (Fig. 2.12).

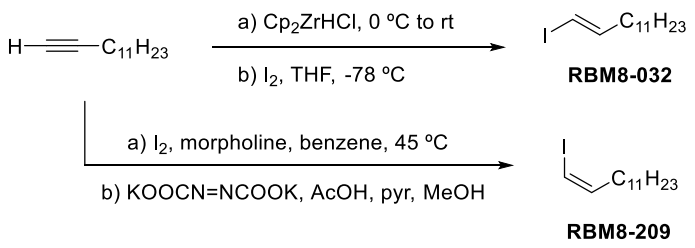

Figure 2.12. *Preparation of E and Z-vinyl iodide* ***RBM8-032*** *and* ***RBM8-209****, respectively.*

With the corresponding building blocks for the Sonogashira coupling in hand, the palladium-catalyzed sp^2-sp coupling between (*E*) or (*Z*)-alkenyl halides **RBM8-032** and **RBM8-209**, respectively, and the terminal alkyne **RBM8-031** was attempted. The process proceeded in good yields (42 and 72%, respectively) under the standard reaction conditions (catalyzed with $Pd(PPh_3)_4$ in combination with copper (I) salt).[117] This Pd-catalyzed cross-coupling reaction represents a facile access to alkynyl vinyl iodides and sets the stage for the partial reduction of the enyne moiety to obtain the required diene sphingoid bases. Thus, the above enynes **RBM8-033** and **RBM8-210** (Fig. 2.11) were stereoselectively reduced with Red-Al[96] (sodium bis(2-methoxyethoxy)aluminum hydride) to the corresponding conjugated (*E,E*) and (*E,Z*) **RBM8-034** and **RBM8-135** dienes, respectively. This process is known to reduce propargylic alcohols to the corresponding allylic alcohols with practically exclusive *trans*-selectivity.[126]

The mechanism of aluminium hydride reductions involves a *trans*-hydroalumination, promoted by the initial coordination of Al to the propargylic hydroxyl group, followed by an external hydride attack leading to a transient cyclic intermediate, whose subsequent hydrolysis leads to the final allylic alcohol (Fig. 2.13).

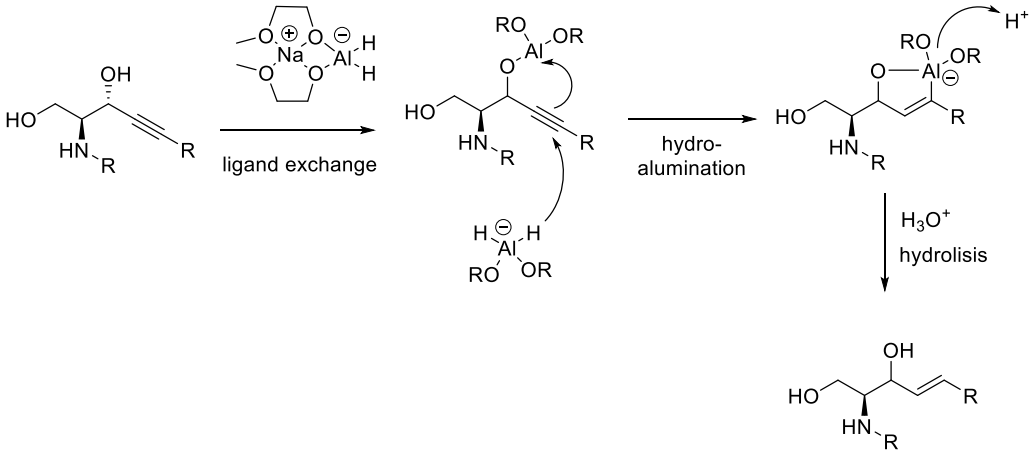

Figure 2.13*. Mechanism of Red-Al reduction of a propargylic alcohol to the corresponding E-allylic alcohol.*

In light of the sensitivity of dienes **RBM8-034** and **RBM8-135** towards the acidic conditions initially tried for the simultaneous *N*-Boc and isopropylidene removal, a sequential two step deprotection, via oxazolidinones **RBM8-041** (for *E,E*) and **RBM8-235** (for *E,Z*) were considered (Fig. 2.11). Gratifyingly, $\Delta^{4,6}$-diene (*E,E*)-**RBM8-043** and (*E,Z*)-**RBM8-137** were readily obtained by this approach. Finally, the target fluorescent Cer analogues **RBM8-053** and **RBM8-138**, as well as the *N*-octanoyl derivatives **RBM2-076** and **RBM8-216**, were obtained by *N*-acylation of the corresponding sphingoid bases with C_6NBD or *n*-octanoic acid, respectively, using HOBt, EDC as coupling partners.

2.3. Validation of the chemical probes

2.3.1. Evaluation of Des1 activity using RBM8-029 and RBM8-126 as substrates

The ability of (*E*) and (*Z*)-Δ^6-dhCer as Des1 substrates was initially tested with the fluorescent C_6NBD probes **RBM8-029** and **RBM8-126** (Fig. 2.4 and 2.7), respectively in HGC 27 cell lysates in the presence of NADH as enzyme cofactor. The conversion of these probes into the corresponding dienes **RBM8-053** [(*E,E*)-$\Delta^{4,6}$] and **RBM8-138** [(*E,Z*)-$\Delta^{4,6}$] was monitored by HPLC-FD, following an optimized protocol developed in our group.[67,127]

As shown in Figure 2.14, HPLC-FD analysis evidenced that the (*E*)-Δ^6-monoene **RBM8-029** afforded the (*E*,*E*)-$\Delta^{4,6}$-diene **RBM8-053**, as concluded by comparison with the synthetic diene standard, although at very low conversion rates. In contrast, incubations using the (*Z*)-Δ^6-monoene **RBM8-126** afforded the corresponding (*E*,*Z*)-$\Delta^{4,6}$-diene **RBM8-138** at similar levels to those observed in a positive control of Des1 activity using dhCerC_6NBD as substrate.[67] As above, the resulting diene was identified by comparison with the synthetic standard.

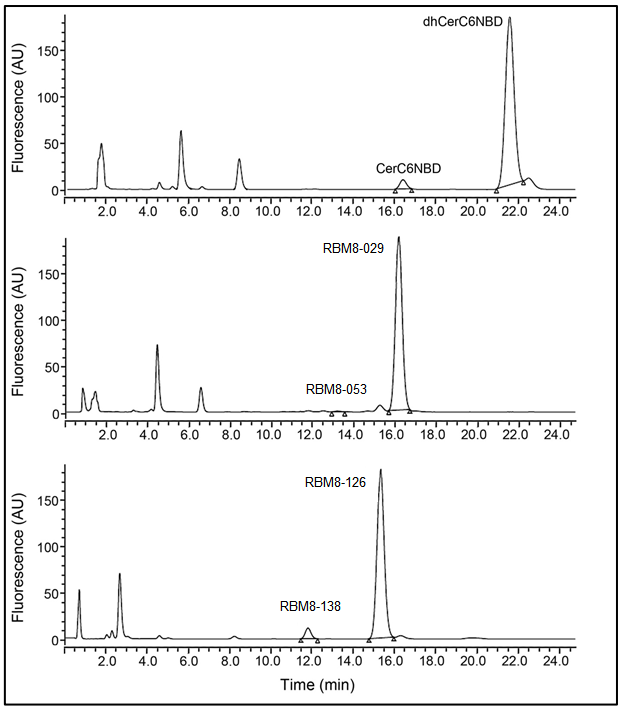

Figure 2.14. *Representative HPLC-FD profiles of fluorescent substrates and products detected in cell lysates incubated with* ***RBM8-029****,* ***RBM8-126*** *and dhCerC$_6$NBD (positive control of Des1 activity).*

These results indicated that the (*Z*)-Δ^6-monoene **RBM8-126** behaves as Des1 substrate, while the *E*-isomer **RBM8-029** is not a Des1 substrate.

2.3.2. Kinetic studies of substrate RBM8-126

To determine the kinetic parameters of **RBM8-126** as Des1 substrate, a plot of substrate concentrations *vs* conversion was constructed, as shown in Figure 2.15.

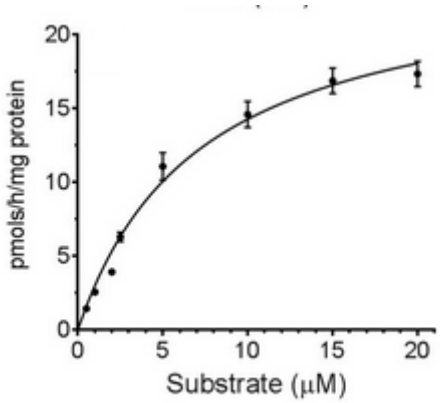

Figure 2.15. *Effect of* ***RBM8-126*** *at different concentrations on Des1 activity (mean ± SD from two experiments with triplicates).*

Kinetic analysis indicated that **RBM8-126** was desaturated with $K_{m(app)}$ and $V_{max(app)}$ values of 7.6 (±1.0) µM and 23.03 (±1.5) pmol/h/mg, respectively. These constants are similar to those of the saturated analogue, dhCerC$_6$NBD ($K_{m(app)}$= 7.7 µM; $V_{max(app)}$= 19.3 pmol/h/mg).[128]

2.3.3. Effects of RBM2-085 and RBM8-202 on the sphingolipidome

This Section was performed by Yadira Ordoñez (Doctoral Thesis, University of Barcelona, 2016) and the results are collected in the following publication: Ana Pou *et al.*, *Chem. Commun.*, **2017**, *53*, 4394-4397.

To further confirm that the (*Z*)-Δ^6-monoene was a good Des1 substrate, intact glioblastoma T98G and U87MG cells were incubated with the *N*-octanoyl derivatives of the *Z* and *E*-Δ^6-monoenes **RBM2-085** and **RBM8-202**, respectively. Cell viability assays at 24 h in both cell lines were first determined by the MTT test.[129]

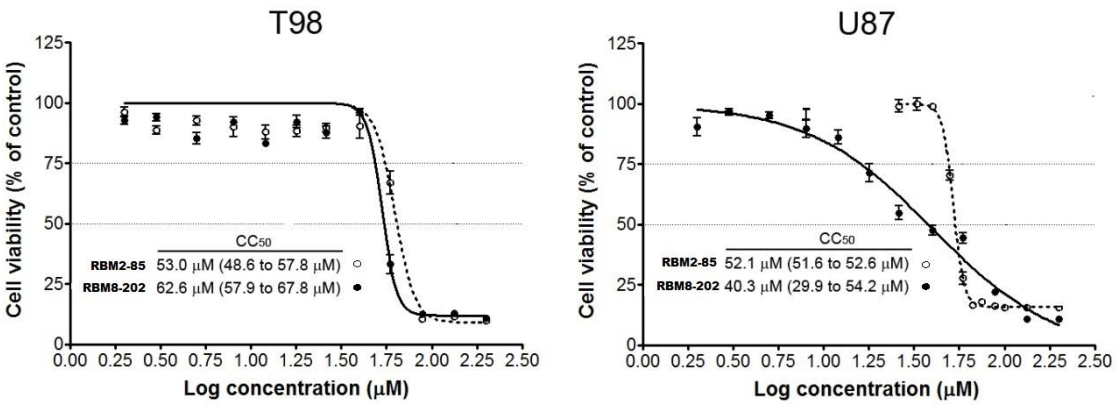

Figure 2.16. *Effect of compounds **RBM2-085** and **RBM8-202** on cell viability. Data correspond to the average ± SD of three independent experiments with triplicates.*

Curve fitting with the sigmoidal dose-response (variable slope) equation afforded the CC_{50} values indicated in Figure 2.16, with 95% confidence intervals.

The effect of the *N*-octanoyl Δ^6-Cer **RBM2-085** and **RBM8-202** on the sphingolipidome was also evaluated after incubation of intact T98 and U87 cells with the target compounds at 10 µM (concentration not affecting cell viability) for 2 and 24 h, and compared with a control experiment (EtOH treatment). Lipids were extracted and processed for UPLC-TOF MS analysis. The results showed that **RBM2-085** and **RBM8-202** were converted into the corresponding diene Cer **RBM2-076** and **RBM8-216**, respectively, which were further metabolized at C1-OH to afford the sphingomyelin analogues (phosphocholine derivatives: PC) (Fig. 2.17A), with negligible levels of glycosylated derivatives.

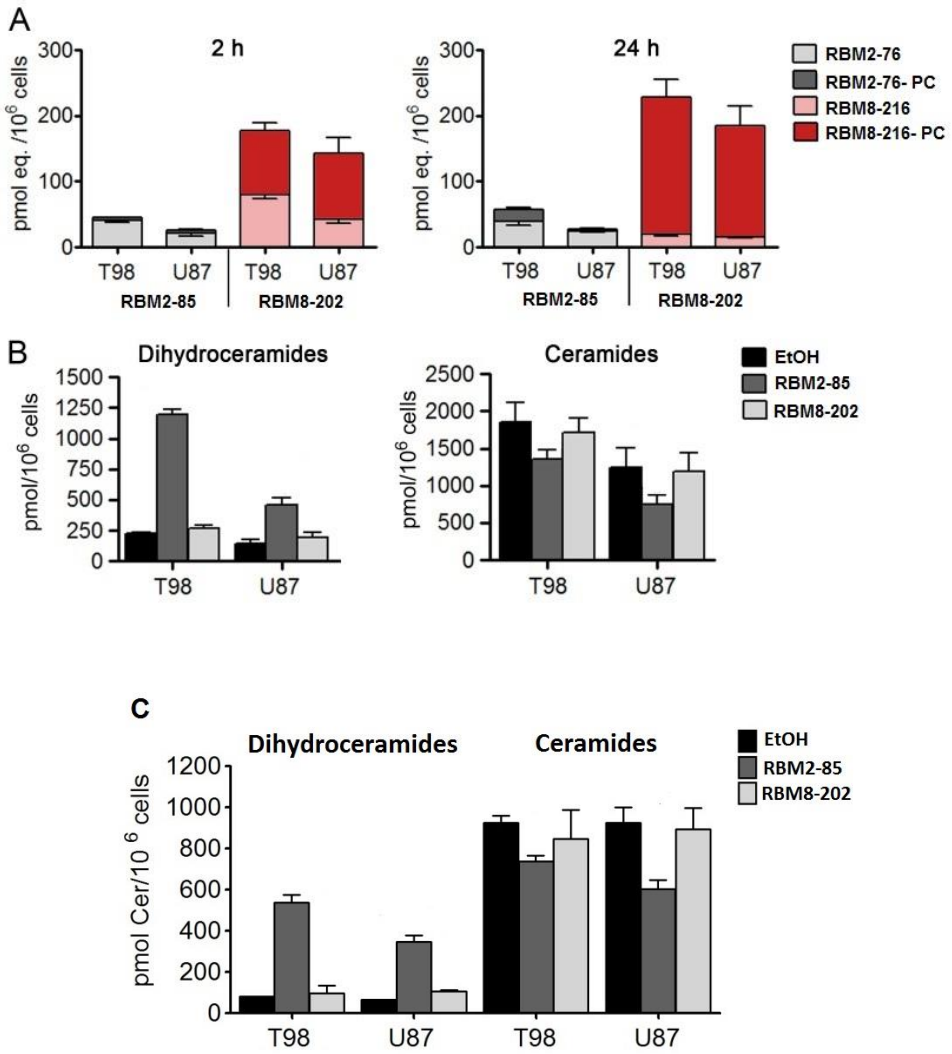

Figure 2.17. *Des1 activity in the presence of compounds* ***RBM2-085*** *and* ***RBM8-202****.* ***A****. Amounts of diene Cer and SM analogues formed from* ***RBM2-085*** *and* ***RBM8-202****. Assignment details are given in Table 5.1 of the Experimental Section.* ***RBM2-076-PC*** *and* ***RBM8-216-PC*** *are the phosphocholine derivatives of* ***RBM2-085*** *and* ***RBM8-202****, respectively.* ***B.*** *Effect of 2 h treatment with* ***RBM2-085*** *and* ***RBM8-202*** *on production of natural dhCers and Cers.* ***C.*** *Effect of 24 h treatment with* ***RBM2-085*** *and* ***RBM8-202*** *on production of natural dhCers and Cers. In* ***A****,* ***B*** *and* ***C,*** *analyses were conducted by UPLC-TOF MS in extracts of cells treated with or without the compounds for the times shown. Results are means ± SD of two independent experiments with triplicates and are normalized with respect to the number of cells extracted.*

Interestingly, analysis of SL composition after treatments showed that **RBM2-085**, but not **RBM8-202**, caused a 3 to 5-fold increase in dhCer levels, which was already evident 2 h after the treatment (Fig. 2.17B) and remained even after 24 h (Fig. 2.17C). These results suggested that the *E* isomer (**RBM2-085**), but not the *Z* isomer (**RBM8-202**) Δ^6-monoene dhCer inhibited Des1. Although dhCer accumulation at 2 h suggests a stronger inhibition of Des1 in T98 cells than in U87 cells, this apparent discrepancy can be explained by considering that the levels of remaining Cer are also higher in T98 than in U87 cells (Fig. 2.17B), which results in similar dhCer/Cer ratios in the presence of **RBM2-085** (T98, 1.2 ± 0.05; U87, 0.84 ± 0.12)

2.3.4. Determination of kinetic parameters for RBM2-085 as Des1 inhibitor

To confirm Des1 inhibition by **RBM2-085**, the *in vitro* Des1 assay was performed incubating cell lysates with dhCerC_6NBD (10 µM) as substrate in the presence of different concentrations of **RBM2-085** (*see* Experimental Section). Concentration-activity determinations showed that **RBM2-085** inhibited Des1 with an IC_{50} value of 155.4 nM (Fig. 2.18).

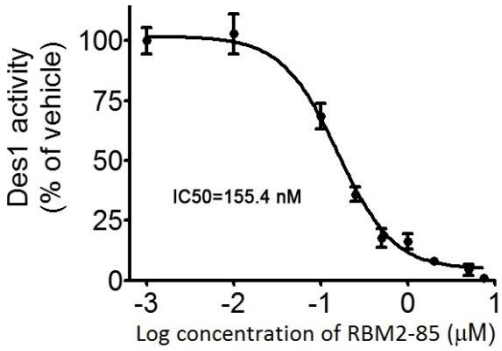

Figure 2.18. *Response effect of* ***RBM2-085*** *on Des1 activity.HGC 27 cell lysates were incubated with* ***RBM2-085*** *as described in the Experimental Section. Data correspond to the average ± SD of three independent experiments with triplicates.*

The kinetic parameters of **RBM2-085** as a Des1 inhibitor were next investigated. To this end, cell lysates were incubated with various amounts of the compound and different substrate concentrations (dhCerC_6NBD) for 4 h. The results showed a concentration-dependent inhibition at all concentrations. Moreover, while $K_{m(app)}$ did not change, $V_{max(app)}$ decreased with increasing concentrations of **RBM2-085** (Fig. 2.19A), which is indicative of non-competitive type of inhibition. By plotting the reciprocal of $V_{max(app)}$ (obtained from the Lineweaver-Burk representation at different inhibitor concentrations) *vs* the inhibitor concentrations, a *K*i of 111.4 nM was calculated for **RBM2-085** (Fig. 2.19B).

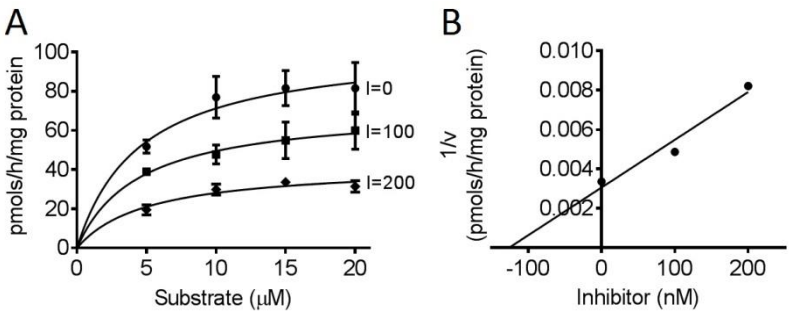

Figure 2.19. *Des1 inhibition by compound* ***RBM2-085*** *at different substrate and inhibitor concentrations. In all experiments, the amount of protein (cell lysates) was 140 µg; Results are the means ± SD of three independent experiments with triplicates.* ***B.*** *Plot of the reciprocal of $V_{max(app)}$ to inhibitor concentration. Linear regression afforded a K_i=111.4 nM (y = 30.7x10^{-5} + 0.034). All curve fittings and regression analysis were carried out in GraphPad Prism 6.*

Finally, a time-dependent inhibition assay was performed to confirm the reversibility of the inhibition. As depicted in Figure 2.20, the inhibition did not change with incubation time, which supports that **RBM2-085** is a Des1 reversible inhibitor.

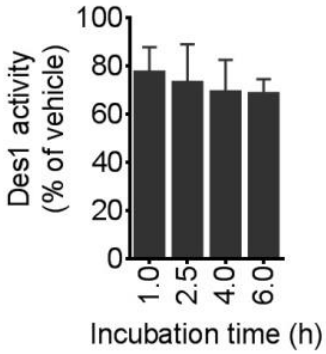

Figure 2.20. *Time-dependence of Des1 inhibition by compound* ***RBM2-085****. Substrate (dhCerC$_6$NBD) concentration was 10 µM and inhibitor concentration was 150 nM. Des1 assay was carried out as detailed in the experimental section. Results are the means ± SD of two independent experiments with triplicates*

In the light of these results, we can conclude that compound **RBM2-085** has an affinity around 18 times higher than **XM462**, a mixed type Des1 inhibitor (K_i = 2 µM).[130] However, the potency of compound **RBM2-085** is about 3-5-fold lower than that of GT11, a competitive Des1 inhibitor,[54] which afforded an IC_{50} value of 52 nM in the above Des1 assay and a calculated K_i value of 22 nM, using the web-based tool reported by Cer *et al.* for a competitive inhibitor.[131]

The IC_{50} value for XM462 as Des1 inhibitor using HGC27 cell lysates is similar to that previously obtained with rat liver microsomes[130]. However, IC_{50} and K_i values of 20 µM and 6 µM, respectively, for GT11 were previously found using *N*-octanoyldihydrosphingosine at 50 µM as substrate.[54] With the substrate used here (dhCerC$_6$NBD at 10 µM), taking into account that Des1 has similar affinities for both substrates (*N*-octanoyldihydrosphingosine: ($K_{m(app)}$ = 5 µM[54], dhCerC$_6$NBD: $K_{m(app)}$ = 7.7 µM),[130] and considering that GT11 is a Des1 competitive inhibitor, the difference in IC_{50} is explained in terms of the different substrate concentrations used in both experiments.

3. DESIGN OF A HTS ASSAY TO MONITOR DES1 ACTIVITY ON SOLID SUPPORT

3. DESIGN OF A HTS ASSAY TO MONITOR DES1 ACTIVITY ON SOLID SUPPORT

3.1. Small molecule microarrays

Microarrays are miniaturized assemblies of molecules organized across a planar surface. The physical location of each spot on the array encodes its identity. Anywhere from the hundreds to tens of thousands of samples may be densely populated on planar surfaces, typically glass slides, and the spectrum of applications is determined by the nature and class of the immobilized molecules.[132]

Small Molecule Microarrays (SMMs), also called chemical microarrays, were introduced around a decade ago and, within a short space of time, have become the next generation platform for HTS assays. DNA microarrays were the first type of arrays developed in this area, which comprise surfaces with addressed oligonucleotides.[133] As the chemistries improved, a variety of molecules, other than DNA, including proteins,[134] peptides,[135] carbohydrates,[136] and chemical libraries[137] were likewise arrayed and presented on this format.

3.1.1. Chemical microarray: a new tool for drug screening and discovery

Over the past decade, HTS has become a powerful tool for the identification of active compounds and pharmacophores against specific biological targets. At the same time, HTS synthesis of small molecules is also widely used to generate large numbers of chemicals in a short time. Thus, different HTS methods have been introduced and widely utilized. To further increase the throughput and reduce the cost of chemicals and targets, the miniaturization of biological assays has been the trend in today's assay development and laboratory automation.[138]

SMMs can rise to this challenge because of their capability to identify and evaluate small molecules as potential hits. During the past few years, the chemical microarray technology, with different surface chemistries and activation strategies, has generated many successful results in the evaluation of chemical–protein interactions, enzyme activity inhibition, target identification, signal pathway elucidation and cell-based functional analysis.[139] The success of the chemical microarray technology will provide unprecedented possibilities and capabilities for parallel functional analysis of tremendous amounts of chemical compounds.

3.1.2. Immobilization methods on solid support

Specific proteins, antibodies, small molecule compounds, peptides, and carbohydrates can be immobilized on solid surfaces to form high-density microarrays. Depending on their chemical nature, the immobilization on the solid support is accomplished by *in situ* synthesis, nonspecific adsorption, specific binding, nonspecific chemical ligation, or chemoselective ligation. These arrays of molecules can then be probed against complex analytes, such as serum, total cell extracts, and whole blood. Interactions between the analytes and the immobilized array of molecules can be evaluated with a number of different detection systems.[140]

Thus, the first step of any SMM experiment involves the design and fabrication of the chips containing the probe molecules of interest. The immobilization methods must consider both the orientation of the probe and its molecular stability. Chemical microarrays consist of arrays of organic compounds, including small organic molecules, peptides, and sugars. Based on how the chemical microarrays are constructed, they can also be categorized as "*in situ* synthesis" arrays or as "spotting" arrays. The chemistry of the *in situ* synthesis approach is more limited, particularly when photochemical reactions are required. As a result, only oligomeric molecules, such as oligonucleotides or peptides are used in this type of array. A spotting array refers to an array of compounds that have been previously synthesized and directly transferred and immobilized on the solid surface. This approach is more versatile and of wider applicability.[140] The addition of the products to the solid support is carried out by means of a device (the "spotter") capable of dispensing nanodrops forming micrometric active areas (spots).

3.1.2.1. Immobilization via physical adsorption

The first and simplest type of immobilization is through surface adsorption. This immobilization is based on electrostatic interactions. In the case of oligonucleotides, the interactions take place between the negatively charged groups of the oligonucleotide chain and the positive charges introduced on the surface. This approach is also useful for proteins, and it has been used in standard ELISA and Western blot for many years.[141] The commonly used solid supports are based on hydrophobic plastics, such as polystyrene. Slides coated with aminosilane or poly-L-lysine[142] have been used to randomly capture oligonucleotides, proteins, and cells via electrostatic interactions or by passive adsorption. Similarly, nitrocellulose has been used as a substrate for the capture of DNA, proteins, and carbohydrates.[143]

3.1.2.2. Immobilization via specific surface interaction

In addition to the immobilization via nonspecific physical adsorption, molecules can be tagged and immobilized through specific noncovalent interactions between the tag and an immobilized suitable capturing molecule. A typical example is the biotin-streptavidin system for immobilizing biotinylated proteins onto streptavidin coated surfaces.[144] Likewise, a small molecule can also be biotinylated and printed onto a surface that has been pre-coated with a monolayer of streptavidin. The adsorption of this kind of molecules is based on the formation of hydrogen bonds, electrostatic interactions, Van der Waals links and hydrophobic interactions.

3.1.2.3. Immobilization via covalent attachment

Although nonspecific physical adsorption can be used to generate a microarray of macromolecules, this approach is less useful for the preparation of small molecule or small peptide microarrays. Alternatively, immobilization *via* covalent attachment to a functional group on the solid surface can be considered. In Figure 3.1, some of the common chemistries used to generate microarrays by covalent attachments are summarized. Chemical modification of the solid surface is necessary to create functional groups for covalent immobilization and to achieve homogeneous immobilization.

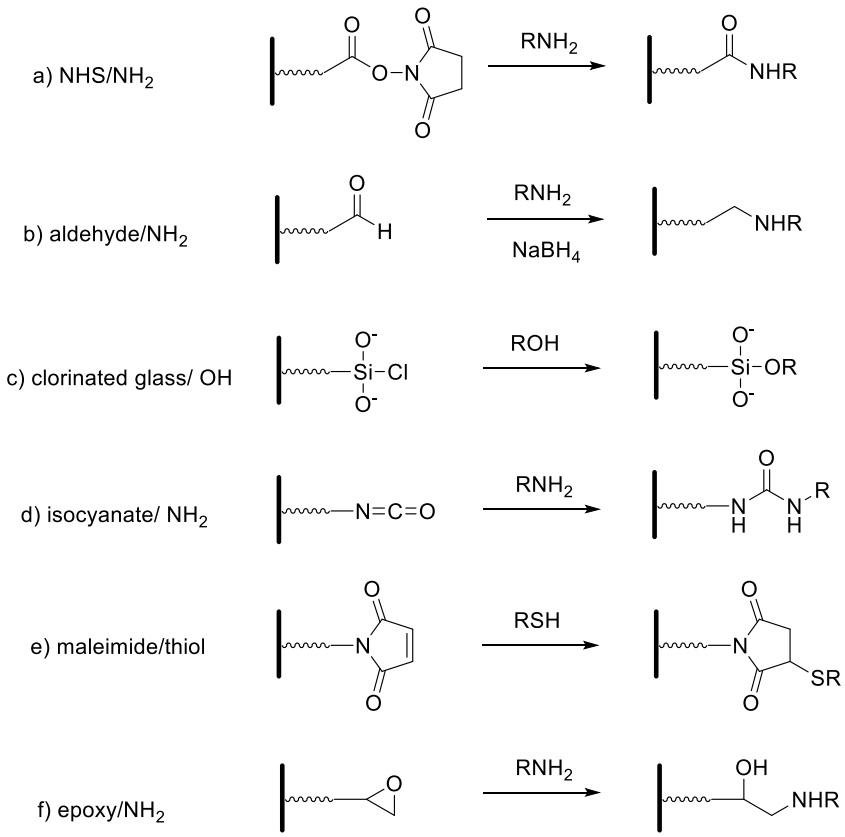

Figure 3.1. *Chemistries for covalent immobilization (non-selective ligation).*

Commercially available aldehyde-derivatized glass slides, commonly used for DNA immobilization, can also be used for protein microarrays.[145] The aldehyde groups on the glass surface react with primary amines present on the protein to form Schiff's base linkages. Furthermore, Benters *et al.* [146] have demonstrated the use of succinimidyl ester or isocyanate functionalized dendrimers on a solid surface for nucleic acid and protein microarrays.

Immobilization of small molecules or short peptides often requires the covalent linkage of the compounds onto the solid support. Michael addition has been used by Schreiber's group to ligate thiol-containing compounds to maleimide-derivatized glass slides to form a microarray of small molecules.[147]

3.1.3. Click Chemistry in Microarrays

3.1.3.1. Azide-alkyne cycloaddition

The azide group is a 1,3-dipole that shares four electrons in a π-system over three centres. It also presents a linear geometry and can undergo reaction with dipolarophiles, such as activated alkynes.[148] These π-systems are both uncommon and inert in biological systems, further enhancing the bioorthogonality of the azide group. The [3+2] cycloaddition between azides and terminal alkynes, to provide stable triazole adducts, was first described by Huisgen in 1963.[149] The reaction is thermodynamically favourable by a 30-35 kcal/mol. Without alkyne activation, however, the reaction requires elevated temperatures or pressures that are not compatible with living systems (Fig. 3.2).

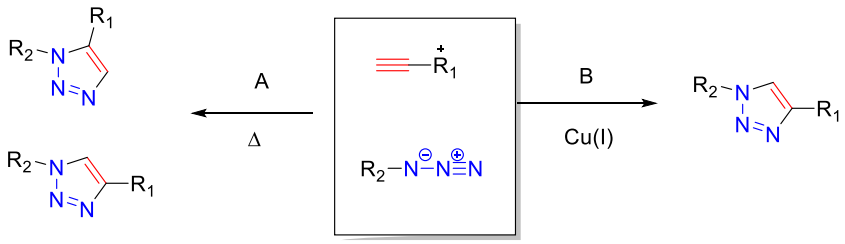

***Figure 3.2. A**. The thermal cycloaddition of alkynes with azides requires elevated temperatures and affords mixtures of the two possible regioisomers. **B.** The copper-catalyzed reaction leads to the 1,4-disubstituted regioisomers at room temperature in high yields.*

One possibility to achieve alkyne activation involves the use of a metal catalyst. In this context, ruthenium and copper have been used to accelerate these types of cycloadditions. In this section, we will focus on copper-catalyzed azide-alkyne cycloadditions (CuAAC) and strain-promoted azide-alkyne cycloadditions (SPAAC), being the last one another kind of cycloaddition where the catalyst is not required.

3.1.3.1.1. Copper-catalyzed [3+2] azide-alkyne cyloaddition (CuAAC)

The copper-catalyzed azide-alkyne cycloaddition (CuAAC) has become the paradigm of the term "click chemistry" coined by Sharpless in 2002.[150] The reaction is an improved version of the Huisgen's [3 + 2] cycloaddition, with little solvent dependence and better compliance to the principles of click chemistry.[151] The presence of copper increases the reaction rates and yields, allowing the processes to be carried out at room temperature or below. However, there is a severe restriction that should not be ignored: the free Cu (I) ions are toxic to living systems. Sodium ascorbate was often used to reduce Cu(II) to the Cu (I) oxidation state, but the Cu/ascorbate system may generate variable amounts of reactive oxygen species (ROS). Some Cu (I)-stabilizing ligands were developed to further accelerate the reaction, such as the C_3-symmetric derivatives (TBTA),[152] or tris (3-hydroxypropyl-triazolylmethyl) amine (THPTA) (Fig. 3.3).[153]

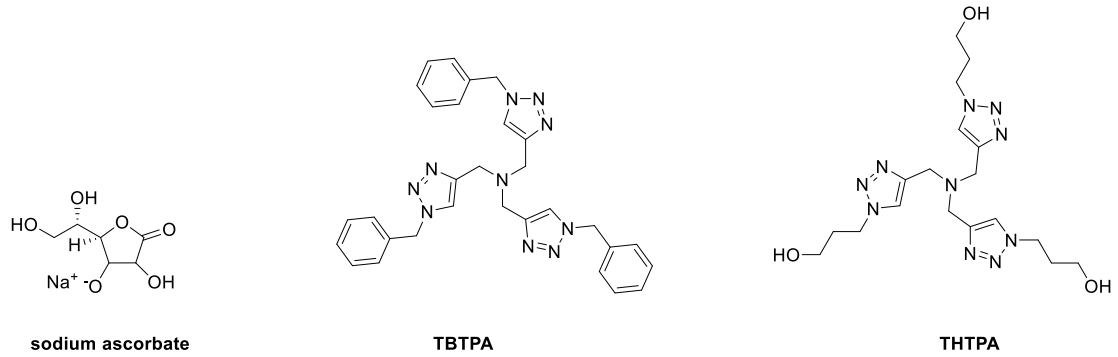

Figure 3.3. *Chemical structures of common additives used in the CuAAC.*

3.1.3.1.2. Strain-promoted azide-alkyne cycloaddition (SPAAC)

As mentioned previously, exogenous metals can have cytotoxic effects in cells. As a result, they can disturb the homestasis of the biological systems under study.[154] In this context, the development of bioorthogonal reactions, based on processes lacking an exogenous metal catalyst, has been crucial in chemical biology.

To activate the alkyne component for the direct [3+2] cycloaddition with azides, the use of ring strain as a way to overcome the sluggish reactivity of the alkynes has been explored. Thus, in 1961, Wittig and Krebs demonstrated for the first time that cyclooctyne, the smallest stable cycloalkyne, reacts with azides to form the corresponding 1,2,3-triazole.[155] The massive bond angle deformation of the alkyne (around 160°) accounts for nearly 18 kcal/mol of ring strain (Fig. 3.4). This destabilization of the ground state *versus* the transition state of the reaction provides a dramatic rate acceleration compared to unstrained alkynes. In contrast to CuAAC, the cycloaddition with cyclooctynes affords a 1:1 mixture of regioisomeric 1,2,3-triazoles. This process is known as "strain promoted alkyne-azide cycloaddition (SPAAC)", due to the requirement of the ring strain in the cyclooctyne system for the click reaction to take place.

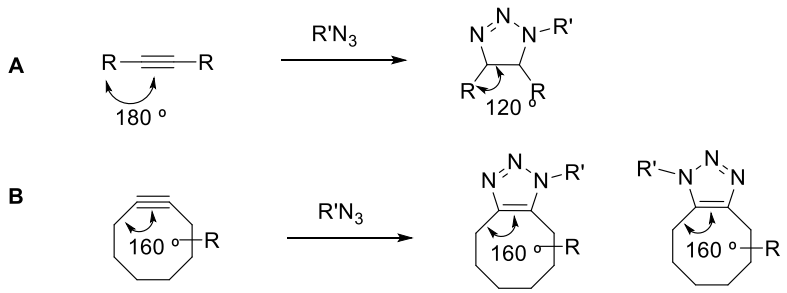

Figure 3.4. *1,3-Dipolar cycloadditions between azides and alkynes.* ***A.*** *Cycloaddition involving azides and linear alkynes.* ***B.*** *Cu-free, strain-promoted cycloaddition between azides and cyclooctynes.*

Several strain-promoted systems, such as oxanorbornadienes, cyclooctynes, and dibenzocyclooctynes (Fig. 3.5) have recently been developed for the fast and selective reaction with azide-containing biomolecules and have found application in tumour imaging, glycan labelling, *in vivo* imaging, and surface modification,[156] among others. Inspired by the dibenzocyclooctyne derivative DIBC (structure **D** in Fig. 3.5) developed by Boons *et al*.[157] and the aza-dimethoxycyclooctyne DIMAC (structure **C** in Fig. 3.5) synthesized by Bertozzi *et al.*,[158] Rutjes and coworkers developed the hybrid structure aza-dibenzocyclooctyne DIBAC (structure **E**).[156]

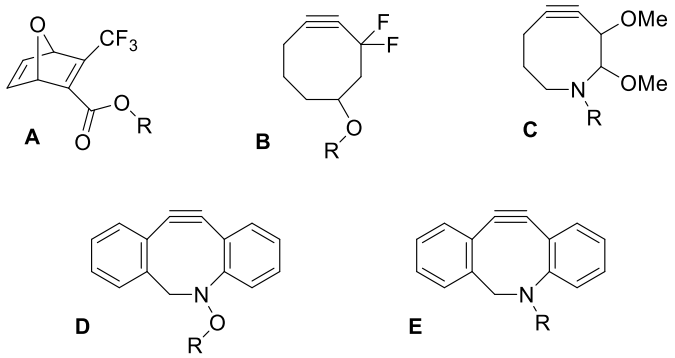

Figure 3.5. *Strain-promoted systems for Cu-free click reactions.*

The aza-dibenzocyclooctyne was designed to combine the favourable kinetics of DIBC (**D**) with the increased hydrophilicity of DIMAC (**C**).[158] With respect to the latter, the nitrogen atom in **E** should allow the straightforward functionalisation of the aniline moiety and the diversification of the system.

3.1.3.2. Applications of Bioorthogonal Click Chemistry in Microarrays

The term bioorthogonal click chemistry was first coined by Carolyn Bertozzi in 2003.[159] It refers to any chemical reaction that can occur inside living systems without interfering with native biochemical processes. The bioorthogonal reagents of click chemistry have demonstrated unique advantages derived from their biocompatibility, high efficiency and high specificity.

Bioorthogonal click chemistry is a two-step reaction that needs a pair of functional groups (Fig. 3.6). First, a functional moiety (chemical reporter) is incorporated into a suitable substrate.

Second, the reporter is covalently linked to an exogenous probe through a click reaction, which allows the detection and isolation of the target. Most importantly, the covalent reaction between these two components must proceed rapidly and selectively in a physiological environment of pH (6–8) and temperature (37 °C). In addition, few non-toxic or no by-products should be formed in the process. Moreover, the chemical reporter should be inert *in vivo*, be unreactive towards the biological environment and small enough to minimally modify the target substrate without giving rise to any functional and/or spatial interference.[160]

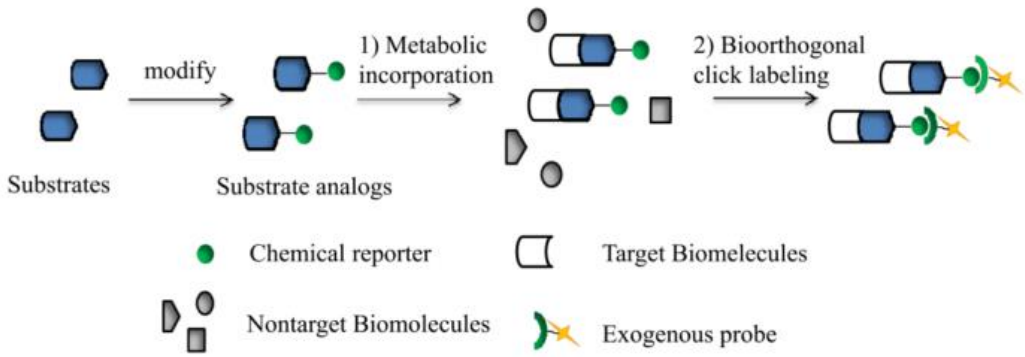

Figure 3.6. *Two-step bioorthogonal chemistry. A chemical reporter linked to a substrate is introduced into a target biomolecule through cellular metabolism. In a second step, the reporter is covalently tagged with an exogenously delivered probe.*

The use of click chemistry in microarrays has become a challenge for the immobilization of some biomolecules. For example, in glycobiology, Wong and co-workers explored the use of Cu(I)-catalyzed azide-alkyne cyclooadditions to attach oligosaccharides on microtiter plates.[161]

Furthermore, peptides can also be immobilized on a solid support by click chemistry. Pfeifer *et al*. immobilized several azide-derivatized and fluorescently-labelled peptides on azadibenzocyclooctyne (ADIBO) activated slide surfaces via a SPAAC reaction. These reactions revealed excellent immobilization kinetics, good spot homogeneities and reproducible fluorescence signal intensities.[162,163]

In the DNA microarray technology, which is used to measure the expression levels of large numbers of genes simultaneously or to genotype multiple regions of a genome, this strategy gives the opportunity to analyse thousands of different DNAs or RNAs in parallel with only a small amount of biological material linked to a solid support.[164] In this context, click chemistry based on the CuAAC method can be easily applied to attach oligonucleotides to functionalised surfaces. They are fairly easy to attach and they are chemically stable under ambient conditions.[165]

Click chemistry has also been applied to the generation of carbohydrate microarrays. This was achieved by reacting an aliphatic azide with the commercially available unsialylated disaccharide *N*-acetylacetosamine. It has been shown that these microarrays can then be incubated with enzymes of interest to identify new inhibitors at the nanomolar range.[166] These last reports are capital for the future of both nucleic acids and protein microarray

development for disparate applications such as basic research, disease diagnosis and drug discovery.

Another application of CuAAC-mediated immobilization is affinity chromatography, by linking a ligand to a support via click chemistry.[167] Indeed, it is possible to envisage the use of commercially available azide or alkyne-functionalised resins to be functionalises in-house "on demand". Furthermore, CuAAC has been used to generate glycol-silica supports for applications in affinity chromatography, in order to overcome the strong electrostatic interactions between silica and proteins which can alter the secondary structure of the protein and diminish its catalytic activity.[168]

3.2. Approaches to the design of a microarray platform for Des1 activity

In the previous chapter, we described the synthesis of a fluorescent Δ^6-dhCer analogue to monitor Des1 activity in solution (Fig. 3.7A). However, this method is not amenable for a HTS format. According to the objectives of this thesis, this chapter will be focused on the design of a new fluorescent assay for Des1 activity, also amenable to microarray formats. In this context, the use of an immobilized Δ^6-(*Z*)-monoene as substrate for a Diels Alder reaction of the resulting diene with a labelable dienophile will be described in the next sections (Fig. 3.7B).

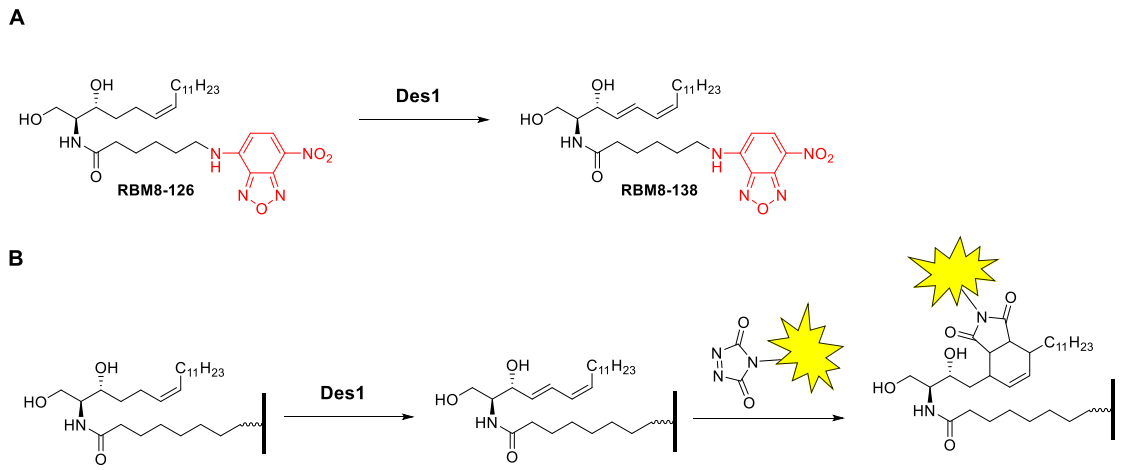

Figure 3.7. *Developed methods to monitor Des1 activity.* ***A.*** *Scheme of the Des1 assay performed in solution using fluorescent Δ^6-dhCer as substrate.* ***B.*** *Scheme of a HTS Des1 assay designed for a solid-supported substrate and the subsequent derivatization of the reaction product with a fluorescent dienophile.*

First, the fluorescent Δ^6-dhCer **RBM8-126** should be replaced by a non-fluorescent dhCer analogue suitable for immobilization on a solid support. Furthermore, we must confirm that the supported monoene is a suitable Des1 substrate and that the resulting diene is able to afford the required Diels Alder reaction with a fluorescent TAD reporter for quantification. At this point, the conditions for each step in the microarray format must be optimized to reduce unspecific reactions and to improve the sensitivity of the quantification.

Although the microarray technique has already been discussed in section 3.1, we should remind that one of the main advantages of this format relies on the miniaturization and parallelization of the experiments, with the resulting savings in reagents and time.

3.3. Design of a TAD-derived fluorescent readout system

3.3.1. Optimization of the Diels Alder reaction with a fluorescent TAD in solution

As stated in the previous section, the search of a TAD-derived fluorescent reported was required at this stage of the project. In light of the promising results obtained with PTAD (*see* Section 2.1), the use of the commercially available fluorescent DMEQ-TAD[169,170] was considered (Table 3.9, entries 1 and 2). In these assays, a single adduct was observed and the yield was notably increased by carrying out the reaction in DMSO, instead of in the initial THF/CH_2Cl_2 mixtures.

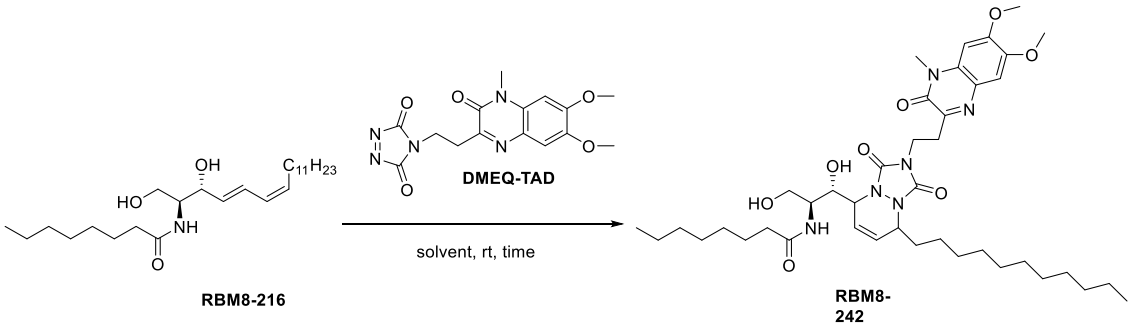

Figure 3.8. *Evaluation of Diels Alder reaction with DMEQ-TAD in solution. Results are summarized in Table 3.9.*

Table 3.9. Reactivity of RBM8-216 with some commercially dienophiles.

Entry	Solvent	Time (h)	Yield (%)
1	THF/CH_2Cl_2	2	60
2	DMSO	2	87

Despite the fluorescent nature of the resulting **RBM8-242**, the low emission wavelength of DMEQ (λ_{em}=440 nm),[171] was unsuitable for the spectral range of our scanner (between 543 and 633 nm, *see* Experimental Section). For this reason, we designed a two-step reporter system (Fig. 3.10), based on the initial reaction of the diene product with the triazolinedione **RBM8-254** (arising from *in-situ* oxidation of the urazole derivative "TAD-azide") followed by a Cu-free reaction with DBCO-PEG_4-TAMRA in a strain-promoted alkyne-azide cycloaddition reaction (SPAAC, *see* Section 3.1.3.1.2).[71,163,172]

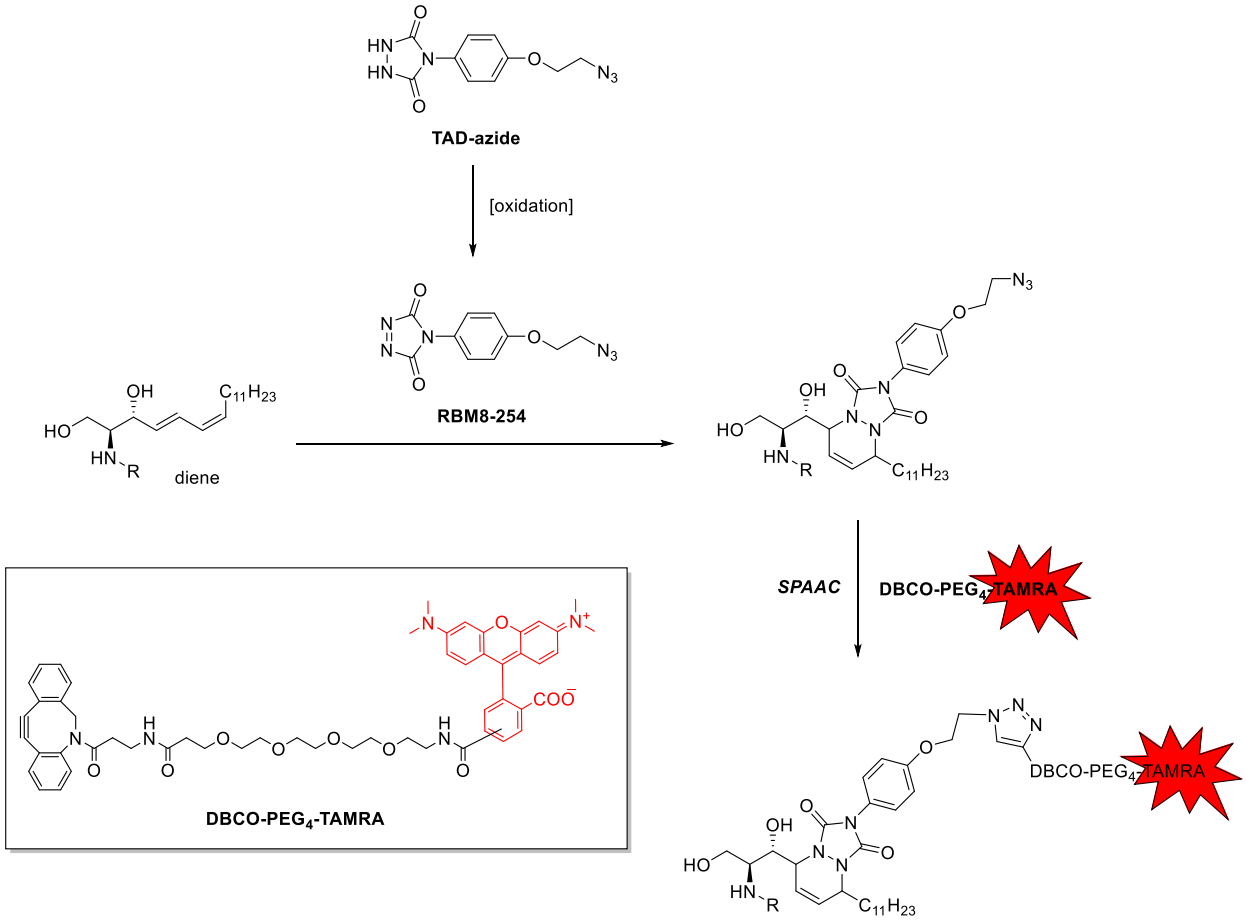

Figure 3.10. *Fluorescent labelling based on SPAAC reaction between* ***RBM8-254*** *and* ***DBCO-PEG$_4$-TAMRA****.*

Azadibenzocyclooctyne-tetramethyl rhodamine (DBCO-TAMRA) is a versatile fluorescent reagent for the labelling of azide containing molecules. The azadibenzocyclooctyne (DBCO) moiety is a strained alkyne that reacts with azides under mild, biocompatible conditions to give a triazole system without the need of the Cu(I) catalysis required for terminal, non-strained alkynes. Furthermore, the excitation and emission wavelenghts of TAMRA fall within the spectral required range of our scanner (λ_{exc}=545 nm, λ_{em}=567 nm).

The reaction between the triazolinedione **RBM8-254** (for its synthesis, *see* Section 3.3.2) and the diene **RBM8-216** in solution afforded the corresponding Diels Alder adduct as a mixture of two diastereomers (exo/endo 1/1), which could be separated by flash chromatography (Fig. 3.11), although they were not configurationally assigned. After 2 h, the starting material **RBM8-216** was totally converted into the corresponding Diels Alder adduct **RBM8-310**, as confirmed by MS.

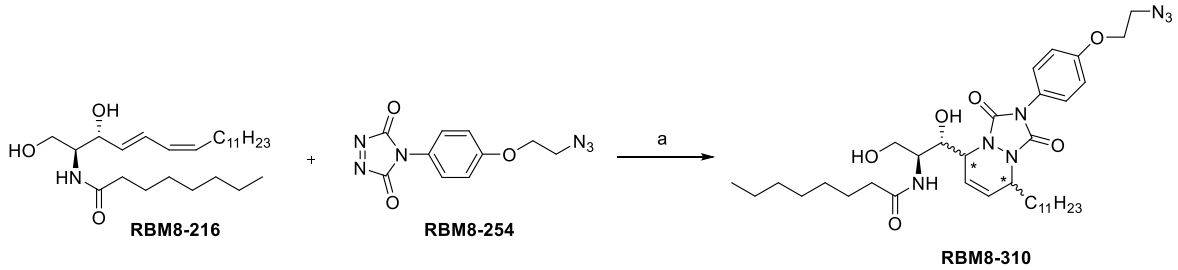

Figure 3.11. *Diels Alder reaction in solution using* ***RBM8-254*** *as dienophile. Reagents and conditions. a) CH_2Cl_2, rt, 2h, d.r.(exo/endo: 1/1), 91% yield.*

3.3.2. Synthesis of RBM8-254

Although TAD-azide is commercially available, this compound was synthesized following the procedure of Barbas and co-workers shown in Fig. 3.12.[85] The aniline **RBM8-080** was synthesized from *p*-(2-bromoethoxy)nitrobenzene by simultaneous reduction and protection of the nitro group as the *N*-Boc derivative **RBM8-078**, nucleophilic addition of azide and final *N*-Boc deprotection. The coupling between ethyl hydrazinecarboxylate and aniline **RBM8-080** was carried out by activation of the hydrazine with carbonyldiimidazole (CDI), followed by addition of the aniline under basic conditions.

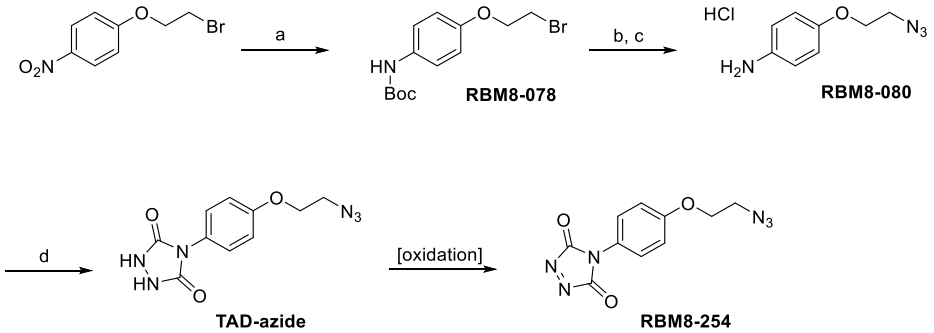

Figure 3.12. *Reagents and conditions. a) Boc_2O, Pd/C, H_2, THF, 58%. b) NaN_3, DMF, 86% c) HCl (4 M), dioxane, 99%. d) ethyl hydrazinecarboxylate, CDI, Et_3N, K_2CO_3, 28%.*

In the last step, TAD-azide was converted into the desired triazole **RBM8-254** by oxidation of the hidrazo moiety to an azo group. There are several methods for the oxidation of 4-substituted urazoles to the corresponding 1,2,4-triazoline-3,5-diones. Some of the most common oxidizing agents are nitric acid (HNO_3), gaseous dinitrogen tetroxide (N_2O_4), halogen-mediated oxidation (Cl_2 or Br_2), hypochlorites (^{t}BuOCl), *in situ* generation of active halogen species (NBS, DABCO-Br), as well as other miscellaneous oxidants, such as iodobenzene diacetate.[71] Unfortunately, none of them can be considered of general applicability and the development of a successful protocol is sometimes a matter of trial and error. Experimentally, the development of a bright colour, characteristic of the azo compounds, is a clear indication of a successful oxidation. However, some triazolinediones are unstable and decompose at room temperature or in the presence of light, humidity and silica gel, so their isolation is not straightforward. This is the case of **RBM8-254**, in contrast with other stable and commercially available triazolinediones, such as PTAD or DMEQ-TAD, which

were used by us for the optimization of the Diels Alder reaction with **RBM8-216** (*see* Section 2.1 and 3.3.1, respectively).

In our case, the formation of **RBM8-254** was first attempted by oxidation of TAD-azide with 1,3-dibromo-5,5-dimethylhydantoin (Table 3.13, entry 1).[85] The reaction was readily monitored by observing the change of the reaction mixture from colourless to a deep red colour. Nevertheless, the isolation of **RBM8-254** was not possible, due to its instability during the chromatographic purification in silica gel. Decomposition products, together with unreacted hydantoin, were isolated in all cases, as confirmed by ^{1}H NMR of some of the column fractions.

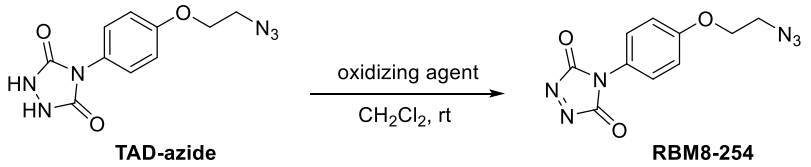

Table 3.13. Oxidation of TAD-azide

Entry	Oxidizing agent	Reaction time (h)	% Conversion
1	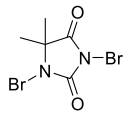 1,3-dibromo-5,5-dimethylhydantoin	2	not isolated
2	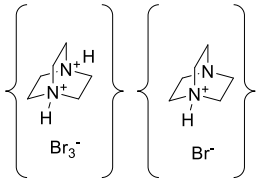 DABCO-Br	1	quantitative

At this point, a modification of the oxidation step was considered. In order to perform the reaction under heterogeneous conditions, DABCO-Br,[172] an oxidizing reagent not soluble in organic solvents, was tested (Table 3.13, entry 2). This reagent exists as a tetrameric complex and it has been found to be particularly useful in heterogeneous systems, where the removal of the excess reagent and by-products can be simplified.[71] Thus, compound **RBM8-254** could be isolated by simple filtration of the crude mixture, once the formation of a red coloured solution was observed. In all cases, this compound was freshly prepared and used immediately to prevent its decomposition.

3.4. Synthesis of immobilized Δ^6-monoene analogues

As already mentioned, the fluorescent Δ^6-dhCer **RBM8-126** used as Des1 substrate in solution, should be replaced by a non-fluorescent Δ^6-dhCer suitable for its ligation to a solid support. In this section, we describe the synthesis and immobilization of a Δ^6-dhCer having a suitable ω-functionalised *N*-acyl chain (Fig. 3.14).

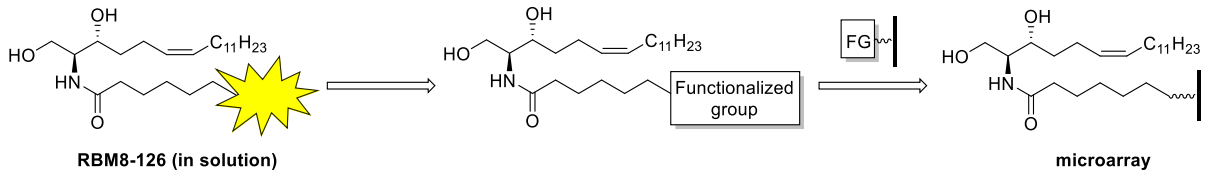

***Figure 3.14**. Modification of the (Z)-Δ^6-dhCer **RBM8-126** for its immobilization on a solid support (FG: functional group)*

To test the suitability of an immobilized dhCer as Des1 substrate, a cleavable linker was first considered. In this way, the formation of the diene reaction product could be easily analysed by UPLC-TOF MS, after cleavage of the enzyme reaction product from the solid support.

3.4.1. Synthesis, immobilization and study of (*Z*)-Δ^6-dhCer RBM8-251 as Des1 substrate

Initial attempts to evaluate the Des1 activity in a microarray format were carried out with immobilized **RBM8-251** as substrate. This compound was synthesized by *N*-acylation of the sphingoid base **RBM8-125** with monomethyl glutarate, followed by ester hydrolysis under basic conditions (Fig. 3.15).

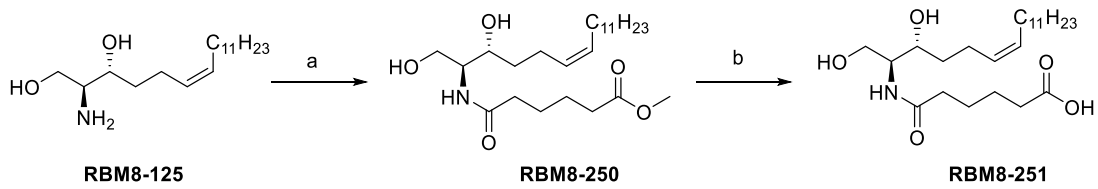

***Figure 3.15**. Synthesis of **RBM8-251**. Reagents and conditions. a) mono-methyl glutarate, EDC, HOBt, CH_2Cl_2, 4h, rt, 60%. b) LiOH, THF, rt, 2h, 87%.*

Figure 3.16 shows the steps required for the immobilization of **RBM8-251** and the evaluation of the Des1 activity in a microarray format.

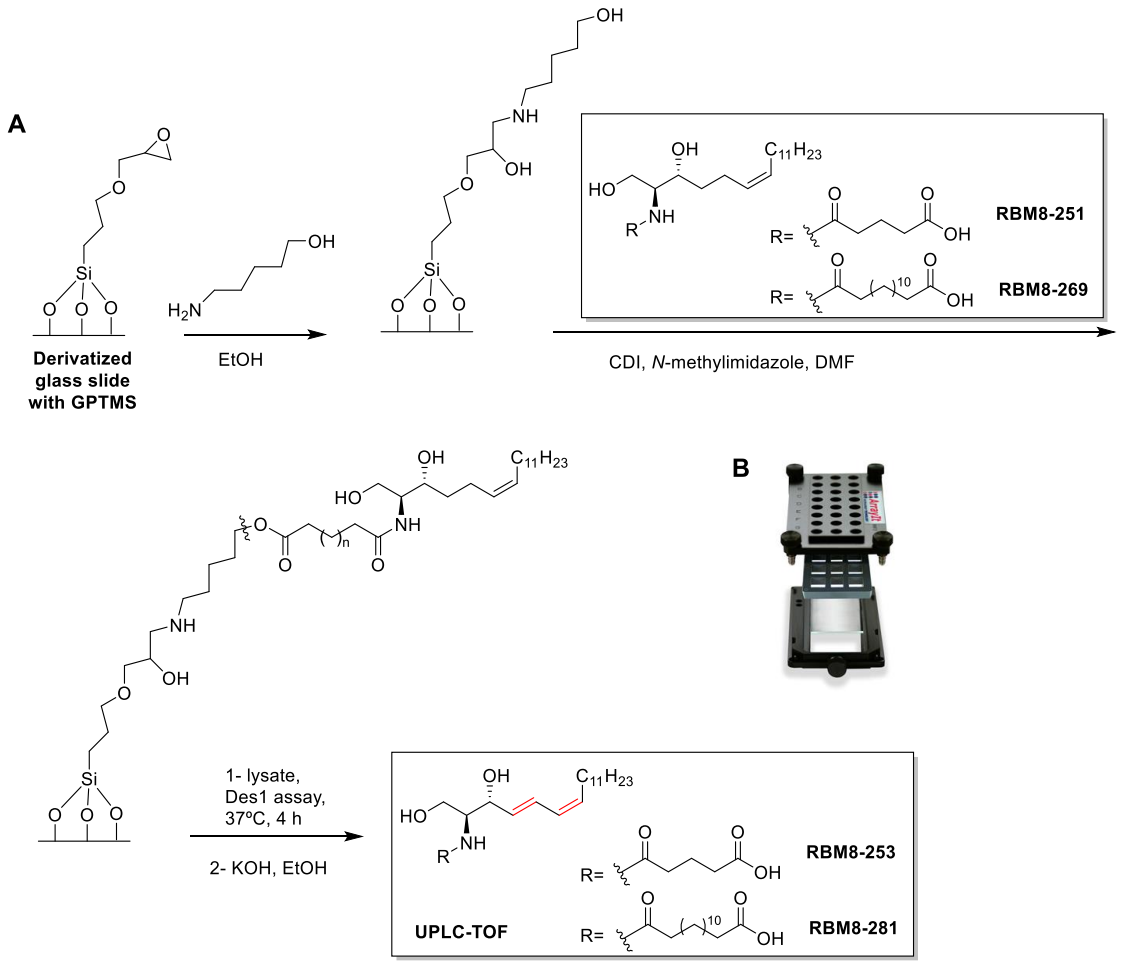

***Figure 3.16. A**. Sequential steps for the evaluation of **RBM8-251** and **RBM8-269** as Des1 substrates in a microarray format. **B.** Microplate microarray Arrayit hardware system (Telechem International Inc.) with a silicon gasket that defines 24 wells per slide.*

The initial step was the reaction of 5-aminopentanol with a derivatized glycidylpropyl trimethylsilyl (GPTMS) glass slide (Fig. 3.16A). Then, **RBM8-251** was immobilized on the solid support by esterification of the terminal carboxylate group with the free hydroxyl groups of the solid support. This functionalized slide was incubated with cell lysates to perform the enzymatic reaction. All these steps were carried out in a microplate microarray with a silicon gasket (Fig. 3.16B) that demarcated into 24 wells per slide. The last step consisted on the alkaline hydrolysis of ester group and the analysis of the free lipids by UPLC-TOF MS Despite this experiment showed the successful immobilization of **RBM8-251**, no trace of the expected diene **RBM8-253** was detected in the lipid extracts.

3.4.2. Synthesis, immobilization and study of (*Z*)-Δ^6-dhCer RBM8-269 as Des1 substrate

The above negative results were attributed to the nature of the linker in **RBM8-251**, probably too short (only three carbon atoms) to allow an efficient access of the substrate to the enzyme active site. Based on this hypothesis, we designed (*Z*)-Δ^6-dhCer **RBM8-269** as an alternative substrate with a 12-carbon atom linker between the sphingoid amide and the terminal carboxylate group.

The synthesis of Δ^6-dhCer **RBM8-269** was performed by *N*-acylation of amino diol **RBM8-125** with 14-methoxy-14-oxotetradecanoic acid,[173] followed by deprotection of the methyl ester under basic conditions (Fig. 3.17).

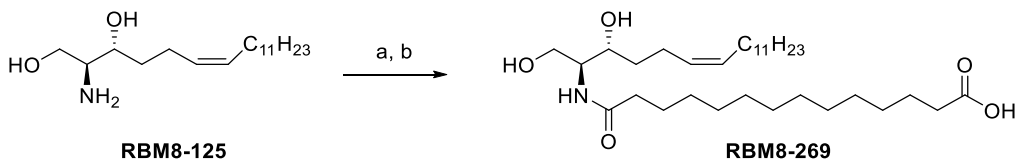

Figure 3.17. *Reagents and conditions. a) EDC, HOBt, 14-methoxy-14-oxotetradecanoic acid, 4 h, rt, 83%. b) LiOH, THF/H_2O, 79%.*

The monoene **RBM8-269** was immobilized, as depicted in Figure 3.16, and evaluated as Des1 substrate. Interestingly, UPLC-TOF MS analysis of the lipid extracts showed, in this case, the formation of the diene Cer product **RBM8-281**, an indication that desaturation of the immobilized **RBM8-269** by Des1 had taken place in the microarray surface. The diene ceramide was identified by comparison with a synthetic sample of **RBM8-281**, prepared as indicated in the Experimental Section.

Average concentrations of 35-45 µg/mL for the immobilized carboxylic acid **RBM8-269** were invariably obtained from 1 or 2 mg/mL DMF solutions, as estimated by UPLC-TOF-MS quantification using the calibration curve shown in Fig. 3.18A.

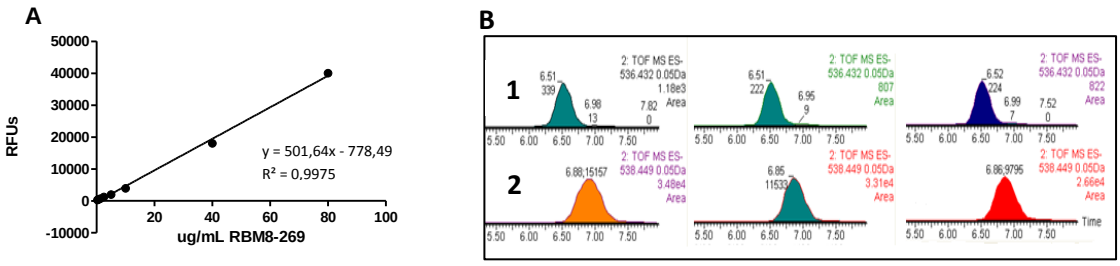

Figure 3.18. A*. Calibration curve to determine concentration of the immobilized compound.* ***B****. UPLC-TOF MS chromatograms operated in negative electrospray ionization mode. Representative [M-H] signals for the diene reaction product* ***RBM8-281*** *(****B1****,[M-H]: 536.432) and monoene substrate* ***RBM8-269*** *(****B2****, [M-H]: 538.449).*

Conversions of the immobilized **RBM8-269** to the corresponding $\Delta^{4,6}$-ceramide **RBM8-281** ranged between 1 and 5 %, similarly as those found for the enzymatic assay in solution (*see*

Section 2.3.1). These results confirmed the suitability of our system to carry out the Des1 assay in a microarray format.

3.5. Optimizing the microarray format for the evaluation of Des1 activity

Focused on our main objective, addressed at the development of a Des1 assay in a microarray format, we next proceeded with the combination of all the partial achievements reported in the previous sections. First, we have designed an immobilized Des1 substrate from **RBM8-269**. Second, we have obtained triazolinedione **RBM8-254** as a dienophile for the Diels Alder reaction with the diene product of the enzymatic reaction, and third, the said Diels Alder adduct has been used in a SPAAC reaction[174,160] with the fluorescent reporter **DBCO-PEG$_4$-TAMRA**.

In this section, we will first describe the validation of the click reaction in microarray format between the azide and the DBCO moieties. On the other hand, the immobilized **RBM8-269**, used in the preliminary assays, will be replaced by a more stable, non-hydrolyzable linker. The conditions for the HTS assay on a microarray format will be optimized by immobilizing the diene Des1 product to verify that the consecutive Diels Alder cycloaddition and copper-free click reaction lead to a fluorescent adduct that can be quantified on the microarray support.

3.5.1. Validation of the click reaction in a microarray system

To evaluate the SPAAC click reaction in a microarray system, the reactivity of an azide and a DBCO group was first considered using commercially available models. This was achieved by derivatization of a GPTMS glass slide with NH_2-$(PEG)_4$-DBCO and its reaction with a fluorescent azide (N_3-$(PEG)_3$-TAMRA) *via* a copper-free click reaction (Fig. 3.19).

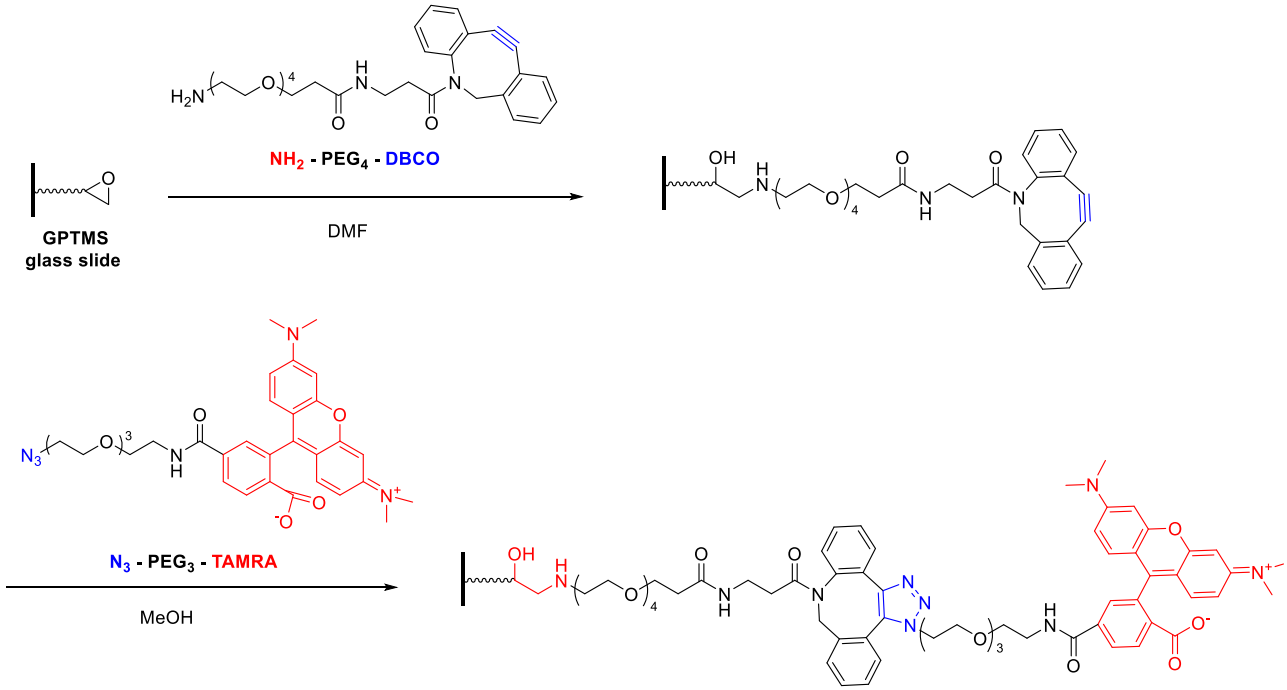

Figure 3.19. *Schematic representation of a strained-promoted azide-alkyne cycloaddition (SPAAC) in a microarray format between commercially available* ***NH_2-PEG_4-DBCO*** *and* ***N_3-PEG_3-TAMRA****.*

The following experiment setup was designed: first, **NH_2-PEG_4-DBCO** was spotted on the derivatized GPTMS glass slide at different concentrations (0, 0.125, 0.25, 0.5, 1 mg/mL in DMF). Then, the slide was placed in a silicon gasket that divides the slide into 24 wells, with 5x5 spots of the **NH_2-PEG_4-DBCO** at 5 different concentrations in each well. A solution of **N_3-PEG_3-TAMRA** was added to each well at 8 different concentrations to perform the click reaction. Finally, the fluorescence of the slide was read with the scanner fixed at the TAMRA λ_{max} of 570 nm.

A schematic representation of the covalent immobilization is shown in Figure 3.20A. The slide is divided into 24 wells (8 rows x 3 columns) with 5 different concentrations and 5 replicates of **NH_2-PEG_4-DBCO** in each well. By using this format, 8 different concentrations of fluorescent **N_3-PEG_3-TAMRA** per row can be used in triplicates. This represents a total of 15 point readouts for each concentration of **NH_2-PEG_4-DBCO** and **N_3-PEG_3-TAMRA** tested.

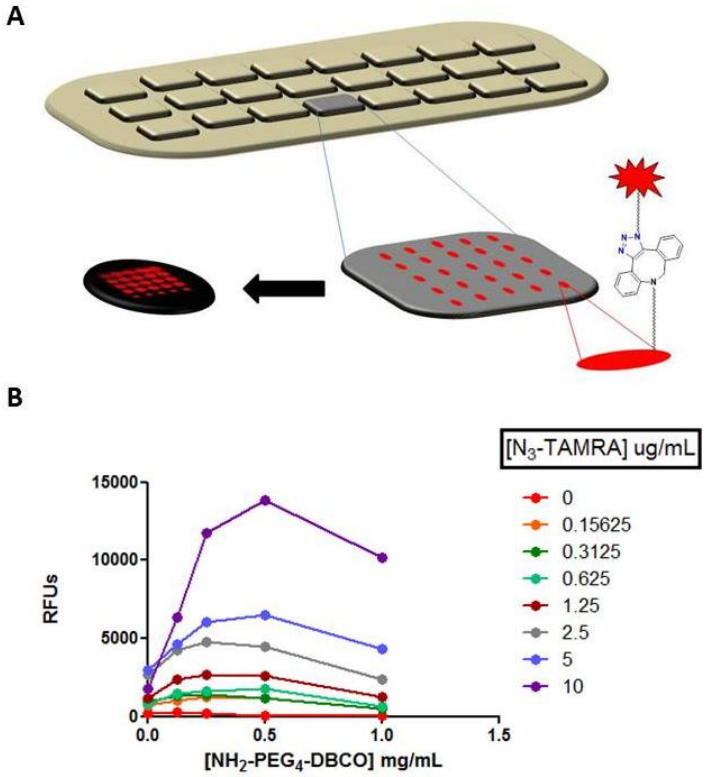

***Figure 3.20. A**. Schematic representation of the preparation of a SPAAC reaction in a microarray format, together with a microarray image of one representative experiment. **B**. Fluorescence signal intensity at λ = 570 nm. Data are mean values ± SD of a simple experiment (1 column). RFU: Relative Fluorescence Units.*

The triazole linker formed in the click reaction had excellent chemical stability, due to the aromatic character of the heterocycle, revealing good spot homogeneities and reproducible fluorescence signal intensities with good selectivity, specificity and the absence of non-specific binding. Furthermore, a saturation curve with a linear slope at low concentrations and a saturation fluorescence intensity at high concentrations was obtained (Fig. 3.20B).

3.5.2. Synthesis and immobilization of (*Z*)-Δ^6-dhCer RBM8-324 and (*Z,E*)-$\Delta^{4,6}$-Cer RBM8-313

Once confirmed the suitability of immobilized **RBM8-269** as Des1 substrate by UPLC-TOF MS analysis (see Section 3.4.2), we considered more convenient the synthesis a non-hydrolytically cleavable version of this substrate for the development of our fluorescent assay.

As shown in Figure 3.21, a new substrate (**RBM8-324**) was designed by the formal replacement of the ester bond with an amide bond in the linker chain. The synthesis of **RBM8-324** was carried out by a convergent approach, based on the initial coupling of partially protected amino acids **RBM8-306** [175] and **RBM8-305** [176] to give the orthogonally protected amino ester **RBM8-307** (Fig. 3.22). The selective deprotection of ester **RBM8-307** in acidic conditions, to preserve the *N*-Fmoc protecting group, led to the carboxylic acid **RBM8-311**, whose coupling with the Δ^6-(*Z*) monoene **RBM8-135** or with the $\Delta^{4,6}$-(*E*,*Z*) diene **RBM8-137** led to the required Des1 substrate Δ^6-dhCer **RBM8-324** or the expected $\Delta^{4,6}$-Cer Des1 reaction product **RBM8-313**,

respectively, after final *N*-Fmoc removal. Both compounds were directly linked to the GPTMS-derivatized glass slide through the terminal amino bond. This strategy avoided the use of the 5-amino-1-pentanol spacer, since this fragment was already incorporated as part of the linker in the final compounds. The diene **RBM8-313** was also immobilized and used as standard for the optimization of the Diels Alder reaction with the TAD-N_3 derivative **RBM8-254** and its subsequent derivatisation with DBCO-PEG_4-TAMRA (*see* Section 3.5.3).

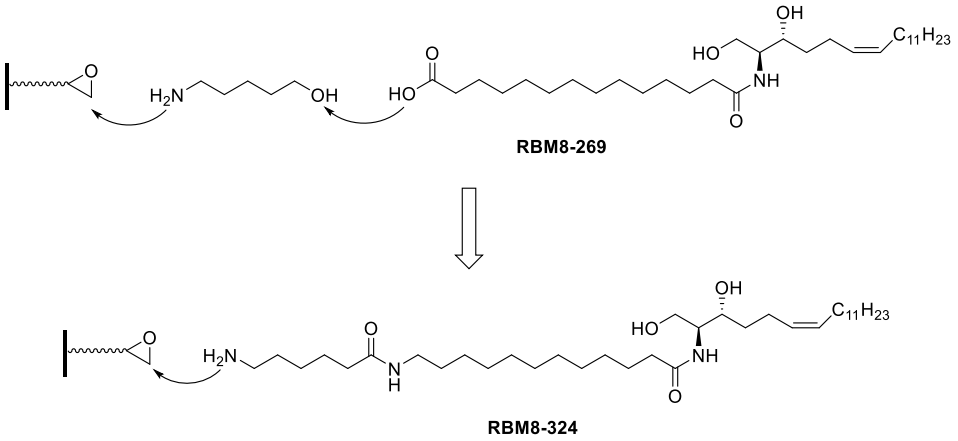

Figure 3.21. *Modification of the N-acyl chain of the substrate by a non hydrolyzable covalent immobilization.*

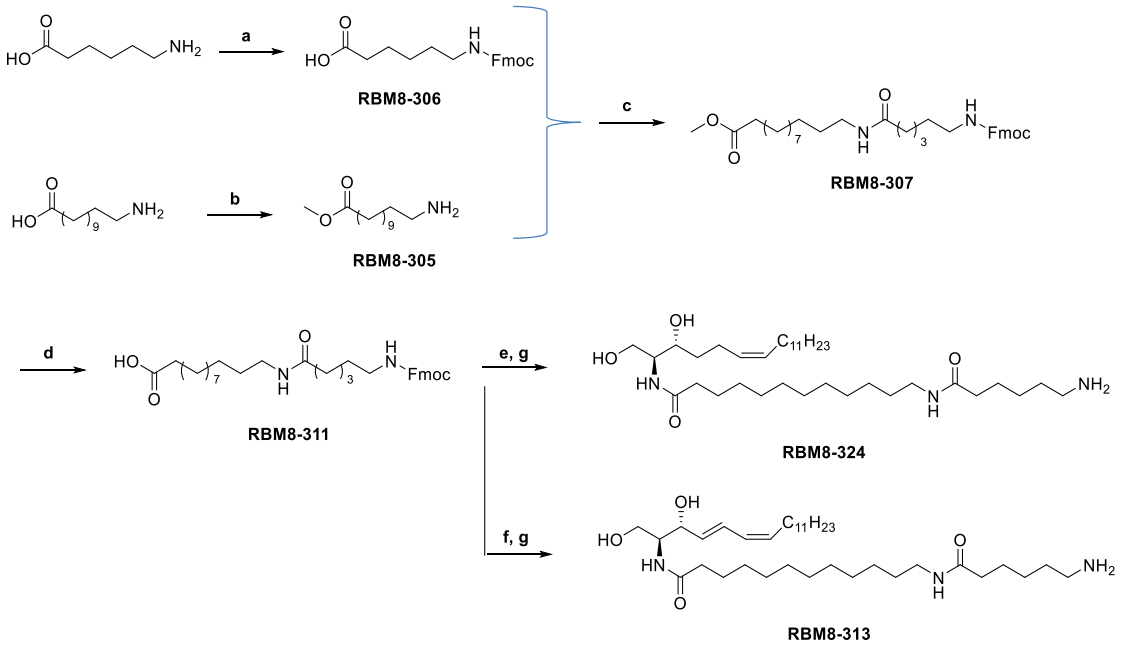

Figure 3.22. *Reagents and conditions. a) Na_2CO_3, H_2O, dioxane, FmocCl, 73%. b) Thionyl chloride, MeOH, quant. c) EDC, HOBt, CH_2Cl_2, 88%. d) HCl 4N, dioxane, 90%. e) EDC, HOBt,* ***RBM8-125****, CH_2Cl_2, 75%. f) EDC, HOBt,* ***RBM8-137****, CH_2Cl_2, 65%. g) piperidine, THF, 83% for* ***RBM8-324*** *and 71% for* ***RBM8-313.***

3.5.3. Optimization of the microarray conditions using the $\Delta^{4,6}$-Cer analogue RBM8-313

As indicated in the previous Section, the immobilized diene **RBM8-313** was used as standard to develop a quantification protocol (Fig. 3.23). Thus, the sequential Diels Alder reaction of **RBM8-313** with the dienophile **RBM8-254**, followed by a SPPAC reaction with **DBCO-PEG$_4$-TAMRA** would allow the fluorescence detection of the above diene in our HTS assay.

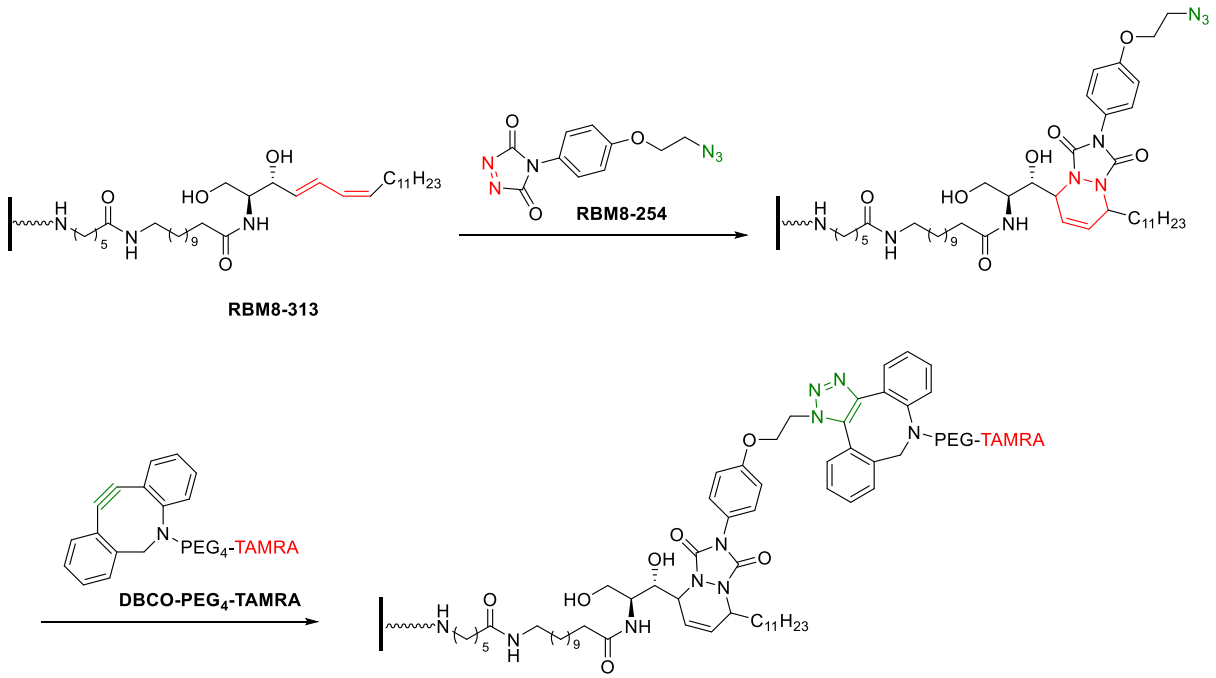

Figure 3.23. *The product of the enzymatic reaction (**RBM8-313**) is immobilized on the microarray. The successive Diels-Alder reaction with **RBM8-254**, followed by the copper-free click reaction with **DBCO-PEG$_4$-TAMRA** is used to determine the best conditions for our HTS assay.*

The optimization process required the initial spotting of the sphingolipid (**RBM8-313**) on the GPTMS glass slide. This was carried out by first dividing the slide into 24 wells. Each well was spotted with 3x3 spots (9 dots) of the sphingolipid at different concentrations (from 10 to 0 mg/mL in DMF). Then, by using the silicon gasket, freshly prepared **RBM8-254** was next added to each well at different concentrations (from 10 to 0 mg/mL in MeOH) to carry out the Diels Alder reaction. After washings, of **DBCO-PEG$_4$-TAMRA** (from 10 to 0 µg/mL in MeOH) was added to each well and the fluorescence of the slide was read on the scanner at λ=543 nm for TAMRA.

Figure 3.24 shows a schematic representation of the optimization experiment. The advantage of the microarray format relies on the possibility of a multiplex detection and characterization, so different variables can be modified simultaneously in a single experiment.

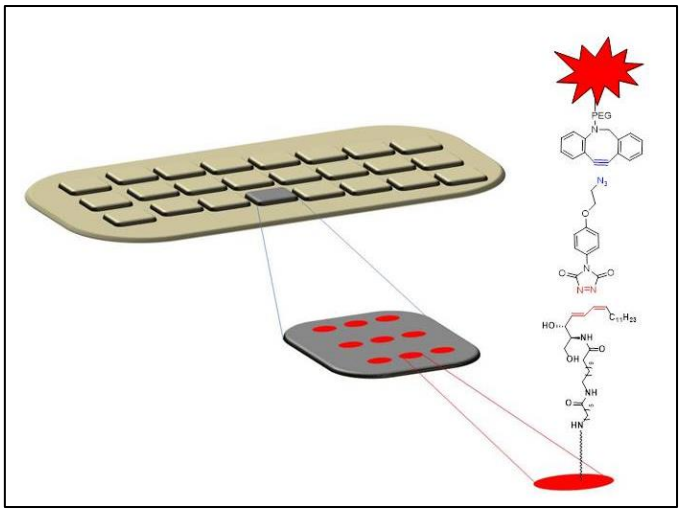

Figure 3.24. *Representative scheme for the optimization of the microarray design using* ***RBM8-313*** *as standard.*

After several attempts, the best conditions were determined. These required the optimization of solvents, reaction times, concentrations, number of washings, etc. for each reaction, as well as the optimization of the fluorescence intensity for the detection and quantification of the TAMRA adducts. The best reaction conditions, after the preliminary screenings, are collected in Table 3.25. Solvent selection and concentrations for each step were based on solubility criteria and also on the intensity of the fluorescence signal. The observation of a minimal background signal, due to the non-specific binding (NSB) of the reagents to the solid surface, was considered a key requirement at this stage of the optimization.

Table 3.25. *Important parameters to consider for the development of the microarray assay.*

Immobilization method	covalent
Humidity and temperature	60 % and 20ºC
Solvent immobilization/concentration of RBM8-313	DMF/ 10 mg mL^{-1} to 0 $mg.mL^{-1}$
Solvent/concentration/reaction time of RBM8-254	MeOH/ 1 mg mL^{-1}/ 1 h
Solvent/concentration/reaction time of DBCO-PEG_4-TAMRA	MeOH/ 1µg mL^{-1}/ 1 h
Final washing stage	MeOH/ MilliQ H_2O

Blocking reagents to reduce non-specific binding

The efficient blocking of the reactive surface groups after arraying is critical for a minimal fluorescence background.[177] Thus, some blocking agents were tested in order to improve the selectivity of the assay by reducing non-specific adsorptions. Using the conditions of Table 3.25, different blocking agents were added after the initial spotting of **RBM8-313**. The best results were obtained with polyvinyl pyrrolidine (PVP), gelatine and milk (Fig. 3.26), which led to a clean increase of the signal to noise ratio. After additional experiments (data not shown), PVP was chosen as the best blocking agent for our microarray assay.

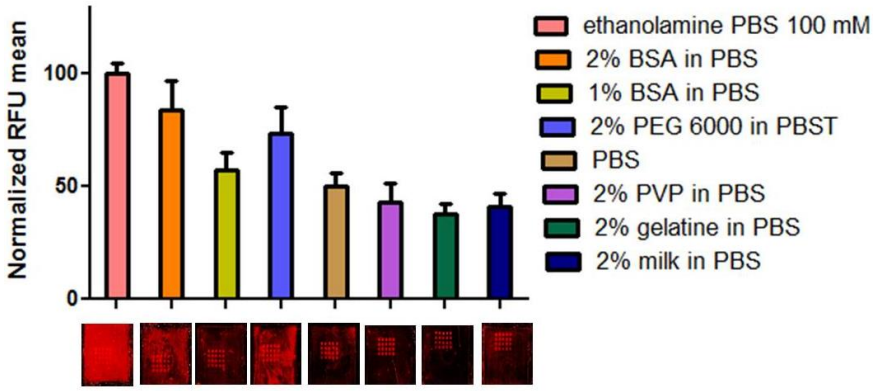

Figure 3.26. *Normalized signal background intensity using different blocking agents and conditions. Data are mean values ± SD at 5 different concentrations of* ***RBM8-313*** *in each well (x5) with triplicates. The scanner images (on the abscissa axis) show one representative well for each blocking agent with the corresponding images obtained with the scanner*

As we mentioned before, the use of a silicon gasket to demarcate each slide into 24 wells (or single microarrays) was crucial for the optimization steps. Nevertheless, we realized that MeOH (used as solvent in **RBM8-254** and **DBCO-PEG$_4$-TAMRA** solutions) caused the damage of the silicon gasket and the appearance of strong unspecific adsorptions on the slide (Fig. 3.27A). For this reason, we decided to use polystyrene trays instead of silicon gaskets during the hybridization stages when MeOH or other organic solvents were required (Fig. 3.27B). The silicon gasket was only used in steps requiring an aqueous media, such as the blocking steps or the enzymatic reactions with cell lysates.

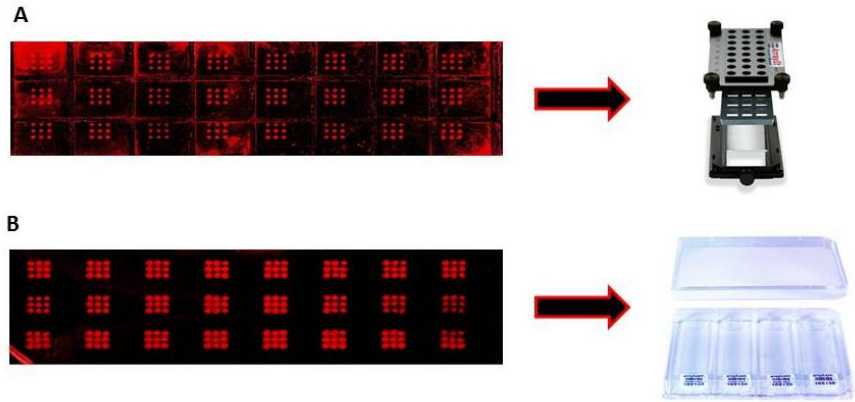

Figure 3.27. A. *Optimized setup using microplate microarrays with a silicon gasket. Non-specific binding (NSB) is observed.* ***B.*** *Optimized setup in which the array is submerged into solutions of the corresponding analytes in a polystyrene tray. Conditions for both steps* ***A*** *and* ***B****: 1 mg/ml (3x3) per well of* ***RBM8-313*** *is spotted, PVP 2% in BSA,* ***RBM8-254*** *(1 mg/ml),* ***DBCO-PEG$_4$-TAMRA*** *(1 ug/ml). For additional details, see the Experimental Section.*

Figure 3.27 shows a representative example illustrating the differences in NSB between an experiment carried out using a silicon gasket (3.27A) or by submerging the array into solutions of the reagents in a polystyrene tray (3.27B). This last approach allowed the reduction of NSB and gave good reproducibility. The disadvantage of the use of a polystyrene tray is the impossibility to use different concentrations of reagents in the same slide, since the whole slide is submerged into a solution of the reagent. However, this was not a severe problem at this stage, since the optimal concentrations of reagents had already been optimized as indicated above.

Optimizing the spotting solutions for increased reproducibility

Finally, one of the key steps we should considered was the morphology of the spots when the sphingolipid was deposited on the glass slide. Although in the above optimization steps the sphingolipid was dissolved in DMF (*see* Table 3.25), we tried to improve the morphology of the spots, as well as their signal intensity, by using different additives, such as trehalose or glycerol at different concentrations in DMF (Fig. 3.28).[177–179]

Figure 3.28*. Representative images for the assays addressed at the improvement of the spots morphology*

None of the additives gave rise to substantial improvements, neither of the spots morphology nor of the signal intensity, in comparison with the previous experiments carried out only in DMF, which was kept as the solvent of choice in all the experiments.

3.5.4. Calibration curves and detection limit for RBM8-313

Once optimized the conditions of the microarray assay, the fluorescence detection limit for the diene **RBM8-313** was evaluated. To reproduce as close as possible the conditions of the real assay, an extra incubation time, to mimic the incubation with the cell lysates that will be required in the Des1 assay with monoene **RBM8-324** (*see* Section 3.6), was also included in the protocol (Table 3.29).

Table 3.29. Optimization of the HTS assay in microarray format.

Immobilization method	covalent
Humidity and temperature	60 % and 20˚C
Immobilization solvent/ RBM8-313 concentration	DMF/ 5, 1, 0.5, 0.25, 0.125, 0.0625, 0.03, 0 mg L^{-1}
Blocking agent	PVP 2% in PBS
Buffer enzymatic reaction/ incubation time	Phosphate buffer pH 7.4/ 4 h, 37˚C
Solvent/concentration/ RBM8-254reaction time	MeOH/ 1 mg mL^{-1}/ 1 h
Solvent/concentration/DBCO-PEG$_4$-TAMRA reaction time	MeOH/ 1µg mL^{-1}/ 1 h
Final washing stage	MeOH/ Milli-Q H_2O

First, the diene **RBM8-313** was anchored on the solid support at 8 different concentrations (rows) with triplicates (columns), and each concentration was spotted 3x3 times (9 dots). Then, the slide was placed in the microplate with a silicon gasket to demarcate 24 wells per slide and 100 µL of 2% PVP BSA solution (blocking agent) was applied in each well. The slide was kept at room temperature for 1 h. This was followed by multiple rinsing with Milli-Q water to avoid non-specific adsorptions. Next, phosphate buffer (100 µl per well) was added and the plate was incubated at 37˚C for 4 h. The plate was next submerged into a freshly prepared solution of TAD-azide **RBM8-254**, to carry out the Diels Alder reaction, for 1 h, followed, after washings, by the addition of a **DBCO-PEG$_4$-TAMRA** solution (1 h). Finally, the plate was scanned for fluorescence reading (for additional details, *see* the Experimental section). As already mentioned, the silicon gaskets were only used for reactions in aqueous media.

Figure 3.30 shows the result of one representative experiment and the corresponding calibration curve for analyte **RBM8-313**. Considering that the immobilization of 1 to 2 mg/ml of

substrate led to conversions between 1 and 5% (*see* Section 3.4.2), the results shown in Figure 3.30 (LOD = 3.3 µg/mL) are promising for the detection of the enzymatic reaction product.

Relative fluorescence units (RFU) were normalized due to the high variability between experiments. Since no appreciable "inter-well" variability was observed, each experiment was designed to include a calibration curve for **RBM8-313**.

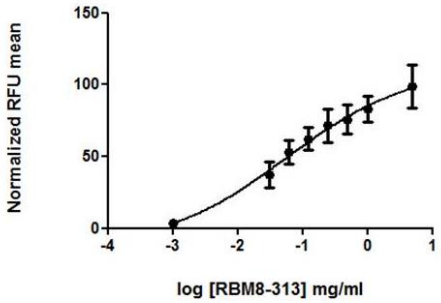

	RBM8-313
Norm. RFU max	102,44 ± 5,44
Norm. RFU min	-0,11 ± 2,80
Slope	0,84 ± 0,22
IC_{50} (µg/mL)	70,75 ± 38,60
LOD (µg/mL)	3,32 ± 1,97
LOQ (µg/mL)	17,16 ± 7,19
r^2	0,98 ± 0,02

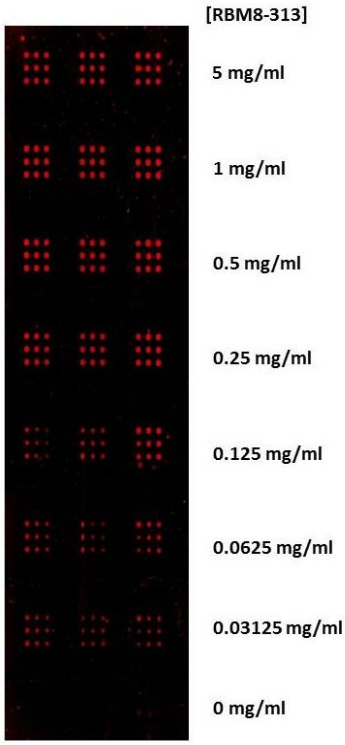

***Figure 3.30**. Calibration curve for the detection of **RBM8-313** and parameters that define this calibration curve. The experiments were performed in triplicate (3 columns) and in three different days. The image shown corresponds to one experiment. RFU: Relative Fluorescence Units. LOD: Limit of Detection. LOQ: Limit of Quantification.*

3.6. Towards a HTS enzymatic assay to evaluate Des1 activity

Once completed the optimization for the quantitative determination of the linked diene **RBM8-313**, the Des1 assay on the microarray support was next attempted. This required the immobilization of the monoene substrate **RBM8-324** onto the microarray surface and the incubation with cell lysates from HGC27 cells, a type of human gastric cancer cells currently used in our group for cellular biology studies.

Thus, substrate **RBM8-324** was deposited on the solid support from a 5 mg/mL DMF solution, and the Des1 assay was carried out using a suspension of 10^6 cells/mL per well (Fig. 3.31). The diene **RBM8-313** resulting from the enzymatic reaction was trapped with the dienophile **RBM8-254** for the subsequent click reaction with the fluorescent reporter **DBCO-PEG$_4$-TAMRA**.

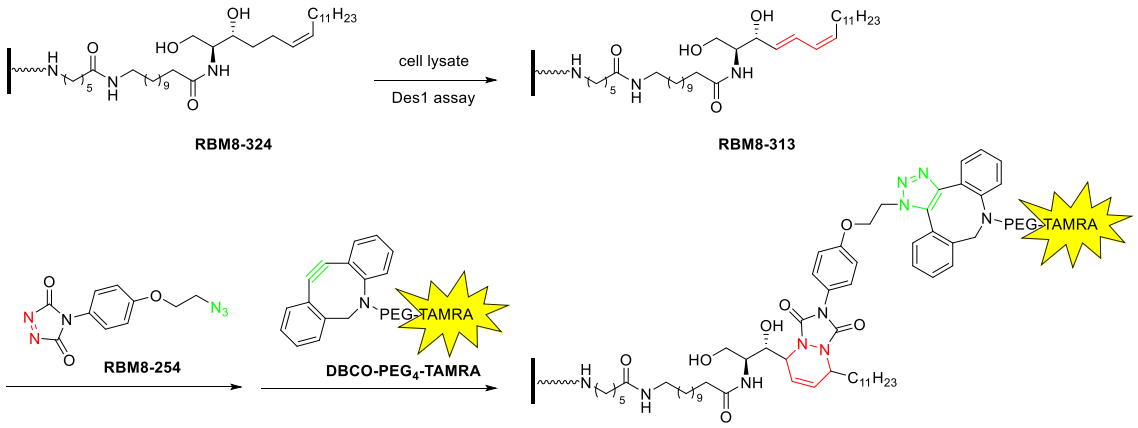

Figure 3.31. *Schematic representation of the reactions involved in the HTS assay to monitor Des1 activity in a microarray format.*

As we mentioned before, a calibration curve was made to consider the variability of the assay. In this experiment, we obtained a LOD of 51 µg/mL of diene **RBM8-313** (Fig. 3.32A), a bit higher to that obtained in the calibration curve of the experiment discussed in Section 3.5.4. Furthermore, the fluorescence signal for diene **RBM8-313** arising from the Des1 reaction gave a mean value of 280 µg/mL, enough for being detected. However, the high fluorescence found for the blank assay (spots of non-treated substrate **RBM8-324** with cell lysates) made not possible to quantify accurately the enzyme reaction product **RBM8-313** under these conditions.

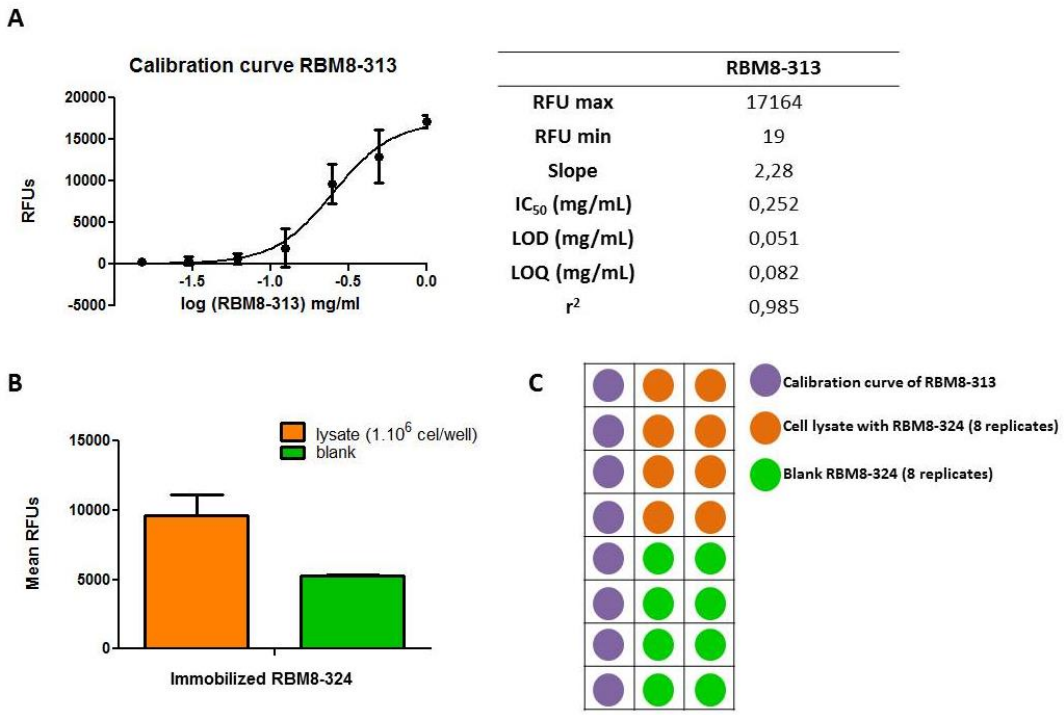

	RBM8-313
RFU max	17164
RFU min	19
Slope	2,28
IC_{50} (mg/mL)	0,252
LOD (mg/mL)	0,051
LOQ (mg/mL)	0,082
r^2	0,985

Figure 3.32. A. *Calibration curve and parameters obtained for diene* ***RBM8-313*** *in the experiment.* ***B.*** *Fluorescence signal after spotting the substrate* ***RBM8-324****, with cell lysates (orange) or blank, without cell lysates (green). Data are the mean values ± SD of 8 wells (3x3 spots in each well at 5 mg/ml in DMF).* ***C.*** *Representative setup design of the slide for each experiment.* ***RBM8-313*** *(3x3 spots in each well at same concentration) at 8 different concentrations was spotted in the first column (to give the maximum theoretical fluorescence). Columns 2 and 3 were spotted with the substrate* ***RBM8-324*** *at 5 mg/ml (3x3 spots in each well). Half of the columns were incubated with cell lysates (to measure the assay fluorescence), while the other half were not treated with cell lysates (to give the background fluorescence).*

Despite the promising results shown above, we were intrigued by the high background fluorescence (*see* Fig. 3.32B). In this context, additional experiments were carried out to check if this fluorescence came from nonspecific adsorptions or from formation of covalent bonds with the support.

As discussed in the next sections, some experiments were performed to explore the reasons for the strong signal background found for the immobilized substrate **RBM8-324** (the blank). In all cases, the immobilized diene **RBM8-324** was used as reference to determine the maximum theoretical fluorescence of the expected Des1 reaction product.

3.6.1. Attempts to increase the fluorescence intensity ratio between the reaction product and the substrate

The first experiments were carried out by immobilization of equimolar concentrations (1 mg/mL in DMF) of monoene **RBM8-324** and diene **RBM8-313**, using PVP 2% BSA solution as blocking agent. Consecutive Diels Alder and copper-free click reactions were performed at different reagent concentrations to obtain a maximum signal ratio ($Signal_{RBM8-313}/Signal_{RBM8-324}$).

The first experiment was carried out at different concentrations of the dienophile (TAD-azide **RBM8-254**), while keeping a fixed concentration of **DBCO-PEG$_4$-TAMRA** (1 µg/mL). As shown in Figure 3.33, the product signal raised at increasing dienophile concentrations , while a stable signal for the monoene substrate **RBM8-324** was observed.

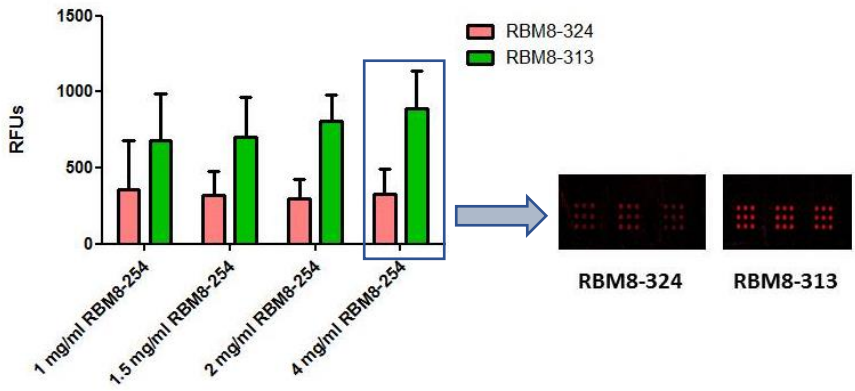

Figure 3.33. *Fluorescence signal for monoene substrate* ***RBM8-324*** *and diene product* ***RBM8-313*** *at different concentrations of the dienophile* ***RBM8-254*** *(1-4 mg/mL in MeOH) and fixed concentration of* ***DBCO-PEG$_4$-TAMRA*** *(1 µg/mL in MeOH). The images represent the best ratio of fluorescence intensities for the diene product and the monoene substrate.*

In contrast, a lineal dependence of fluorescence intensities for both substrate **RBM8-324** and product **RBM8-313** was observed using different **DBCO-PEG$_4$-TAMRA** concentrations (1, 0.8, 0.5, 0.3 µg/mL in MeOH) at a fixed dienophile concentration (**RBM8-254** at 4 mg/mL in MeOH). The best fluorescence intensity ratio between product and substrate was obtained at 1 µg/mL **DBCO-PEG$_4$-TAMRA** (Fig. 3.34).

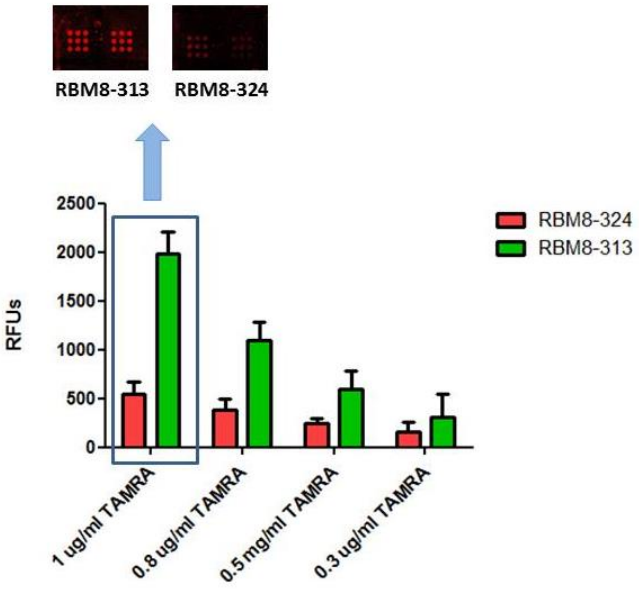

Figure 3.34. *Fluorescence signal for substrate* ***RBM8-324*** *and diene product* ***RBM8-313*** *at different DBCO-PEG$_4$-TAMRA concentrations (1-0.3 µg/mL in MeOH) and fixed concentration of the dienophile* ***RBM8-254 (****4 mg/mL in MeOH). The images represent the best ratio of fluorescence intensities between the diene product and the monoene substrate.*

This behaviour would be consistent with unspecific adsorptions of TAMRA, due to its linear concentration dependence. At this point, an alternative fluorophore was considered (Section 3.6.2). From these experiments, the best concentration of the dienophile **RBM8-254** was set at 4 mg/mL. However, the origin of the strong background fluorescence could not be determined and additional experiments were considered.

3.6.2. Use of an alternative fluorophore

To evaluate the possibility of a nonspecific adsorption of **TAMRA** on the solid surface, we carried out a control experiment in which **DBCO-PEG$_4$-TAMRA** was replaced by the DBCO-containing fluorescent cyanine dye DBCO-Cy3 (Fig. 3.35A).

In this experiment, both substrate **RBM8-324** and product **RBM8-313**, were spotted at 1 mg/mL in DMF, and the slide was next blocked with PVP 2% BSA solution, submerged with a 4 mg/mL solution of **RBM8-254** and, finally, treated with aqueous solutions of DBCO-Cy3 at different concentrations (*see* Fig. 3.35C for an schematic representation).

As it can be seen in Figure 3.35C, only slightly minor fluorescence intensities were observed for the monoene substrate **RBM8-324** in comparison with the diene reaction product **RBM8-313** (Fig 3.35B). Furthermore, a nonspecific background fluorescence was also observed in all cases, which led us to disregard any specific reactivity of **DBCO-PEG$_4$-TAMRA** as the origin of the strong background.

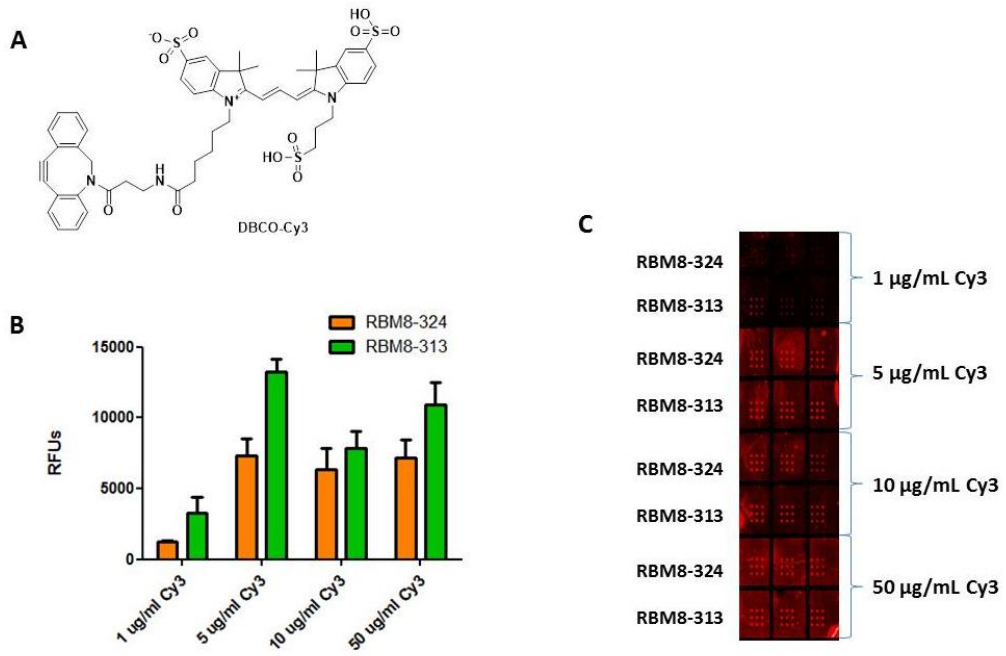

Figure 3.35. A. *Chemical structure of DBCO-Cy3.* ***B.*** *Fluorescence signal of substrate* ***RBM8-324*** *and the diene reaction product* ***RBM8-313*** *(spotted at 1 mg/ml in DMF)* ***C.*** *Image from the scanner for this experiment.*

3.6.3. Evaluation of the SPAAC reaction as the cause of nonspecific fluorescence

The SPAAC reaction between **DBCO-PEG$_4$-TAMRA** and the azide-labeled reaction partner **RBM8-254** (Fig. 3.10, Section 3.3.1) was also investigated to evaluate this reaction as the cause of the unwanted nonspecific fluorescence with the immobilized substrate **RBM8-324**. To this end, the DBCO group was replaced by a terminal alkyne, which required the use of a Cu-catalysed azide-alkyne cycloaddition (CuAAC) reaction. In addition to the substrate and the diene reaction product, the “linker-free” amino diol **RBM8-125** and the “sphingolipid-free” protected amino acid **RBM8-305** (Fig. 3.36) were independently anchored to the array for the evaluation of a putative nonspecific fluorescence background with these fragments.

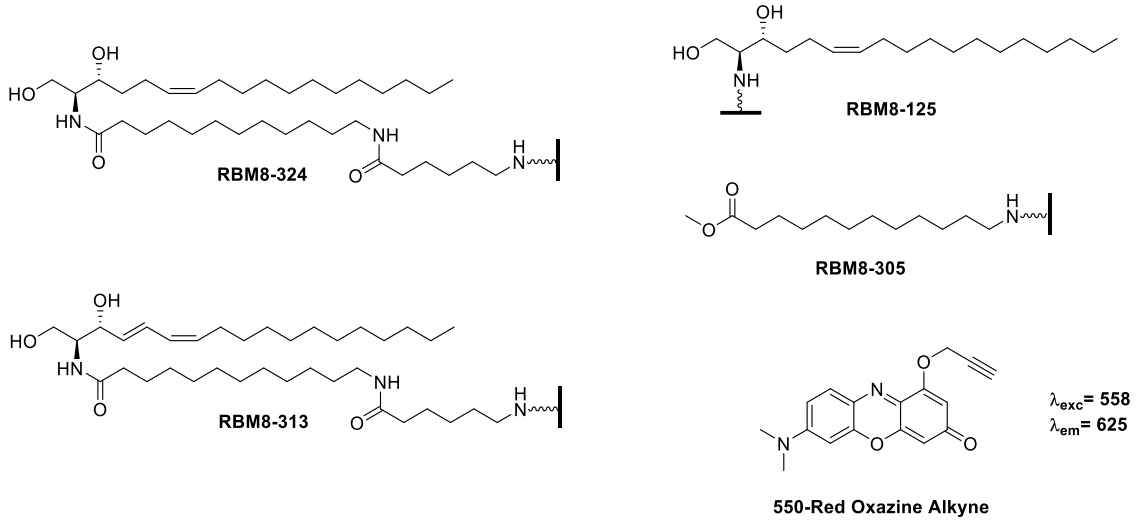

Figure 3.36. *Chemical structures of the immobilized compounds described in this section and the structure of 550-Red oxazine alkyne used to perform the CuAAC reaction in microarray format.*

Two identical slides containing compounds **RBM8-305**, **RBM8-125**, **RBM8-324** and **RBM8-313** (spotted at 1 mg/mL in DMF) were prepared in a matrix format of 3x3 spots per well; this matrix was repeated six times for each compound for a total of 24 wells per slide. Then, the slides were blocked with PVP 2% in BSA solution for 1 h and submerged into a 4 mg/mL solution of **RBM8-254** in MeOH. One of the slides was treated with an aqueous solution of **550-Red-Oxazine Alkyne** (1 µg/mL) (Fig. 3.36) in the presence of $CuSO_4$, sodium ascorbate and THTPA (*see* Experimental Section). In contrast, the other slide was submerged into **DBCO-PEG$_4$-TAMRA** (1 µg/mL in MeOH) for a standard SPAAC reaction. The results are summarized in Figure 3.37.

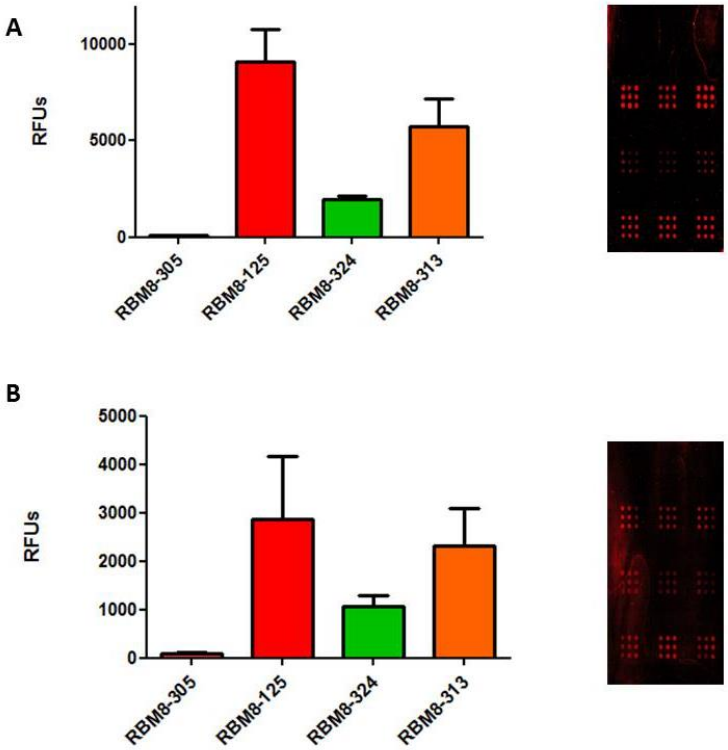

***Figure 3.37. A**. Bar graph showing the quantified fluorescent signal of compounds **RBM8-324, RBM8-313, RBM8-305** and **RBM8-125** (spotted at 1 mg/mL in DMF) using **DBCO-PEG$_4$-TAMRA** (1 µg/mL in MeOH) for the click reaction step. Bars show the average and standard deviation of signals recorded from 9 spots x 3 rows in duplicate for each compound. **B.** Bar graph showing the quantified fluorescence signal of compounds described in **A**, but using **550-Red-oxazine alkyne** (1 µg/ml in H_2O) for the click reaction step. Bars show the average and standard deviation of signals recorded from 9 spots x 3 rows in duplicate for each compound. **A,B**. Representative scanner images of half of slide with immobilization of **RBM8-305** (row 1), **RBM8-125** (row 2), **RBM8-324** (row 3) and **RBM8-313** (row 4).*

As observed in the graphics **A** and **B**, the fluorescence intensities were higher in the SPAAC reaction than in the CuAAC reaction. In addition, the non-specific binding of the background using dye Red-Oxazine observed in image **B** was attributed at the non-previous optimization of reaction conditions with some other blocking agents. Moreover, as we expected, immobilization of amino acid **RBM8-305** did not lead to fluorescence signal. Surprisingly, despite no fluorescence signal was expected for the anchored sphingoid base **RBM8-125**, its fluorescence intensity was even higher than that of the diene **RBM8-313**. This could be indicative of the sphingoid Δ^6-double bound as the origin of the background fluorescence of the substrate **RBM8-324**, for which significant fluorescence was again observed in these experiments.

In summary, these experiments made us conclude that the DBCO moiety is not related to the background fluorescence, since comparable results were obtained in the CuAAC reaction. Furthermore, the high fluorescence observed for amino diol **RBM8-125** indicates that the *cis*-Δ^6-double bond of the sphingoid base can be the origin of the unwanted background signal of the monoene substrate **RBM8-324**.

3.6.4. Evaluation of the Alder-ene reaction in solution using RBM8-125 as a model

As discussed in Section 2.1, the initial attempts to develop an HTS assay based on the use of the a dhCer derivative as Des1 substrate were unsuccessful, due to the lack of reactivity of the reaction product (Δ^4-Cer derivative) in an Alder-ene type reaction with PTAD. This finding made us assume that a Δ^6-dhCer derivative would also be unreactive under the same conditions and that it could be used safely as Des1 substrate for a subsequent Diels Alder reaction of the resulting diene with a suitable TAD derivative. However, the strong fluorescence signal observed in the above experiments with the immobilized Δ^6-dhCer **RBM8-324** and the Δ^6-sphingoid base **RBM8-125**, seemed to indicate that a specific reaction had taken place with these monoene substrates. *Surprisingly, it seems that a Δ^6-double bond can react with a TAD derivative through an Alder-ene reaction, while a Δ^4-double bond cannot*. Based on this assumption, we were prompted to check the Alder-ene reaction in solution between the sphingoid base **RBM8-125** and the triazolinedione **RBM8-254** (Fig. 3.38).

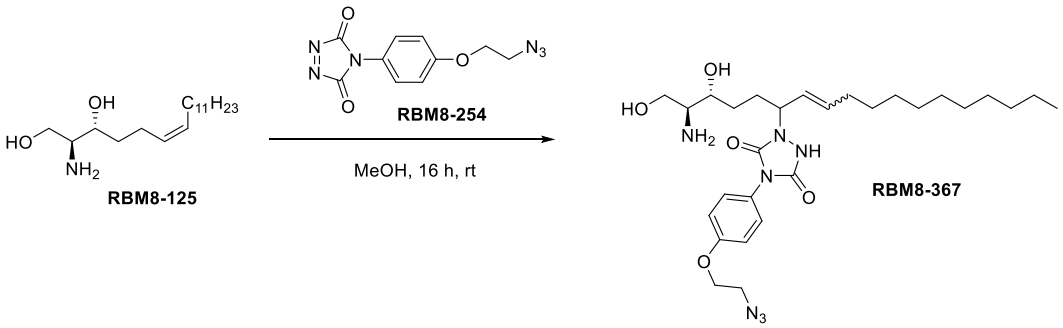

Figure 3.38. *Reaction of Δ^6-**RBM8-125** with **RBM8-254** as enophile in an Alder-ene reaction in solution.*

Much to our regret, the Δ^6-dhCer **RBM8-125** afforded the Alder-ene adduct, as evidenced by the NMR spectra and the MS of the major reaction product, which were in agreement with **RBM8-367**. This adduct was obtained as a single stereoisomer, although the configuration of the double bond was not determined. The spectral data (^{1}H NMR, HSQC and COSY) of **RBM8-367** were in agreement with the proposed structure. The regiochemistry of the Alder-ene reaction was inferred by comparison with the starting material **RBM8-125**, in particular with carbons C1 and C2 (Fig. 3.39A), which remained practically unaltered in the final adduct. This result rules out the regiochemical course depicted in Figure 3.39B, by which C2 would become an olefin carbon.

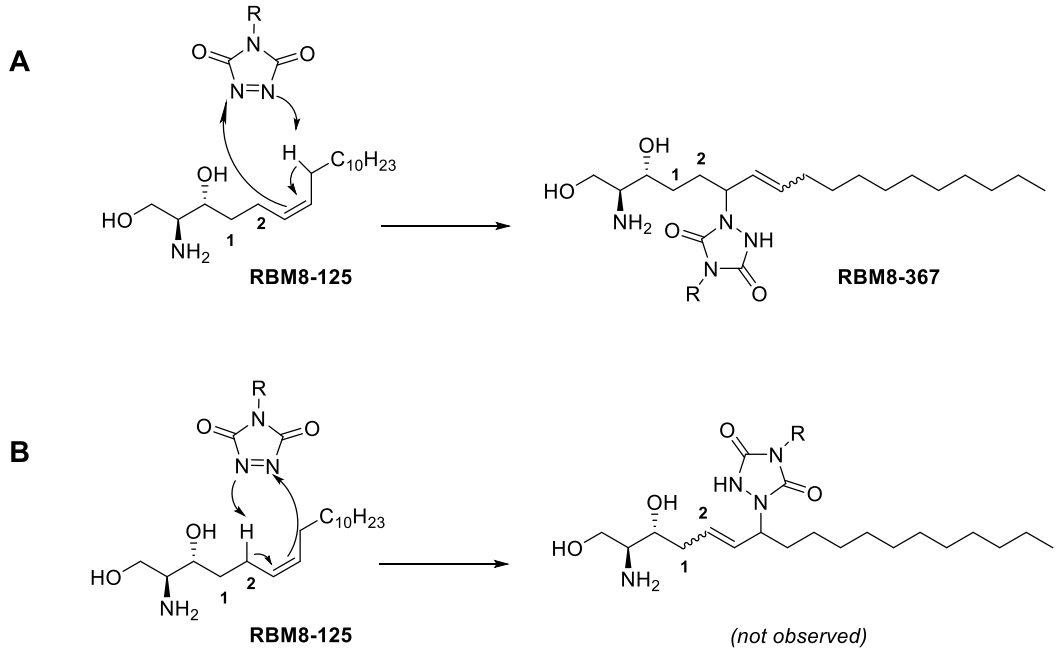

Figure 3.39. *Mechanistic postulation of the Alder-ene reaction of* ***RBM8-125*** *with* ***RBM8-254****.* ***A*** *and* ***B****. Two possible Alder-ene adducts can be obtained.*

These results made us conclude that the strong background fluorescence intensities observed in our microarray systems can be mostly attributed to an Alder-ene reaction between the TAD-azide **RBM8-254** and the Des1 substrate **RBM8-324**. This is also in agreement with the strong fluorescence signal observed for immobilized **RBM8-125**, as discussed in the previous section.

3.6.5. Immobilization of dhCer RBM8-337 and Δ^4-Cer RBM8-351

To further corroborate the above assumptions, we undertook the immobilization of the natural Δ^4-Cer **RBM8-351** and dhCer **RBM8-337**, to compare their reactivity in the microarray surface with that of Δ^6-dhCer **RBM8-324** and the $\Delta^{4,6}$ diene **RBM8-313**, which were taken as positive controls (Fig. 3.40). The synthesis of the Δ^4-Cer monoene **RBM8-351** and the dhCer **RBM8-337** was carried out following standard protocols (see Experimental) and they were immobilized on the microarray surface similarly as described in the precedent sections for the related Δ^6 monoene and $\Delta^{4,6}$ diene, **RBM8-324** and **RBM8-313**, respectively.

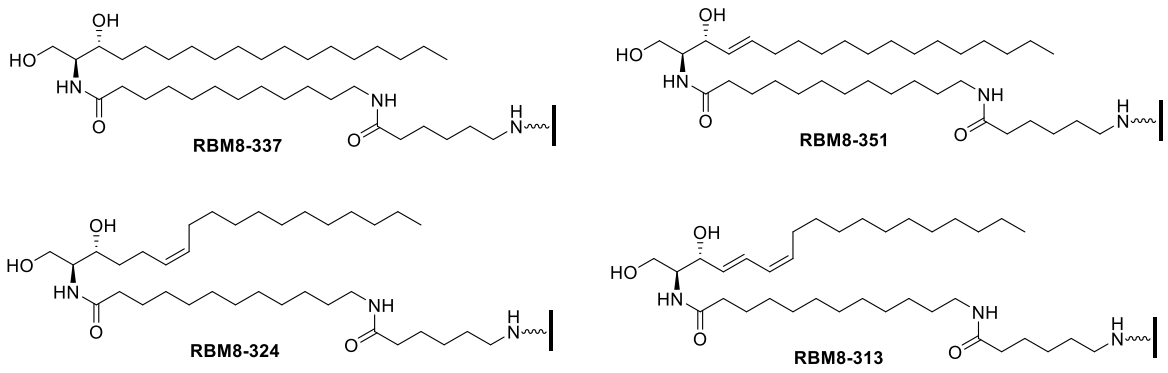

Figure 3.40. *Chemical structures of the immobilized compounds mentioned in this section.*

Compounds **RBM8-337**, **RBM8-351**, **RBM8-324** and **RBM8-313** were spotted at 1 mg/mL in DMF and the slides were next blocked with PVP 2% in BSA solution, submerged into a 4 mg/mL MeOH solution of **RBM8-254** and, finally, treated with **DBCO-PEG$_4$-TAMRA** (1 µg/ml in MeOH) for 1 h.

As shown in Figure 3.41, a strong fluorescence for the corresponding Δ^6-dhCer and $\Delta^{4,6}$-Cer **RBM8-324** and **RBM8-313**, respectively, was observed. In agreement with the results shown in the previous sections, the fluorescence signal of Δ^6-dhCer **RBM8-324** was now interpreted as a result of an Alder-ene reaction with the triazolinedione **RBM8-254**. On the other hand, the fluorescence signal of $\Delta^{4,6}$-Cer **RBM8-313** may be interpreted as result of a Diels Alder reaction with triazolinedione **RBM8-254**. Despite the Diels Alder reaction pathway from diene **RBM8-313** gives higher fluorescence intensity than that arising from the Alder-ene pathway from monoene **RBM8-324**, the strong background fluorescence makes the system unpracticable.

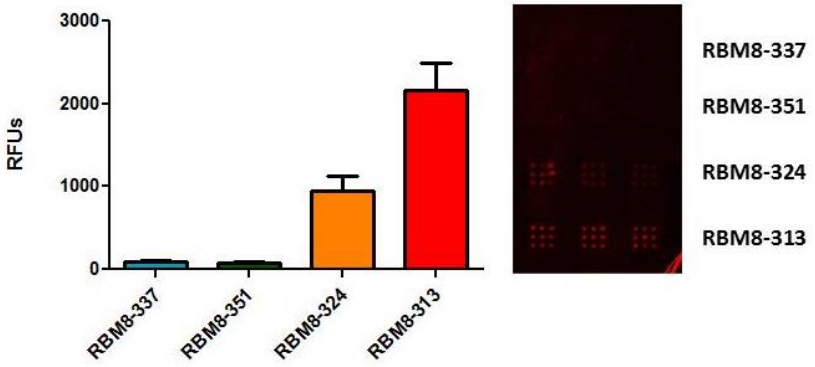

***Figure 3.41**. Fluorescence intensities of compounds **RBM8-337**, **RBM8-351**, **RBM8-324** and **RBM8-313**. Bars show the average and the standard deviation of signals recorded from 9 spots x 3 rows in duplicate of each compound. Representative scanner image of the experiment.*

Finally, we want to stress on the striking difference of reactivity between Δ^4-Cer and Δ^6-Cer towards **TAD** reagents. Thus, while Δ^6-dhCer is reactive, both in solution and on the microarray support, the isomeric Δ^4-Cer is inert under identical conditions. The allylic nature of the double bond in Δ^4-Cer may be responsible for its lack of reactivity. However, this assumption would require additional experiments that are beyond the scope of this Thesis Dissertation.

4. SUMMARY AND CONCLUSIONS

4. SUMMARY AND CONCLUSIONS

1) Depending on the geometry, the introduction of a double bond at C6 of dhCer has different effects on Des1 activity. Thus, while the *Z* isomer **RBM8-126** is desaturated by Des1 to afford the conjugated (4*E*,6*Z*)-diene **RBM8-138**, with K_M values of 7.6 (±1.0) µM and 23.03 (±1.5) pmol/h/mg, the *N*-octanoyl (*E*)-Δ^6-dhCer **RBM2-085** is a non-competitive Des1 inhibitor with a Ki value of 111.4 nM, using dhCerC_6NBD as substrate. Furthermore, in agreement with this inhibitory activity, this compound gives rise to increased dhSph levels in intact cells.

2) Preliminary experiments (Section 2.1, Approach A) were carried out to explore the suitability of a dhCer as substrate for a Des1 assay based on an Alder-ene reaction with the resulting Cer. The lack of reactivity of the model *trans*-Δ^4-Cer **RBM8-349** with TAD-azide **RBM8-254** made us disregard this approach. However, the observed Diels Alder reaction between (4*E*,6*Z*)-diene **RBM8-216** and TAD-azide **RBM8-254** (Section 2.1, Approach B), made us consider a non-natural (*Z*)-Δ^6-dhCer as a suitable substrate for the development of a Des1 assay.

3) The synthesis of the fluorescent *E* and *Z*-Δ^6-dhCer **RBM8-029** and **RBM8-126**, respectively, has been required to perform the Des1 assay in cell lysates in solution. Furthermore, the isomeric dienes **RBM8-053** and **RBM8-138**, the expected Des1 reaction products, were also synthesized and used as analytical standards. In addition, the *N*-octanoyl isomeric (*E*) and (*Z*)-dhCer substrates (**RBM2-085** and **RBM8-202**, respectively), as well as the standards (*E,E*) and (*E,Z*) dienes **RBM2-076** and **RBM8-216**, respectively, were also synthesized to study their activity as Des1 substrates in intact cells.

4) The design of an HTS assay to monitor Des1 activity on solid support has been attempted. Desaturation takes place on a microarray support, as evidenced by the conversion (checked by UPLC-TOF MS) of an immobilized substrate (*Z*-Δ^6-dhCer **RBM8-269**) into the corresponding (4*E*,6*Z*) diene.

5) A versatile fluorescent reporter system has been designed, based on a two-step reaction between triazolinedione **RBM8-254** (arising from the *in-situ* oxidation of the corresponding urazole precursor) followed by a Cu-free reaction with DBCO-PEG_4-TAMRA.

6) An optimization of the detection conditions for the immobilized diene (*E,Z*)-$\Delta^{4,6}$-Cer **RBM8-313** has been carried out. Reagent concentrations, solvents, non-specific binding, spot morphology and blocking agents have been carefully optimized. Under the best set of conditions, a LOD = 3.32 µg/mL for diene **RBM8-313** has been determined.

7) The anchored substrate (*Z*)-Δ^6-dhCer **RBM8-324** is desaturated to diene (*E,Z*)-$\Delta^{4,6}$-Cer **RBM8-313** in our microarray format using lysates from HGC27 cells. The resulting diene can be visualized by the fluorescence reporter system mentioned above (conclusion 5). However, a strong fluorescence background was observed under all the conditions tested.

8) The strong fluorescence background has been attributed to an Alder-ene reaction between TAD-azide **RBM8-254** and the olefinic (*Z*)-Δ^6 double bond present in the immobilized substrate **RBM8-324**. This has been evidenced by the formation of the Alder-ene adduct **RBM8-367** by

reaction between the model (*Z*)-Δ^6-**RBM8-125** and TAD-azide **RBM8-254** in solution. This assumption was fully corroborated on the microarray format by comparing the fluorescence of the immobilized dhCer **RBM8-337**, (*E*)-Δ^4-Cer **RBM8-351**, (Z)-Δ^6-Cer **RBM8-324**, and diene $\Delta^{4,6}$-Cer **RBM8-313** using our two-step reporter system.

9) Although the preliminary experiments (see conclusion 2) made us disregard the Alder-ene reaction between a (*E*)-Δ^4-Cer and TAD derivatives, the results obtained in this thesis indicate a surprisingly different reactivity pattern between a (*E*)-Δ^4-Cer and a (*Z*)-Δ^6-Cer towards this reaction. Unfortunately, this finding, despite its interest, has hampered the achievement of one of our final goals.

5. EXPERIMENTAL SECTION

5. EXPERIMENTAL SECTION

5.1. Synthesis and product characterization

5.1.1. General remarks

All chemicals were purchased from commercial sources and used as received unless otherwise noted. Dry solvents were obtained by passing through an activated alumina column on a Solvent Purification System (SPS). Synthesis grade or HPLC–grade solvents were used for extractions and purifications. Anhydrous EtOH and Et_3N were prepared by distillation at atmospheric pressure over calcium hydride under N_2 atmosphere, and stored over 4 Å molecular sieves and argon atmosphere. Molecular sieves were previously dried in a dry flask, heated to 120°C under high vacuum for 5 h, and refilled under argon atmosphere.

All reactions were monitored by TLC analysis using ALUGRAM® SIL G/UV_{254} precoated aluminum sheets (0.2 mm-thickness) (Macherey-Nagel). UV light was used as the visualising agent (at λ = 254 nm or λ = 365 nm), and a 5% (w/v) ethanolic solution of phosphomolybdic acid or as the developing agent. Flash column chromatography was carried out with the indicated solvents using flash-grade silica-gel 60 Å (37-70 µm). Yields refer to chromatographically and spectroscopically pure compounds, unless otherwise noted.

NMR spectra were recorded at RT on a Varian Mercury 400 instrument. The chemical shifts (δ) are reported in parts per million (ppm) relative to the solvent signal, and coupling constants (J) are reported in Hertz (Hz). The following abbreviations are used to define the multiplicities in ^{1}H NMR spectra: s = singlet, d = doublet, t = triplet, q = quartet, dd = doublet of doublets, ddd = doublet of doublet of doublets, m = multiplet and br = broad signal.

Specific optical rotations were recorded on a digital Perkin-Elmer 341 polarimeter at 25°C in 1-dm 1-mL cell, using a sodium light lamp (λ = 589 nm). Specific optical rotations values $[\alpha]_D$ are expressed in $10^{-1}\cdot deg\cdot cm^3\cdot g^{-1}$, and concentrations ($c$) are reported in g/100 mL of solvent.

High Resolution Mass Spectrometry analyses were recorded on an Acquity UPLC system coupled to a LCT Premier orthogonal accelerated time-of-flight mass spectrometer (Waters) using electrospray ionization (ESI) technique. Data were acquired in positive ESI. Samples were analysed by FIA (Flow Injection Analysis), using CH_3CN/water (70:30) as mobile phase. Samples were analysed using a 10 µL volumee injection. *m/z* ratios are reported in atomic mass units.

HPLC analyses were performed with an Alliance apparatus coupled to a fluorescence detector using a C18 column (Kromasil, 100 C18, 5µm, 15x0.40 cm, Tracer) precolumn equipped (precolumn ODS, Tracer). Compounds were eluted with 25% H_2O and 75% acetonitrile, flowing at 1 mL/min. The detector was set at an excitation wavelength of 465 nm and measure the emission wavelength at 530 nm. Each sample was run for up to 22 min.

5.1.2. Synthesis of (*E*)-Δ^6-dhCer analogues

(4*S*)-*tert*-butyl 4-(1-hydroxypent-4-en-1-yl)-2,2-dimethyloxazolidine-3-carboxylate (RBM8-005)

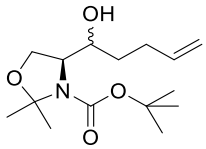

3-Butenylmagnesium bromide (0.5M solution in THF, 6.15 mL, 3.1 mmol) was added dropwise to a cooled solution of Garner's aldehyde[180] (500 mg, 2.1 mmol) in anhydrous THF (7 mL) at -78 °C. The reaction mixture was stirred at that temperature for 2 h and then allowed to warm to rt. Next, saturated aqueous NH_4Cl was carefully added. The aqueous phase was extracted with Et_2O (3 x 15 mL). The combined organic layers were dried over $MgSO_4$, filtered, and concentrated *in vacuo*. The resulting residue was purified by flash chromatography (hexane/EtOAc 80:20) to give 376 mg (1.31 mmol, 76%) of **RBM8-005** as an inseparable mixture of diastereomers.

^{1}H NMR (δ, 400 MHz, $CDCl_3$, mixture of diastereomers (2*S*, 3*R,S*): 5.88-5.76 (m, 1H), 5.03 (d, J= 17.0 Hz, 1H), 4.95 (d, J= 9.5 Hz, 1H), 4.15-3.63 (m, 4H), 2.31-2.26 (m, 1H), 2.22-2.08 (m, 1H), 1.67-1.35 (m, 17H).

^{13}C NMR (δ, 101 MHz, $CDCl_3$, mixture of diastereomers): 155.8, 138.1, 115.2, 99.2, 79.5, 74.0, 70.6, 65.5, 33.7, 30.9, 29.9, 29.0, 28.5.

HRMS calculated for $C_{15}H_{27}NNaO_4$: 308.1838 $[M+ Na]^+$. Found: 308.1823.

Analytical data match those reported for this compound in the literature.[181]

(*S*)-t*ert*-butyl 4-((*R*)-1-((*R*)-2-methoxy-2-phenylacetoxy)pent-4-en-1-yl)-2,2-dimethyloxazolidine-3-carboxylate (RBM8-009)

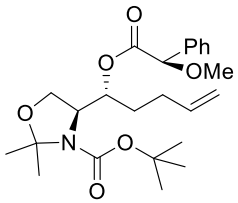

A solution of (*R*)-α-methoxy-α-phenylacetic acid (58 mg, 0.35 mmol), EDC (34 mg, 0.18 mmol) and DMAP (22 mg, 0.18 mmol) in dry CH_2Cl_2 (3 mL) was added dropwise to a solution of **RBM8-005** (50 mg, 0.18 mmol) in CH_2Cl_2 (2 mL) under argon. The reaction was stirred at rt for 7 h. The organic layer was sequentially washed with 1*N* HCl, sat $NaHCO_3$, and water (2 x 1mL each), then dried over $MgSO_4$ and concentrated under reduced pressure affording crude **RBM8-009** as an approximate 4:1 mixture of two diastereomers. After careful chromatographic purification with hexane/EtOAc 90:10, major diastereomer

(2*S*,3*R*)(*R*)-**RBM8-009** was isolated in a 57% yield. Following the methodology of Riguera,[182] the absolute configuration at C3 was assigned as *R*.

R_f (2*S,3R*)(*R*): 0.54; **R_f** (2*S,3S*)(*R*): 0.40

^{1}H NMR (δ, 400 MHz, $CDCl_3$. peaks assigned by HSQC): (*S,R,R*) 7.41-7.37 (m, 2H), 7.31-7.23 (m, 3H), 5.77-5.62 (m, 1H, C6H), 5.21 (br, 1H, C3H), 4.94-4.87 (m, 2H, $C7H_2$), 4.70 (s, 1H, CαH), 3.93-3.51 (m, 3H, C2H+$C1H_2$), 3.36 (s, 3H, OMe), 2.07-1.88 (m, 2H,$C5H_2$), 1.66-1.52 (m, 2H, $C4H_2$), 1.40 (s, 9H, 2x$C9H_3$+1x$C12H_3$)(*), 1.32 (broad, 1H, 1x$C12H_3$)(*), 1.17 (s, 3H, 1x$C12H_3$)(*);

^{13}C NMR (δ, 101 MHz, $CDCl_3$): 170.0 (C12), 152.9+151.9 (C10)(*), 137.5+137.0 (C6)(*), 136.1 (Cq arom), 128.7, 128.5, 127.3 (C arom), 115.5+115.0 (C7)(*), 94.2+93.7 (C8)(*), 82.8 (Cα), 80.3 (C11), 73.6+73.1 (C3)(*), 63.5 (C1), 59.2 (C2), 57.3 (OMe), 31.5+31.0 (C4)(*), 29.6 (C5), 28.3 (2xC9 + 1xC12), 26.8+25.9 (1xC12)(*), 24.3+23.0 (1xC12)(*)

(*): signal splitting due to rotameric equilibria; see NMR traces for numbering

HRMS (ESI): calculated for $C_{24}H_{36}NO_6$ $[M+H]^+$ 434.2543; found 434.2540.

(*S*)-t*ert*-butyl 4-((*R,E*)-1-((*R*)-2-methoxy-2-phenylacetoxy)hexadec-4-en-1-yl)-2,2-dimethyloxazolidine-3-carboxylate (RBM8-027)

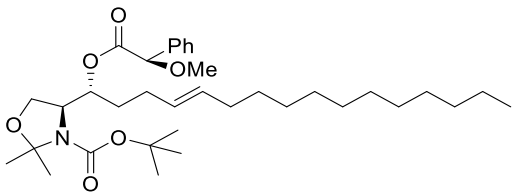

A two-necked round bottom flask fitted with a reflux condenser under argon atmosphere, was charged with **RBM8-009** (550 mg, 1.26 mmol) and tridecene (1.92 mL, 8.11 mmol) in previously degassed CH_2Cl_2 (15 mL). Next, Grubb's 2nd generation catalyst (68 mg, 0.08 mmol) was added portionwise, and the resulting mixture was stirred at reflux temperature for 5 h. The mixture was next allowed to cool down to rt and concentrated in vacuo. Purification of the crude with hexane/EtOAc 80:20 afforded **RBM8-027** (393 mg, 53%) as a mixture of two isomers (d.r. (*E:Z*) = 6:1; major *E*-isomer: **R_f** = 0.53).

^{1}H NMR (δ, 400 MHz, $CDCl_3$) for major *E* isomer: 7.43-7.39 (m, 2H), 7.34-7.26 (m, 3H), 5.37-5.23 (m, 4H), 4.72 (s, 1H), 3.95-3.52 (m, 4H), 3.38 (s, 3H), 1.97-1.85 (m, 4H), 1.62-1.50 (m, 2H), 1.42 (s, 9H), 1.39-1.15 (m, 22H), 0.85 (m, 3H).

^{13}C NMR (δ, 101 MHz, $CDCl_3$) for major *E* isomer: 170.1, 152.8/151.6 (rotamers), 135.9, 131.2, 130.8, 128.7/128.5 (rotamers), 127.3, 94.3/93.7 (rotamers), 82.9, 80.3, 73.8 (broad due to rotamers), 63.5, 59.2, 57.4, 31.9, 29.6-29.5 (12 C), 28.3, 27.2, 14.1

HRMS (ESI): calculated for $C_{35}H_{58}NO_6$ $[M+H]^+$ 588.4264; found 588.4273.

(*S*)-t*ert*-butyl 4-((*R,E*)-1-hydroxyhexadec-4-en-1-yl)-2,2-dimethyloxazolidine-3-carboxylate (RBM8-028)

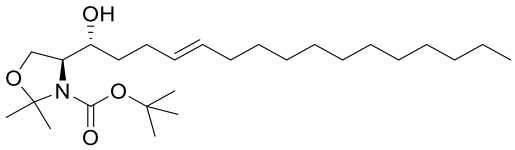

To a solution of **RBM8-027** (389 mg, 0.66 mmol) in MeOH (10 mL), was added K_2CO_3 (281 mg, 2.03 mmol). The mixture was stirred for 6 h at rt. Next, MeOH was concentrated and the mixture was diluted with EtOAc, washed with water and brine, dried over $MgSO_4$, filtered, and concentrated *in vacuo*. Purification of the crude with hexane/EtOAc 8:2 afforded **RBM8-028** (**R_f** = 0.45,75%) as a colourless oil.

^{1}H NMR ($CDCl_3$): δ 5.48-5.33 (m, 2H), 4.12-3.63 (m, 5H), 2.20 (brs, 2H), 2.12-1.99 (m, 2H), 1.98-1.90 (m, 2H), 1.55 (brs, 3H), 1.52-1.38 (s, 12H), 1.33-1.17 (m, 18H), 0.85 (m, 3H),

^{13}C NMR ($CDCl_3$): δ 131.4, 129.5, 94.3, 72.3, 64.6, 62.5, 32.6, 31.9, 29.8, 29.78, 29.72, 29.6, 29.5, 29.3, 29.1, 29.0, 28.3, 26.4, 22.6, 14.1.

HRMS (ESI): calculated for $C_{26}H_{50}NO_4$ $[M+H]^+$ 440.3740; found 440.3752.

(1*R*,7a*S*)-1-(but-3-en-1-yl)-5,5-dimethyldihydro-1*H*,3*H*,5*H*-oxazolo[3,4-c]oxazol-3-one (RBM8-139)

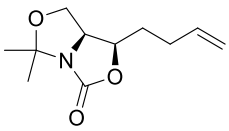

A solution of methyltriphenylphosphonium bromide (167 mg, 0.47 mmol) in anhydrous THF (10 mL) was added KHDMS (94 mg, 0.47 mmol) at 0°C. The mixture was stirred for 30 min under argon atmosphere and then warmed to rt. A solution of aldehyde **RBM8-105** (50 mg, 0.23 mmol) in anhydrous THF (5 mL) was added. After vigorous stirring at rt for 3 h, the reaction mixture was quenched by addition of aqueous saturated NH_4Cl (10 mL). The aqueous phase was extracted with EtOAc (3 x 10 mL), and the combined organic layers were dried over $MgSO_4$ and filtered. Concentration under reduced pressure afforded a crude, which was

purified by flash chromatography (10:0 to 7:3 hexane/EtOAc gradient) to afford 27 mg (0.13 mmol, 56%) of **RBM8-139** as a colourless oil.

^{1}H NMR ($CDCl_3$): δ 5.74 (ddt, *J* = 17.1, 10.2, 6.7 Hz, 1H), 5.14 – 4.91 (m, 2H), 4.64 – 4.52 (m, 1H), 4.27 (ddd, *J* = 15.8, 9.2, 5.9 Hz, 1H), 3.87 (dt, *J* = 17.3, 8.7 Hz, 1H), 3.68 (t, *J* = 8.7 Hz, 1H), 2.30 – 2.18 (m, 1H), 2.16 – 2.05 (m, 1H), 1.86 – 1.74 (m, 1H), 1.68 (s, 3H), 1.62 – 1.51 (m, 1H), 1.40 (s, 3H).

^{13}C NMR ($CDCl_3$): δ 156.7, 136.3, 116.2, 94.7, 73.8, 63.6, 61.1, 29.9, 29.7, 28.1, 23.4.

HRMS (ESI): calculated for $C_{11}H_{18}NO_3$ $[M+H]^+$ 212.1287; found 212.1272.

(1*R*,7aS)-5,5-dimethyl-1-((*E*)-pentadec-3-en-1-yl)dihydro-1H,3H,5H-oxazolo[3,4-c]oxazol-3-one (RBM8-140)

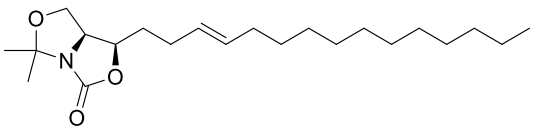

A two necked round bottom flask fitted with a reflux condenser under argon atmosphere, was charged with **RBM8-139** (18 mg, 0.09 mmol) and tridecene (0.12 mL, 0.50 mmol) in previously degassed CH_2Cl_2 (5 mL). Next, Grubb's 2nd generation catalyst (5 mg, 0.01 mmol) was added portionwise, and the resulting mixture was stirred at reflux temperature for 5 h. The mixture was next allowed to cool down to rt and concentrated in vacuo. Purification of the crude with hexane/EtOAc 80:20 afforded **RBM8-140** (20 mg, 63%) as a colourless oil (d.r. (*E/Z*) = 6/1).

^{1}H NMR ($CDCl_3$): major isomer (*E*) δ 5.45 (t, *J* = 10.9 Hz, 1H), 5.39 – 5.26 (m, 1H), 4.66 – 4.50 (m, 1H), 4.36 – 4.20 (m, 1H), 3.89 (dd, *J* = 8.5, 6.2 Hz, 1H), 3.69 (t, *J* = 8.7 Hz, 1H), 2.17 (d, *J* = 6.3 Hz, 1H), 2.11 – 2.00 (m, 1H), 1.96 (dd, *J* = 13.8, 6.9 Hz, 2H), 1.79 (d, *J* = 8.7 Hz, 1H), 1.70 (s, 3H), 1.65 – 1.45 (m, 2H), 1.42 (s, 3H), 1.38 – 1.10 (m, 17H), 0.86 (t, *J* = 6.8 Hz, 3H).

^{13}C NMR ($CDCl_3$): major isomer (*E*) δ 156.8, 132.7, 127.5, 94.8, 73.8, 63.6, 61.2, 32.5, 31.9, 30.6, 29.64, 29.60, 29.59, 29.46, 29.40, 29.3, 29.2, 28.6, 28.2, 23.4, 22.7, 14.1.

HRMS (ESI): calculated for $C_{22}H_{40}NO_3$ $[M+H]^+$ 366.3008; found 366.3011.

***N*-((2*S*,3*R*,*E*)-1,3-dihydroxyoctadec-6-en-2-yl)-6-((7-nitrobenzo[c][1,2,5]oxadiazol-4-yl)amino)hexanamide (RBM8-029)**

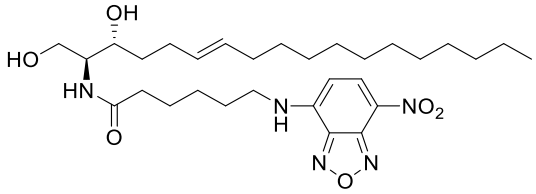

To a solution of **RBM8-028** (52 mg, 0.12 mmol) in MeOH (3 mL) was added acetyl chloride (0.2 mL, 6 % volumee) and the mixture was vigorous stirred at rt for 1 h. Then, MeOH was concentrated under reduced pressure and the crude was used in the next step without further purification.

A solution of EDC (36 mg, 0.19 mmol), HOBt (10 mg, 0.14 mmol) and C_6NBD acid (38 mg, 0.13 mmol) in anhydrous CH_2Cl_2 (2 mL) was stirred under argon atmosphere at rt for 10 min, and next added dropwise to a solution of the crude amino diol (0.12 mmol) and Et_3N (40 µL,0.24 mmol) in anhydrous CH_2Cl_2 (2 mL). The reaction mixture was stirred at rt for 4 h under argon atmosphere. The mixture was diluted by addition of CH_2Cl_2 (5 mL) and washed successively with water (10 mL) and brine (10 mL). The organic layer was dried over $MgSO_4$, and filtered. Concentration under reduced pressure afforded a residue, which was purified by flash chromatography with hexane/EtOAc (9:1 to 7:3) followed by CH_2Cl_2/MeOH (100:0 to 97:3) to afford **RBM8-029** (22 mg, 32% in two steps) as an orange solid.

R_f =0.40 (hexane/EtOAc 7:3)

^{1}H NMR ($CDCl_3$): δ 8.44 (d, *J*= 8.6 Hz, 1H), 6.88 (brs, 1H), 6.53 (brs, 1H), 6.14 (d, *J*= 8.5 Hz, 1H), 5.42 (dt, *J*= 16.5, 6.4 Hz, 2H), 4.01 (m, 1H), 3.91-3.70 (m, 3H), 3.55-3.45 (m, 2H), 2.29 (t, *J*= 6.6 Hz, 2H), 2.18 (dt, *J*= 14.2, 6.9 Hz, 1H), 2.08 (dt, *J*= 14.2, 6.9 Hz, 1H), 1.94 (q, *J*= 6.4 Hz, 2H), 1.86-1.69 (m, 4H), 1.65-1.45 (m, 4H), 1.34-1.14 (m, 18H), 0.85 (t, *J*= 6.7 Hz, 3H).

^{13}C NMR ($CDCl_3$): δ 172.9, 144.2, 143.9, 136.5, 132.2, 128.9, 123.4, 98.6, 73.9, 62.4, 53.6, 43.6, 36.0, 34.2, 32.5, 31.8, 29.7, 29.6, 29.5 (2C), 29.3, 29.2, 27.8, 26.2, 24.7, 22.7, 14.1.

HRMS (ESI): calculated for $C_{30}H_{50}N_5O_6$ $[M + H]^+$ 576.3761; found 576.3757.

Analytical HPLC-FD: Column (Kromasil 100, C18, 5 µm, 15 x 0.4 cm); Isocratic method 75:25 ACN:H_2O; R_t: 16.4 min.; Sample volumee: 10 µL; **RBM8-029** (1mg/ mL in MeOH); λ_{abs}= 440; λ_{em}= 540

$[\alpha]^{20}_D$ = - 8 (*c* = 1.1, MeOH).

***N*-((2*S*,3*R*,*E*)-1,3-dihydroxyoctadec-6-en-2-yl)octanamide (RBM2-085)**

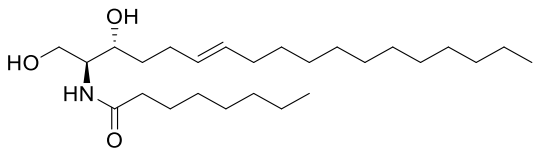

To a solution of **RBM8-028** (52 mg, 0.12 mmol) in MeOH (3 mL) was added acetyl chloride (0.2 mL, 6 % volume) and the mixture was vigorously stirred at rt for 1 h. Then, MeOH was concentrated under reduced pressure and the crude was used in the next step without further purification.

A solution of EDC (36 mg, 0.19 mmol), HOBt (10 mg, 0.14 mmol) and octanoic acid (55 mg, 0.13 mmol) in anhydrous CH_2Cl_2 (2 mL) was stirred under argon atmosphere at rt for 10 min, and next added dropwise to a solution of the crude amino diol (0.12 mmol) and Et_3N (40 µL,0.24 mmol) in anhydrous CH_2Cl_2 (2 mL). The reaction mixture was stirred at rt for 4 h under argon atmosphere. The mixture was diluted by addition of CH_2Cl_2 (5 mL) and washed successively with water (10 mL) and brine (10 mL). The organic layer was dried over $MgSO_4$, and filtered. Concentration under reduced pressure afforded crude compound, which was purified by flash chromatography with CH_2Cl_2/MeOH (100:0 to 93:7) to afford **RBM2-085** (30 mg, 60%) as a yellow oil.

R_f = 0.35, hexane/EtOAc 7:3.

^{1}H NMR ($CDCl_3$): δ 6.15 (d, J=8.0 Hz, 1H), 5.52-5.34 (m, 2H), 3.98 (t, J=6.0 Hz, 1H), 3.95-3.89 (m, 1H), 3.88-3.75 (m, 2H), 2.66 (brs, 1H), 2.59 (brs, 1H), 2.24 (t, J=8.0 Hz, 2H), 2.10 (q, J=7.0 Hz, 2H), 1.97 (q, J=8.5 Hz, 2H), 1.70-1.49 (m, 4H), 1.41-1.14 (m, 26H), 0.88 (t, J=7.0 Hz, 6H).

^{13}C NMR ($CDCl_3$): δ 174.1, 132.0, 129.2, 73.0, 65.8, 53.3, 37.1, 34.2, 32.7, 32.1, 31.9, 29.9, 29.8, 29.7, 29.7, 29.5, 29.4, 29.2, 29.0, 26.0, 22.9, 22.8, 14.3, 14.2.

HRMS (ESI): calculated for $C_{26}H_{52}NO_3$ $[M + H]^+$ 426.3947; found 426.3954.

$[\alpha]^{20}_D$ = -1.3 (*c* = 1.2, $CHCl_3$).

5.1.3. Synthesis of (*Z*)-Δ^6-dhCer analogues

***tert*-Butyldimethyl(prop-2-yn-1-yloxy)silane (RBM8-090)**

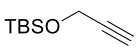

To a solution of propargyl alcohol (1.4 mL, 23.4 mmol) in dry CH_2Cl_2 (10 mL) under argon was added *tert*-butyldimethylsilyl chloride (3.5 g, 23.4 mmol) followed by imidazole (3.2 g, 46.8 mmol). The flask was equipped with a condenser after which the solution was heated to reflux.

After 4 h, the starting material was consumed (as checked by TLC) and the flask was allowed to cool to rt. The reaction was quenched with 10 mL of ice-cold water. The resulting mixture was filtered through a pad of Celite®. The filtrate was transferred to a separating funnel and the phases were separated. The aqueous phase was extracted 3 x 10 mL CH_2Cl_2. The combined organic phases were washed with brine, dried over $MgSO_4$ and the solvent was evaporated, to afford 3.9 g (98%) of a colourless liquid without further purification. The physical and spectroscopic data of compound **RBM8-090** were identical to those reported in the literature.[183]

^{1}H NMR ($CDCl_3$): δ 4.31 (d, *J*= 2.4 Hz, 2H), 2.38 (t, *J*= 2.5 Hz, 1H), 0.91 (s, 9H), 0.13 (s, 6H)

(*S*)-t*ert*-Butyl 4-((*R*)-4-((*tert*-butyldimethylsilyl)oxy)-1-hydroxybut-2-yn-1-yl)-2,2-dimethyloxazolidine-3-carboxylate (RBM8-092)

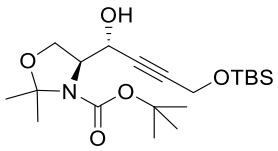

A dried flask under argon was charged with **RBM8-090** (0.83 g, 4.9 mmol) and 15 mL of dry THF. The solution was cooled to -78 °C and *n*BuLi (1.9 mL, 4.6 mmol, 2.5 M hexane) was added over 10 min. The resulting mixture was stirred for 1 h. Then Garner's aldehyde[180] (0.9 g, 3.75 mmol) was added to the mixture with 10 mL of dry THF. The resulting solution was stirred for 4 h and quenched by adding sat. NH_4Cl. The cooling bath was removed and replaced by a warm water bath. After reaching rt, the aqueous layer was extracted with EtOAc (2 x 30 mL). The combined organic phases were dried over $MgSO_4$ and concentrated to yield 1.5 g of a crude product as a mixture of two diastereomers (**d.r.** (erythro/threo) = 36/1). Purification of the crude by flash chromatography with hexane/EtOAc (10:0 to 9:1) allowed the isolation of **RBM8-092** (1.3 g, 89 % yield, single diastereomer) as a yellow oil. The compound was synthesized as reported in the literature.[183]

^{1}H NMR ($CDCl_3$): δ 4.73 (br, s, 1H), 4.56 (br, s, 1H), 4.33 (s, 2H), 4.10 (br, 2H), 3.93 (br, 1H), 1.49 (m, 15H), 0.88 (s, 9H), 0.09 (s, 6H).

^{13}C NMR ($CDCl_3$): δ 154.5, 94.9, 84.5, 82.5, 81.3, 65.0, 64.2, 62.5, 51.6, 28.3, 26.5, 25.8, 25.7, 25.2, 17.6, -5.22.

HRMS (ESI): calcd. for $C_{19}H_{36}NO_5Si$ $[M + H]^+$ 386.2363; found 386.2363.

$[\alpha]^{20}_D$ = -33 (*c* = 1.36, $CHCl_3$)

(*S*)-*tert*-Butyl 4-((*R*)-4-((tert-butyldimethylsilyl)oxy)-1-hydroxybutyl)-2,2-dimethyloxazolidine-3-carboxylate (RBM8-095)

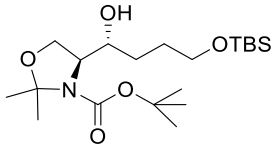

Rhodium on alumina (36 mg, 18% by weight) was added to a solution of **RBM8-092** (200 mg, 0.5 mmol) in freshly degassed MeOH (10 mL). The resulting mixture was vigorously stirred at rt for 3 h under H_2 (1 atm). The mixture was next filtered through a plug of Celite, and the solid was rinsed with MeOH (3 x 10 mL). The combined filtrates were concentrated in vacuo to afford 300 mg of a crude, which was purified by flash chromatography (8/2 hexane/EtOAc) to give 201 mg (99%) of **RBM8-095** as a yellow oil.

^{1}H NMR ($CDCl_3$): δ 4.11-3.77 (m, 4H), 3.69 (br, 1H), 3.61 (t, *J* = 4.9 Hz, 2H), 1.68-1.49 (m, 4H), 1.48-1.34 (m, 15H), 0.84 (s, 9H), 0.02 (s, 6H).

^{13}C NMR ($CDCl_3$): δ 153.9, 94.1, 80.7, 72.4, 64.5, 63.1, 62.3, 28.3, 26.4, 25.8, 18.2, -5.4.

HRMS (ESI): calcd. for $C_{20}H_{42}NO_5Si$ $[M + H]^+$ 404.2832; found 404.2835.

$[\alpha]^{20}_D$ = -19.8 (*c* = 1.0, $CHCl_3$).

(1*R*,7a*S*)-1-(3-((tert-Butyldimethylsilyl)oxy)propyl)-5,5-dimethyldihydro-1H-oxazolo[3,4-c]oxazol-3(5H)-one (RBM8-097)

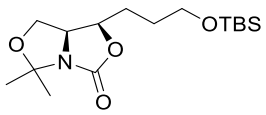

To a solution of **RBM8-095** (370 mg, 0.9 mmol) in anydrous THF (15 mL) was added to a suspension of NaH (60% in mineral oil, 370 mg, 9.2 mmol) in anhydrous THF (5 mL) at rt. The reaction mixture was vigorously stirred for 16 h at 50 °C and under argon atmosphere. The reaction was next quenched by dropwise addition of aqueous sat. $NaHCO_3$ at 0 °C, until H_2 evolution was not observed. The aqueous phase was next extracted with EtOAc (3 x 40 mL). The combined organic layers were dried over $MgSO_4$, filtered, and concentrated in vacuo, giving a crude which was purified by flash chromatography (80:20 hexane/EtOAc, $\mathbf{R_f}$ = 0.45) to afford 258 mg (85%) of **RBM8-097**.

^{1}H NMR ($CDCl_3$): δ 4.61 (td, *J* = 8.3, 4.9 Hz, 1H), 4.30 (td, *J* = 8.5, 6.3 Hz, 1H), 3.90 (dd, *J* = 8.5, 6.2 Hz, 1H), 3.79-3.49 (m, 3H), 1.78-1.58 (m, 5H), 1.58-1.46 (m, 1H), 1.41 (s, 3H), 0.85 (s, 9H), 0.03 (s, 6H).

^{13}C NMR ($CDCl_3$): δ 156.8, 94.7, 74.4, 63.5, 62.1, 61.2, 28.7, 28.2, 27.4, 25.9, 23.4, 18.2, -5.4.

HRMS (ESI): calcd. for $C_{16}H_{32}NO_4Si$ $[M + H]^+$ 330.2101; found 330.2016

$[\alpha]^{20}_D$ = -29.8 (*c* = 1.1, $CHCl_3$)

(1*R*,7a*S*)-1-(3-Hydroxypropyl)-5,5-dimethyldihydro-*1H,3H,5H*-oxazolo[3,4-*c*]oxazol-3-one (RBM8-103)

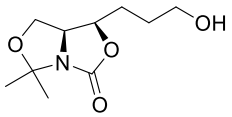

A solution of TBAF (0.61 mL, 0.61 mmol, 1M in THF) was added to a solution of **RBM8-097** (200 mg, 0.61 mmol) in THF (5 mL) at 0°C. The reaction was stirred for 1 h at rt. An excess of aqueous NH_4Cl was added and the aqueous phase was extracted with EtOAc (3 x 10 mL). The combined organic layers were dried over $MgSO_4$, filtered and concentrated *in vacuo*, giving 86% yield of **RBM8-103**, which was used in the next step without further purification.

^{1}H NMR ($CDCl_3$): δ 4.65 (qd, *J*= 8.8, 8.2, 4.8 Hz, 1H), 4.34 (td, *J*= 8.5, 6.2 Hz, 1H), 3.93 (dd, *J*= 8.5, 6.2 Hz, 1H), 3.82-3.62 (m, 3H), 1.82-1.73 (m, 2H), 1.72 (s, 3H), 1.71-1.58 (m, 2H), 1.44 (s, 3H).

^{13}C NMR ($CDCl_3$): δ 156.8, 94.8, 74.5, 63.6, 61.8, 61.2, 28.8, 28.1, 27.3, 23.4.

HRMS (ESI): calcd. for $C_{10}H_{17}NNaO_4$ $[M + Na]^+$ 238.1055; found 238.1048.

$[\alpha]^{20}_D$ = -25.7 (*c* = 1.09, $CHCl_3$).

3-((1*R*,7a*S*)-5,5-Dimethyl-3-oxodihydro-1H,3H,5H-oxazolo[3,4-c]oxazol-1-yl)propanal (RBM8-105)

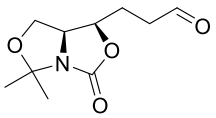

To a solution of **RBM8-103** (100 mg, 0.46 mmol) in EtOAC (20 mL) was added 2-iodoxybenzoic acid (195 mg, 0.70 mmol) at rt and under argon atmosphere. The reaction was warmed to 85 °C and stirred at this temperature for 16 h. Then the mixture was cooled down to rt and left in an ice-bath for additional 2 h. The suspension was filtered through a medium porosity sintered-glass funnel, the solid was repeatedly rinsed with EtOAC, and the filtrates were concentrated in vacuo. Purification of the crude with CH_2Cl_2/MeOH (100% to 95%) gave 85 mg (87%) of **RBM8-105**.

^{1}H NMR ($CDCl_3$): δ 9.71 (s, 1H), 4.53 (ddd, *J* = 10.1, 8.1, 3.9 Hz, 1H), 4.36 (td, *J*= 8.3, 6.3, 1H), 3.87 (dd, *J*=, 8.7, 6.3, 1H), 3.68 (t, *J*= 8.6, 1H), 2.77-2.52 (m, 2H), 1.90-1.73 (m, 2H), 1.61 (s, 3H), 1.34 (s, 3H).

^{13}C NMR ($CDCl_3$): δ 220.2, 156.3, 94.8, 73.6, 63.4, 61.1, 39.9, 27.8, 23.4, 23.1.

HRMS (ESI): calcd. for $C_{10}H_{16}NO_4$ $[M + H]^+$ 214.1079; found 214.1059.

$[\alpha]^{20}_D$ = -12.02 (*c* = 1.0, $CHCl_3$)

Dodecyltriphenylphosphonium bromide (RBM8-104)

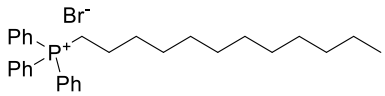

To a 50 mL necked round bottom flask fitted with a reflux condenser, PPh_3 (7.63 g, 29 mmol) was added portionwise to neat 1-bromododecane (2.35 mL, 9.8 mmol). The reaction mixture was heated at 90°C, and allowed to stir at this temperature overnight. After cooling down to rt, the resulting precipitate was washed with hexane and Et_2O successively (x 10) to afford 4.9 g (9.57 mmol, 98%) of a white solid.[184]

^{1}H NMR ($CDCl_3$): δ 8.23-7.28 (m, 15H), 3.38 (d, *J*= 2.6 Hz, 2H), 1.64 (s, 2H), 1.53 (s, 2H), 1.38-1.16 (m, 16H), 0.87 (t, *J*= 6.9 Hz, 3H).

^{13}C NMR ($CDCl_3$): δ 134.83, 134.80, 133.4, 133.3, 130.2, 130.0, 119.0, 118.2, 31.6, 30.2, 30.1, 29.3, 29.1, 29.0, 28.5, 22.3, 22.2, 21.5, 21.0, 13.1.

(1*R*,7a*S*)-5,5-Dimethyl-1-((*Z*)-pentadec-3-en-1-yl)dihydro-1H-oxazolo[3,4-c]oxazol-3(5*H*)-one (RBM8-123)

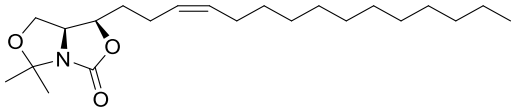

Method A: (Wittig reaction, from Fig. 2.7) A solution of dodecyltriphenylphosphonium bromide (300 mg, 0.58 mmol) in anhydrous THF (10 mL) and HMPA (0.75 mL) was cooled down to -78°C, followed by dropwise addition of *n*BuLi (0.24 mL, 0.61 mmol, 2.5 M in hexane) over 30 min. under argon. The resulting mixture was allowed to warm to 0°C, and next stirred for 30 min. After cooling down to -78°C, a solution of aldehyde **RBM8-105** (78 mg, 0.36 mmol) in anhydrous THF (5 mL) was added dropwise. After vigorous stirring at -78°C for 15 min, the reaction was allowed to warm to rt and kept at this temperature for 2 h under stirring. The reaction mixture was next quenched by addition of aqueous saturated NH_4Cl (10 mL), and stirred for 30 min. The aqueous phase was extracted with EtOAc (3 x 10 mL), and the combined organic layers were dried over $MgSO_4$ and filtered. Concentration under reduced pressure afforded a crude, which was purified by flash chromatography (10:0 to 8:2 hexane/EtOAc gradient) to afford 83 mg (0.23 mmol, 64%) of **RBM8-123** as a colourless oil.[185] (d.r. (E/Z) = 1/30).

Method B: (Cross Metathesis reaction, from Fig. 2.8) A two necked round bottom flask fitted with a reflux condenser under argon atmosphere, was charged with **RBM8-139** (18 mg, 0.09 mmol) and 1-tridecene (0.12 mL, 0.50 mmol) in previously degassed CH_2Cl_2 (5 mL). Next, ruthenium catalyst (5 mg, 0.06 mmol) was added portionwise, and the resulting mixture was stirred at reflux temperature for 5 h. The mixture was next allowed to cool down to rt and concentrated in vacuo. Purification of the crude with hexane/EtOAc 80:20 afforded **RBM8-123** (19 mg, 60%) as a colourless oil (d.r. (*E/Z*) = 1/8).

R_f = 0.25 in hexane/EtOAc 9:1

^{1}H NMR ($CDCl_3$): δ 5.53-5.35 (m, 1H), 5.30 (dt, *J*= 10.8, 7.3 Hz, 1H), 4.69-4.52 (m, 1H), 4.30 (td, *J*= 8.5, 6.2 Hz, 1H), 3.91 (dd, *J*= 8.5, 6.2 Hz, 1H), 3.71 (t, *J*= 8.8 Hz, 1H), 2.28-2.10 (m, 2H), 2.02 (q, *J*= 6.7 Hz, 2H), 1.85-1.75 (m, 1H), 1.72 (s, 3H), 1.58-1.48 (m, 1H), 1.44 (s, 3H), 1.35-1.21 (m, 14 H), 0.94-0.81 (m, 3H).

^{13}C NMR ($CDCl_3$): δ 156.8, 132.2, 126.9, 94.8, 73.9, 63.6, 61.2, 31.9, 30.7, 29.63, 29.60, 29.52, 29.31, 29.27, 28.18, 28.17, 27.2, 23.4, 23.3, 22.6, 14.1.

HRMS (ESI): calcd. For $C_{22}H_{40}NO_3$ $[M+H]^+$ 366.3008; found 366.3013**.**

$[\alpha]^{20}_D$ = -17.6 (*c* = 1.05, $CHCl_3$).

(4*S*,5*R*)-4-(Hydroxymethyl)-5-((*Z*)-pentadec-3-en-1-yl)oxazolidin-2-one (RBM8-124)

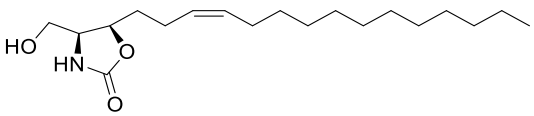

Solid *p*TsOH (7 mg, 0.03 mmol) was added portionwise to a solution of **RBM8-123** (80 mg, 0.22 mmol) in MeOH (5 mL). After vigorous stirring at rt for 3 h, Et_3N was added dropwise and the reaction mixture was concentrated *in vacuo*. Purification of the crude (95:5 to 80:20 CH_2Cl_2:MeOH gradient) gave 60 mg (0.18 mmol, 84%) of **RBM8-123** as a white solid.

R_f = 0.25 in hexane/EtOAc 1.1.

^{1}H NMR ($CDCl_3$): δ 6.76 (s, 1H), 5.51-5.39 (m, 1H), 5.37-5.24 (m, 1H), 4.64 (ddd, *J*= 10.1, 7.7, 3.7 Hz, 1H), 3.95-3.84 (m, 1H), 3.80 (td, *J*= 7.5, 7.0, 3.6 Hz, 1H), 3.73-3.62 (m, 2H), 2.30-2.09 (m, 2H), 2.01 (qd, *J*= 7.1, 1.5 Hz, 2H), 1.96-1.81 (m, 1H), 1.61 (dddd, *J*= 14.0, 8.7, 7.3, 3.8 Hz, 1H), 1.41-1.09 (m, 14H), 0.94-0.80 (m, 3H).

^{13}C NMR ($CDCl_3$): δ 160.7, 131.9, 127.3, 79.0, 61.0, 56.8, 31.9, 29.7, 29.64, 29.62, 29.56, 29.32, 20.30, 28.9, 27.2, 23.7, 22.7, 14.1.

HRMS (ESI): calcd. For $C_{19}H_{36}NO_3$ $[M+H]^+$ 326.2695; found 326.2704.

$[\alpha]^{20}_D$ = -11.3 (*c* = 0.99, $CHCl_3$).

(2*S*,3*R*,*Z*)-2-Aminooctadec-6-ene-1,3-diol (RBM8-125)

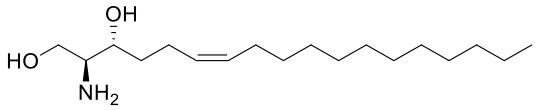

To a solution of **RBM8-124** (50 mg, 0.15 mmol) in EtOH (5 mL) was added NaOH 2M (5 mL) and the mixture was vigorous stirred at reflux temperature for 2 h. The reaction mixture was cooled to rt, concentrated under reduced pressure, and extracted with CH_2Cl_2 (3 x 10 mL). The combined organic layers were dried over $MgSO_4$, filtered, and concentrated *in vacuo* to give a crude, which was purified by flash chromatography (100:0 to 90:10 CH_2Cl_2/EtOAc), affording 32 mg (70 %) of **RBM8-125** as a white waxy solid.

R_f = 0.20 in hexane/EtOAc 1.1

^{1}H NMR (CD_3OD): δ 5.42 (td, *J* = 7.9, 6.9, 3.9 Hz, 2H), 3.76 (dd, *J* = 10.9, 4.1 Hz, 1H), 3.63-3.47 (m, 2H), 2.85-2.70 (m, 1H), 2.29 (ddt, *J* = 19.3, 10.1, 4.4 Hz, 1H), 2.22-2.05 (m, 3H), 1.61 (tdd, *J* = 16.6, 8.4, 5.0 Hz, 1H), 1.50 (ddt, *J* = 19.3, 10.1, 4.4 Hz, 1H), 1.45-1.24 (m, 18 H), 1.01-0.85 (m, 3H).

^{13}C NMR (CD_3OD): δ 129.9, 128.8, 72.1, 62.7, 56.7, 33.1, 31.7, 29.5, 29.41, 29.40, 29.38, 29.31, 29.1, 29.04, 26.8, 23.3, 22.3, 13.1.

HRMS (ESI): calcd. For $C_{18}H_{38}NO_2$ $[M+H]^+$ 300.2903; found 300.2903.

$[\alpha]^{20}_D$ = -0.7 (*c* = 1.0, $CHCl_3$)

***N*-((2*S*,3*R*,*Z*)-1,3-Dihydroxyoctadec-6-en-2-yl)-6-((7-nitrobenzo[c][1,2,5]oxadiazol-4-yl)amino)hexanamide (RBM8-126)**

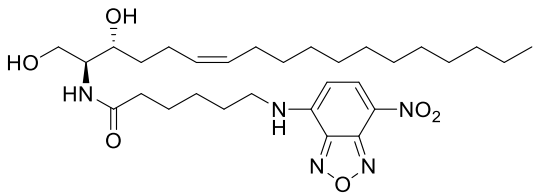

A solution of EDC (36 mg, 0.19 mmol), HOBt (28 mg, 0.21 mmol) and C_6-NBD acid (82 mg, 0.28 mmol) in anhydrous CH_2Cl_2 (7 mL) was stirred under argon atmosphere at rt for 10 min, and next added dropwise to a solution of **RBM8-125** (53 mg, 0.17 mmol) in anhydrous CH_2Cl_2 (8 mL). The reaction mixture was stirred at rt for 5 h under argon atmosphere. The mixture was diluted by addition of CH_2Cl_2 (10 mL) and washed successively with water (10 mL) and brine (10 mL). The organic layer was dried over $MgSO_4$, and filtered. Concentration under reduced pressure afforded crude compound, which was purified by flash chromatography with hexane/EtOAc (9:1 to 7:3) followed by CH_2Cl_2/MeOH (100:0 to 97:3) to afford **RBM8-126** (80%) as an orange solid.

R_f = 0.35 in hexane/EtOAc 1:1.

^{1}H NMR ($CDCl_3$): δ 8.49 (d, *J*= 8.6 Hz, 1H), 6.64 (s, 1H), 6.41 (d, *J*= 7.7 Hz, 1H), 6.17 (d, *J*= 8.7 Hz, 1H), 5.40 (tdd, *J*= 18.0, 10.9, 9.7 Hz, 2H), 4.05 (dd, *J*= 11.3, 3.4 Hz, 1H), 3.94-3.85 (m, 1H), 3.85-3.80 (m, 1H), 3.78 (dd, *J*= 11.3, 3.0 Hz, 1H), 3.52 (dt, *J*= 10.6, 5.4 Hz, 2H), 2.32 (q, *J*= 7.6 Hz, 2H), 2.18 (ddt, *J*= 20.8, 14.2, 7.4 Hz, 2H), 2.03 (q, *J*= 6.8 Hz, 2H), 1.91-1.71 (m, 4H), 1.71-1.46 (m, 4H), 1.25 (m, 18H), 0.88 (t, *J*= 6.9 Hz, 3H).

^{13}C NMR ($CDCl_3$): δ 172.8, 144.2, 143.9, 136.4 (C *o*-NO_2), 131.6 (C=), 128.3 (C=), 98.5 (C *m*-NO_2), 74.2, 62.4, 53.6, 43.4, 36.0, 34.4, 31.9, 29.7, 29.6, 29.5, 29.3, 27.9, 27.3, 26.1, 24.6, 23.8, 22.7, 14.1.

HSQC (see figure in NMR spectra for atom numbering)

HRMS (ESI): calcd. For $C_{30}H_{50}N_5O_6$ $[M+H]^+$ 576.3761; found 576.3779.

Analytical HPLC-FD: Column (Kromasil 100, C18, 5 µm, 15 x 0.4 cm); Isocratic method 75:25 ACN:H_2O; R_t: 17.3 min.; Sample volume: 10 µL; RBM8-053 (1mg/ mL in MeOH); λ_{abs}= 440; λ_{em}= 540.

$[\alpha]^{20}_D$ = - 13 (*c* = 0.8, MeOH).

N-((2*S*,3*R*,*Z*)-1,3-Dihydroxyoctadec-6-en-2-yl)octanamide (RBM8-202)

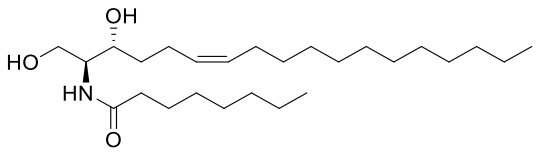

A solution of EDC (42 mg, 0.22 mmol), HOBt (28 mg, 0.20 mmol) and octanoic acid (38 mg, 0.28 mmol) in anhydrous CH_2Cl_2 (7 mL) was stirred under argon atmosphere at rt for 10 min, and next added dropwise to a solution of **RBM8-125** (51 mg, 0.17 mmol) in anhydrous CH_2Cl_2 (8 mL). The reaction mixture was stirred at rt for 5 h under argon atmosphere. The mixture was diluted by addition of CH_2Cl_2 (10 mL) and washed successively with water (10 mL) and brine (10 mL). The organic layer was dried over $MgSO_4$, and filtered. Concentration under reduced pressure afforded crude, which was purified by flash chromatography with CH_2Cl_2/MeOH (100:0 to 90:10) to afford **RBM8-202** (87%) as a white solid.

R_f = 0.35 in hexane/EtOAc 1:1

^{1}H NMR ($CDCl_3$): δ 6.38 (br, 1H), 5.51-5.31 (m, 2H), 3.99 (dd, J= 11.3, 3.3 Hz, 1H), 3.92-3.67 (m, 3H), 2.25-2.19 (m, 2H), 2.03 (q, *J*= 13.5, 6.5 Hz, 2H), 1.61 (td, *J*= 13.0, 6.4, 4H), 1.36-1.21 (m, 28H), 0.87 (t, *J*= 6.8, 6H).

^{13}C NMR ($CDCl_3$): δ 173.6, 131.4, 128.4, 73.9, 62.5, 53.9, 36.8, 34.3, 31.9, 31.6, 29.7, 29.7, 29.6, 29.5, 29.3, 29.2, 28.9, 27.3, 25.7, 23.8, 22.6, 22.6, 14.1, 14.02.

HRMS (ESI): calcd. For $C_{26}H_{52}NO_3$ $[M+H]^+$ 426.3947; found 426.3807.

$[\alpha]^{20}_D$ = -1.02 (*c* = 1.3, $CHCl_3$).

Methyl 5-(((2*S*,3*R*,*Z*)-1,3-dihydroxyoctadec-6-en-2-yl)amino)-5-oxopentanoate (RBM8-250)

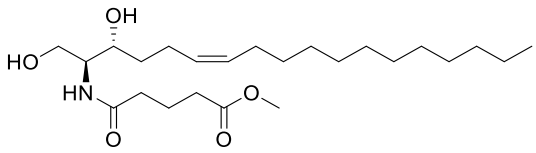

A solution of EDC (20 mg, 0.10 mmol), HOBt (11 mg, 0.08 mmol) and mono-methyl glutarate (15 mg, 0.10 mmol) in anhydrous CH_2Cl_2 (5 mL) was stirred under argon atmosphere at rt for 10 min, and next added dropwise to a solution of **RBM8-125** (25 mg, 0.08 mmol) in anhydrous CH_2Cl_2 (3 mL). The reaction mixture was stirred at rt for 4 h under argon atmosphere. The mixture was diluted by addition of CH_2Cl_2 (5 mL) and washed successively with water (5 mL) and brine (5 mL). The organic layer was dried over $MgSO_4$, and filtered. Concentration under reduced pressure afforded crude compound, which was purified by flash chromatography with CH_2Cl_2/MeOH (100:0 to 94:6) to afford **RBM8-250** (60%) as a white solid.

^{1}H NMR ($CDCl_3$): δ 6.45 (d, *J* = 7.1 Hz, 1H), 5.36 (ddt, *J* = 17.8, 10.8, 5.4 Hz, 2H), 3.98 (d, *J* = 11.3 Hz, 1H), 3.85 – 3.68 (m, 3H), 3.66 (s, 3H), 2.98 (br, 1H), 2.38 (t, *J* = 7.0 Hz, 2H), 2.33 – 2.05 (m, 4H), 2.00 (dq, *J* = 14.2, 6.9 Hz, 4H), 1.71 – 1.46 (m, 2H), 1.41 – 1.05 (m, 19H), 0.86 (t, *J* = 6.8 Hz, 3H).

^{13}C NMR ($CDCl_3$): δ 173.9, 172.3, 131.3, 128.4, 73.8, 62.2, 53.8, 51.7, 35.5, 34.3, 33.1, 31.9, 29.68, 29.65, 29.62, 29.55, 29.3, 27.3, 23.8, 22.7, 20.9, 14.1.

HRMS (ESI): calcd. For $C_{24}H_{46}NO_5$ $[M+H]^+$ 428.3376; found 428.3382.

$[\alpha]^{20}_D$ = -1.1 (*c* = 1.2, $CHCl_3$).

5-(((2*S*,3*R*,*Z*)-1,3-Dihydroxyoctadec-6-en-2-yl)amino)-5-oxopentanoic acid (RBM8-251)

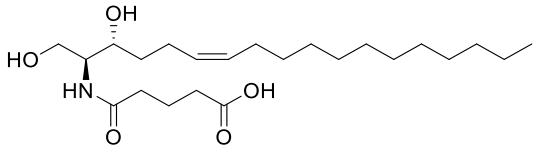

The ester **RBM8-250** (24 mg, 0.06 mmol) was dissolved in THF and water (3:1), and LiOH (21 mg, 0.08 mmol) was added. After stirring 2 h at rt the mixture was concentrated. The residue was taken up in water, acidified with 5% HCl, and extracted three times with ethyl acetate. The combined organic extracts were washed with brine, dried over $MgSO_4$, and concentrated in vacuo. Purification by flash chromatography with CH_2Cl_2/MeOH (9:1) afforded **RBM8-251** (20 mg, 87%) as a white solid.[186]

^{1}H NMR ($CDCl_3$): δ 7.15 (s, 1H), 5.47 – 5.25 (m, 2H), 3.96 (m, 2H), 3.82 (d, *J* = 18.5 Hz, 2H), 2.52 – 2.26 (m, 4H), 2.17 (d, *J* = 34.2 Hz, 2H), 1.99 (dd, *J* = 14.3, 7.0 Hz, 4H), 1.70-1.47 (m, 2H), 1.25 (d, *J* = 10.9 Hz, 18H), 0.86 (t, *J* = 6.7 Hz, 3H).

^{13}C NMR ($CDCl_3$): δ 176.6, 173.0, 131.3, 128.2, 73.9, 61.8, 53.7, 35.2, 34.1, 32.9, 31.9, 29.70, 29.67, 29.63, 29.59, 29.3, 27.3, 23.7, 22.7, 20.8, 14.1.

HRMS (ESI): calcd. For $C_{23}H_{44}NO_5$ $[M+H]^+$ 414.3219; found 414.3219.

$[\alpha]^{20}_D$ = -7.5 (*c* = 1.32, $CHCl_3$).

Methyl 14-(((2*S*,3*R*,*Z*)-1,3-dihydroxyoctadec-6-en-2-yl)amino)-14-oxotetradecanoate (RBM8-268)

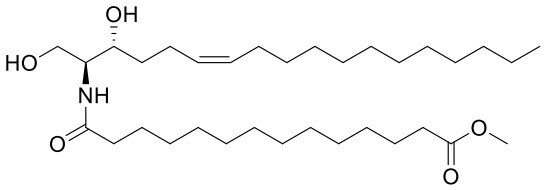

A solution of EDC (15 mg, 0.08 mmol), HOBt (8 mg, 0.06 mmol) and 14-methoxy-14-oxotetradecanoic acid [173] (24 mg, 0.08 mmol) in anhydrous CH_2Cl_2 (5 mL) was stirred under argon atmosphere at rt for 10 min, and next added dropwise to a solution of **RBM8-125** (20 mg, 0.06 mmol) in anhydrous CH_2Cl_2 (3 mL). The reaction mixture was stirred at rt for 4 h under argon atmosphere. The mixture was diluted by addition of CH_2Cl_2 (5 mL) and washed successively with water (5 mL) and brine (5 mL). The organic layer was dried over $MgSO_4$, and filtered. Concentration under reduced pressure afforded **RBM8-268** (83%) as a white solid, which was used without further purification.

^{1}H NMR ($CDCl_3$): δ 6.44 (d, *J* = 6.9 Hz, 1H), 5.45 – 5.26 (m, 2H), 4.06 – 3.88 (m, 1H), 3.86 – 3.68 (m, 3H), 3.64 (s, 3H), 2.26 (q, *J* = 9.2, 8.4 Hz, 2H), 2.23 – 2.15 (m, 2H), 2.11 – 1.92 (m, 2H), 1.59 (dt, *J* = 13.7, 6.6 Hz, 4H), 1.23 (s, 38H), 0.85 (t, *J* = 6.7 Hz, 3H).

^{13}C NMR ($CDCl_3$): δ 174.4, 173.6, 131.2, 128.5, 73.7, 62.4, 53.9, 53.4, 51.4, 43.8, 36.8, 34.3, 34.1, 31.9, 29.69, 29.66, 29.62, 29.56, 29.50, 29.48, 29.41, 29.36, 29.32, 29.30, 29.25, 29.19, 29.09, 27.3, 25.7, 24.9, 23.8, 22.7, 14.1.

HRMS (ESI): calcd. For $C_{33}H_{64}NO_5$ $[M+H]^+$ 554.4784; found 554.4807.

$[\alpha]^{20}_D$ = +0.4 (*c* = 1.0, $CHCl_3$).

14-(((2*S*,3*R*,*Z*)-1,3-Dihydroxyoctadec-6-en-2-yl)amino)-14-oxotetradecanoic acid (RBM8-269)

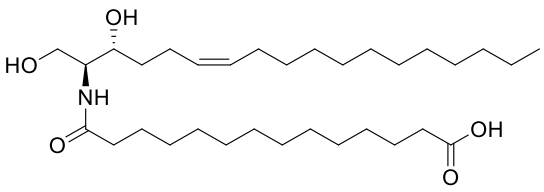

The ester **RBM8-268** (50 mg, 0.09 mmol) was dissolved in THF and water (3:1), and LiOH (3 mg, 0.13 mmol) was added. After stirring 2 h at rt the mixture was concentrated. The residue was taken up in water, acidified with 5% HCl, and extracted three times with ethyl acetate. The combined organic extracts were washed with brine, dried over $MgSO_4$, and concentrated in vacuo. Purification by flash chromatography with CH_2Cl_2/MeOH (9:1) afforded **RBM8-269** (37 mg, 79%) as a white solid.[186]

^{1}H NMR ($CDCl_3$): δ 6.89 (d, *J* = 7.3 Hz, 1H), 5.37 (tdd, *J* = 17.8, 10.9, 7.1 Hz, 2H), 3.97 (dd, *J* = 11.4, 3.5 Hz, 1H), 3.82 (ddt, *J* = 22.0, 12.1, 6.4 Hz, 3H), 2.32 (t, *J* = 7.2 Hz, 2H), 2.24 (d, *J* = 8.1 Hz, 3H), 2.19 – 2.08 (m, 1H), 2.01 (d, *J* = 6.7 Hz, 2H), 1.61 (s, 4H), 1.37 – 1.13 (m, 35H), 0.86 (t, *J* = 6.8 Hz, 3H).

^{13}C NMR ($CDCl_3$): δ 177.2, 174.2, 131.4, 128.3, 74.0, 62.4, 53.7, 36.6, 34.2, 33.7, 31.9, 30.9, 29.67, 29.63, 29.57, 29.3, 28.9, 28.8, 28.6, 28.53, 28.49, 27.3, 25.6, 24.5, 23.8, 22.7, 14.1

HRMS (ESI): calcd. For $C_{30}H_{63}NO_5Na$ $[M+Na]^+$ 540.4604; found 540.4611.

$[\alpha]^{20}_D$ = - 4 (*c* = 0.7, $CHCl_3$:MeOH 1:2).

(9*H*-Fluoren-9-yl)methyl (6-((12-(((2*S*,3*R*,*Z*)-1,3-dihydroxyoctadec-6-en-2-yl)amino)-12-oxododecyl)amino)-6-oxohexyl)carbamate (RBM8-319)

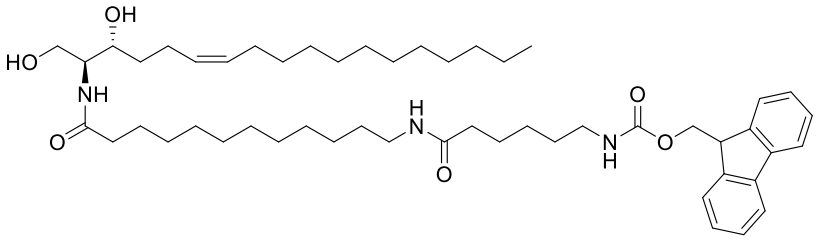

A solution of EDC (25 mg, 0.13 mmol), HOBt (14 mg, 0.10 mmol) and **RBM8-311** (65 mg, 0.12 mmol) in anhydrous CH_2Cl_2 (5 mL) was stirred under argon atmosphere at rt for 10 min, and next added dropwise to a solution of **RBM8-125** (30 mg, 0.10 mmol) in anhydrous CH_2Cl_2 (5 mL). The reaction mixture was stirred at rt for 4 h under argon atmosphere. The mixture was diluted by addition of CH_2Cl_2 (10 mL) and washed successively with water and brine. The organic layer was dried over $MgSO_4$, and filtered. Concentration under reduced pressure afforded crude compound, which was purified by flash chromatography with CH_2Cl_2/MeOH (100% to 95%) to afford **RBM8-319** (62 mg, 75%) as a white solid.

^{1}H NMR ($CDCl_3$): δ 7.74 (d, *J* = 7.5 Hz, 1H), 7.57 (d, *J* = 7.5 Hz, 1H), 7.37 (t, *J* = 7.4 Hz, 1H), 7.29 (t, *J* = 7.1 Hz, 1H), 6.48 (d, *J* = 7.6 Hz, 1H), 5.62 (s, 1H), 5.36 (ddd, *J* = 16.4, 10.8, 4.0 Hz, 2H), 4.98 (s, 1H), 4.36 (d, *J* = 6.9 Hz, 1H), 4.19 (d, *J* = 5.9 Hz, 1H), 3.97 (dd, *J* = 11.3, 3.4 Hz, 1H), 3.88 – 3.65 (m, 3H), 3.19 (dt, *J* = 12.4, 6.3 Hz, 4H), 2.18 (dh, *J* = 21.0, 7.1, 6.5 Hz, 6H), 2.10 – 1.93 (m, 2H), 1.72 – 1.39 (m, 8H), 1.23 (s, 24H), 0.86 (t, *J* = 6.7 Hz, 3H).

^{13}C NMR ($CDCl_3$): δ 173.5, 173.0, 143.9, 141.3, 131.2, 128.5, 127.9, 127.6, 127.3, 127.0, 124.9, 119.9, 73.7, 66.5, 62.5, 53.9, 47.2, 40.7, 39.5, 36.8, 36.5, 34.3, 31.9, 29.70, 29.66, 29.62, 29.57, 29.49, 29.33, 29.16, 29.11, 29.03, 28.9, 27.3, 26.7, 26.2, 25.6, 25.2, 23.9, 22.7, 14.1.

HRMS (ESI): calcd. For $C_{51}H_{81}N_3O_6Na$ $[M+Na]^+$ 854.6023; found 854.6087.

$[\alpha]^{20}_D$ = - 1 (*c* = 1.1, $CHCl_3$).

12-(6-Aminohexanamido)-*N*-((2*S*,3*R*,*Z*)-1,3-dihydroxyoctadec-6-en-2-yl)dodecanamide (RBM8-324)

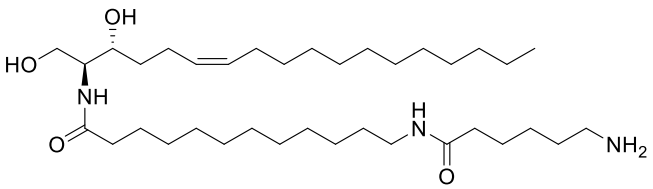

To a solution of **RBM8-319** (60 mg, 0.07 mmol) in anhydrous THF (5 mL) was added piperidine (400 µL, 2.1 mmol) at rt. After stirring for 4 h, the mixture was diluted with EtOAc. The organic phase was washed with water and brine, dried over anhydrous MgSO4, and concentrated under reduced pressure. The residue was purified by flash column chromatography on silica gel (DCM:MeOH; stepwise gradient from 10% to 20% of MeOH) to give **RBM8-324** as a white solid (35 mg, 83%). [187,188]

^{1}H NMR (CD_3OD): δ 5.36 (t, *J* = 5.2 Hz, 2H), 3.87 – 3.79 (m, 1H), 3.75 – 3.66 (m, 2H), 3.65 – 3.58 (m, 1H), 3.15 (t, *J* = 7.1 Hz, 2H), 2.94 – 2.80 (m, 2H), 2.21 (q, *J* = 7.7 Hz, 6H), 2.14 – 2.01 (m, 4H), 1.71 – 1.44 (m, 10H), 1.44 – 1.14 (m, 32H), 0.90 (t, *J* = 6.9 Hz, 3H).

^{13}C NMR (CD_3OD): δ 174.8, 174.4, 129.9, 128.8, 70.5, 61.0, 55.3, 40.4, 38.9, 35.9, 35.5, 33.7, 31.7, 30.6, 29.5, 29.38, 29.37, 29.34, 29.30, 29.26, 29.24, 29.21, 29.09, 29.06, 29.02, 29.00, 28.99, 28.94, 26.8, 26.6, 25.9, 25.7, 25.3, 22.9, 22.3, 13.0.

HRMS (ESI): calcd. For $C_{36}H_{72}N_3O_4$ $[M+H]^+$ 610.5523; found 610.5541.

$[\alpha]^{20}_D$ = - 3.1 (*c* = 0.8, $CHCl_3$).

5.1.4. Synthesis of (*E,E*)-Δ^6-Cer analogues

(*S*)-*tert*-Butyl 4-((*R*)-1-hydroxyprop-2-yn-1-yl)-2,2-dimethyloxazolidine-3-carboxylate (RBM8-031)

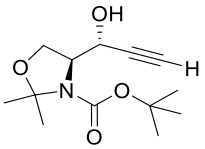

To a solution of ethynyltrimethylsilane (2.0 mL, 14.15 mmol) in dry THF (20 mL) was added dropwise *n*BuLi (6.9 mL, 17.16 mmol, 2.5 M in hexanes) at -78°C under argon atmosphere. After vigorous stirring at -78°C for 1 h, was added HMPA (2.8 mL, 16.09 mmol), followed by a solution of Garner's aldehyde[180] (2.0 g, 8.72 mmol) in dry THF (8 mL). After stirred at -78 for 2 h, the reaction mixture was quenched with dropwise addition of aqueous saturated NH_4Cl, and next allowed to warm to rt. The resulting white residue was taken up in water and the aqueous phase was extracted with Et_2O (3 x 20 mL). The combined organic layers were washed successively with 0.5 *N* HCl and brine, dried over $MgSO_4$ and filtered. The solvent was removed *in vacuo,* and the resulting residue was used without further purification. To a solution of the crude residue (1.73 g, 5.28 mmol) in MeOH (50 mL) was added solid K_2CO_3 (7.3 g, 52.8 mmol). After vigorous stirring at rt for 3 h, the reaction mixture was concentrated *in vacuo*. The resulting residue was taken up in water (25 mL), and the aqueous phase was extracted with EtOAc (3 x 30 mL). The combined organic layers were dried over $MgSO_4$ and filtered. Concentration under reduced pressure afforded compound **RBM8-031** as a colourless oil. The overall yield was 73% (2.6 g) over two steps and the compound was used without further purification. The physical and spectroscopic data of the compound were identical to those reported in the literature.[120]

^{1}H NMR ($CDCl_3$): δ 5.04 (d, *J*= 6.8 Hz, 1H), 4.57-4.47 (m, 1H), 4.23-4.05 (m, 1H), 3.95-3.85 (m, 1H), 1.61 (s, 3H), 1.57 (s, 3H), 1.50 (s, 9H).

(*E*)-1-Iodotridec-1-ene (RBM8-032)

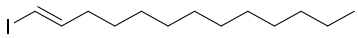

Schwartz reagent, Cp_2ZrHCl, (0.56 g, 5.19 mmol) was dissolved in THF (5 mL) at 0 ˚C. To the solution was added 1-tridecyne (0.76 ml, 3.24 mmol). The ice bath was removed and the mixture stirred for 2 h at rt. The vinylzirconium solution was cooled to -78˚C and a solution of I_2 (1.0 g, 3.89 mmol) in THF (5 mL) was added dropwise. The reaction was stirred for 2 h at -78˚C

and quenched with HCl 0.1 M (9 mL). The aqueous layer was extracted with Et2O (3 x 5 mL) and the combined organic layers were washed with a saturated solution of $NaHCO_3$ (4 mL), $Na_2S_2O_3$ (4 mL) and NaCl (4 mL). The organic layer was dried over $MgSO_4$ and the solvent concentrated *in vacuo*. Purification by flash chromatography (hexane) provided **RBM8-032** (0.8 g, 80%) as a light-yellow oil. The physical and spectroscopic data of compound **RBM8-032** were identical to those reported in the literature.[117]

^{1}H NMR ($CDCl_3$): δ 6.51 (td, *J* = 16.0, 4.0 Hz, 1H), 5.97 (dt, *J* = 16.0, 4.0 Hz, 1 H), 2.04 (q, *J* = 8.0 Hz, 2H), 1.38 (t, *J* = 8.0 Hz, 2H), 1.27 (s, 18H), 0.88 (t, *J* = 8.0 Hz, 3H).

^{13}C NMR ($CDCl_3$): δ 146.8, 76.2, 36.0, 31.9, 29.6, 29.5, 29.4, 29.36, 29.32, 28.9, 29.3, 22.6, 14.1.

***tert*-Butyl (*S*)-4-((*R,E*)-1-hydroxyhexadec-4-en-2-yn-1-yl)-2,2-dimethyloxazolidine-3-carboxylate (RBM8-033)**

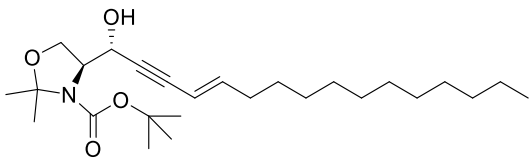

To a solution of $Pd(PPh_3)_4$ (0.10 g, 0.16 mmol) and CuI (0.03 g, 0.16 mmol) in piperidine (15 mL) was added a solution of **RBM8-031** (0.254 g, 1.63 mmol) in THF (20 mL) and a solution of (*E*)-1-iodotridec-1-ene **RBM8-032** (0.60 g, 1.94 mmol) in piperidine (15 mL). The reaction mixture was stirred at rt for 2 h and quenched by addition of a saturated solution of NH_4Cl (40 mL) at 0 ˚C. The aqueous layer was extracted with Et_2O (4 x 20 mL). The resulting organic layer was then dried over $MgSO_4$ and concentrated to give a crude that was purified by flash chromatography (hexane/EtOAc 90/10) to give **RBM8-033** (0.298 g, 42% yield) as a colourless oil.[117]

R_f = 0.35 hexane/EtOAc 7:3

^{1}H NMR ($CDCl_3$): δ 6.09 (dt, *J* = 15.2, 7.1 Hz, 1H), 5.43 (dq, *J* = 15.9, 1.7 Hz, 1H), 4.98 (d, *J* = 8.7 Hz, 1H), 4.56 (d, *J* = 8.5 Hz, 1H), 4.11 (dt, *J* = 35.1, 7.1 Hz, 2H), 3.86 (dd, *J* = 9.2, 5.0 Hz, 1H), 2.05 (qd, *J* = 7.2, 1.6 Hz, 2H), 1.66 – 1.53 (m, 3H), 1.48 (m, 9H), 1.38 – 1.13 (m, 21H), 0.91 – 0.78 (m, 3H).

^{13}C NMR ($CDCl_3$): δ 145.5, 108.8, 94.9, 85.4, 81.3, 65.2, 64.8, 62.9, 33.1, 33.0, 31.9, 29.6, 29.58, 29.57, 29.54, 29.45, 29.4, 29.3, 29.0, 28.8, 28.6, 28.4, 28.3, 25.7, 22.7, 14.1.

HRMS (ESI): calculated for $C_{26}H_{46}NO_4$ $[M + H]^+$ 436.3427; found 436.3427.

***Tert*-Butyl (*S*)-4-((*R*,2*E*,4*E*)-1-hydroxyhexadeca-2,4-dien-1-yl)-2,2-dimethyloxazolidine-3-carboxylate (RBM8-034)**

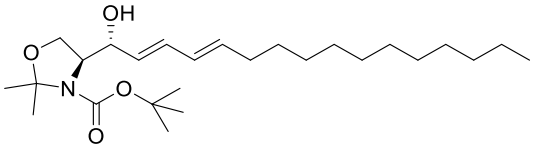

To a solution of **RBM8-033** (0.100 g, 0.23 mmol) in THF (2 mL) previously cooled to 0°C, was added dropwise a solution of RedAl (wt. 65% in toluene, 0.7 mL, 2.31 mmol). The mixture was stirred at rt for 5 h. After this time, the mixture was cooled to 0°C and quenched by addition of MeOH (5 mL) at 0°C. After dilution with Et_2O (5 mL) a saturated solution of Rochelle's salt (Na-K tartrate, 5 mL) was added. The aqueous layer was extracted with Et_2O (5 x 5 mL). The organic layers were washed with a saturated solution of Rochelle's salt (2 x 5 mL) and dried over $MgSO_4$. Purification by flash chromatography (hexane/ethyl acetate) yielded 0.085 g of **RBM8-034** (85%) as colourless oil.[117]

R_f = 0.30 hexane/EtOAc 8:2

^{1}H NMR ($CDCl_3$): δ 6.25 (dd, *J* = 15.2, 10.4 Hz, 1H), 6.08 – 5.92 (m, 1H), 5.73 – 5.59 (m, 1H), 5.52 (dd, *J* = 15.3, 6.0 Hz, 1H), 4.06 (dd, *J* = 113.1, 64.0 Hz, 4H), 2.04 (q, *J* = 7.1 Hz, 2H), 1.45 (s, 14H), 1.23 (m, 19H), 0.96 – 0.72 (m, 3H).

^{13}C NMR ($CDCl_3$): δ 135.5, 131.94, 129.4, 128.8, 94.4, 73.6, 64.6, 62.5, 32.6, 31.9, 29.6, 29.6, 29.58, 29.56, 29.47, 29.3, 29.2, 29.19, 29.14, 28.3, 22.6, 14.1.

HRMS (ESI): calculated for $C_{26}H_{47}NO_4Na$ $[M + Na]^+$ 460.3403; found 460.3396.

(1*R*,7a*S*)-5,5-Dimethyl-1-((1*E*,3*E*)-pentadeca-1,3-dien-1-yl)dihydro-1*H*,3*H*,5*H*-oxazolo[3,4-*c*]oxazol-3-one (RBM8-041)

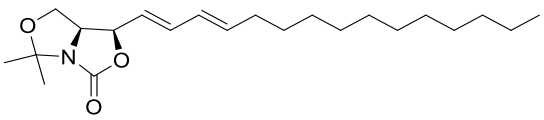

A solution of **RBM8-034** (40 mg, 0.09 mmol) in anydrous THF (2 mL) was added to a suspension of NaH (60% in mineral oil, 36 mg, 0.90 mmol) in anhydrous THF (2 mL) at rt. The reaction mixture was vigorously stirred for 16 h at 50 °C and under argon atmosphere. The reaction was next quenched by dropwise addition of aqueous sat. $NaHCO_3$ at 0 °C, until H_2 evolution was not observed. The aqueous phase was next extracted with EtOAc (3 x 10 mL). The combined organic layers were dried over $MgSO_4$, filtered, and concentrated in vacuo, giving a crude which was purified by flash chromatography (70:30 hexane/EtOAc), affording 23 mg (70%) of pure *trans/trans* **RBM8-041** as a colourless oil.

^{1}H NMR ($CDCl_3$): δ 6.33 (dd, *J* = 15.2, 10.4 Hz, 1H), 6.02 (dd, *J* = 15.2, 10.4 Hz, 1H), 5.80 (dt, *J* = 14.7, 6.9 Hz, 1H), 5.43 (dd, *J* = 15.2, 7.3 Hz, 1H), 5.13 – 4.98 (m, 1H), 4.37 (td, *J* = 8.3, 6.3 Hz,

1H), 3.86 (dd, *J* = 8.7, 6.4 Hz, 1H), 3.69 (t, *J* = 8.6 Hz, 1H), 2.21 – 1.98 (m, 2H), 1.70 (s, 3H), 1.42 (s, 3H), 1.37 (t, *J* = 6.8 Hz, 2H), 1.24 (s, 16H), 0.86 (t, *J* = 6.8 Hz, 3H).

^{13}C NMR ($CDCl_3$): δ 159.8, 138.9, 135.7, 128.2, 121.6, 95.1, 75.2, 64.3, 61.7, 32.6, 31.9, 29.61, 29.58, 29.53, 29.42, 29.29, 29.16, 28.9, 27.8, 23.4, 22.6, 14.1.

HRMS (ESI): calculated for $C_{22}H_{38}NO_3$ $[M + H]^+$ 364.2852; found 364.2852.

(4*S*,5*R*)-4-(Hydroxymethyl)-5-((1*E*,3*E*)-pentadeca-1,3-dien-1-yl)oxazolidin-2-one (RBM8-042)

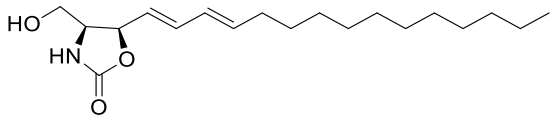

Solid *p*TsOH (2 mg, 0.01 mmol) was added portion wise to a solution of **RBM8-041** (23 mg, 0.06 mmol) in MeOH (2 mL). After vigorous stirring at rt for 3 h, Et_3N was added dropwise and the reaction mixture was concentrated *in vacuo*. Purification of the crude (95:5 to 80:20 CH_2Cl_2:MeOH gradient) gave 16 mg (82%) of **RBM8-042** as a white solid.

R_f = 0.25, hexane/EtOAc 1:1

^{1}H NMR (CD_3OD): δ 6.35 (dd, *J* = 15.2, 10.4 Hz, 1H), 6.10 (dd, *J* = 15.2, 10.4 Hz, 1H), 5.76 (ddd, *J* = 39.0, 14.8, 7.6 Hz, 2H), 5.19 – 5.07 (m, 1H), 3.84 (ddd, *J* = 8.2, 5.8, 4.3 Hz, 1H), 3.52 (qd, *J* = 11.4, 5.1 Hz, 2H), 2.21 – 1.99 (m, 2H), 1.39 (t, *J* = 7.1 Hz, 2H), 1.28 (d, *J* = 6.0 Hz, 16H), 1.04 – 0.79 (m, 3H).

^{13}C NMR (CD_3OD): δ 137.3, 135.8, 128.8, 122.5, 79.9, 60.7, 57.3, 48.2, 48.0, 47.8, 47.6, 47.3, 47.1, 46.9, 32.2, 29.3, 29.2, 22.3, 13.0.

HRMS (ESI): calculated for $C_{19}H_{34}NO_3$ $[M + H]^+$ 324.2539; found 324.2549.

(2*S*,3*R*,5*E*,7*E*)-2-Aminononadeca-5,7-diene-1,3-diol (RBM8-043)

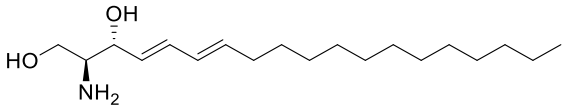

To a solution of **RBM8-042** (16 mg, 0.05 mmol) in EtOH (2 mL) was added NaOH 2M (2 mL) and the mixture was vigorously stirred at reflux for 4 h. Next, the reaction mixture was cooled to rt, concentrated under reduced pressure., and extracted with CH_2Cl_2. The aqueous residue was extracted with CH_2Cl_2 (3 x 10 mL) and the combined organic phases were dried and evaporated to dryness. The resulting compound **RBM8-043** (12 mg, 82 %) was used in the next step without further purification.

^{1}H NMR ($CDCl_3$): δ 6.26 (dd, *J* = 15.3, 10.4 Hz, 1H), 6.03 (dd, *J* = 15.2, 10.4 Hz, 1H), 5.72 (dt, *J* = 14.6, 7.0 Hz, 1H), 5.55 (dd, *J* = 15.3, 7.0 Hz, 1H), 4.10 (br, 1H), 3.65 (br, 2H), 2.98 – 2.75 (m, 1H), 2.07 (q, *J* = 7.2 Hz, 2H), 1.37 (t, *J* = 7.2 Hz, 2H), 1.25 (s, 16H), 0.87 (t, *J* = 6.7 Hz, 3H).

^{13}C NMR ($CDCl_3$): δ 136.4, 133.0, 129.6, 129.1, 75.1, 63.9, 56.2, 32.6, 31.9, 29.7, 29.6, 29.6, 29.5, 29.3, 29.23, 29.17, 22.7, 14.1.

HRMS (ESI): calculated for $C_{18}H_{36}NO_2$ $[M + H]^+$ 298.2746; found 298.2740.

***N*-((2*S*,3*R*,4*E*,6*E*)-1,3-Dihydroxyoctadeca-4,6-dien-2-yl)-6-((7-nitrobenzo[c][1,2,5]oxadiazol-4-yl)amino)hexanamide (RBM8-053)**

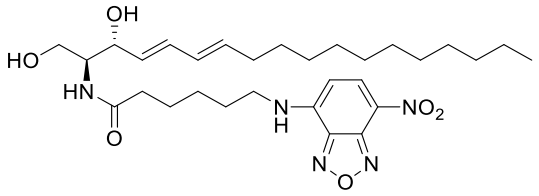

A solution of EDC (52 mg, 0.27 mmol), HOBt (27 mg, 0.20 mmol) and C_6NBD acid (53 mg, 0.18 mmol) in anhydrous CH_2Cl_2 (7 mL) was stirred under argon atmosphere at rt for 10 min, and next added dropwise to a solution of **RBM8-043** (50 mg, 0.17 mmol) in anhydrous CH_2Cl_2 (8 mL). The reaction mixture was stirred at rt for 2.5 h under argon atmosphere. The mixture was diluted by addition of CH_2Cl_2 (10 mL) and washed successively with water (10 mL) and brine (10 mL). The organic layer was dried over $MgSO_4$, and filtered. Concentration under reduced pressure afforded crude compound, which was purified by flash chromatography with CH_2Cl_2/MeOH (100:0 to 90:10) to afford **RBM8-053** (66%) as an orange waxy solid.

R_f = 0.30 in hexane/EtOAc 1:1.

^{1}H NMR ($CDCl_3$): δ 8.45 (d, *J*= 8.6 Hz, 1H), 6.86 (brs, 1H), 6.40 (d, *J*= 7.5 Hz, 1H), 6.28 (dd, *J*= 15.3, 10.4 Hz, 1H), 6.14 (d, *J*= 8.7, 1H), 6.01 (dd, *J*= 15.2, 10.4 Hz, 1H), 5.72 (dt, *J*= 14.6, 7.0 Hz,

1H), 5.60 (dd, *J*= 15.3, 6.2 Hz, 1H), 4.42-4.38 (m, 1H), 4.00-3.94 (m, 2H), 3.73-3.66 (m, 1H), 3.55-3.46 (m, 2H), 2.29 (t, *J*= 7.0 Hz, 2H), 2.05 (q, *J*= 7.2 Hz, 2H), 1.87-1.78 (m, 2H), 1.77-1.68 (m, 2H), 1.56-1.45 (m, 2H), 1.34 (q, J= 7.1 Hz, 2H), 1.29-1.17 (m, 18H), 0.86 (t, *J*= 6.8 Hz, 3H).

^{13}C NMR ($CDCl_3$): δ 173.3, 144.23, 143.9, 136.9, 136.5, 132.8, 128.8, 128.7, 74.4, 62.3, 54.3, 43.6, 36.0, 32.7, 31.9, 29.7, 29.60, 29.57, 29.47, 29.31, 29.22, 29.13, 27.8, 26.1, 24.7, 22.7, 14.1.

HRMS (ESI): calcd. for $C_{30}H_{48}N_5O_6$ $[M + H]^+$ 576.3605; found 576.3611.

Analytical HPLC-FD: Column (Kromasil 100, C18, 5 µm, 15 x 0.4 cm); Isocratic method 75:25 ACN:H_2O; R_t: 13.2 min.; Sample volume: 10 µL; RBM8-053 (1mg/ mL in MeOH); λ_{abs}= 465; λ_{em}= 530.

$[\alpha]^{20}_D$ = - 4 (*c* = 0.9, MeOH).

***N*-((2*S*,3*R*,4*E*,6*E*)-1,3-Dihydroxyoctadeca-4,6-dien-2-yl)octanamide (RBM2-076)**

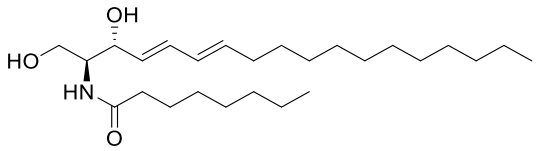

A solution of EDC (20 mg, 0.14 mmol), HOBt (12 mg, 0.11 mmol) and octanoic acid (15 mg, 0.11 mmol) in anhydrous CH_2Cl_2 (4 mL) was stirred under argon a at rt for 10 min, and next added dropwise to a solution of **RBM8-043** (22 mg, 0.11mmol) in anh. CH_2Cl_2 (3 mL). The reaction mixture was stirred at rt for 2 h under argon. The mixture was next diluted by addition of CH_2Cl_2 (5 mL) and washed successively with water (5 mL) and brine (5 mL). The organic layer was dried over $MgSO_4$ and filtered. Concentration under reduced pressure afforded a residue, which was purified by flash chromatography with CH_2Cl_2/MeOH (100:0 to 95:5) to afford **RBM2-076** (81%) as a white waxy solid. **R_f** = 0.30 in hexanes/EtOAc 1:1.

^{1}H NMR ($CDCl_3$): δ 0.88 (t, *J*=7.0 Hz, 10H), 1.20-4.42 (m, 45.5H), 1.60-1.68 (m, 3.8H), 2.08 (q, *J*=7.0 Hz, 1.3H), 2.18 (q, *J*=7.5 Hz, 2H), 2.21-2.27 (m, 2.8H), 3.68-3.74 (m, 1.5H), 3.91-4.01 (m, 2.6H), 4.41 (t, *J*=4.5 Hz, 0.5H), 4.46 (t, *J*=4.5 Hz, 0.7H), 5.50 (dd, *J*=18.0, 7.5, 0.9H), 5.61 (dd, *J*=15.5, 6.5, 0.7H), 5.67-5.78 (m, 1.5H), 5.95-6.08 (m, 1.6H), 6.21-6.34 (m, 2H), 6.62 (dd, *J*=15.0, 11.0 Hz, 0.8H).

HRMS (ESI): calculated for $C_{26}H_{49}NNaO_3$: 446.3610 $[M+Na]^+$. Found: 446.3603.

5.1.5. Synthesis of (*E,Z*)-$\Delta^{4,6}$-Cer analogues

1-Iodotridec-1-yne (RBM8-207)

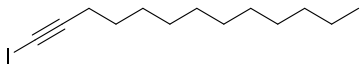

Iodine (3.2 g, 12.7 mmol) and morpholine (3.6 g, 41.2 mmol) were dissolved in benzene (10 mL) and 1-tridecyne (1.8 g, 9.8 mmol) in benzene (5 mL) was added dropwise. The solution was stirred at 45 °C for 20 h under reduced pressure. The suspension was filtered and the residue was washed with Et_2O (2 x 20 mL). The combined organic layers were washed with saturated aqueous solutions of NH_4Cl, $NaHCO_3$ and H_2O. The organic layer was dried over $MgSO_4$ and filtered. The solvent was removed under reduced pressure to obtain 2.95 g (98%) of a brown oil. The physical and spectroscopic data of compound **RBM8-207** were identical to those reported in the literature.[123,122]

^{1}H NMR ($CDCl_3$): δ 2.35 (t, *J* = 7.1 Hz, 2H), 1.51 (p, *J* = 7.0 Hz, 2H), 1.42 – 1.32 (m, 2H), 1.26 (s, 14H), 0.88 (t, *J* = 6.8 Hz, 3H)

^{13}C NMR ($CDCl_3$): δ 94.8, 31.9, 29.6, 29.5, 29.3, 29.0, 28.8, 28.5, 22.7, 20.8, 14.1, -7.72.

(*Z*)-1-Iodotridec-1-en (RBM8-209)

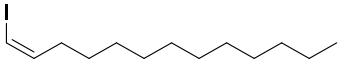

Crude **RBM8-207** (500 mg, 1.6 mmol) was dissolved in 20 mL of MeOH and 0.6 mL of pyridine and 3 g (15.4 mmol) of dipotassium azodicarboxylate were added. Glacial acetic acid (2.5 mL) was added slowly and stirring continued overnight. An additional 2 g of dipotassium azodicarboxylate and 2.5 mL of glacial acetic acid were added and stirred for additional 8 h. Any remaining diimide precursor was destroyed by carefully addition of 10 mL HCl 5% with vigorous stirring. The organic layer was separated and the aqueous layer was extracted with ether (2 x 20 mL). The combined organic layers were washed with 5% HCl 5%, 5% sodium bicarbonate and dried over $MgSO_4$. The solvents were removed under reduced pressure to give an oil, which was dissolved in 20 mL of ether and stirred with 10 mL of 50% aqueous butan-1-amine for 2 h to remove over reduced material. The ether solution was washed with 5% HCl, 5% sodium bicarbonate and dried over $MgSO_4$, and ether was removed in vacuo. Purification by chromatography in silica gel (hexane 100%) gave pure **RBM8-209** (370 mg, 74%) as a colourless oil.[119]

^{1}H NMR ($CDCl_3$): δ 6.18 – 6.10 (m, 2H), 2.11 (ddt, *J* = 11.5, 7.7, 5.8 Hz, 2H), 1.40 (p, *J* = 6.6 Hz, 2H), 1.26 (d, *J* = 11.9 Hz, 16H), 0.86 (t, *J* = 6.8 Hz, 3H).

^{13}C NMR ($CDCl_3$): δ 141.4, 82.1, 34.7, 31.9, 29.62, 29.61, 29.5, 29.4, 29.3, 29.10, 27.9, 22.6, 14.1.

(*S*)-*tert*-Butyl 4-((*R,Z*)-1-hydroxyhexadec-4-en-2-yn-1-yl)-2,2-dimethyloxazolidine-3-carboxylate (RBM8-210)

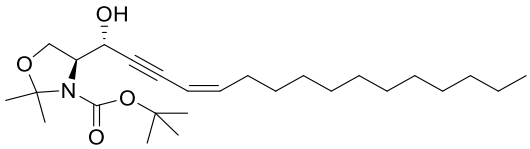

To a solution of $Pd(PPh_3)_4$ (570 mg, 0.5 mmol) and CuI (93 mg, 0.5 mmol) in piperidine (30 mL) was added a solution of **RBM8-031** (1.25 g, 4.9 mmol) in THF (50 mL) and a solution of **RBM8-209** (1.48 g, 4.9 mmol) in piperidine (20 mL). The reaction mixture was stirred at rt for 1.5 h and then quenched by adding a saturated solution of NH_4Cl (50 mL) at 0 °C. The aqueous layer was extracted with Et_2O (3 x 20 mL). The resulting organic layer was then dried over $MgSO_4$ and concentrated to give a crude that was purified by flash chromatography (hexane/ethyl acetate 90/10, $\mathbf{R_f}$ = 0.45) to give compound **RBM8-210** (1.5 g, 72%) as a colourless oil.[117]

^{1}H NMR ($CDCl_3$): δ 5.87 (d, *J* = 9.1 Hz, 1H), 5.42 (d, *J* = 10.8 Hz, 1H), 4.86 – 4.58 (m, 1H), 4.36 – 3.79 (m, 3H), 2.25 (q, *J* = 7.2 Hz, 2H), 1.73 – 1.40 (m, 15H), 1.23 (s, 18H), 0.85 (t, *J* = 6.8 Hz, 3H).

^{13}C NMR ($CDCl_3$): δ 144.7, 108.2, 95.0, 91.1, 81.3, 82.8, 65.1, 64.7, 62.7, 31.9, 30.3, 29.62, 29.60, 29.56, 29.49, 29.3, 29.2, 28.8, 28.3, 25.8, 25.3, 22.6, 14.1.

HRMS (ESI): calcd. For $C_{26}H_{46}NO_4[M+H]^+$ 436.3427; found 436.3422.

$[\alpha]^{20}_{D}$ = -54 (*c* = 1.08, $CHCl_3$).

(*S*)-*tert*-Butyl 4-((*R*,2*E*,4*Z*)-1-hydroxyhexadeca-2,4-dien-1-yl)-2,2-dimethyloxazolidine-3-carboxylate (RBM8-135)

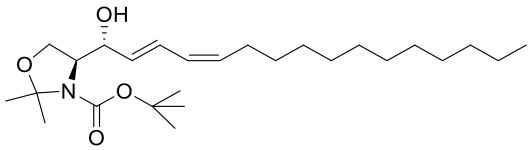

To a solution of **RBM8-210** (40 mg, 0.1 mmol) in THF (2 mL) was added dropwise RedAl (0.28 mL, aprox 60% in toluene) at 0 °C, and the mixture was stirred at rt for 2 h. After this time, the mixture was cooled to 0˚C and quenched by adding MeOH (5 mL) at 0˚C. After dilution with

Et_2O (5 mL) a saturated solution of Rochelle's Salt (Na-K tartrate, 5 mL) was added. The aqueous layer was extracted with Et_2O (5 x 5 mL). The combined ethereal extracts were washed with water and brine, dried over $MgSO_4$ and concentrated under reduced pressure. Purification by flash chromatography with silica gel (hexane/EtOAc 80:20, $\mathbf{R_f}$ = 0.35) gave 37 mg (95 %) of **RBM8-135**.[117]

^{1}H NMR ($CDCl_3$): δ 6.69-6.42 (m, 1H), 5.95 (t, *J*= 11.0 Hz, 1H), 5.73-5.51 (m, 1H), 4.49-3.70 (m, 4H), 2.13 (q, *J*= 6.9 Hz, 2H), 1.44 (s, 9H), 1.37-1.11 (m, 18 H), 0.85 (t, *J*= 6.8 Hz, 3H).

^{13}C NMR ($CDCl_3$): δ 132.8, 131.2, 127.7, 126.8, 94.4, 81.1, 73.9, 64.9, 62.4, 31.9, 29.62, 29.60, 29.57, 29.51, 29.31, 29.26, 28.3, 27.8, 26.2, 24.5, 22.7, 14.1.

HRMS (ESI): calcd. For $C_{26}H_{47}NO_4Na[M+Na]^+$ 460.3403; found 460.3386.

$[\alpha]^{20}_D$ = -12 (*c* = 1.0, $CHCl_3$).

(1*R*,7a*S*)-5,5-Dimethyl-1-((1*E*,3*Z*)-pentadeca-1,3-dien-1-yl)dihydro-1*H*-oxazolo[3,4-c]oxazol-3(5*H*)-one (RBM8-235)

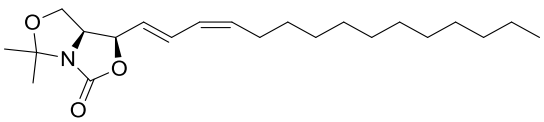

A solution of **RBM8-135** (50 mg, 0.11 mmol) in anydrous THF (3 mL) was added dropwise to a suspension of NaH (60% in mineral oil, 46 mg, 1.14 mmol) in anh THF (2 mL) at rt. The reaction mixture was vigorously stirred for 16 h at 50 °C and under argon atmosphere. The reaction was next quenched by dropwise addition of aqueous sat. $NaHCO_3$ at 0 °C, until H_2 evolution was ceased. The aqueous phase was next extracted with EtOAc (3 x 10 mL). The combined organic layers were dried over $MgSO_4$, filtered, and concentrated in vacuo to give a crude which was purified by flash chromatography (100:0 to 80:20 hexane/EtOAc), affording 32 mg (80 %) of **RBM8-235**.

$\mathbf{R_f}$ = 0.35 in hexane/EtOAc 8:2.

^{1}H NMR ($CDCl_3$): δ 6.67 (dd, *J* = 15.1, 11.1 Hz, 1H), 5.98 (t, *J* = 11.0 Hz, 1H), 5.69 – 5.42 (m, 2H), 5.13 (t, *J* = 7.6 Hz, 1H), 4.40 (td, *J* = 8.3, 6.4 Hz, 1H), 3.96 – 3.80 (m, 1H), 3.69 (t, *J* = 8.6 Hz, 1H), 2.27 – 2.07 (m, 2H), 1.72 (s, 3H), 1.45 (s, 3H), 1.37 – 1.10 (m, 18H), 0.86 (t, *J* = 11.0 Hz, 3H).

^{13}C NMR ($CDCl_3$): δ 156.7, 136.1, 130.5, 126.4, 123.8, 95.1, 75.0, 64.3, 61.7, 31.9, 29.7, 29.62, 29.60, 29.57, 29.47, 29.45, 29.3, 29.2, 27.9, 23.4, 22.7, 14.1.

HRMS (ESI): calcd. For $C_{22}H_{38}NO_3[M+H]^+$ 364.2852; found 364.2842.

$[\alpha]^{20}_D$ = -17 (*c* = 0.975, $CHCl_3$).

(4*S*,5*R*)-4-(Hydroxymethyl)-5-((1*E*,3*Z*)-pentadeca-1,3-dien-1-yl)oxazolidin-2-one (RBM8-236)

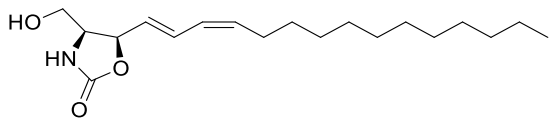

Solid *p*TsOH (3 mg, 0.01 mmol) was added to a solution of **RBM8-235** (50 mg, 0.13 mmol) in MeOH (3 mL). After vigorous stirring at rt for 1 h, Et_3N was added dropwise and the reaction mixture was concentrated *in vacuo*. Purification of the crude (100:0 to 97:03 CH_2Cl_2:MeOH gradient) gave 36 mg (85%) of **RBM8-236** as a white waxy solid.

R_f = 0.45 in hexane/EtOAc 1:1

^{1}H NMR ($CDCl_3$): δ 6.65 (dd, *J* = 15.2, 11.1 Hz, 1H), 6.58 (s, 1H), 5.99 (t, *J* = 11.1 Hz, 1H), 5.73 (dd, *J* = 15.2, 8.3 Hz, 1H), 5.62 – 5.50 (m, 1H), 5.16 (t, *J* = 8.2 Hz, 1H), 3.88 (ddd, *J* = 8.4, 6.0, 3.9 Hz, 1H), 3.70 – 3.54 (m, 2H), 3.40 (brs, 1H), 2.16 (q, *J* = 6.9 Hz, 2H), 1.34 (dd, *J* = 19.7, 5.5 Hz, 18H), 0.86 (t, *J* = 6.8 Hz, 3H).

^{13}C NMR ($CDCl_3$): δ 160.2, 135.9, 131.7, 126.6, 123.7, 80.1, 61.7, 57.5, 31.9, 29.63, 29.60, 29.57, 29.49, 29.32, 29.26, 27.9, 22.7, 14.1.

HRMS (ESI): calcd. For $C_{19}H_{34}NO_3[M+H]^+$ 324.2539; found 324.2531.

$[\alpha]^{20}_D$ = - 23 (*c* = 1.0, $CHCl_3$).

(2*S*,3*R*,4*E*,6*Z*)-2-Aminooctadeca-4,6-diene-1,3-diol (RBM8-137)

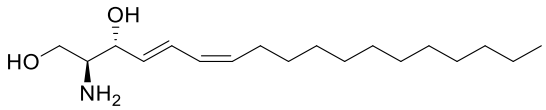

A solution of 2*N* NaOH (5 mL) was added dropwise to a solution of **RBM8-236** (50 mg, 0.18 mmol) in EtOH (5 mL). After vigorously stirring at reflux temperature for 2 h, the reaction mixture was cooled to rt, concentrated under reduced pressure to eliminate EtOH, and extracted with CH_2Cl_2 (3 x 10 mL). The combined organic extracts were dried over $MgSO_4$, filtered, and concentrated *in vacuo* to give a crude, which was purified by flash chromatography (100:0 to 90:10 CH_2Cl_2/EtOAc) to afford 45 mg (98 %) of **RBM8-137** as a white waxy solid.

R_f = 0.40 in hexane/EtOAc 1:1

^{1}H NMR (CD_3OD): δ 6.63 (dd, *J*= 15.2, 11.1 Hz, 1H), 6.05 (t, *J* = 11.1 Hz, 1H), 5.72 (dd, *J* = 15.2, 6.9 Hz, 1H), 5.47 (dt, *J*= 10.7, 7.7 Hz, 1H), 4.12 (t, *J* = 6.5 Hz, 1H), 3.68 (dd, *J* = 11.0, 4.5 Hz, 1H), 3.52 (dd, *J* = 11.0, 7.3 Hz, 1H), 2.81 (q, *J*= 6.3, 1H), 2.27-2.19 (m, 2H), 1.46-1.26 (m, 18H), 0.99-0.72 (m, 3H).

^{13}C NMR (CD_3OD): δ 132.22, 132.19, 127.7, 127.4, 73.4, 62.9, 56.7, 31.7, 29.42, 29.39, 29.36, 29.27, 29.1, 29.0, 27.3, 22.3, 13.1.

HRMS (ESI): calcd. For $C_{18}H_{36}NO_2[M+H]^+$ 298.2746; found 298.2729.

$[\alpha]^{20}_D$ = +4 (*c* = 1.0, $CHCl_3$).

***N*-((2*S*,3*R*,4*E*,6*Z*)-1,3-Dihydroxyoctadeca-4,6-dien-2-yl)-6-((7-nitrobenzo[*c*][1,2,5]oxadiazol-4-yl)amino)hexanamide (RBM8-138)**

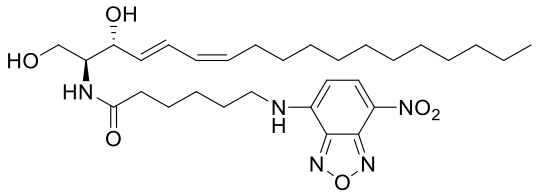

A solution of EDC (38 mg, 0.18 mmol), HOBt (29 mg, 0.21 mmol) and C_6NBD acid (88 mg, 0.30 mmol) in anhydrous CH_2Cl_2 (7 mL) was stirred under argon atmosphere at rt for 10 min, and next added dropwise to a solution of **RBM8-137** (53 mg, 0.18 mmol) in anhydrous CH_2Cl_2 (5 mL). The reaction mixture was stirred at rt for 5 h under argon atmosphere. The mixture was diluted by addition of CH_2Cl_2 (10 mL) and washed successively with water (10 mL) and brine (10 mL). The organic layer was dried over $MgSO_4$, and filtered. Concentration under reduced pressure afforded crude compound, which was purified by flash chromatography with CH_2Cl_2/MeOH (100:0 to 95:5) to afford **RBM8-138** (80%) as a red solid.

R_f = 0.35 in hexane/EtOAc 1:1

^{1}H NMR ($CDCl_3$): 8.44 (d, *J*= 8.7 Hz, 1H), 6.87 (s, 1H), 6.60 (dd, *J*= 15.2, 11.1 Hz, 1H), 6.44 (d, *J*= 7.8 Hz, 1H), 6.14 (d, *J*= 8.7 Hz, 1H), 5.95 (t, *J*= 11.0 Hz, 1H), 5.69 (dd, *J*= 15.2, 6.2 Hz, 1H), 5.47 (dt, *J*= 10.7, 7.6 Hz, 1H), 4.44 (s, 1H), 4.10-3.86 (m, 2H), 3.78-3.65 (m, 1H), 3.50 (d, *J*= 5.7 Hz, 2H), 2.29 (d, *J*= 7.0 Hz, 2H), 2.18-2.09 (m, 2H), 1.86-1.67 (m, 4H), 1.28-1.11 (m, 20H), 0.85 (t, J= 6.8 Hz, 3H).

^{13}C NMR ($CDCl_3$): 173.4, 144.2, 136.6, 134.2, 131.0, 127.7, 127.1, 74.5, 62.2, 54.3, 43.6, 36.0, 31.9, 29.64, 29.60, 29.59, 29.52, 29.31, 29.29, 27.9, 27.8, 26.2, 24.7, 22.7, 14.1.

HRMS (ESI): calcd. For $C_{30}H_{47}N_5NaO_6[M+Na]^+$ 596.3424; found 596.3415.

$[\alpha]^{20}_D$ = -11 (*c* = 0.45, MeOH).

_N_-((2_S_,3_R_,4_E_,6_Z_)-1,3-Dihydroxyoctadeca-4,6-dien-2-yl)octanamide (RBM8-216)

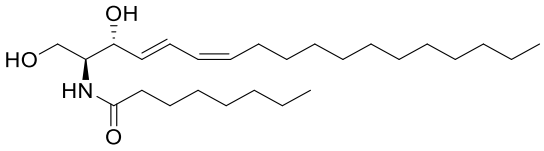

A solution of EDC (13 mg, 0.09 mmol), hydroxybenzotriazole (HOBt) (8 mg, 0.07 mmol) and octanoic acid (10 mg, 0.09 mmol) in anhydrous CH_2Cl_2 (3 mL) was stirred under argon atmosphere at rt for 10 min, and next added dropwise to a solution of **RBM8-137** (15 mg, 0.07 mmol) in anhydrous CH_2Cl_2 (3 mL). The reaction mixture was stirred at rt for 2 h under argon atmosphere. The mixture was diluted by addition of CH_2Cl_2 (5 mL) and washed successively with water (5 mL) and brine (5 mL). The organic layer was dried over $MgSO_4$, and filtered. Concentration under reduced pressure afforded crude compound, which was purified by flash chromatography with CH_2Cl_2/MeOH (100:0 to 95:5) to afford **RBM8-216** (87%) as a white solid.

R_f = 0.30 in hexane/EtOAc 1:1.

^{1}H NMR ($CDCl_3$): δ 6.60 (dd, *J*= 15.2, 11.1 Hz, 1H), 6.26 (d, *J*= 7.4 Hz, 1H), 5.97 (t, *J*= 11.0 Hz, 1H), 5.68 (dd, *J*= 15.2, 6.2 Hz, 1H), 5.54-5.40 (m, 1H), 4.49-4.35 (m, 1H), 4.08-3.83 (m, 2H), 3.76-3.64 (m, 1H), 2.38-1.99 (m, 4H), 1.69-1.52 (m, 2H), 1.43-1.16 (m, 22H), 1.06-0.64 (m, 6H).

^{13}C NMR ($CDCl_3$): δ 173.9, 134.1, 131.2, 127.6, 127.2, 74.6, 62.4, 54.4, 36.8, 31.9, 31.6, 29.64, 29.61, 29.59, 29.52, 29.32, 29.29, 29.19, 28.98, 27.9, 25.7, 22.7, 22.6, 14.1, 14.0.

HRMS (ESI): calcd. For $C_{26}H_{49}NNaO_3[M+Na]^+$ 446.3610; found 446.3605.

$[\alpha]^{20}_D$ = -22 (*c* = 0.99, MeOH).

Methyl 14-(((2_S_,3_R_,4_E_,6_Z_)-1,3-dihydroxyoctadeca-4,6-dien-2-yl)amino)-14-oxotetradecanoate (RBM8-274)

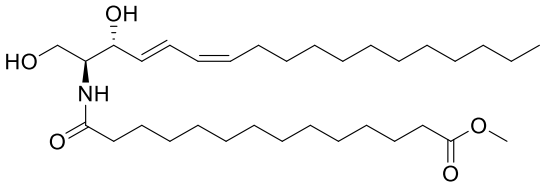

A solution of EDC (17 mg, 0.09 mmol), HOBt (10 mg, 0.07 mmol) and 14-methoxy-14-oxotetradecanoic acid [173] (24 mg, 0.09 mmol) in anhydrous CH_2Cl_2 (5 mL) was stirred under argon atmosphere at rt for 10 min, and next added dropwise to a solution of **RBM8-137** (20 mg, 0.07 mmol) in anhydrous CH_2Cl_2 (5 mL). The reaction mixture was stirred at rt for 4 h under argon atmosphere. The mixture was diluted by addition of CH_2Cl_2 (10 mL) and washed successively with water and brine. The organic layer was dried over $MgSO_4$, and filtered. Concentration under reduced pressure afforded a crude compound, which was purified by flash chromatography with CH_2Cl_2/MeOH 90:10 to afford **RBM8-274** (95%) as a white solid.

^{1}H NMR ($CDCl_3$): δ 6.58 (dd, *J* = 15.1, 11.1 Hz, 1H), 6.32 (d, *J* = 7.3 Hz, 1H), 5.95 (t, *J* = 11.0 Hz, 1H), 5.67 (dd, *J* = 15.2, 6.2 Hz, 1H), 5.56 – 5.36 (m, 1H), 4.40 (s, 1H), 3.92 (q, *J* = 8.3, 6.0 Hz, 2H), 3.64 (s, 4H), 2.32 – 2.10 (m, 6H), 1.66 – 1.53 (m, 2H), 1.23 (s, 36H), 0.94 – 0.76 (m, 3H).

^{13}C NMR ($CDCl_3$): δ 174.4, 174.0, 133.9, 131.3, 127.5, 127.2, 74.4, 62.4, 54.5, 51.4, 36.8, 34.1, 31.9, 29.64, 29.60, 29.53, 29.50, 29.48, 29.40, 29.36, 29.31, 29.30, 29.22, 29.19, 29.09, 27.8, 25.7, 24.9, 22.7, 14.1.

HRMS (ESI): calcd. For $C_{33}H_{61}NO_5Na$ $[M+Na]^+$ 574.4447; found 574.4424.

$[\alpha]^{20}_D$ = - 6 (*c* = 1.02, $CHCl_3$).

14-(((2*S*,3*R*,4*E*,6*Z*)-1,3-Dihydroxyoctadeca-4,6-dien-2-yl)amino)-14-oxotetradecanoic acid (RBM8-281)

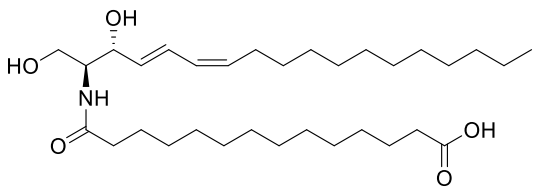

The ester **RBM8-274** (58 mg, 0.1 mmol) was dissolved in THF and water (3:1), and LiOH (4 mg, 0.16 mmol) was added. After stirring 2 h at rt the mixture was concentrated. The residue was taken up in water, acidified with 5% HCl, and extracted three times with ethyl acetate. The combined organic extracts were washed with brine, dried over $MgSO_4$, and concentrated in vacuo. Purification by flash chromatography with CH_2Cl_2/MeOH (99:1 to 95:5) afforded **RBM8-281** (52 mg, 96%) as a white solid.[186]

^{1}H NMR ($CDCl_3$): δ 6.72 – 6.48 (m, 2H), 5.96 (t, *J* = 11.0 Hz, 1H), 5.67 (dd, *J* = 15.2, 6.1 Hz, 1H), 5.53 – 5.40 (m, 1H), 4.42 (s, 1H), 3.82 (dd, *J* = 93.6, 8.3 Hz, 3H), 2.41 – 2.07 (m, 6H), 1.68 – 1.50 (m, 2H), 1.25 (d, *J* = 9.7 Hz, 36H), 0.86 (t, *J* = 6.7 Hz, 3H).

^{13}C NMR ($CDCl_3$): δ 178.2, 174.5, 133.9, 131.0, 127.6, 127.2, 74.3, 62.2, 54.4, 36.6, 33.9, 31.9, 29.7, 29.6, 29.5, 29.3, 29.10, 29.08, 28.97, 28.85, 28.77, 27.86, 25.7, 24.6, 22.7, 14.1.

HRMS (ESI): calcd. For $C_{32}H_{60}NO_5$ $[M+H]^+$ 538.4471; found 538.4451.

$[\alpha]^{20}_D$ = - 5.6 (*c* = 1.00, $CHCl_3$).

(9*H*-Fluoren-9-yl)methyl (6-((12-(((2*S*,3*R*,4*E*,6*Z*)-1,3-dihydroxyoctadeca-4,6-dien-2-yl)amino)-12-oxododecyl)amino)-6-oxohexyl)carbamate (RBM8-312)

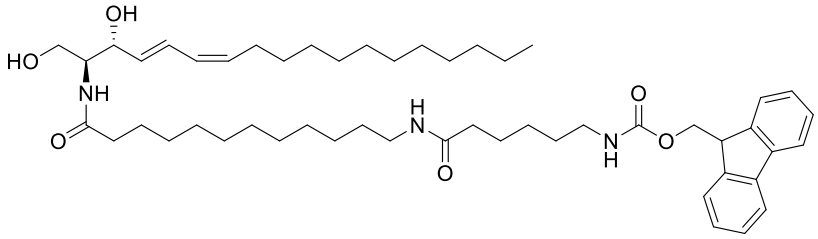

A solution of EDC (25 mg, 0.13 mmol), HOBt (14 mg, 0.10 mmol) and **RBM8-311** (65 mg, 0.12 mmol) in anhydrous CH_2Cl_2 (5 mL) was stirred under argon atmosphere at rt for 10 min, and next added dropwise to a solution of **RBM8-137** (30 mg, 0.10 mmol) in anhydrous CH_2Cl_2 (5 mL). The reaction mixture was stirred at rt for 4 h under argon atmosphere. The mixture was diluted by addition of CH_2Cl_2 (10 mL) and washed successively with water and brine. The organic layer was dried over $MgSO_4$, and filtered. Concentration under reduced pressure afforded crude compound, which was purified by flash chromatography with CH_2Cl_2/MeOH (100% to 95%) to afford **RBM8-312** (54 mg, 65%) as a white solid.

^{1}H NMR ($CDCl_3$): δ 7.74 (d, *J* = 7.5 Hz, 1H), 7.57 (d, *J* = 7.5 Hz, 1H), 7.37 (q, *J* = 6.7, 6.1 Hz, 2H), 7.28 (d, *J* = 14.6 Hz, 1H), 6.58 (dd, *J* = 15.0, 11.2 Hz, 1H), 6.45 (d, *J* = 6.9 Hz, 1H), 5.95 (t, *J* = 10.9 Hz, 1H), 5.67 (dd, *J* = 15.3, 6.1 Hz, 2H), 5.51 – 5.38 (m, 1H), 4.99 (s, 1H), 4.48 – 4.31 (m, 3H), 4.19 (d, *J* = 6.1 Hz, 1H), 3.93 (d, *J* = 9.0 Hz, 3H), 3.68 (dd, *J* = 12.4, 4.4 Hz, 1H), 3.19 (dt, *J* = 12.5, 6.2 Hz, 4H), 2.30 – 2.03 (m, 6H), 1.72 – 1.54 (m, 2H), 1.55 – 1.39 (m, 4H), 1.23 (s, 30H), 0.86 (t, *J* = 6.7 Hz, 3H).

^{13}C NMR ($CDCl_3$): δ 173.9, 172.9, 143.9, 141.3, 133.7, 131.5, 127.6, 127.3, 127.0, 125.0, 119.9, 74.4, 66.5, 62.4, 54.5, 47.2, 40.7, 39.5, 36.7, 36.5, 31.9, 29.7, 29.61, 29.60, 29.54, 29.48, 29.32, 29.31, 29.2, 29.11, 29.10, 29.04, 29.00, 28.93, 27.85, 26.6, 26.2, 25.6, 25.2, 22.7, 14.1.
HRMS (ESI): calcd. For $C_{51}H_{79}N_3O_6Na$ $[M+Na]^+$ 852.5867; found 852.5993.
$[\alpha]^{20}_D$ = - 15 (c = 1.0, MeOH/$CHCl_3$ 1/1).

12-(6-Aminohexanamido)-*N*-((2*S*,3*R*,4*E*,6*Z*)-1,3-dihydroxyoctadeca-4,6-dien-2-yl)dodecanamide (RBM8-313)

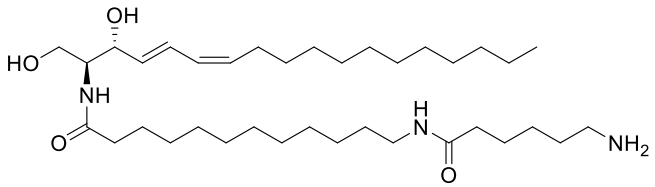

To a solution of **RBM8-312** (50 mg, 0.06 mmol) in anhydrous THF (2 mL) was added piperidine (180 µL, 1.8 mmol) at rt. After stirring for 5 h, the mixture was diluted with EtOAc. The organic phase was washed with water and brine, dried over anhydrous $MgSO_4$, and concentrated under reduced pressure. The residue was purified by flash column chromatography on silica

gel (DCM:MeOH; stepwise gradient from 0 to 10% of MeOH) to give **RBM8-313** as a white solid (25 mg, 71%). [187,188]

^{1}H NMR (CD_3OD): δ 6.55 (dd, *J* = 15.2, 11.1 Hz, 1H), 5.97 (t, *J* = 11.1 Hz, 1H), 5.65 (dd, *J* = 15.2, 7.3 Hz, 1H), 5.43 (dt, *J* = 10.7, 7.7 Hz, 1H), 4.22 – 4.12 (m, 1H), 3.89 (dt, *J* = 7.3, 5.1 Hz, 1H), 3.74 – 3.65 (m, 2H), 3.15 (t, *J* = 7.1 Hz, 2H), 2.80 – 2.68 (m, 2H), 2.19 (td, *J* = 7.6, 2.7 Hz, 4H), 1.72 – 1.43 (m, 8H), 1.43 – 1.16 (m, 25H), 0.93 (dt, *J* = 18.7, 7.2 Hz, 3H).

^{13}C NMR (CD_3OD): δ 174.9, 174.3, 132.6, 132.1, 127.8, 127.1, 72.0, 60.8, 55.3, 39.8, 38.9, 35.9, 35.3, 31.7, 29.45, 29.38, 29.34, 29.28, 29.26, 29.17, 29.11, 29.05, 28.99, 28.95, 28.83, 27.3, 26.6, 25.8, 25.7, 25.1, 22.3, 13.0.

HRMS (ESI): calcd. For $C_{36}H_{70}N_3O_4$ $[M+H]^+$ 608.5366; found 608.5278.
$[\alpha]^{20}_D$ = -3 (c: 1.3, MeOH/$CHCl_3$ 1:1)

5.1.6. Synthesis of RBM8-311

Methyl 12-aminododecanoate (RBM8-305)

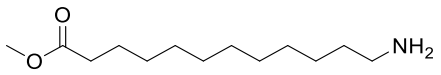

Thionyl chloride (0.52 mL, 7.2 mmol) was added dropwise to a cold suspension (0 ˚C) of 12-aminododecanoic acid (620 mg, 2.9 mmol) in 6 mL MeOH. The resulting mixture was refluxed overnight. The solvent and the excess of thionyl chloride were removed under reduced pressure. Trituration with EtOAc of the resulting white solid yielded quantitatively **RBM8-305**.[176]

^{1}H NMR ($CDCl_3$): δ 8.27 (s, 2H), 3.64 (s, 3H), 2.96 (s, 2H), 2.28 (t, *J* = 7.5 Hz, 2H), 1.84 – 1.67 (m, 2H), 1.59 (d, *J* = 14.7 Hz, 2H), 1.45 – 1.16 (m, 14H).

^{13}C NMR ($CDCl_3$): δ 174.3, 51.4, 39.9, 34.1, 29.4, 29.33, 29.29, 29.20, 29.10, 28.9, 27.7, 26.4, 24.9.
HRMS (ESI): calcd. For $C_{13}H_{28}NO_2$ $[M+H]^+$ 230.2120; found 230.2054.

6-((((9*H*-Fluoren-9-yl)methoxy)carbonyl)amino)hexanoic acid (RBM8-306)

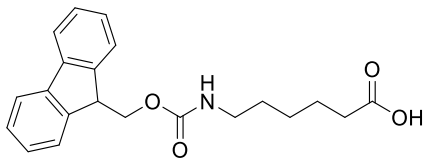

6-Aminohexanoic acid (500 mg, 3.80 mmol) and Na_2CO_3 (1.6 g, 7.60 mmol) were taken in 8 mL of water and the mixture was stirred with 7 mL of dioxane at 0 ˚C. To this mixture, Fmoc

chloride (1 g, 3.8 mmol) in 5 mL of dioxane was added dropwise and stirred for 1 h at 0°C and for additional 18 h at rt. The reaction mixture was poured into 100 mL of cold water and extracted with Et_2O. The ether extracts were discarded and the aqueous phase was adjusted to pH 2-3 and extracted with EtOAc. The organic layer was dried by rotatory evaporation and the crude was recrystallized from EtOAc-hexane to give of **RBM8-306**[175] (0.96 g, 73%) as a white solid.

^{1}H NMR ($CDCl_3$): δ 7.74 (d, *J* = 7.5 Hz, 2H), 7.57 (d, *J* = 7.4 Hz, 2H), 7.38 (t, *J* = 7.4 Hz, 2H), 7.33 – 7.26 (m, 2H), 4.76 (s, 1H), 4.39 (d, *J* = 6.8 Hz, 2H), 4.20 (d, *J* = 6.8 Hz, 1H), 3.18 (q, *J* = 6.6 Hz, 2H), 2.34 (t, *J* = 7.3 Hz, 2H), 1.71 – 1.56 (m, 2H), 1.56 – 1.43 (m, 2H), 1.43 – 1.29 (m, 2H).

^{13}C NMR ($CDCl_3$): δ 143.9, 141.3, 127.6, 126.9, 124.9, 119.9, 66.5, 47.3, 40.7, 33.6, 29.6, 26.1, 24.2.
HRMS (ESI): calcd. For $C_{21}H_{24}NO_4$ $[M+H]^+$ 354.1681; found 354.1640.

Methyl 12-(6-((((9*H*-fluoren-9-yl)methoxy)carbonyl)amino)hexanamido)dodecanoate (RBM8-307)

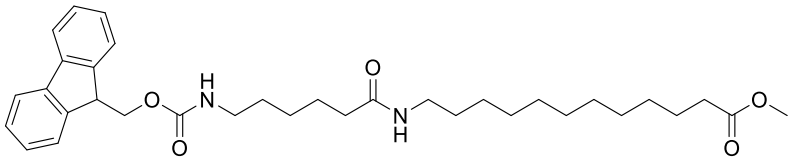

A solution of EDC (117 mg, 0.61 mmol), HOBt (64 mg, 0.47 mmol) and **RBM8-306** (200 mg, 0.56 mmol) in anhydrous CH_2Cl_2 (5 mL) was stirred under argon atmosphere at rt for 10 min, and next added dropwise to a solution of **RBM8-305** (108 mg, 0.47 mmol) in anhydrous CH_2Cl_2 (5 mL). The reaction mixture was stirred at rt for 3 h under argon atmosphere. The mixture was diluted by addition of CH_2Cl_2 (10 mL) and washed successively with water and brine. The organic layer was dried over $MgSO_4$, and filtered. Concentration under reduced pressure afforded the crude compound, which was purified by flash chromatography with CH_2Cl_2/MeOH 98:2 to afford **RBM8-307** (234 mg, 88%) as a white solid.

^{1}H NMR ($CDCl_3$): δ 7.73 (d, *J* = 7.5 Hz, 2H), 7.56 (d, *J* = 7.4 Hz, 2H), 7.36 (t, *J* = 7.4 Hz, 2H), 7.27 (t, *J* = 7.4 Hz, 2H), 5.60 (s, 1H), 4.99 (s, 1H), 4.35 (d, *J* = 6.9 Hz, 2H), 4.17 (t, *J* = 6.7 Hz, 1H), 3.63 (s, 3H), 3.17 (dq, *J* = 11.7, 6.6 Hz, 4H), 2.26 (t, *J* = 7.5 Hz, 2H), 2.12 (t, *J* = 7.3 Hz, 2H), 1.60 (tt, *J* = 14.7, 7.3 Hz, 4H), 1.47 (dt, *J* = 21.6, 6.9 Hz, 4H), 1.37 – 1.11 (m, 16H).

^{13}C NMR ($CDCl_3$): δ 174.4, 172.8, 156.6, 144.1, 141.4, 127.7, 127.1, 125.1, 120.0, 66.6, 51.5, 47.4, 40.8, 39.6, 36.6, 34.2, 29.7, 29.6, 29.5, 29.4, 29.34, 29.29, 29.19, 26.9, 26.4, 25.3, 25.0.

HRMS (ESI): calcd. For $C_{34}H_{49}N_2O_5$ $[M+H]^+$ 565.3641; found 565.3636.

12-(6-((((9*H*-Fluoren-9-yl)methoxy)carbonyl)amino)hexanamido)dodecanoic acid (RBM8-311)

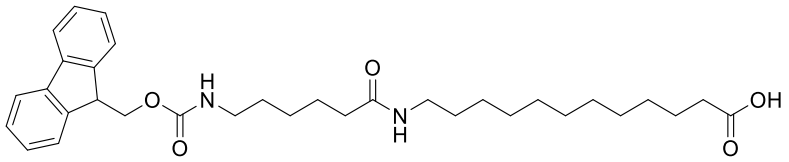

To a solution of **RBM8-307** (225 mg, 0.40 mmol) in dioxane (5 mL) was added a 4N aqueous solution of HCl (5 mL). The mixture was heated at 50°C for 18 h and then EtOAc was the added. The organic layer was washed with water until pH 7, brine, and dried over $MgSO_4$. The solvent was evaporated in vacuo and the residue was purified by flash chromatography with CH_2Cl_2/MeOH (98:2) affording **RBM8-311** (192 mg, 90%).[189]

^{1}H NMR ($CDCl_3$): δ 7.74 (d, *J* = 7.5 Hz, 2H), 7.57 (d, *J* = 7.5 Hz, 2H), 7.38 (t, *J* = 7.4 Hz, 2H), 7.33 – 7.25 (m, 2H), 5.49 (s, 1H), 4.87 (s, 1H), 4.37 (d, *J* = 6.9 Hz, 2H), 4.20 (d, *J* = 6.9 Hz, 1H), 3.20 (dq, *J* = 13.3, 6.4 Hz, 4H), 2.32 (t, *J* = 7.4 Hz, 2H), 2.15 (t, *J* = 7.4 Hz, 2H), 1.77 – 1.39 (m, 8H), 1.29 (d, *J* = 44.8 Hz, 14H).

^{13}C NMR ($CDCl_3$): δ 178.3, 173.1, 156.5, 143.9, 141.3, 132.6, 127.9, 127.6, 127.3, 126.9, 125.5, 125.0, 120.8, 119.9, 66.6, 66.1, 47.2, 40.7, 39.6, 36.5, 34.0, 29.5, 29.31, 29.26, 29.21, 29.13, 29.05, 28.9, 26.8, 26.2, 25.2, 24.7.

HRMS (ESI): calcd. For $C_{33}H_{47}N_2O_5$ $[M+H]^+$ 551.3485; found 551.3490.

5.1.7. Synthesis of sphinganine derivatives

(9*H*-Fluoren-9-yl)methyl (6-((12-(((2*S*,3*R*)-1,3-dihydroxyoctadecan-2-yl)amino)-12-oxododecyl)amino)-6-oxohexyl)carbamate (RBM8-336)

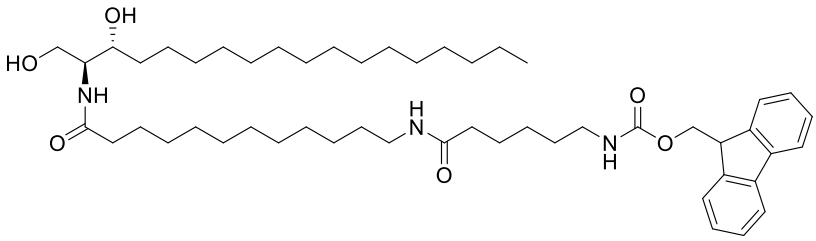

A solution of EDC (8 mg, 0.04 mmol), HOBt (5 mg, 0.03 mmol) and **RBM8-311** (21 mg, 0.04 mmol) in anhydrous CH_2Cl_2 (3 mL) was stirred under argon atmosphere at rt for 10 min, and next added dropwise to a solution of dihydrosphingosine [190] (10 mg, 0.03 mmol) in anhydrous CH_2Cl_2 (3 mL). The reaction mixture was stirred at rt for 2 h under argon atmosphere. The mixture was diluted by addition of CH_2Cl_2 (5 mL) and washed successively with water and brine. The organic layer was dried over $MgSO_4$, and filtered. Concentration under reduced pressure afforded the crude compound, which was purified by flash chromatography with CH_2Cl_2/MeOH (100% to 95%) to afford **RBM8-336** (20 mg, 74%) as a white solid.

^{1}H NMR ($CDCl_3$): δ 7.75 (d, *J* = 7.5 Hz, 1H), 7.57 (d, *J* = 7.4 Hz, 1H), 7.38 (t, *J* = 7.4 Hz, 1H), 7.30 (d, *J* = 7.4 Hz, 1H), 6.45 (d, *J* = 7.5 Hz, 1H), 5.53 (s, 1H), 4.86 (d, *J* = 51.9 Hz, 1H), 4.37 (d, *J* = 6.8 Hz, 1H), 4.28 – 4.11 (m, 1H), 3.99 (dd, *J* = 11.4, 3.4 Hz, 1H), 3.74 (s, 2H), 3.19 (dd, *J* = 13.5, 6.8 Hz, 4H), 2.18 (dt, *J* = 20.9, 7.3 Hz, 4H), 1.84 – 1.40 (m, 6H), 1.39-1.12 (m, 30H), 0.86 (t, *J* = 6.8 Hz, 3H).

^{13}C NMR ($CDCl_3$): δ 143.9, 141.3, 127.6, 127.0, 125.0, 119.9, 120.0, 106.5, 74.2, 66.5, 62.5, 53.7, 53.4, 47.3, 39.4, 36.8, 36.5, 34.5, 31.9, 29.7, 29.63, 29.57, 29.55, 29.48, 29.33, 29.26, 29.24, 29.17, 29.10, 29.04, 29.03, 28.97, 28.86, 26.6, 26.2, 25.9, 25.6, 25.2, 22.7, 14.1

HRMS (ESI): calcd. For $C_{51}H_{84}N_3O_6$ $[M+H]^+$ 834.6360; found 834.6357.

12-(6-Aminohexanamido)-N-((2*S*,3*R*)-1,3-dihydroxyoctadecan-2-yl)dodecanamide

(RBM8-337)

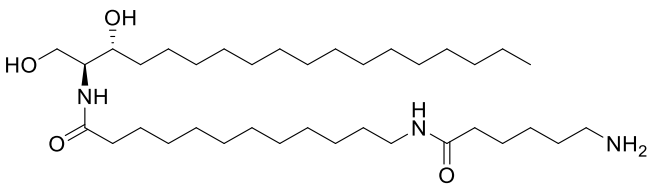

To a solution of **RBM8-336** (10 mg, 0.01 mmol) in anhydrous THF (2 mL) was added piperidine (400 µL, 0.36 mmol) at rt. After stirring for 4 h, the mixture was diluted with EtOAc. The organic phase was washed with water and brine, dried over anhydrous MgSO4, and concentrated under reduced pressure. The residue was purified by flash column chromatography on silica gel (DCM:MeOH; stepwise gradient from 10 to 50% of MeOH) to give **RBM8-337** as a white solid (7 mg, 97%). [187,188]

^{1}H NMR (CD_3OD): δ 3.89 – 3.78 (m, 1H), 3.71 (dd, *J* = 5.0, 2.6 Hz, 2H), 3.65 – 3.56 (m, 1H), 3.36 (s, 1H), 3.16 (q, *J* = 6.2 Hz, 4H), 2.99 – 2.88 (m, 2H), 2.23 (q, *J* = 7.3 Hz, 2H), 1.81 (p, *J* = 5.6 Hz, 4H), 1.77 – 1.39 (m, 12H), 1.31 (d, *J* = 9.3 Hz, 30H), 0.91 (t, *J* = 6.9 Hz, 3H).

^{13}C NMR (CD_3OD): δ 174.8, 174.2, 70.9, 61.0, 55.3, 44.3, 39.1, 38.9, 35.8, 35.2, 33.5, 31.6, 29.4, 29.34, 29.32, 29.28, 29.25, 29.24, 29.21, 29.10, 29.04, 28.98, 28.91, 26.8, 26.6, 25.7, 25.5, 25.1, 24.9, 22.33, 22.30, 21.6, 13.00.

HRMS (ESI): calcd. For $C_{36}H_{74}N_3O_4$ $[M+H]^+$ 612,5679; found 612.5670.

5.1.8. Synthesis of sphingosine derivatives

_N_-((2_S_,3_R_,_E_)-1,3-Dihydroxyoctadec-4-en-2-yl)octanamide (RBM8-349)

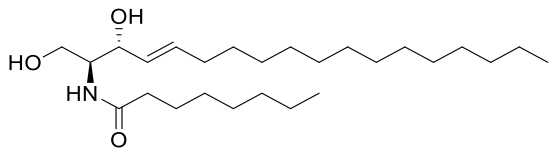

A solution of EDC (58 mg, 0.30 mmol), HOBt (31 mg, 0.23 mmol) and octanoic aicd (40 mg, 0.28 mmol) in anhydrous CH_2Cl_2 (5 mL) was stirred under argon atmosphere at rt for 10 min, and next added dropwise to a solution of sphingosine[191] (70 mg, 0.23 mmol) in anhydrous CH_2Cl_2 (5 mL). The reaction mixture was stirred at rt for 16 h under argon atmosphere. The mixture was diluted by addition of CH_2Cl_2 (5 mL) and washed successively with water and brine. The organic layer was dried over $MgSO_4$, and filtered. Concentration under reduced pressure afforded crude compound, which was purified by flash chromatography with CH_2Cl_2/MeOH (100% to 95%) to afford **RBM8-349** (82 mg, 84%) as a white solid.

^{1}H NMR ($CDCl_3$): δ 6.33 (d, J = 7.3 Hz, 1H), 5.86 – 5.67 (m, 1H), 5.59 – 5.40 (m, 1H), 4.28 (s, 1H), 4.05 – 3.79 (m, 2H), 3.68 (d, J = 8.7 Hz, 1H), 3.23 (s, 1H), 2.34 – 2.08 (m, 2H), 2.13 – 1.88 (m, 2H), 1.58 (dt, J = 62.8, 31.3 Hz, 2H), 1.44 – 1.08 (m, 30H), 0.87 (t, J = 6.8 Hz, 6H).

^{13}C NMR ($CDCl_3$): δ 174.2, 134.3, 128.91, 74.5, 62.5, 54.7, 36.9, 32.5, 32.1, 31.8, 29.8, 29.8, 29.8, 29.7, 29.5, 29.40, 29.38, 29.30, 29.2, 25.9, 22.82, 22.75, 14.3, 14.2.

HRMS (ESI): calcd. For $C_{26}H_{52}NO_3$ $[M+H]^+$ 426.3947; found 426.3942.

(9_H_-Fluoren-9-yl)methyl (6-((12-(((2_S_,3_R_,_E_)-1,3-dihydroxyoctadec-4-en-2-yl)amino)-12-oxododecyl)amino)-6-oxohexyl)carbamate (RBM8-350)

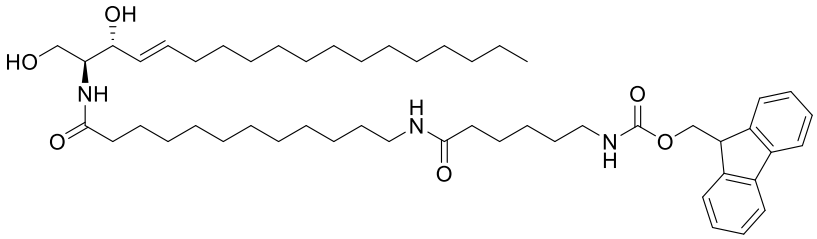

A solution of EDC (37 mg, 0.20 mmol), HOBt (20 mg, 0.15 mmol) and **RBM8-311** (100 mg, 0.18 mmol) in anhydrous CH_2Cl_2 (3 mL) was stirred under argon atmosphere at rt for 10 min, and next added dropwise to a solution of sphingosine[191] (51 mg, 0.15 mmol) in anhydrous CH_2Cl_2 (3 mL). The reaction mixture was stirred at rt for 2 h under argon atmosphere. The mixture was diluted by addition of CH_2Cl_2 (5 mL) and washed successively with water and brine. The organic layer was dried over $MgSO_4$, and filtered. Concentration under reduced pressure afforded

crude compound, which was purified by flash chromatography with CH_2Cl_2/MeOH (98% to 95%) to afford **RBM8-350** (91 mg, 65%) as a white solid.

^{1}H NMR (CD_3OD): δ 7.93 (d, *J* = 7.5 Hz, 2H), 7.78 (s, 2H), 7.55 (t, *J* = 7.4 Hz, 2H), 7.51 – 7.45 (m, 2H), 5.94 – 5.81 (m, 1H), 5.72 – 5.57 (m, 1H), 4.51 (d, *J* = 7.0 Hz, 2H), 4.36 (t, *J* = 6.9 Hz, 1H), 4.28 (t, *J* = 6.6 Hz, 1H), 4.08 – 3.97 (m, 1H), 3.99 – 3.88 (m, 1H), 3.83 (ddd, *J* = 11.3, 7.2, 4.1 Hz, 1H), 3.30 (dd, *J* = 16.1, 7.3 Hz, 4H), 2.35 (dd, *J* = 16.0, 8.2 Hz, 2H), 2.28 – 2.11 (m, 2H), 1.77 (tt, *J* = 14.4, 7.4 Hz, 2H), 1.67 (td, *J* = 14.9, 7.3 Hz, 2H), 1.59 – 1.30 (m, 44H), 1.04 (t, *J* = 6.8 Hz, 3H).

^{13}C NMR (CD_3OD): δ 174.8, 174.5, 143.8, 141.2, 133.7, 129.2, 127.5, 126.8, 124.9, 119.7, 72.7, 66.4, 61.2, 55.0, 47.1, 40.3, 39.3, 36.2, 35.9, 32.2, 31.7, 29.50, 29.49, 29.45, 29.44, 29.36, 29.30, 29.22, 29.16, 29.13, 29.11, 29.09, 29.06, 26.8, 26.0, 25.7, 25.3, 22.5, 13.5.

HRMS (ESI): calcd. For $C_{51}H_{82}N_3O_6$ $[M+H]^+$ 832.6204; found 832.6207.

12-(6-Aminohexanamido)-*N*-((2*S*,3*R*,*E*)-1,3-dihydroxyoctadec-4-en-2-yl)dodecanamide (RBM8-351)

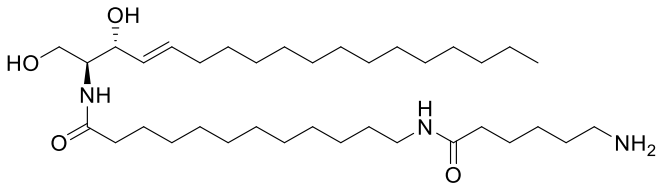

To a solution of **RBM8-350** (55 mg, 0.07 mmol) in anhydrous THF (10 mL) was added piperidine (200 µL, 1.98 mmol) at rt. After stirring for 3 h, the mixture was diluted with EtOAc. The organic phase was washed with water and brine, dried over anhydrous MgSO4, and concentrated under reduced pressure. The residue was purified by flash column chromatography on silica gel (DCM:MeOH; stepwise gradient from 10 to 20% of MeOH) to give **RBM8-350** as a white solid (30 mg, 75%).

^{1}H NMR (CD_3OD): δ 7.98 (s, 1H), 7.76 – 7.64 (m, 1H), 5.77 – 5.64 (m, 1H), 5.48 (dt, *J* = 15.4, 7.8 Hz, 1H), 4.07 (t, *J* = 7.4 Hz, 1H), 3.95 – 3.82 (m, 1H), 3.70 (d, *J* = 5.1 Hz, 1H), 3.20 – 3.11 (m, 4H), 2.98 – 2.89 (m, 2H), 2.22 (dd, *J* = 14.2, 7.0 Hz, 4H), 2.13 – 1.98 (m, 2H), 1.88 – 1.77 (m, 4H), 1.76 – 1.55 (m, 6H), 1.49 (dd, *J* = 15.8, 9.8 Hz, 2H), 1.46 – 1.17 (m, 36H), 0.99 – 0.83 (m, 3H).

^{13}C NMR (CD_3OD): δ 174.9, 174.2, 133.3, 129.8, 72.2, 60.9, 55.3, 44.3, 39.1, 39.0, 35.9, 35.2, 32.0, 31.6, 29.4, 29.4, 29.34, 29.33, 29.27, 29.20, 29.14, 29.10, 29.04, 28.99, 28.97, 28.95, 28.94, 26.8, 26.6, 25.7, 25.5, 24.9, 22.3, 21.6, 13.0.

HRMS (ESI): calcd. For $C_{36}H_{72}N_3O_4$ $[M+H]^+$ 610.5523; found 610.5523.

5.1.9. Synthesis of triazolinedione RBM8-254

***tert*-Butyl (4-(2-bromoethoxy)phenyl)carbamate (RBM8-078)**

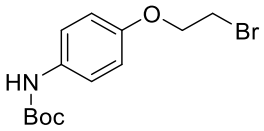

A suspension of 1-(2-bromoethoxy)-4-nitrobenzene (3 g, 11.5 mmol) and 5% Pd/C (600 mg) in THF (50 mL) was stirred at room temperatura for 4 h under a hydrogen atmosphere. Hydrogen was replaced with argon, and a solution of $(Boc)_2O$ (2.5 g, 11.5 mmol) in THF (10 mL) was added. After overnight stirring, the catalyst was removed through Celite. After evaporation, the remaining solids were washed with Hexane/Et_2O, and the residue was purified by flash column chromatography on silica gel (Hexane/EtOAc 90/10 to 80/20) to give **RBM8-078** as a white solid (730 mg, 58%).

^{1}H NMR ($CDCl_3$) δ 7.27 (d, *J* = 8.3 Hz, 2H), 6.85 (d, *J* = 9.0 Hz, 2H), 6.35 (s, 1H), 4.25 (t, *J* = 6.3 Hz, 2H), 3.61 (t, *J* = 6.3 Hz, 2H), 1.51 (s, 9H).

Analytical data match those reported for this compound in the literature.[85]

***Tert*-butyl (4-(2-azidoethoxy)phenyl)carbamate (RBM8-079)**

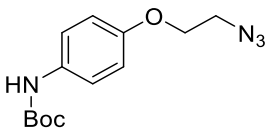

A suspension of **RBM8-078** (700 mg, 2.12 mmol) and NaN_3 (689 mg, 10.6 mmol) in DMF (15 mL) was stirred at 50°C for 3 h. Then, EtOAc and water were added. The organic layer was separated and washed once with water. The resulting aqueous layer was extracted once with EtOAc. The combined organic layer was dried over $MgSO_4$, and concentrated *in vacuo*. The residue was purified by a filtration through a short plug of silica gel (Hexane/EtOAc 10/0 to 7/3) to give **RBM8-079** (507 mg, 86%) as white crystals.

^{1}H NMR ($CDCl_3$): δ 7.25 (d, *J* = 7.7 Hz, 2H), 7.01 – 6.68 (m, 2H), 6.44 (s, 1H), 4.09 (dd, *J* = 10.2, 5.2 Hz, 2H), 3.64 – 3.39 (m, 2H), 1.48 (s, 9H).

Analytical data match those reported for this compound in the literature.[85]

4-(2-Azidoethoxy)aniline hydrochloride (RBM8-080)

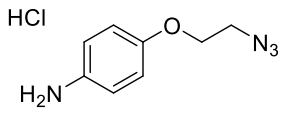

A solution of **RBM8-079** (500 mg, 1.80 mmol) in 4 M HCl/dioxane (10 mL) was stirred at rt for 3 h. The solvent was removed *in vacuo* and the resulting pale brown solids were washed with EtOAc to give **RBM8-080** (380 mg, 99%).

^{1}H NMR (CD_3OD): δ 7.39 – 7.33 (m, 2H), 7.13 – 7.08 (m, 2H), 4.23 – 4.18 (m, 2H), 3.61 (dd, *J* = 8.7, 3.7 Hz, 2H).

4-(4-(2-Azidoethoxy)phenyl)-1,2,4-triazolidine-3,5-dione (TAD-Azide)

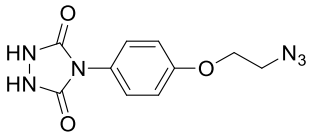

To a 0.2 M solution of ethyl hydrazinecarboxylate (243 mg, 2.33 mmol) in THF (12 mL) was added 1,1'-carbonyldiimidazole (CDI, 378 mg, 2.33 mmol) at rt. The resulting solution was stirred at rt for 2 h. Aniline **RBM8-080** (500 mg, 2.33 mmol) and Et_3N (0.65 mL, 4.66 mmol) were next added at rt and stirring was maintained overnight. Then, EtOAc and 10% HCl were added. The organic layer was separated and washed once with 10% HCl and water. The resulting aqueous layer was extracted once with EtOAc. The combined organic layer was dried over $MgSO_4$, and concentrated *in vacuo*. The resulting crude solid was washed with EtOAc, dried and taken up in MeOH (0.2 M solution), followed by addition of K_2CO_3 (3 equiv.). The resulting suspension was stirred at reflux temperature for 3 h. Then, the reaction mixture was acidified with 12 N HCl to pH 2 and then concentrated *in vacuo*. The resulting withe solids were washed with water and EtOAc to give **TAD-azide** (2 steps, 28%).

^{1}H NMR (DMSO): δ 10.40 (s, 2H), 7.35 (d, *J* = 9.0 Hz, 2H), 7.06 (d, *J* = 9.0 Hz, 2H), 4.31 – 4.12 (m, 2H), 3.79 – 3.58 (m, 2H).

^{13}C NMR (DMSO): δ 157.2, 153.6, 127.7, 124.9, 114.7, 67.1, 49.5.

The physical and spectroscopic data were identical to those reported.[85]

1,4-Diazabicyclo[2.2.2]octane bromine (DABCO-Br)

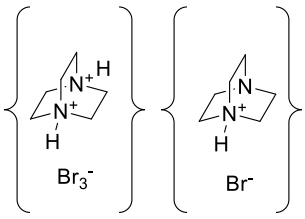

This compound was synthesized as reported in the literature.[89,192] Thus, 1,4-diazabicyclo[2.2.2]octane (2 g, 18.0 mmol) was dissolved in chloroform (20mL). A solution of Br_2 (6 g, 37.0 mmol) in chloroform (10 mL) was next added dropwise using an addition funnel. The resulting mixture was stirred under inert atmosphere for 1 h. The yellow precipitate was filtered off, washed with chloroform (50mL) and dried overnight under vacuum.

4-(4-(2-Azidoethoxy)phenyl)-3*H*-1,2,4-triazole-3,5(4*H*)-dione (RBM8-254)

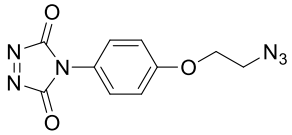

A mixture of TAD-Azide (100 mg, 0.38 mmmol), DABCO-Br (120 mg, 0.07 mmol) and CH_2Cl_2 (3 mL) was stirred for 1 h at rt, until the development of deep red coloured solution. The reaction mixture was filtered off, the residue washed with dichloromethane and the filtrate concentrated in vacuo to obtain **RBM8-254** (98 mg, 99%) as a red solid.[85,89] The activated reagent should be used immediately due to its apparent instability against light, humidity and silica gel.

^{1}H NMR ($CDCl_3$): δ 7.40 – 7.32 (m, 2H), 7.10 – 7.03 (m, 2H), 4.23 – 4.16 (m, 2H), 3.67 – 3.60 (m, 2H).

^{13}C NMR ($CDCl_3$): δ 158.7, 157.8, 125.6, 122.4, 115.7, 67.4, 49.9.

5.1.10. Diels Alder adducts

N-((1*S*,2*S*)-1-(1,3-Dioxo-2-phenyl-8-undecyl-2,3,5,8-tetrahydro-1*H*-[1,2,4]triazolo[1,2-a]pyridazin-5-yl)-1,3-dihydroxypropan-2-yl)octanamide (RBM8-217)

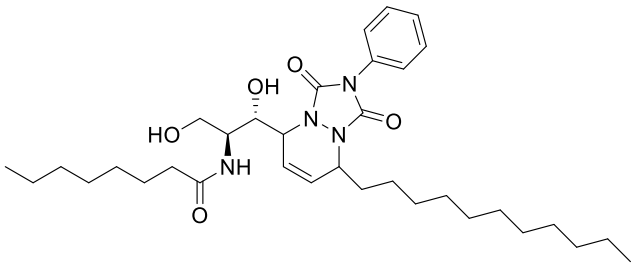

To a solution of **RBM8-216** (25 mg, 0.05 mmol) in THF/CH_2Cl_2 (1 mL/1 mL) was added dropwise a solution of PTAD [193,194] (43 mg, 0.25 mmol) in 1 mL of CH_2Cl_2/THF (1/1). The mixture was stirred at rt for 16 h. The solvent was concentrated in vacuo and the residue was purified by flash chromatography on silica gel (CH_2Cl_2/MeOH, stepwise gradient from 0 to 3% of MeOH) to obtain 15 mg (50%) of **RBM8-217** as a single diastereomer.

^{1}H NMR ($CDCl_3$): δ 7.55 – 7.30 (m, 5H), 6.12 (s, 2H), 4.60 (s, 1H), 4.54 (s, 1H), 4.33 (d, *J* = 10.5 Hz, 1H), 4.14 – 3.95 (m, 2H), 3.55 (d, *J* = 11.6 Hz, 1H), 2.20 (s, 2H), 1.80 (d, *J* = 6.5 Hz, 2H), 1.61 (br, 2H), 1.24 (d, *J* = 18.6 Hz, 24H), 0.85 (d, *J* = 7.1 Hz, 6H).

^{13}C NMR ($CDCl_3$): δ 173.7, 151.1, 149.9, 130.4, 129.5, 129.3, 128.7, 128.5, 127.7, 125.5, 125.3, 119.0, 68.4, 62.1, 54.7, 53.5, 51.3, 36.5, 31.9, 31.7, 29.55, 29.47, 29.37, 29.34, 29.29, 29.21, 28.9, 25.6, 24.3, 22.64, 22.56, 14.08, 14.04.

HRMS (ESI): calcd. For $C_{34}H_{55}N_4O_5$ $[M+H]^+$ 599.4172; found 599.4168.

***N*-((1*S*,2*S*)-1-(2-(2-(6,7-Dimethoxy-4-methyl-3-oxo-3,4-dihydroquinoxalin-2-yl)ethyl)-1,3-dioxo-8-undecyl-2,3,5,8-tetrahydro-1*H*-[1,2,4]triazolo[1,2-a]pyridazin-5-yl)-1,3-dihydroxypropan-2-yl)octanamide (RBM8-242)**

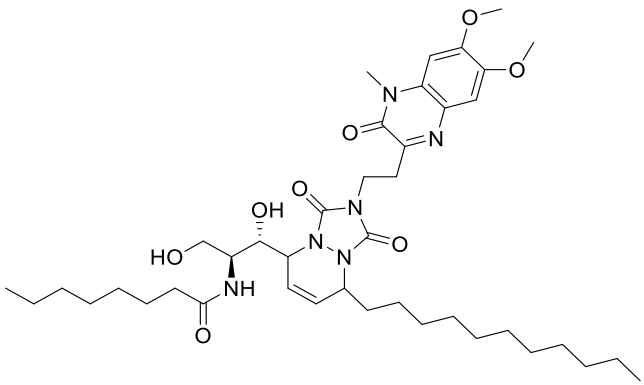

To a solution of **RBM8-216** (13 mg, 0.03 mmol) in DMSO (1 mL) was added dropwise a solution of DMEQ-TAD [169,195] (11 mg, 0.03 mmol) in 1 mL of DMSO. The mixture was stirred at rt for 2 h.

Water (5 mL) was next added, and the solution was extracted with Et_2O (3 x 3 mL), and the organic phases were washed with brine and concentrated in vacuo. The residue was purified by flash chromatography on silica gel (CH_2Cl_2/MeOH 10/90) to obtain 20 mg (87%) of **RBM8-242** as a single diastereomer.

^{1}H NMR ($CDCl_3$): δ 7.20 (s, 1H), 6.78 (d, *J* = 9.2 Hz, 1H), 6.64 (s, 1H), 6.20 (dd, *J* = 10.7, 3.2 Hz, 1H), 6.06 (dd, *J* = 10.5, 2.7 Hz, 1H), 4.94 (d, *J* = 5.1 Hz, 1H), 4.56 (s, 1H), 4.47 (dd, *J* = 9.9, 4.7 Hz, 1H), 4.33 (s, 1H), 4.11 (q, *J* = 15.0, 14.1 Hz, 2H), 3.95 (d, *J* = 28.9 Hz, 6H), 3.69 – 3.60 (m, 1H), 3.50 – 3.34 (m, 2H), 3.00 – 2.74 (m, 2H), 2.36 – 2.13 (m, *J* = 7.7 Hz, 2H), 2.00 (s, 2H), 1.75 (s, 2H), 1.70 – 1.43 (m, 6H), 1.42 – 0.98 (m, 28H), 0.85 (dt, *J* = 6.9, 3.2 Hz, 6H).

^{13}C NMR ($CDCl_3$): δ 173.5, 155.4, 154.2, 152.2, 151.84, 151.76, 146.6, 127.9, 127.7, 127.3, 119.9, 110.5, 95.9, 68.8, 62.1, 56.4, 56.2, 55.0, 53.1, 50.9, 38.0, 36.7, 32.9, 31.9, 31.7, 29.71, 29.66, 29.54, 29.52, 29.45, 29.41, 29.32, 29.28, 29.26, 28.97, 25.7, 24.4, 22.63, 22.56, 14.07, 14.04.

HRMS (ESI): calcd. For $C_{41}H_{65}N_6O_8$ $[M+H]^+$ 769.4864; found 769.4896.

N-((1*S*,2*S*)-1-(2-(4-(2-Azidoethoxy)phenyl)-1,3-dioxo-8-undecyl-2,3,5,8-tetrahydro-1*H*-[1,2,4]triazolo[1,2-a]pyridazin-5-yl)-1,3-dihydroxypropan-2-yl)octanamide (RBM8-310)

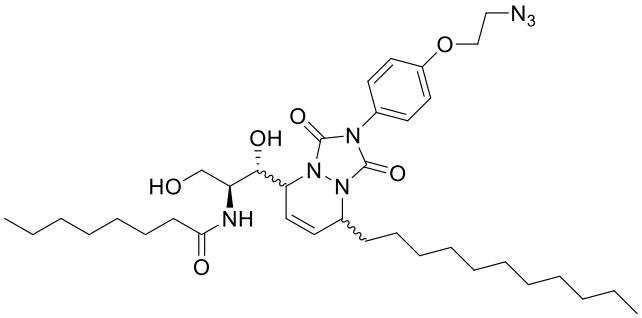

To a solution of **RBM8-216** (15 mg, 0.05 mmol) in CH_2Cl_2 (2 mL) was added dropwise a solution of **RBM8-254** (20 mg, 0.10 mmol) in 1 mL of CH_2Cl_2. The mixture was stirred at rt for 2 h. The solvent was concentrated in vacuo to afford a mixture of two diastereomers (**d.r.** (exo/endo)= 1/1), which were separated by flash chromatography on silica gel (CH_2Cl_2/MeOH stepwise gradient from 0 to 3% of MeOH) to obtain 15 mg and 16 mg (91% total yield) of **RBM8-310(f1)** and **RBM8-310(f2)**, respectively. The configuration of the two diastereomers (exo/endo) was not determined.

^{1}H NMR (RBM8-310f1, $CDCl_3$): δ 7.37 (t, *J* = 10.8 Hz, 2H), 6.96 (t, *J* = 9.5 Hz, 2H), 5.99 (qd, *J* = 10.7, 3.8 Hz, 2H), 4.83 – 4.72 (m, 1H), 4.50 (dt, *J* = 8.7, 4.1 Hz, 1H), 4.20 – 3.94 (m, 6H), 3.82 (d, *J* = 10.5 Hz, 2H), 3.58 (t, *J* = 5.0 Hz, 4H), 2.14 (t, *J* = 7.7 Hz, 2H), 1.78 (q, *J* = 8.3, 7.9 Hz, 2H), 1.57 (s, 2H), 1.44 – 1.03 (m, 24H), 0.96 – 0.78 (m, 6H).

HRMS (RBM8-310f1, ESI): calcd. For $C_{36}H_{58}N_7O_6$ $[M+H]^+$ 684.4449; found 684.4449.

^{1}H NMR (RBM8-310f2, $CDCl_3$): δ 7.29 – 7.18 (m, 2H), 6.95 (t, *J* = 7.8 Hz, 2H), 6.12 (d, *J* = 1.9 Hz, 2H), 4.64 – 4.51 (m, 2H), 4.34 (d, *J* = 10.4 Hz, 1H), 4.13 (q, *J* = 5.5, 5.1 Hz, 3H), 4.10 – 4.00 (m, 2H), 3.64 – 3.49 (m, 4H), 2.20 (t, *J* = 7.6 Hz, 2H), 1.79 (q, *J* = 7.3 Hz, 2H), 1.63 (dq, *J* = 15.0, 9.0, 8.1 Hz, 2H), 1.43 – 1.02 (m, 28H), 0.85 (td, *J* = 6.8, 3.3 Hz, 6H).

HRMS (RBM8-310f2, ESI): calcd. For $C_{36}H_{58}N_7O_6$ $[M+H]^+$ 684.4449; found 684.4471.

5.1.11. Alder-ene adducts

1-((2*S*,3*R*)-2-Amino-1,3-dihydroxyheptadec-7-en-6-yl)-4-(4-(2-azidoethoxy)phenyl)-1,2,4-triazolidine-3,5-dione (RBM8-367)

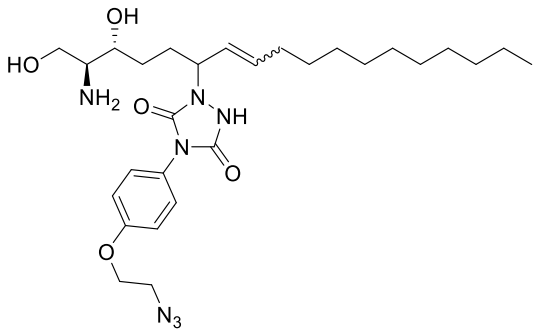

Freshly prepared **RBM8-254** (134 mg, 0.58 mmol) was added to a solution of **RBM8-125** (20 mg, 0.07 mmol) in MeOH (5 mL). The reaction mixture was stirred at rt. After 16h, the solvent was removed and the residue was purified by flash chromatography (CH_2Cl_2/MeOH 100% to 90%) to afford **RBM8-367** (25 mg, 70%) as a brown solid.

^{1}H NMR (CD_3OD): δ 9.13 (d, *J* = 7.8 Hz, 1H), 7.14 – 7.08 (m, 2H), 7.00 – 6.93 (m, 2H), 5.44 – 5.33 (m, 2H), 4.18 (dd, *J* = 10.2, 5.2 Hz, 2H), 3.96 (s, 1H), 3.81 (dt, *J* = 12.7, 5.5 Hz, 2H), 3.78 – 3.71 (m, 2H), 3.68 (s, 2H), 3.61 – 3.58 (m, 2H), 2.27 (ddd, *J* = 14.3, 9.9, 5.1 Hz, 1H), 2.19 – 1.98 (m, 3H), 1.63 (m, 1H), 1.58 – 1.48 (m, 1H), 1.45 – 1.17 (m, 16H), 0.96 – 0.84 (m, 3H).

^{13}C NMR ($CDCl_3$): δ 157.8, 156.3, 154.6, 131.3, 130.5, 129.7, 128.5, 127.5, 115.3, 114.8, 73.7, 67.3, 67.2, 62.5, 55.8, 53.9, 50.0, 49.9, 34.1, 31.9, 29.67, 29.61, 29.55, 29.3, 27.3, 23.8, 22.7, 14.1.

HRMS (RBM8-310f2, ESI): calcd. For $C_{28}H_{46}N_7O_5$ $[M+H]^+$ 560.3560; found 560.3456.

5.2. Biochemistry

5.2.1. Cell culture

The human gastric cancer cell line HGC 27 was cultured at 37°C in 5% CO_2 in minimum essential medium supplemented with 10% foetal bovine serum, 1% nonessential amino acids, and 100 ng/ml each of penicillin and streptomycin. Cells were routinely grown at a 60% maximum confluence. Human glioblastoma cell lines T98 and U87 were cultured at 37°C in 5% CO_2 in Dulbecco's modified Eagle's medium supplemented with 10% foetal bovine serum and 100 ng/ml each of penicillin and streptomycin. All cell lines were obtained from American Type Culture Collection.

5.2.2. Cell viability

In all cell lines, cell viability was measured in triplicate by the colorimetric 3-(4,5-dimethylthiazol-2-yl)-2,5-diphenyl tetrazolium bromide (MTT) assay. Cells were seeded in 96 well plates at a density of $1x10^5$ cells/mL and then subjected to the treatments for 24 h. At the end of the treatments, MTT was added to each well and incubated for 3 h. The supernatant was aspirated, and the resulting crystals (formazan) were dissolved in DMSO. The absorbance was measured at 570 nm with a Spectramax Plus Reader (Molecular Device Corporation).

5.2.3. Des1 activity assay in cell lysates

Des1 activity was determined in HGC27 cell lysates as reported,[62] using the fluorescent derivatives **RBM8-29**, **RBM8-126**, or dhCerC_6NBD as a positive control of enzyme activity. In the inhibition studies by **RBM2-085** and **RBM8-202** dhCerC_6NBD was used as substrate.

To prepare the cell lysates, a suspension of 10^6 cells/mL per sample was centrifuged (1400 *rpm*/3 min), the pellets were washed twice with PBS and resuspended in 0.4 ml of 0.2 M phosphate buffer pH 7.4 (PB). Then 100 µL of PB were added to each pellet and sonicated at 75 Watts (Branson SFX150 sonicator) for 5 seconds. A 3.5 % (v/v) solution of the required amount of stock substrate solution (1 mM in EtOH) in a BSA solution (3.3 mg/ml in PB) was prepared to have the needed substrate concentrations (35 µM for a 10 µM final concentration in standard assays). In inhibition studies, the required amount of test compound was added at this point. To each tube containing the lysate from 10^6 cells was added: 85 µL of the BSA-substrate-inhibitor/vehicle mix (final substrate concentrations in standard assays was 10 µM), 30 µL of NADH solution (20 mg/ml in PB) and 85 µL of PB to have a final volume of 300 µL. Unless otherwise indicated, the reaction mixture was incubated at 37°C for 4 h. To stop the reaction, 700 µL/sample of methanol was added to each tube and the reaction mixture was vortexed and kept at 4°C overnight. The mixture was centrifuged (10.000 *rpm*/3 min), the clear supernatants were transferred to HPLC vials and 20 µL were injected. HPLC analyses were

performed with an Alliance apparatus coupled to a fluorescence detector using a C18 column (Kromasil 100 C18, 5 µm, 15 x 0.40 cm, Tracer) equipped with a precolumn (ODS, Tracer). Compounds were eluted with 25% H_2O and 75% acetonitrile, at 1 mL/min flow rate. The detector was set at an excitation wavelength of 465 nm and an emission wavelength at 530 nm. Each sample was run for up to 22 min.

Specific assays conditions

a) To determine the kinetic parameters of **RBM8-126** as Des1 substrate (Fig. 2.13), concentrations of **RBM8-126** were 20, 15, 10, 5, 2.5, 1.25, 0.675, 0.327 and 0 µM. Amount of protein (cell lysates) were 140 µg.

b) To determine the IC_{50} value of compound **RBM2-085** (Fig. 2.16), compound concentrations were 7.5, 5.0, 2.5, 2.0, 1.0, 0.5, 0.25, 0.1, 0.01 and 0 µM. Amount of protein (cell lysates) were 140 µg. Reaction time was 4 h.

c) To determine reversibility of Des1 inhibition by **RBM2-085** (Fig. 2.18), substrate concentration (dhCerC_6NBD) was 10 µM, test compound concentration was 150 nM and the reaction times were 1, 2.5, 4 and 6 h. Amount of protein (cell lysates) were 140 µg.

d) For Ki determination (Fig. 2.17), substrate (dhCerC_6NBD) concentrations were 20, 15, 10 and 5 µM and inhibitor concentrations were 200, 100 and 0 nM. Amount of protein (cell lysates) were 140 µg. Reaction time was 4 h.

5.2.4. Lipid analyses

Cells were seeded at $1x10^5$ cells into 6 well plates (1 ml/well) and were allowed to adhere for 24 h. The medium was replaced with fresh medium containing the test compounds at the specified concentrations or EtOH for the control. The medium was removed after 2 and 24 h, and cells were washed with PBS and harvested by trypsinization. Sphingolipid extracts, fortified with internal standards *N*-dodecanoylsphingosine, *N*-dodecanoylglucosylsphingosine, *N*-dodecanoylsphingosylphosphorylcoline, C17-sphinganine and C17-sphinganine 1-phosphate, 0.2 nmol each) were prepared and analysed by UPLC-TOF MS.[62]

The liquid chromatography-mass spectrometer consisted of a Waters Aquity UPLC system connected to a Waters LCT Premier orthogonal accelerated time of flight mass spectrometer (Waters, Millford, MA), operated in positive electrospray ionisation mode. Full scan spectra from 50 to 1500 Da were acquired and individual spectra were summed to produce data points each 0.2 s. Mass accuracy and reproducibility were maintained by using an independent reference spray by the LockSpray interference. The analytical column was a 100 mm x 2.1mm i.d., 1.7 mm C8 Acquity UPLC BEH (Waters). The two mobile phases were phase A: methanol/water/formic acid (74/25/1 v/v/v); phase B: methanol/formic acid (99/1 v/v), both also contained 5mM ammonium formate. A linear gradient was programmed— 0.0 min: 80% B; 3 min: 90% B; 6 min: 90% B; 15 min: 99% B; 18 min: 99% B; 20 min: 80% B. The flow rate was 0.3 ml min^{-1}. The column was held at 30°C. Quantification was carried out using the extracted ion chromatogram of each compound, using 50 mDa. windows. The linear dynamic range was determined by injecting standard mixtures. Positive identification of compounds was based on

the accurate mass measurement with an error <5 ppm and its LC retention time, compared to that of a standard (±2%).

Table 5.1. MS-Based assignments of metabolites of **RBM2-085** and **RBM8-202** present in cell lipid extracts.

Compound	Exp. Mass[a]	Calc. Mass[a]	Error (ppm)	Formula	rt (min)[b]
RBM2-085	426.3957	426.3947	-2,3	C26H52NO3	4.11[c]
RBM8-202	426.3967	426.3947	-4,7	C26H52NO3	4.11[c]
RBM2-76	424.3804	424.3791	-3,1	C26H50NO3	3.83[c]
RBM8-216	424.3778	424.3791	3,1	C26H50NO3	3.83[c]
RBM2-085-PC	591.4497	591.4502	0,8	C31H64N2O6P	3.92
RBM8-202-PC	591.4511	591.4502	-1,5	C31H62N2O6P	4.08
RBM2-76-PC	589.4373	589.4346	-4,6	C31H62N2O6P	3.61
RBM8-216-PC	589.4356	589.4346	-1,7	C31H62N2O6P	3.70

[a]in ESI-positive mode. [b]rt, retention time. [c]identical to synthetic standards.

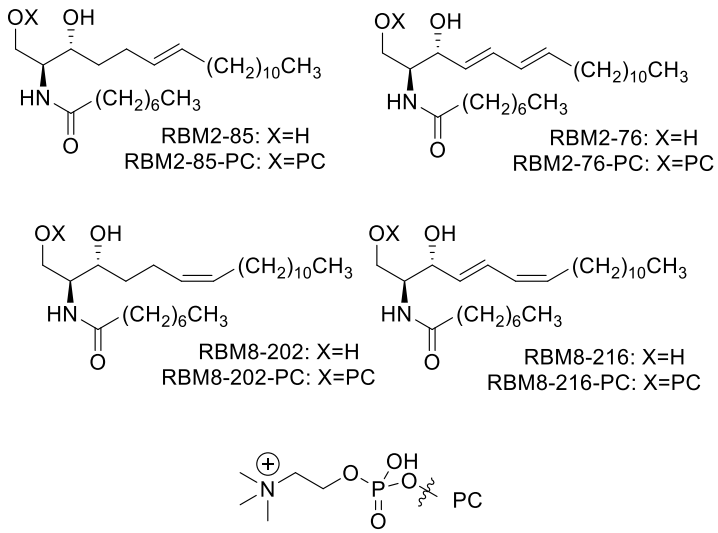

5.3. Microarray assays

5.3.1. Reagents, buffers and blocking agents

The chemical reagents (compounds **RBM8-**) used in this study were synthetized in our laboratory (*see* Experimental section, synthesis and product characterization). DBCO-PEG$_4$-TAMRA (Dibenzylcyclooctyne-PEG4-5/6-Tetramethylrhodamine) were obtained from Jena Bioscience (Jena, Germany).

PBS was 0.01 M phosphate buffer in a 0.8% saline solution (137 mmol/L NaCl, 2.7 mmol/L KCl; pH =7.5). PBST was PBS with 0.05% Tween 20. The washing stations were carried out with MilliQ water (Milli-Q® Ultrapure Water Solutions) and MeOH (for liquid chromatography LiChrosolv®, Merck).

Blocking agents used in this study were ethanolamine (100 mM in PBS), BSA (1 and 2%) in PBS, 2% PEG6000 in PBST, PBS, 2% PVP in PBS, 2% gelatine in PBS and 2% milk in PBS.

5.3.2. Instrumentation

5.3.2.1. Microarray printing

Sphingolipid chains were spotted onto derivatized solid support using BioOdissey Calligrapher MiniArrayer (Bio-Rad Laboratories, Inc. USA) in a 60% relative humidity and at 22˚C.

5.3.2.2. ScanArray Gx Plus (Microarray scanner)

Fluorescent measurements were recorded on a ScanArray Gx PLUS (Perkin Elmer, USA) with a TAMRA optical filter with 5-µm resolution. The laser power and PMT were set to 90% and 70%, respectively. The spots were measured by F543_Mean-B543 (Mean TAMRA foreground intensity minus mean TAMRA background intensity). Fluorescence intensity values were expressed normalized or in relative units as average and standard deviation of three replicate wells. The competitive curves were analysed with a four-parameter logistic equation using software [SoftmaxPro v4.7 (Molecular Devices) and GraphPad Prism v 4 (GraphPad Software Inc., San Diego, CA, USA)]. The standard curves were fitted to a four-parameter equation according to the following formula: Y = [(A _ B)/1 _ (x/C)D] + B, where A is the maximal fluorescence, B the minimum fluorescence, C the concentration producing 50% of the difference between A and B (or IC50), and D the slope at the inflection point of the sigmoid curve. The limit of detection (LOD) was defined as the concentration producing 90% of the maximal fluorescence (IC90).

5.3.3. Microarray steps for a HTS assay

5.3.3.1. Slides derivatization with GPTMS

Glass slides (drawer 3.5, Corning® 2947-75x25) were marked in the bottom right corner and washed with soap and water. Then, they were submerged into a piranha solution (H_2SO_4 conc.: H_2O_2 7:3 (v/v)) for 30 min. and rinsed with water (x6). For the surface activation (Fig. 5.2), slides were submerged into a 10% NaOH solution for 30 min. and then rinsed with water (x3) and ethanol (x3). Next, the glass slides were submerged into a solution of GPTMS (2,5% in EtOH) and 10 mM acetic acid for 3 h. To remove de excess of GPTMS, slides were submerged into EtOH and left in an ultrasonic bath for 30 min, dried in an air current and stored in a desiccator.

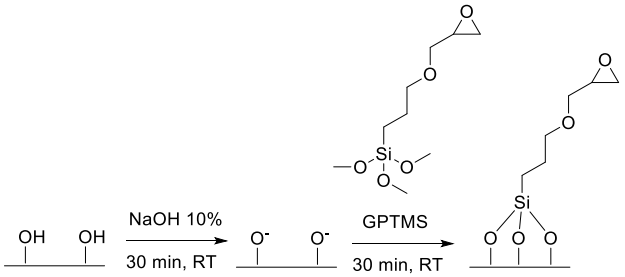

Figure 5.2. Functionalization of the glass support with GPTMS.

5.3.3.2. Validation of click reaction

A solution of NH_2-PEG_4-DBCO (0, 0.125, 0.25, 0.5, 1 mg/mL in DMF) was used to charge a 96 well plate (100 µL per well), which was placed inside the Bioodissey ™ Calligrapher ™ Miniarrayer (Bio-Rad Laboratories, Inc. USA). The content of each well was spotted (100 µm) onto the GPTMS derivatized solid support (*see* above) kept a 60% relative humidity at 22˚C. Each glass slide contained 24 subarrays defined by a 5x5 spot matrix on each well with 5 different concentrations (1, 0.5, 0.25, 0.125, 0 mg/mL) and 5 replicates for each concentration. After 16 h, the slide was placed on a microplate microarray ArrayIt hardware system (Telechem International Inc.) with a silicon gasket that demarcated 24 subarrays per slide (8 rows x 3 columns) and 100 µL of N_3-PEG_3-TAMRA at concentrations of 10, 5, 2.5, 1.25, 0.625, 0.313, 0.15, 0 µg/mL in MeOH were added to each well (x 3 columns) for 1 h. Then, the slide was washed with MeOH and MilliQ water, dried and read in the ScanArray G_x.

5.3.3.3. Sphingolipid binding of compounds RBM8-251 and RBM8-269 to the derivatized surface

The derivatized GPTMS slide was submerged in a 2.5% EtOH solution of 5-aminopentan-1-ol for 1 h. The slide was washed with EtOH, dried, and placed on a microplate microarray Arrayit hardware system (Telechem International Inc.) with a silicon gasket that demarcated 24 wells. On the other hand, 500 µL of **RBM8-251** (4 mg/mL in DMF, 1 mmol) or **RBM8-269** (4 mg/mL in DMF, 1 mmol) were mixed with 250 µL of *N*-metylimidazole (2.4 mg/mL in DMF, 1 mmol) and 250 µL of CDI (14.4 mg/mL, 3 mmol) for 10 min. After this time, 100 µL of the above mixture was added to each well and left on standing for 3 h. The final concentration of the substrates was 5, 2 and 1 mg/ml per well. The slide was next washed with DMF, dried on air and the silicon gasket was placed again. After carrying out the enzymatic reaction with the cell lysates (*see* Section 5.3.3.6), 100 µL of a 1 M KOH solution in EtOH was added to each well, and allowed to react for 1 h. The content of each well was next transferred to HPLC vials for UPLC-TOF MS analysis.

The lipid extracts were taken up in 150 µl of methanol. The liquid chromatography-mass spectrometer consisted of a Waters Aquity UPLC system connected to a Waters LCT Premier Orthogonal Accelerated Time of Flight Mass Spectrometer (Waters, Millford, MA), operated in positive or negative electrospray ionization mode. Full scan spectra from 50 to 1500 Da were obtained. Mass accuracy and reproducibility were maintained by using an independent reference spray via LockSpray. A 100 mm 2.1 mm id, 1.7 mm C18 Acquity UPLC® BEH LCT Premier Xe (Waters) analytical column was used. The two mobile phases used were 20 mM HCOOH in MeCN (phase A) and 20 mM HCOOH in H_2O (phase B) and mixtures at 0.3 mL/min were used as mobile phase. The column was run at 30°C. Quantification was carried out using the ion chromatogram obtained for each compound using 50 mDa windows.

5.3.3.4. Sphingolipid attachment of RBM8-313 and RBM8-324 to the microarray surface

The target sphingolipids were dissolved in DMF (concentrations ranged between 10 to 0 mg/mL, depending on the assay). This solution was transferred to a 96 well plate (100 µL per well), which was placed inside the Bioodissey ™ Calligrapher ™ Miniarrayer (Bio-Rad Laboratories, Inc. USA). The sphingolipids were spotted onto the GPTMS derivatized solid support (*see* Section 5.3.3.1) in a 60% relative humidity chamber at 22°C. Each glass slide contained 24 wells of a 3x3 spot matrix per well with nine spots with 3 replicates per well.

5.3.3.5. Blocking agents

The slide was placed on a microplate microarray ArrayIt hardware system (Telechem International Inc.) with a silicon gasket that demarcated into 24 wells per slide. Before starting the assay, the slides were blocked (100 µL/well-blocking solution) for 1 h, washed four times with MilliQ water and dried.

5.3.3.6. Enzymatic assay in cell lysates

To prepare the cell lysates, a suspension of 10^6 cells/ml of the HGC27 cell line per sample was centrifuged (1400 *rpm*/3 min) and the pellets were washed twice with PBS and resuspended in 180 µL of 0.2 M phosphate buffer pH 7.4 and kept under ice. The ice cooled suspension was sonicated for 5 seconds. Next, 20 µL of a NADH solution (20 mg/ml in 0.2 M phosphate buffer pH 7.4) to have a final volume of 200 µL was added.

The slide was placed again on the microplate microarray with a silicon gasket to demarcate 24 wells per slide, and the above 200 µl of cell lysate were added in each well. The reaction mixture was incubated at 37 °C for 4 h. After this time, the slide was washed with MilliQ water and dried using compressed air.

5.3.3.7. Diels Alder reaction

The above slide was placed in a Arrayit Microarray Reaction Trays (Arrayit® Corporation) and submerged into 5 mL of **RBM8-254** (4 mg/ml) in MeOH for 1 h at rt. Then, the slide was rinsed with MeOH, Milli-Q water and dried with compressed air.

5.3.3.8. SPAAC reaction

The above slide was placed again in the Arrayit Microarray Reaction Trays and submerged into 5 ml of **DBCO-PEG$_4$-TAMRA** (1 µg/ml) in MeOH. After 1 h of incubation at rt, the slide was rinsed with MeOH, H_2O and dried under compressed air.

5.3.3.9. CuAAC reaction

After the Diels Alder reaction, the slide was placed in the Arrayit Microarray Reaction Trays and submerged into 5 ml of **550-Red Oxazine alkyne** solution (1 µg/mL in H_2O), previously activated with Cu_2SO_4 (17 eq.), sodium ascorbate (40 eq.) and THTPA (10 eq.). After 1 h of incubation at rt, the slide was rinsed with MilliQ water and dried under compressed air.

5.3.3.10. Fluorescence reading

The fluorescence of the slide was read with ScanArray G_x PLUS (*see* Section 5.3.2.2). The exciting source was set up at 543 nm and the fluorescence readout was collected at 570 nm.

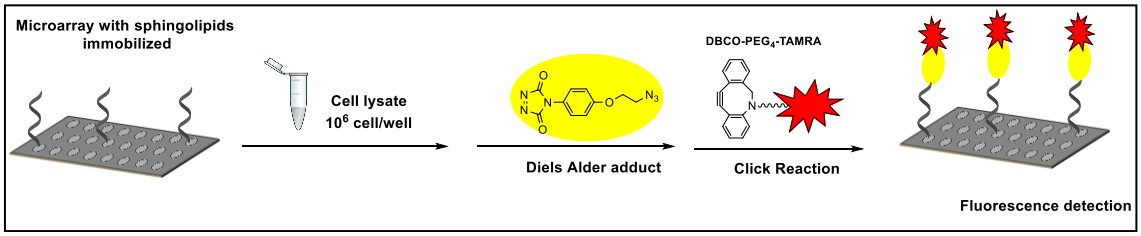

6. REFERENCES

6. REFERENCES

(1) Yang, J.; Yu, Y.; Sun, S.; Duerksen-Hughes, P. J. Ceramide and Other Sphingolipids in Cellular Responses. *Cell Biochem. Biophys.* **2004**, *40* (3), 323–350.

(2) Futerman, A. H.; Hannun, Y. A. The Complex Life of Simple Sphingolipids. *EMBO Rep.* **2004**, *5* (8), 777–782.

(3) Ohanian, J.; Ohanian, V. Cellular and Molecular Life Sciences Sphingolipids in Mammalian Cell Signalling. *Cell. Mol. Life Sci.* **2001**, *58* (14), 2053–2068.

(4) Merril, A. H.; Sandhoff, K. *Sphingolipids: Metabolism and Cell Signalling*; Elsevier Masson SAS, 2002; Vol. 31.

(5) Merrill, A. H. De Novo Sphingolipid Biosynthesis: A Necessary, but Dangerous, Pathway. *J. Biol. Chem.* **2002**, *277* (29), 25843–25846.

(6) Hannun, Y. A.; Obeid, L. M. Many Ceramides. *J. Biol. Chem.* **2011**, *286* (32), 27855–27862.

(7) Ogretmen, B.; Hannun, Y. A. Biologically Active Sphingolipids in Cancer Pathogenesis and Treatment. *Nat. Rev. Cancer* **2004**, *4* (8), 604–616.

(8) Hannun, Y. a; Obeid, L. M. Principles of Bioactive Lipid Signalling: Lessons from Sphingolipids. *Nat. Rev. Mol. Cell Biol.* **2008**, *9* (2), 139–150.

(9) Wattenberg, B. W.; Pitson, S. M.; Raben, D. M. The Sphingosine and Diacylglycerol Kinase Superfamily of Signaling Kinases: Localization as a Key to Signaling Function. *J. Lipid Res.* **2006**, *47* (6), 1128–1139.

(10) Johnson, K. R.; Johnson, K. Y.; Becker, K. P.; Bielawski, J.; Mao, C.; Obeid, L. M. Role of Human Sphingosine-1-Phosphate Phosphatase 1 in the Regulation of Intra- and Extracellular Sphingosine-1-Phosphate Levels and Cell Viability. *J. Biol. Chem.* **2003**, *278* (36), 34541–34547.

(11) Levy, M.; Futerman, A. H. Mammalian Ceramide Synthases. *IUBMB Life* **2010**, *62* (5), 347–356.

(12) Maceyka, M.; Spiegel, S. Sphingolipid Metabolites in Inflammatory Disease. *Nature* **2014**, *510* (7503), 58–67.

(13) Hanada, K.; Kumagai, K.; Yasuda, S.; Miura, Y.; Kawano, M.; Fukasawa, M.; Nishijima, M. Molecular Machinery for Non-Vesicular Trafficking of Ceramide. *Nature* **2003**, *426* (6968), 803–809.

(14) Hannun, Y. A.; Luberto, C.; Mao, C.; Obeid, L. M. Bioactive Sphingolipids in Cancer Biology and Therapy. In *Bioactive Sphingolipids in Cancer Biology and Therapy*; Springer, 2015; pp 1–486.

(15) Carvajal, A.; Menendez, A.; Bowen, W.; Wanebo, H. Sphingolipid Biology and Its Role in Cancer Development and Therapy. *Clin. Case Reports Rev.* **2016**, *2* (4), 369–374.

(16) Pralhada Rao, R.; Vaidyanathan, N.; Rengasamy, M.; Mammen Oommen, A.; Somaiya, N.; Jagannath, M. R. Sphingolipid Metabolic Pathway: An Overview of Major Roles

Played in Human Diseases. *J. Lipids* **2013**, *2013*, 1–12.

(17) Borodzicz, S.; Czarzasta, K.; Kuch, M.; Cudnoch-Jedrzejewska, A. Sphingolipids in Cardiovascular Diseases and Metabolic Disorders. *Lipids Health Dis.* **2015**, *14* (1), 1–8.

(18) Stover, T.; Kester, M. Liposomal Delivery Enhances Short-Chain Ceramide-Induced Apoptosis of Breast Cancer Cells. *J. Pharmacol. Exp. Ther.* **2003**, *307* (2), 468–475.

(19) Jazvinšćak Jembrek, M.; Hof, P. R.; Šimić, G. Ceramides in Alzheimer's Disease: Key Mediators of Neuronal Apoptosis Induced by Oxidative Stress and Aβ Accumulation. *Oxid. Med. Cell. Longev.* **2015**, *2015*, 1–17.

(20) Katsel, P.; Li, C.; Haroutunian, V. Gene Expression Alterations in the Sphingolipid Metabolism Pathways during Progression of Dementia and Alzheimer's Disease: A Shift toward Ceramide Accumulation at the Earliest Recognizable Stages of Alzheimer's Disease. *Neurochem. Res.* **2007**, *32* (4–5), 845–856.

(21) Van Echten-Deckert, G.; Walter, J. Sphingolipids: Critical Players in Alzheimer's Disease. *Prog. Lipid Res.* **2012**, *51* (4), 378–393.

(22) 1,2-Diacylglycerol and Ceramide Levels in Insulin-Resistant Tissues of the Rat in Vivo. *J. Biol. Chem.* **1990**, *265* (28), 16880–16885.

(23) Ussher, J. R.; Koves, T. R.; Cadete, V. J. J.; Zhang, L.; Jaswal, J. S.; Swyrd, S. J.; Lopaschuk, D. G.; Proctor, S. D.; Keung, W.; Muoio, D. M.; Lopaschuk, G. D. Inhibition of de Novo Ceramide Synthesis Reverses Diet-Induced Insulin Resistance and Enhances Whole-Body Oxygen Consumption. *Diabetes* **2010**, *59* (10), 2453–2464.

(24) Holland, W. L.; Brozinick, J. T.; Wang, L. P.; Hawkins, E. D.; Sargent, K. M.; Liu, Y.; Narra, K.; Hoehn, K. L.; Knotts, T. A.; Siesky, A.; Nelson, D. H.; Karathanasis, S. K.; Fontenot, G. K. K.; Birnbaum, M. J.; Summers, S. A. Inhibition of Ceramide Synthesis Ameliorates Glucocorticoid-, Saturated-Fat-, and Obesity-Induced Insulin Resistance. *Cell Metab.* **2007**, *5* (3), 167–179.

(25) Masako Sugiura, Keita Kono, Hong Liu, Tetsuya Shimizugawa, Hiroyuki Minekura, S. S. and T. K. Ceramide Kinase, a Novel Lipid Kinase. Molecular Cloning and Functional Characterization. *The Journal of Biological Chemistry*. 2002, pp 23294–23300.

(26) Yehezkel Barnholz, A. R. and S. G. Enzymatic Hydrolysis of Sphingolipids. II. Hydrolysis of Sphingomyelin by an Enzyme from Rat Brain. *J. Biol. Chem.* **1966**, *241*, 3731–3737.

(27) Nikolova-Karakashian, M. Assays for the Biosynthesis of Sphingomyelin and Ceramide Phosphoethanolamine. *Methods Enzymol.* **1999**, *311* (1972), 31–42.

(28) Schulze, H.; Michel, C.; Van Echten-Deckert, G. Dihydroceramide Desaturase. *Methods Enzymol.* **1999**, *311* (1993), 22–30.

(29) Rui-Dong Duan, A. N. Sphingolipid Hydrolyzing Enzymes in the Gastrointestinal Tract. *Methods Enzymol.* **2000**, *311* (1968), 276–286.

(30) Anna Maria, V.; Takuro, K.; Kunihiko, S. Comparison of Synthetic and Natural Glucosylceramides as Substrate for Glucosylceramidase Assay. *Clin. Chim. Acta* **1982**, *118* (1), 1–7.

(31) Van Veldhoven, P. P. Sphingolipid Metabolism and Cell Signaling Part A. *Methods*

Enzymol. **2000**, *311* (D), 244–254.

(32) Spassieva, S.; Bielawski, J.; Anelli, V.; Obeid, L. M. Combination of C17 Sphingoid Base Homologues and Mass Spectrometry Analysis as a New Approach to Study Sphingolipid Metabolism. *Methods Enzymol.* **2007**, *434* (7), 233–241.

(33) Abad, J. L.; Nieves, I.; Rayo, P.; Casas, J.; Fabriàs, G.; Delgado, A. Straightforward Access to Spisulosine and 4,5-Dehydrospisulosine Stereoisomers: Probes for Profiling Ceramide Synthase Activities in Intact Cells. *J. Org. Chem.* **2013**, *78* (12), 5858–5866.

(34) Kim, H. J.; Qiao, Q.; Toop, H. D.; Morris, J. C.; Don, A. S. A Fluorescent Assay for Ceramide Synthase Activity. *J. Lipid Res.* **2012**, *53* (8), 1701–1707.

(35) Billich, A.; Ettmayer, P. Fluorescence-Based Assay of Sphingosine Kinases. *Anal. Biochem.* **2004**, *326* (1), 114–119.

(36) French, K. J.; Zhuang, Y.; Maines, L. W.; Gao, P.; Wang, W.; Beljanski, V.; Upson, J. J.; Green, C. L.; Keller, S. N.; Smith, C. D. Pharmacology and Antitumor Activity of ABC294640, a Selective Inhibitor of Sphingosine Kinase-2. *J. Pharmacol. Exp. Ther.* **2010**, *333* (1), 129–139.

(37) Nikolova-Karakashian, M.; Morgan, E. T.; Alexander, C.; Liotta, D. C.; Merrill, A. H. Bimodal Regulation of Ceramidase by Interleukin-1β. Implications for the Regulation of Cytochrome P450 2C11 (CYP2C11). *J. Biol. Chem.* **1997**, *272* (30), 18718–18724.

(38) Bhabak, K. P.; Hauser, A.; Redmer, S.; Banhart, S.; Heuer, D.; Arenz, C. Development of a Novel FRET Probe for the Real-Time Determination of Ceramidase Activity. *ChemBioChem* **2013**, *14* (9), 1049–1052.

(39) Munoz-Olaya, J. M.; Matabosch, X.; Bedia, C.; Egido-Gabás, M.; Casas, J.; Llebaria, A.; Delgado, A.; Fabriàs, G. Synthesis and Biological Activity of a Novel Inhibitor of Dihydroceramide Desaturase. *ChemMedChem* **2008**, *3* (6), 946–953.

(40) Casasampere, M.; Ordoñez, Y. F.; Pou, A.; Casas, J. Inhibitors of Dihydroceramide Desaturase 1: Therapeutic Agents and Pharmacological Tools to Decipher the Role of Dihydroceramides in Cell Biology. *Chem. Phys. Lipids* **2016**, *197*, 33–44.

(41) Rodriguez-Cuenca, S.; Barbarroja, N.; Vidal-Puig, A. Dihydroceramide Desaturase 1, the Gatekeeper of Ceramide Induced Lipotoxicity. *Biochim. Biophys. Acta - Mol. Cell Biol. Lipids* **2015**, *1851* (1), 40–50.

(42) Bielawska, A.; Crane, H. M.; Liotta, D.; Obeid, L. M.; Hannun, Y. A. Selectivity of Ceramide-Mediated Biology: Lack of Activity of Erythro-Dihydroceramide. *J. Biol. Chem.* **1993**, *268* (35), 26226–26232.

(43) Kraveka, J. M.; Li, L.; Szulc, Z. M.; Bielawski, J.; Ogretmen, B.; Hannun, Y. A.; Obeid, L. M.; Bielawska, A. Involvement of Dihydroceramide Desaturase in Cell Cycle Progression in Human Neuroblastoma Cells. *J. Biol. Chem.* **2007**, *282* (23), 16718–16728.

(44) Zheng, W.; Kollmeyer, J.; Symolon, H.; Momin, A.; Munter, E.; Wang, E.; Kelly, S.; Allegood, J. C.; Liu, Y.; Peng, Q.; Ramaraju, H.; Sullards, M. C.; Cabot, M.; Merrill, A. H. Ceramides and Other Bioactive Sphingolipid Backbones in Health and Disease: Lipidomic Analysis, Metabolism and Roles in Membrane Structure, Dynamics, Signaling and Autophagy. *Biochim. Biophys. Acta - Biomembr.* **2006**, *1758* (12), 1864–1884.

(45) Stiban, J.; Fistere, D.; Colombini, M. Dihydroceramide Hinders Ceramide Channel Formation: Implications on Apoptosis. *Apoptosis* **2006**, *11* (5), 773–780.

(46) Cadena, D. L.; Kurten, R. C.; Gill, G. N. The Product of the MLD Gene Is a Member of the Membrane Fatty Acid Desaturase Family: Overexpression of MLD Inhibits EGF Receptor Biosynthesis. *Biochemistry* **1997**, *36* (23), 6960–6967.

(47) Omae, F.; Miyazaki, M.; Enomoto, A.; Suzuki, M.; Suzuki, Y.; Suzuki, A. DES2 Protein Is Responsible for Phytoceramide Biosynthesis in the Mouse Small Intestine. *Biochem. J.* **2004**, *379* (Pt 3), 687–695.

(48) Fabrias, G.; Muñoz-Olaya, J.; Cingolani, F.; Signorelli, P.; Casas, J.; Gagliostro, V.; Ghidoni, R. Dihydroceramide Desaturase and Dihydrosphingolipids: Debutant Players in the Sphingolipid Arena. *Prog. Lipid Res.* **2012**, *51* (2), 82–94.

(49) Geeraert, L.; Mannaerts, G. P.; van Veldhoven, P. P. Conversion of Dihydroceramide into Ceramide: Involvement of a Desaturase. *Biochem. J.* **1997**, *327*, 125–132.

(50) Michel, C.; van Echten-Deckert, G.; Rother, J.; Sandhoff, K.; Wang, E.; Merrill, A. H. Characterization of Ceramide Synthesis. *J. Biol. Chem.* **1997**, *272* (36), 22432–22437.

(51) Enomoto, A.; Omae, F.; Miyazaki, M.; Kozutsumi, Y.; Yubisui, T.; Suzuki, A. Dihydroceramide:sphinganine C-4-Hydroxylation Requires Des2 Hydroxylase and the Membrane Form of Cytochrome b5. *Biochem. J.* **2006**, *397* (2), 289–295.

(52) Camacho, L.; Simbari, F.; Garrido, M.; Abad, J. L.; Casas, J.; Delgado, A.; Fabriàs, G. 3-Deoxy-3,4-Dehydro Analogs of XM462. Preparation and Activity on Sphingolipid Metabolism and Cell Fate. *Bioorganic Med. Chem.* **2012**, *20* (10), 3173–3179.

(53) Triola, G.; Fabriàs, G.; Llebaria, A. Synthesis of a Cyclopropene Analogue of Ceramide, a Potent Inhibitor of Dihydroceramide Desaturase. *Angew. Chemie Int. Ed.* **2001**, *40* (10), 1960–1962.

(54) Triola, G.; Fabriàs, G.; Casas, J.; Llebaria, A. Synthesis of Cyclopropene Analogues of Ceramide and Their Effect on Dihydroceramide Desaturase. *J. Org. Chem.* **2003**, *68* (26), 9924–9932.

(55) De Jonghe, S.; Van Overmeire, I.; Van Calenbergh, S.; Hendrix, C.; Busson, R.; De Keukeleire, D.; Herdewijn, P. Synthesis of Fluorinated Sphinganine and Dihydroceramide Analogues. *European J. Org. Chem.* **2000**, No. 18, 3177–3183.

(56) Brodesser, S.; Kolter, T. Dihydroceramide Desaturase Inhibition by a Cyclopropanated Dihydroceramide Analog in Cultured Keratinocytes. *J. Lipids* **2011**, *2011*, 1–8.

(57) Mody, N.; McIlroy, G. D. The Mechanisms of Fenretinide-Mediated Anti-Cancer Activity and Prevention of Obesity and Type-2 Diabetes. *Biochem. Pharmacol.* **2014**, *91* (3), 227–286.

(58) Pervaiz, S.; Holme, A. L. Resveratrol: Its Biological Targets and Functional Activity. *Antioxid Redox Signal* **2009**, *11* (11).

(59) Kartal, M.; Saydam, G.; Sahin, F.; Baran, Y. Resveratrol Triggers Apoptosis Through Regulating Ceramide Metabolizing Genes in Human K562 Chronic Myeloid Leukemia Cells. *Nutr. Cancer* **2011**, *634* (4), 637–644.

(60) Cakir, Z.; Saydam, G.; Sahin, F.; Baran, Y. The Roles of Bioactive Sphingolipids in Resveratrol-Induced Apoptosis in HL60 Acute Myeloid Leukemia Cells. *J. Cancer Res. Clin. Oncol.* **2011**, *137* (2), 279–286.

(61) Dolfini, E.; Roncoroni, L.; Dogliotti, E.; Sala, G.; Erba, E.; Sacchi, N.; Ghidoni, R. Resveratrol Impairs the Formation of MDA-MB-231 Multicellular Tumor Spheroids Concomitant with Ceramide Accumulation. *Cancer Lett.* **2007**, *249* (2), 143–147.

(62) Cingolani, F.; Casasampere, M.; Sanllehi, P.; Casas, J.; Bujons, J.; Fabrias, G. Inhibition of Dihydroceramide Desaturase Activity by the Sphingosine Kinase Inhibitor SKI II. *J. Lipid Res.* **2014**, *55* (8), 1711–1720.

(63) Casasampere, M.; Ordoñez, Y. F.; Pou, A.; Casas, J. Inhibitors of Dihydroceramide Desaturase 1: Therapeutic Agents and Pharmacological Tools to Decipher the Role of Dihydroceramides in Cell Biology. *Chem. Phys. Lipids* **2016**, *197*, 33–44.

(64) Michel, C.; Echten-deckert, G. Van; Sandhoff, K.; Wang, E.; Merrill, A. H. Characterization of Ceramide Synthesis. **1997**, *272* (36), 22432–22437.

(65) Raith, K.; , Jorg Darius, R. H. H. N. Ceramide Analysis Utilizing Gas Chromatography – Mass Spectrometry. *J. Chromatogr.* **2000**, *876*, 229–233.

(66) Kok, J. W.; Nikolova-karakashian, M.; Klappe, K.; Alexander, C.; Merrill, A. H. Dihydroceramide Biology Structure-Specific Metabolism and Intracellular Localization. *J. Biol. Chem.* **1997**, *272* (34), 21128–21136.

(67) Munoz-Olaya, J. M.; Matabosch, X.; Bedia, C.; Egido-Gabás, M.; Casas, J.; Llebaria, A.; Delgado, A.; Fabriàs, G. Synthesis and Biological Activity of a Novel Inhibitor of Dihydroceramide Desaturase. *ChemMedChem* **2008**, *3* (6), 946–953.

(68) Cookson, R. C. 4-Phenyl-1,2,4-Triazolin-3,5-Dione: A Powerful Dienophile. *Tetrahedron Lett.* **1962**, *1* (14), 615–618.

(69) Leach, A. G.; Houk, K. N. Diels–Alder and Ene Reactions of Singlet Oxygen, Nitroso Compounds and Triazolinediones: Transition States and Mechanisms from Contemporary Theory. *Chem. Commun.* **2002**, No. 12, 1243–1255.

(70) Radl, S. 1,2,4-Triazoline-3,5-Diones. *Adv. Heterocycl. Chem.* **1996**, *67* (30), 119–205.

(71) De Bruycker, K.; Billiet, S.; Houck, H. A.; Chattopadhyay, S.; Winne, J. M.; Du Prez, F. E. Triazolinediones as Highly Enabling Synthetic Tools. *Chem. Rev.* **2016**, *116* (6), 3919–3974.

(72) Pounder, R. J.; Stanford, M. J.; Brooks, P.; Richards, S. P.; Dove, A. P. Metal Free Thiol-Maleimide "Click" Reaction as a Mild Functionalisation Strategy for Degradable Polymers. *Chem Commun* **2008**, No. 41, 5158–5160.

(73) Dewar, M. J. S.; Olivella, S.; Stewart, J. J. P. Mechanism of the Diels-Alder Reaction: Reactions of Butadiene with Ethylene and Cyanoethylenes. *J. Am. Chem. Soc.* **1986**, *108* (19), 5771–5779.

(74) Hagarty, J. D.; Gillis, B. T. The Reaction of 4-Phenyl-1,2,4-Triazoline-3,5-Dione with Conjugated Dienes. *J. Org. Chem.* **1966**, *32* (2), 330–333.

(75) Korobitsyna, I. K.; Khalikova, A. V.; Rodina, L. L.; Shusherina, N. P. 4-Phenyl-I, 2,4-

Triazoline-3,5-Dione in Organic Synthesis. *Khimiya Geterotsiklicheskikh Soedin.* **1983**, No. 2, 117–136.

(76) Jensen, F.; Foote, C. S. Reaction of 4-Phenyl-1,2,4-Triazoline-3,5-Dione with Substituted Butadienes. A Nonconcerted Diels-Alder Reaction. *J. Am. Chem. Soc.* **1987**, *109* (21), 6376–6385.

(77) Higashi, T.; Shibayama, Y.; Fuji, M.; Shimada, K. Liquid Chromatography-Tandem Mass Spectrometric Method for the Determination of Salivary 25-Hydroxyvitamin D3: A Noninvasive Tool for the Assessment of Vitamin D Status. *Anal. Bioanal. Chem.* **2008**, *391* (1), 229–238.

(78) Wang, H.; Liu, Y.; Li, M.; Huang, H.; Xu, H. M.; Hong, R. J.; Shen, H. Multifunctional TiO2 Nanowires-Modified Nanoparticles Bilayer Film for 3D Dye-Sensitized Solar Cells. *Optoelectron. Adv. Mater. Rapid Commun.* **2010**, *4* (8), 1166–1169.

(79) Ban, H.; Gavrilyuk, J.; Barbas, C. F. Tyrosine Bioconjugation through Aqueous Ene-Type Reactions: A Click-like Reaction for Tyrosine. *J. Am. Chem. Soc.* **2010**, *132* (5), 1523–1525.

(80) Martin E. Burrage, Richard C. Cookson, S. S. G. and I. D. R. S. Substituent and Solvent Effects on the Diels-Alder Reactions of Triazolinediones. *J. Chem. Soc., Perkin Trans. 2* **1975**, 1325–1334.

(81) Hoffmann, H. M. R. The Ene Reaction. *Angew. Chemie Int. Ed.* **1969**, *8* (8), 556–577.

(82) Kurt; Alder; Franz; Pascher; Und; Andreas; Schmitz. Über Die Anlagerung von Maleinsäure-Anhydrid Und Azodicarbonsäure-Ester an Einfach Ungesättigte Koh an Einfach Ungesättigte Kohlenwasserstoffe. Zur Kenntnis von Substitutionsvorgängen in Der Allyl-Stellung. *Eur. J. Inorg. Chem.* **1943**, *76* (1), 27–53.

(83) Clarke, M. L.; France, M. B. The Carbonyl Ene Reaction. *Tetrahedron* **2008**, *64* (38), 9003–9031.

(84) Squillacote, M.; Mooney, M.; Felippis, J. De; Paxton, R. J.; Beatty, B. G.; Curtis, F. L. An Aziridinium Imide Intermediate in the Ene Reaction of Trans-Cycloheptene and N-Methyl- 1,2,4- Triazoline-3,5-Dione. *J. Am. Chem. Soc.* **1990**, *112*, 5364–5365.

(85) Ban, H.; Nagano, M.; Gavrilyuk, J.; Hakamata, W.; Inokuma, T.; Barbas, C. F. Facile and Stabile Linkages through Tyrosine: Bioconjugation Strategies with the Tyrosine-Click Reaction. *Bioconjug. Chem.* **2013**, *24* (4), 520–532.

(86) Murao, N.; Ishigai, M.; Sekiguchi, N.; Takahashi, T.; Aso, Y. Ferrocene-Based Diels-Alder Derivatization for the Determination of 1-Hydroxyvitamin D3 in Rat Plasma by High-Performance Liquid Chromatography-Electrospray Tandem Mass Spectrometry. *Anal. Biochem.* **2005**, *346* (1), 158–166.

(87) Tasdelen, M. A. Diels–Alder “click” Reactions: Recent Applications in Polymer and Material Science. *Polym. Chem.* **2011**, *2* (10), 2133.

(88) Roling, O.; De Bruycker, K.; Vonhören, B.; Stricker, L.; Körsgen, M.; Arlinghaus, H. F.; Ravoo, B. J.; Du Prez, F. E. Rewritable Polymer Brush Micropatterns Grafted by Triazolinedione Click Chemistry. *Angew. Chemie Int. Ed.* **2015**, *54* (44), 13126–13129.

(89) Billiet, S.; Bruycker, K. De; Driessen, F.; De Bruycker, K.; Driessen, F.; Goossens, H.; Van

Speybroeck, V.; Winne, J. M.; Du Prez, F. E. Triazolinediones Enable Ultrafast and Reversible Click Chemistry for the Design of Dynamic Polymer Systems. *Nat. Chem.* **2014**, *6* (9), 815–821.

(90) Rahmaniyan, M.; Curley, R. W.; Obeid, L. M.; Hannun, Y. A.; Kraveka, J. M. Identification of Dihydroceramide Desaturase as a Direct in Vitro Target for Fenretinide. *J. Biol. Chem.* **2011**, *286* (28), 24754–24764.

(91) Savile, C. K.; Fabriàs, G.; Buist, P. H. Dihydroceramide Δ4 Desaturase Initiates Substrate Oxidation at C-4. *J. Am. Chem. Soc.* **2001**, *123* (19), 4382–4385.

(92) Triola, G.; Fabriàs, G.; Llebaria, A. Synthesis of a Cyclopropene Analogue of Ceramide, a Potent Inhibitor of Dihydroceramide Desaturase. *Angew. Chemie - Int. Ed.* **2001**, *40* (10), 1960–1962.

(93) Harvey, S. C. Maleimide as a Dienophile. *J. Am. Chem. Soc.* **1949**, *71* (1), 1121–1122.

(94) Richard Cremlyn, F. S. and R. N. Diels-Alder Reactions Using N-(P-Chlorosulfonylphenyl)-Maleimide as Dienophile. *Phosphorus and Sulfur* **1987**, *33*, 65–67.

(95) Gacal, B.; Durmaz, H.; Tasdelen, M. A.; Hizal, G.; Tunca, U.; Yagci, Y.; Demirel, A. L. Anthracene-Maleimide-Based Diels-Alder "click Chemistry" as a Novel Route to Graft Copolymers. *Macromolecules* **2006**, *39* (16), 5330–5336.

(96) Abad, J. L.; Camps, F.; Fabriàs, G. Substrate-Dependent Stereochemical Course of the (Z)-13-Desaturation Catalyzed by the Processionary Moth Multifunctional Desaturase. *J. Am. Abad, J. L.; Camps, F.; Fabriàs, G. Substrate-Dependent Stereochem. Course (Z)-13-Desaturation Catalyzed by Process. Moth Multifunct. Desaturase. J. Am. Chem. Soc. 2007, 129 (48), 15007–15012. Chem. Soc* **2007**, *129* (48), 15007–15012.

(97) Liénard, M. A.; Strandh, M.; Hedenström, E.; Johansson, T.; Löfstedt, C. Key Biosynthetic Gene Subfamily Recruited for Pheromone Production prior to the Extensive Radiation of Lepidoptera. *BMC Evol. Biol.* **2008**, *8*, 270.

(98) Liénard, M. A.; Lassance, J.-M.; Wang, H.-L.; Zhao, C.-H.; Piskur, J.; Johansson, T.; Löfstedt, C. Elucidation of the Sex-Pheromone Biosynthesis Producing 5,7-Dodecadienes in Dendrolimus Punctatus (Lepidoptera: Lasiocampidae) Reveals Delta 11- and Delta 9-Desaturases with Unusual Catalytic Properties. *Insect Biochem. Mol. Biol.* **2010**, *40* (6), 440–452.

(99) Rodríguez, S.; Hao, G.; Liu, W.; Piña, B.; Rooney, A. P.; Camps, F.; Roelofs, W. L.; Fabriàs, G. Expression and Evolution of Δ9 and Δ11 Desaturase Genes in the Moth Spodoptera Littoralis. *Insect Biochem. Mol. Biol.* **2004**, *34* (12), 1315–1328.

(100) Liu, W.; Jiao, H.; Murray, N. C.; O'Connor, M.; Roelofs, W. L. Gene Characterized for Membrane Desaturase That Produces (E)-11 Isomers of Mono- and Diunsaturated Fatty Acids. *Proc. Natl. Acad. Sci. U. S. A.* **2002**, *99* (2), 620–624.

(101) Abad, J. L.; Camps, F.; Fabriàs, G. Stereospecificity of the (Z)-9 Desaturase That Converts (E)-11-Tetradecenoic Acid into (Z,E)-9,11-Tetradecadienoic Acid in the Biosynthesis of Spodoptera Littoralis Sex Pheromone. *Insect Biochem. Mol. Biol.* **2001**, *31* (8), 799–803.

(102) Garner, P. Stereocontrolled Addition to a Penaldic Acid Equivalent: An Asymmetric of Threo-β-Hydroxy-L-Glutamic Acid. *Tetrahedron Lett.* **1984**, *25* (51), 5855–5858.

(103) Passiniemi, M.; Koskinen, A. M. P. Garner's Aldehyde as a Versatile Intermediate in the Synthesis of Enantiopure Natural Products. *Beilstein J. Org. Chem.* **2013**, *9*, 2641–2659.

(104) Chun, J.; Li, G.; Byun, H. S.; Bittman, R. Synthesis of New Trans Double-Bond Sphingolipid Analogues: Δ (4,6) and Δ (6) Ceramides. *J. Org. Chem.* **2002**, *67* (8), 2600–2605.

(105) Garrido, M.; Abad, J. L.; Fabrias, G.; Casas, J.; Delgado, A. Azide-Tagged Sphingolipids: New Tools for Metabolic Flux Analysis. *ChemBioChem* **2015**, *16* (4), 641–650.

(106) Seco, J. M.; Quioá, E.; Riguera, R. A Practical Guide for the Assignment of the Absolute Configuration of Alcohols, Amines and Carboxylic Acids by NMR. *Tetrahedron Asymmetry* **2001**, *12* (21), 2915–2925.

(107) Gruza, H.; Kiciak, K.; Krasiński, A.; Jurczak, J. The Highly Diastereocontrolled Addition of the Lithium Derivative of Tert Butyldimethylsilyl Propargyl Ether to N-Boc-N,O-Isopropylidene-L-Serinal. *Tetrahedron Asymmetry* **1997**, *8* (15), 2627–2631.

(108) Garner, P.; Park, J. M.; Malecki, E. A Stereodivergent Synthesis of D-Erythro-Sphingosine and D-Threo-Sphingosine from L-Serine. *J. Org. Chem.* **1988**, *53*, 4395–4398.

(109) Collington, E. W.; Finch, H.; Smith, I. J. Selective Deprotection of Alcoholic and Phenolic Silyl Ethers. *Tetrahedron Lett.* **1985**, *26* (5), 681–684.

(110) Bartlett, S. L.; Beaudry, C. M. High-Yielding Oxidation of β-Hydroxyketones to β-Diketones Using O-Iodoxybenzoic Acid. *J. Org. Chem.* **2011**, *76* (23), 9852–9855.

(111) Keitz, B. K.; Endo, K.; Patel, P. R.; Herbert, M. B.; Grubbs, R. H. Improved Ruthenium Catalysts for Z -Selective Olefin Metathesis. *J. Am. Chem. Soc.* **2012**, *134*, 693–699.

(112) Occhipinti, G.; Hansen, F. R.; To, K. W.; Jensen, V. R. Simple and Highly Z - Selective Ruthenium-Based Olefin Metathesis Catalyst. *J. Am. Chem. Soc.* **2013**, *135*, 3331–3334.

(113) Gottumukkala, A. L.; Madduri, A. V. R.; Minnaard, A. J. Z-Selectivity: A Novel Facet of Metathesis. *ChemCatChem* **2012**, *4* (4), 462–467.

(114) Endo, K.; Herbert, M. B.; Grubbs, R. H. Investigations into Ruthenium Metathesis Catalysts with Six- Membered Chelating NHC Ligands: Relationship between Catalyst Structure and Stereoselectivity. **2013**.

(115) Chinchilla, R.; Najera, C. The Sonogashira Reaction: A Booming Methodology in Synthetic Organic Chemistry. *Chem. Rev.* **2007**, *107* (3), 874–922.

(116) Schilz, M.; Plenio, H. A Guide to Sonogashira Cross-Coupling Reactions: The Influence of Substituents in Aryl Bromides, Acetylenes, and Phosphines. *J. Org. Chem.* **2012**, *77* (6), 2798–2807.

(117) Moreno, M.; Murruzzu, C.; Riera, A. Enantioselective Synthesis of Sphingadienines and Aromatic Ceramide Analogs. *Org. Lett.* **2011**, *13* (19), 5184–5187.

(118) Hart, D. W.; Schwartz, J. Hydrozirconation. Organic Synthesis via Organozirconium Intermediates. Synthesis and Rearrangement of Alkylzirconium (IV) Complexes and Their Reaction with. *J. Am. Chem. Soc.* **1974**, *199* (1972), 8115.

(119) C. Luethy, Peter Konstantin, K. G. U. Total Synthesis of Dl-19-Hydroxyprostaglandin E1 and Dl-13-Cis-15-Epi-19-Hydroxyprostaglandin E1. *J. Am. Chem. Soc.* **1978**, *100* (19),

6211–6217.

(120) Herold, P. Synthesis of D-Erythro and D-Threo Sphingsosine. *Helv. Chim. Acta* **1988**, *71* (2), 354–362.

(121) Garner, P.; Park, J. M. Glycosyl Alpha-Amino Acids via Stereocontrolled Buildup of a Penaldic Acid Equivalent. A Novel Synthetic Approach to the Nucleosidic Component of the Polyoxins and Related Substances. *J. Org. Chem.* **1990**, *55* (12), 3772–3787.

(122) Corey, E. J.; Barton, A. Synthesis of Three Potential Inhibitors of the Biosynthesis of Leukotrienes A–E. *Tetrahedron Lett.* **1980**, *21* (44), 4243–4246.

(123) Hashmi, A. S. K.; Döpp, R.; Lothschütz, C.; Rudolph, M.; Riedel, D.; Rominger, F. Scope and Limitations of Palladium-Catalyzed Cross-Coupling Reactions with Organogold Compounds. *Adv. Synth. Catal.* **2010**, *352* (8), 1307–1314.

(124) Dieck, H. A.; Heck, R. F. Palladium-Catalyzed Conjugated Diene Synthesis from Vinylic Halides and Olefinic Compounds. *J. Org. Chem.* **1975**, *40* (8), 1083–1090.

(125) Pasto, D. J. Potassium Azodicarboxylate. *Encycl. Reagents Org. Synth.* **2001**, No. 1, 2.

(126) Marshall, J.; Grote, J.; Shearer, B. A Stereoselective Synthesis of the Hydronaphthalene Substructure of Kijanolide. *J. Org. Chem.* **1986**, *51* (9), 1633–1635.

(127) Cingolani, F.; Casasampere, M.; Sanllehí, P.; Casas, J.; Bujons, J.; Fabrias, G. Inhibition of Dihydroceramide Desaturase Activity by the Sphingosine Kinase Inhibitor SKI II. **2014**, *55*, 1711–1720.

(128) Pou, A.; Abad, J.-L.; Ordóñez, Y. F.; Garrido, M.; Casas, J.; Fabriàs, G.; Delgado, A. From the Configurational Preference of Dihydroceramide Desaturase-1 towards Δ^{6}-Unsaturated Substrates to the Discovery of a New Inhibitor. *Chem. Commun.* **2017**, *53* (31), 4394–4397.

(129) Stockert, J. C.; Blázquez-Castro, A.; Cañete, M.; Horobin, R. W.; Villanueva, Á. MTT Assay for Cell Viability: Intracellular Localization of the Formazan Product Is in Lipid Droplets. *Acta Histochem.* **2012**, *114* (8), 785–796.

(130) Munoz-Olaya, J. M.; Matabosch, X.; Bedia, C.; Egido-Gabas, M.; Casas, J.; Llebaria, A.; Delgado, A.; Fabrias, G. Synthesis and Biological Activity of a Novel Inhibitor of Dihydroceramide Desaturase. *ChemMedChem* **2008**, *3* (6), 946–953.

(131) Cer, R. Z.; Mudunuri, U.; Stephens, R.; Lebeda, F. J. IC50-to-Ki: A Web-Based Tool for Converting IC50 to Ki Values for Inhibitors of Enzyme Activity and Ligand Binding. *Nucleic Acids Res.* **2009**, *37*, 441–445.

(132) Uttamchandani, M.; Yao, S. Q. *Small Molecule Microarrays. Methods and Protocols*; 2010.

(133) Park, H.; Chant, J.; Schena, M.; Shalon, D.; Davis, R. W.; Brownt, P. Quantitative Monitoring of Gene Expression Patterns with a Complementary DNA Microarray. *Science (80-.).* **1995**, *270*, 467–470.

(134) Uttamchandani, M.; Yao, S. Q. Protein and Small Molecule Microarrays : Powerful Tools for High-Throughput Proteomics. *Mol. Biosyst.* **2006**, *2*, 58–68.

(135) Falsey, J. R.; Renil, M.; Park, S.; Li, S.; Lam, K. S. Peptide and Small Molecule Microarray

for High Throughput Cell Adhesion and Functional Assays. *Bioconjug. Chem.* **2001**, *12*, 346–353.

(136) Soc, C.; Okuda, J.; Verch, S.; Sturmer, R.; Beard, T.; Turner, N. J.; Commun, C.; Ager, D. J.; Turner, N. J.; Lett, T.; Park, S.; Shin, I. Fabrication of Carbohydrate Chips for Studying Protein-Carbohydrate Interactions. *Angew. Chem.* **2002**, *114* (17), 3312–3314.

(137) Kuruvilla, F. G.; Shamji, A. F.; Sternson, S. M. Dissecting Glucose Signalling with Diversity-Oriented Synthesis and Small-Molecule Microarrays. *Nature* **2002**, *416* (April), 653–657.

(138) Horiuchi, H. M. and K. Y. Chemical Microarray: A New Tool for Drug Screening and Discovery. *Computer (Long. Beach. Calif).* **2008**, *144* (5), 724–732.

(139) Spring, D. R.; Spring, D. Chemical Genetics to Chemical Genomics : Small Molecules Offer Big Insights. *Chem. Soc. Rev.* **2005**, *34* (September 2004), 472–482.

(140) Xu, Q.; Lam, K. S. Protein and Chemical Microarrays — Powerful Tools for Proteomics. *J. Biomed. Biotechnol.* **2003**, *5*, 257–266.

(141) Belosludtsev, Y.; Iverson, B.; Lemeshko, S.; Eggers, R.; Wiese, R.; Lee, S.; Powdrill, T.; Hogan, M. DNA Microarrays Based on Noncovalent Oligonucleotide Attachment and Hybridization in Two Dimensions. *Anal. Biochem.* **2001**, *256*, 250–256.

(142) Martin, B. D.; Gaber, B. P.; Patterson, C. H.; Turner, D. C. Direct Protein Microarray Fabrication Using a Hydrogel. *Langmuir* **1998**, *14* (15), 3971–3975.

(143) Online, V. A.; Homepage, J. Small-Molecule Microarrays as Tools in Ligand Discovery. *Chem. Soc. Rev.* **2008**, *37*, 1385–1394.

(144) Martin, T. L.; Zaugg, F. G.; Witte, K.; Indermuhle, P.; Nock, S.; Wagner, P. Monolayers of Derivatized Poly (L-Lysine) Grafted Poly (Ethylene Glycol) on Metal Oxides as a Class of Biomolecular Interfaces. *PNAS* **2001**, *98* (3), 852–857.

(145) Macbeath, G.; Schreiber, S. L. Printing Proteins as Microarrays for High-Throughput Function Determination. *Science (80-.).* **2012**, *289* (5485), 1760–1763.

(146) Benters, R.; Niemeyer, C. M.; Wöhrle, D. Dendrimer-Activated Solid Supports for Nucleic Acid and Protein Microarrays. *ChemBioChem* **2001**, No. 2, 686–694.

(147) Macbeath, G.; Koehler, A. N.; Schreiber, S. L. Printing Small Molecules as Microarrays and Detecting Protein - Ligand Interactions En Masse. *J. Am. Chem. Soc.* **1999**, No. 121, 7967–7968.

(148) Padwa, A. Book Reviews. *J. Heterocycl. Chem.* **1986**, *44*, 1899.

(149) Huisgen, R. 1,3-Dipolar Cycloadditions. Past and Future. *Angew. Chem. Int. Ed.* **1963**, *2* (10), 565–598.

(150) Demko, Z. P.; Sharpless, K. B. A Click Chemistry Approach to Tetrazoles by Huisgen 1,3-Dipolar Cycloaddition: Synthesis of 5-Acyltetrazoles from Azides and Acyl Cyanides. *Angew. Chem. Int. Ed.* **2002**, *41* (12), 2113–2116.

(151) Kolb, H. C.; Finn, M. G.; Sharpless, K. B. Click Chemistry: Diverse Chemical Function from a Few Good Reactions. *Angew. Chem. Int. Ed.* 2001, pp 2004–2021.

(152) Chan, T. R.; Hilgraf, R.; Sharpless, K. B.; Fokin, V. V. Polytriazoles as Copper (I) -Stabilizing Ligands in Catalysis. *Org. Lett.* **2004**, *6* (27), 2853–2855.

(153) Hong, V.; Steinmetz, N. F.; Manchester, M.; Finn, M. G. Labeling Live Cells by Copper-Catalyzed Alkyne-Azide Click Chemistry. *Bioconjug. Chem.* **2010**, *21* (10), 1912–1916.

(154) Gaetke, L. M.; Chow, C. K. Copper Toxicity, Oxidative Stress, and Antioxidant Nutrients. *Toxicology* **2003**, *189* (1–2), 147–163.

(155) Banert, K. *Organic Azides*; 2010.

(156) Debets, M. F.; Van Berkel, S. S.; Schoffelen, S.; Rutjes, F. P. J. T.; Van Hest, J. C. M.; Van Delft, F. L. Aza-Dibenzocyclooctynes for Fast and Efficient Enzyme PEGylation via Copper-Free (3+2) Cycloaddition. *Chem. Commun.* **2010**, *46* (1), 97–99.

(157) Ning, X.; Guo, J.; Wolfert, M. A.; Boons, G. J. Visualizing Metabolically Labeled Glycoconjugates of Living Cells by Copper-Free and Fast Huisgen Cycloadditions. *Angew. Chemie Int. Ed.* **2008**, *47* (12), 2253–2255.

(158) Van Berkel, S. S.; Dirks, A. J.; Meeuwissen, S. A.; Pingen, D. L. L.; Boerman, O. C.; Laverman, P.; van Delft, F. L.; Cornelissen, J. J. L. M.; Rutjes, F. P. J. T. Application of Metal-Free Triazole Formation in the Synthesis of Cyclic RGD-DTPA Conjugates. *ChemBioChem* **2008**, *9* (11), 1805–1815.

(159) Sletten, E. M.; Bertozzi, C. R. Bioorthogonal Chemistry: Fishing for Selectivity in a Sea of Functionality. *Angew. Chem. Int. Ed.* **2009**, *48* (38), 6974–6998.

(160) Zhang, X.; Zhang, Y. Applications of Azide-Based Bioorthogonal Click Chemistry in Glycobiology. *Molecules* **2013**, *18* (6), 7145–7159.

(161) Fazio, F.; Bryan, M. C.; Blixt, O.; Paulson, J. C.; Wong, C. H. Synthesis of Sugar Arrays in Microtiter Plate. *J. Am. Chem. Soc.* **2002**, *124* (48), 14397–14402.

(162) Kuzmin, A.; Poloukhtine, A.; Wolfert, M. A.; Popik, V. V. Surface Functionalization Using Catalyst-Free Azide-Alkyne Cycloaddition. *Bioconjug. Chem.* **2010**, *21* (11), 2076–2085.

(163) Prim, D.; Rebeaud, F.; Cosandey, V.; Marti, R.; Passeraub, P.; Pfeifer, M. E. ADIBO-Based "click" chemistry for Diagnostic Peptide Micro-Array Fabrication: Physicochemical and Assay Characteristics. *Molecules* **2013**, *18* (8), 9833–9849.

(164) Uszczyńska, B.; Ratajczak, T.; Frydrych, E.; Maciejewski, H.; Figlerowicz, M.; Markiewicz, W. T.; Chmielewski, M. K. Application of Click Chemistry to the Production of DNA Microarrays. *Lab Chip* **2012**, *12* (6), 1151–1156.

(165) Stefan Brase, Carmen Gil, Kerstin Knepper, and V. Z. Organic Azides: An Exploding Diversity of a Unique Class of Compounds. *Angew. Chem. Int. Ed.* **2005**, *44* (33), 5188–5240.

(166) Harris, F.; Pierpoint, L. PhotodynamicTherapy Based on 5-Aminolevulinic Acid and Its Use as an Antimicrobial Agent. *Med. Res. Rev.* **2012**, *29* (6), 1292–1327.

(167) Punna, S.; Kaltgrad, E.; Finn, M. G. " Clickable " Agarose for Affinity Chromatography Edited by Foxit Reader. *Bioconjug. Chem.* **2005**, *16*, 1536–1541.

(168) Ortega-Muñoz, M.; Lopez-Jaramillo, J.; Hernandez-Mateo, F.; Santoyo-Gonzalez, F. Synthesis of Glyco-Silicas by Cu(I)-Catalyzed "click-Chemistry" and Their Applications in

Affinity Chromatography. *Adv. Synth. Catal.* **2006**, *348* (16–17), 2410–2420.

(169) Higashi, T.; Awada, D.; Shimada, K. Simultaneous Determination of 25-Hydroxyvitamin D2 and 25-Hydroxyvitamin D3 in Human Plasma by Liquid Chromatography-Tandem Mass Spectrometry Employing Derivatization with a Cookson-Type Reagent. *Biol. Pharm. Bull.* **2001**, *24* (7), 738–743.

(170) Shimizu, M.; Kamachi, S.; Nishii, Y.; Yamada, S. Synthesis of a Reagent for Fluorescence-Labeling of Vitamin D and Its Use in Assaying Vitamin D Metabolites. *Anal. Biochem.* **1991**, *194* (1), 77–81.

(171) Yasumoto, T.; Takizawa, A. Fluorometric Measurement of Yessotoxins in Shellfish by High-Pressure Liquid Chromatography. *Biosci. Biotechnol. Biochem.* **1997**, *61* (10), 1775–1777.

(172) Xiao, L.; Chen, Y.; Zhang, K. Efficient Metal-Free “grafting Onto” method for Bottlebrush Polymers by Combining RAFT and Triazolinedione-Diene Click Reaction. *Macromolecules* **2016**, *49* (12), 4452–4461.

(173) Wang, L.; Hou, X.; Fu, H.; Pan, X.; Xu, W.; Tang, W.; Fang, H. Design, Synthesis and Preliminary Bioactivity Studies of 1,3,4-Thiadiazole Hydroxamic Acid Derivatives as Novel Histone Deacetylase Inhibitors. *Bioorganic Med. Chem.* **2012**, *20* (15), 3865–3872.

(174) Kim, D. W. Bioorthogonal Click Chemistry for Fluorine-18 Labeling Protocols under Physiologically Friendly Reaction Condition. *J. Fluor. Chem.* **2015**, *174*, 142–147.

(175) Narasimhan, C.; Lai, C.-S.; Joseph, J. Syntheses and Transglutaminase-Catalyzed Incorporation of Novel Spin-Labeled Primary Amines into Proteins. *Bioorg. Chem.* **1996**, *24* (1), 50–58.

(176) Kastl, R.; Wennemers, H. Peptide-Catalyzed Stereoselective Conjugate Addition Reactions Generating All-Carbon Quaternary Stereogenic Centers. *Angew. Chem. Int. Ed.* **2013**, *52* (28), 7228–7232.

(177) Preininger, C.; Sauer, U.; Dayteg, J.; Pichler, R. Optimizing Processing Parameters for Signal Enhancement of Oligonucleotide and Protein Arrays on ARChip Epoxy. *Bioelectrochemistry* **2005**, *67*, 155–162.

(178) Kusnezow, W.; Jacob, A.; Walijew, A.; Diehl, F.; Hoheisel, J. D. Antibody Microarrays: An Evaluation of Production Parameters. *Proteomics* **2003**, *3* (3), 254–264.

(179) Uttamchandani, M.; Wang, J.; Yao, S. Q. Protein and Small Molecule Microarrays: Powerful Tools for High-Throughput Proteomics. *Mol. Biosyst.* **2006**, *2* (1), 58–68.

(180) Campbell, a D.; Raynham, T. M.; Taylor, R. J. K. A Simplified Route to the (R)-Garner Aldehyde and (S)-Vinyl Glycinol. *Synthesis (Stuttg).* **1998**, No. Scheme 1, 1707–1709.

(181) Bayquen, A. V; Read, R. W. Total Synthesis of Micropine and Epimicropine. *Tetrahedron* **1996**, *52* (42), 13467–13482.

(182) Seco, M.; Quiñoá, E.; Riguera, R. A Practical Guide for the Assignment of the Absolute Configuration of Alcohols , Amines and Carboxylic Acids by NMR. *Tetrahedron: Asymmetry* **2002**, *12* (53), 2915–2925.

(183) Karjalainen, O. K.; Koskinen, A. M. P. Rapid and Practical Synthesis of (-)-1-

Deoxyaltronojirimycin. *Org. Biomol. Chem.* **2011**, *9* (4), 1231–1236.

(184) Beaulieu, P. L.; Duceppe, J.-S.; Johnson, C. Synthesis of Chiral Vinylglycines. *J. Org. Chem.* **1991**, *56* (13), 4196–4204.

(185) Schlosser, M.; Tuong, H. B.; Schaub, B. The Betaine-Ylid Route to Trans-Alkenols. *Tetrahedron Lett.* **1985**, *26* (3), 311–314.

(186) Gary L. Bolton, Bruce D. Roth, and B. K. T.; Depsrtment. Synthesis of Conformationally Constrained Macrocyclic Analogs of the Potent and Selective CCK-B Antagonist CI-988. *Tetrahedron* **1993**, *49* (3), 525–536.

(187) Carpino, L. A.; Han, G. Y. The 9-Fluorenylmethoxycarbonyl Amino-Protecting Group. *J. Org. Chem.* **1972**, *37* (22), 3404–3409.

(188) Tashiro, T.; Hongo, N.; Nakagawa, R.; Seino, K. ichiro; Watarai, H.; Ishii, Y.; Taniguchi, M.; Mori, K. RCAI-17, 22, 24-26, 29, 31, 34-36, 38-40, and 88, the Analogs of KRN7000 with a Sulfonamide Linkage: Their Synthesis and Bioactivity for Mouse Natural Killer T Cells to Produce Th2-Biased Cytokines. *Bioorganic Med. Chem.* **2008**, *16* (19), 8896–8906.

(189) Patino, N.; Di Giorgio, C.; Dan-Covalciuc, C.; Peytou, V.; Terreux, R.; Cabrol-Bass, D.; Bailly, C.; Condom, R. Modelling, Synthesis and Biological Evaluation of an Ethidium-Arginine Conjugate Linked to a Ribonuclease Mimic Directed against TAR RNA of HIV-1. *Eur. J. Med. Chem.* **2002**, *37* (7), 573–584.

(190) Herold, P. Synthesis of D-Erythro- and D-Threo-Sphingosine Derivatives from L-Serine. *Helv. Chim. Acta.* **1988**, *71* (2), 354–362.

(191) Christopher Curfman and Dennis Liotta. Synthesis of Sphingosine and Sphingoid Bases Sphingosine from Serine. *Methods Enzymol.* **1999**, *311*, 391–440.

(192) Vandewalle, S.; Billiet, S.; Driessen, F.; Du Prez, F. E. Macromolecular Coupling in Seconds of Triazolinedione End-Functionalized Polymers Prepared by RAFT Polymerization. *ACS Macro Lett.* **2016**, *5* (6), 766–771.

(193) Shimada, K.; Oe, T.; Mizuguchi, T. Cookson-Type Reagents: Highly Sensitive Derivatization Reagents for Conjugated Dienes in High-Performance Liquid Chromatography. *Analyst* **1991**, *116* (December), 1393–1397.

(194) Ogawa, S.; Ooki, S.; Morohashi, M.; Yamagata, K.; Higashi, T. A Novel Cookson-Type Reagent for Enhancing Sensitivity and Specificity in Assessment of Infant Vitamin D Status Using Liquid Chromatography/tandem Mass Spectrometry. *Rapid Commun. Mass Spectrom.* **2013**, *27* (21), 2453–2460.

(195) Shimada, K.; Higashi, T.; Mitamura, K. Development of Analyses of Biological Steroids Using Chromatography. Special Reference to Vitamin D Compounds and Neurosteroids. **2003**, *24* (1).

7. SUMMARY IN CATALAN

7. SUMMARY IN CATALAN

Introducció

Els esfingolípids (SLs) constitueixen una àmplia família de lípids d'origen natural que formen part de cèl·lules eucariotes. Durant anys s'han considerat simples components estructurals de les membranes cel·lulars. No obstant, en les últimes dècades, s'ha establert el seu paper com a molècules bioactives, les quals intervenen en la senyalització i en la regulació de varis processos cel·lulars. [1,2]

Els SLs estan formats generalment per un grup polar i dues cues: una cadena d'amino alcohol de 18 carbonis, també coneguda com a base esfingoide, i una cadena d'àcid gras que s'uneix a la amina per mitjà d'un enllaç *N*-acil (Fig. 7.1). Els principals SLs bioactius són la ceramida (Cer), la esfingosina (So) i els seus corresponents anàlegs fosforilats, la ceramida 1-fosfat (C1P) i la esfingosina 1-fosfat (S1P). Com s'observa en la figura 7.1, estructuralment els SLs bioactius comparteixen la base esfingoide eritro (*E, 2S, 3R*)-2-aminoocatec-4-ene-1,3-diol.

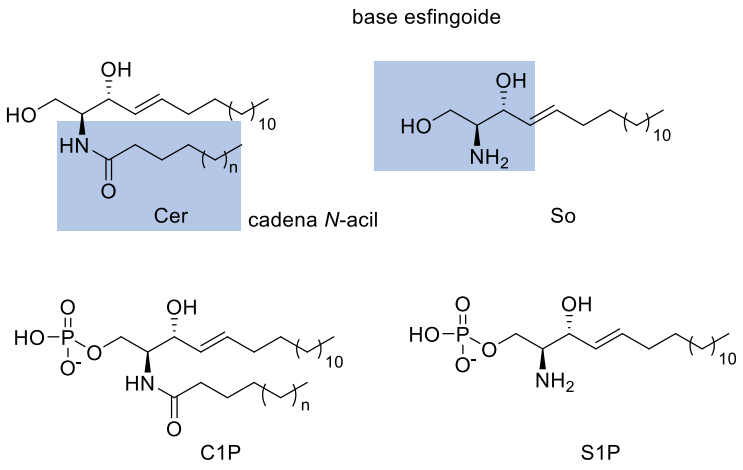

***Figura 7.1**. Estructura dels principals SLs bioactius. (n representa diferents llargades de cadena N-acil).*

Els SLs es sintetitzen majoritàriament en el reticle endoplasmàtic i en l'aparell de Golgi i són transportats a la membrana plasmàtica i altres orgànuls. El seu metabolisme inclou una sèrie de reaccions biosintètiques i catabòliques, en les que la Cer participa com a molècula central. Principalment, la Cer es pot generar per mitjà de dos mecanismes: i) biosíntesi *de novo*, ii) "la via de reciclatge", el qual comprèn la hidròlisi de glicoesfingolípids i el cicle de la esfingomielina.[3] L'alteració d'aquest metabolisme pot causar processos patològics i contribuir en diverses malalties.[4]

L'ús de sondes específiques per tal de controlar l'activitat enzimàtica de certs enzims que formen part dels processos metabòlics dels SLs, així com el seu tràfic i la seva localització intracel·lular, està guanyant importància en la química biològica i en el disseny de fàrmacs.[4] La rellevància biològica i el creixent interès per alguns enzims que metabolitzen els SLs, útils com a dianes terapèutiques, ha donat lloc a la necessitat de trobar inhibidors potents i selectius que modulin de manera eficient les seves activitats. En aquest context, la identificació de manera

ràpida i eficient d'aquests inhibidors en el metabolisme d'SLs es podria aconseguir per mitjà d'un cribratge massiu de biblioteques químiques. No obstant, això requeriria la disponibilitat de mètodes HTS (high throughput screening), on actualment se'n disposen de molt pocs.

Inicialment, la majoria de determinacions enzimàtiques es duien a terme amb substrats radioactius.[5] L'inconvenient, però, de treballar amb aquest tipus de materials va estimular el desenvolupament de substrats no naturals per monitoritzar l'activitat dels enzims metabolitzadors dels SLs. Avui dia, els substrats no naturals més usats són els fluorescents. Per exemple, l'esfinganina NBD (SaNBD, Fig. 7.2) és comercial i s'utilitza com a substrat de la ceramida sintasa (CerS)[6] per tal d'estudiar el seu metabolisme. Pel que fa a l'activitat de la ceramidasa (CDase), Merrill i col·laboradors van dissenyar un assaig tant *in vitro* com en cèl·lules d'hepatòcits on feien ús del substrat fluorescent (NBD)C_6Cer (Fig. 7.2).[7] Un altre exemple de substrat fluorescent és la de la dhCerC_6NBD (Fig. 7.2), utilitzat per a la monitorització de l'enzim dihidroceramida desaturasa (Des1).[4]

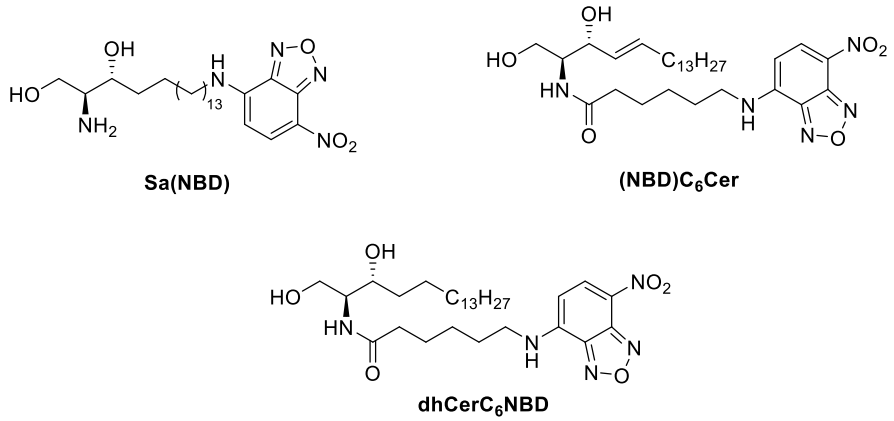

***Figura 7.2**. Substrats fluorescents per tal d'estudiar l'activitat de certs enzims en el metabolisme d'SLs.*

L'enzim Des1 catalitza l'últim pas de reacció de la via *de novo* en la biosíntesi d'SLs. La seva funció és la d'introduir un doble enllaç *trans* en la posició 4 (Δ^4) en la cadena de la dihidroceramida (dhCer) per generar la Cer corresponent (Fig. 7.3).[8] Com a resultat, aquest enzim és crucial per a la regulació del balanç entre els SLs i els dihidroesfingolípids (dhSLs).

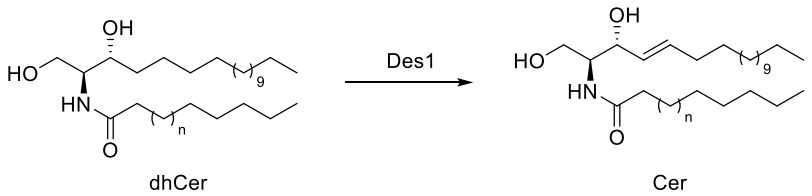

***Figura 7.3.** Dessaturació del C4 de la dhCer per formar la Cer corresponent per mitjà de l'acció de l'enzim Des1.*

Les dhCers es van considerar com a intermediaris inerts de la Cer en base a enfocaments *in vitro*.[9] A més a més, s'utilitzaven com a control per tal estudiar la inhibició del creixement cel·lular, apoptosi i mort cel·lular en certs tipus de cèl·lules.[10] No obstant, publicacions recents[11] indiquen que les dhCer són lípids bioactius tot i que el seu efecte pot ser diferent a

l'obtingut per les Cers. L'ús de models biofísics, genètics i farmacològics per disminuir l'activitat de Des1 han demostrat ser crucials per revelar l'activitat biològica dels derivats de dhCer.

La disponibilitat d'inhibidors de Des1 i el seu ús com a eines farmacològiques ha ajudat a refutar la innocuïtat biològica de la dhCer. La majoria de les evidències venen d'estudis on la inhibició de Des1 causa una acumulació de dhCer. S'han descrit diversos fàrmacs que inhibeixen l'activitat de Des1, incloent la GT11[8] o XM462[12] (Fig. 7.4). A part d'aquests, una sèrie de fàrmacs i productes naturals també han mostrat un efecte inhibitori en l'activitat d'aquest enzim, incloent la fenretinida, resveratrol, celecoxib, tetrahidrocannabiol, entre d'altres.[13–16]

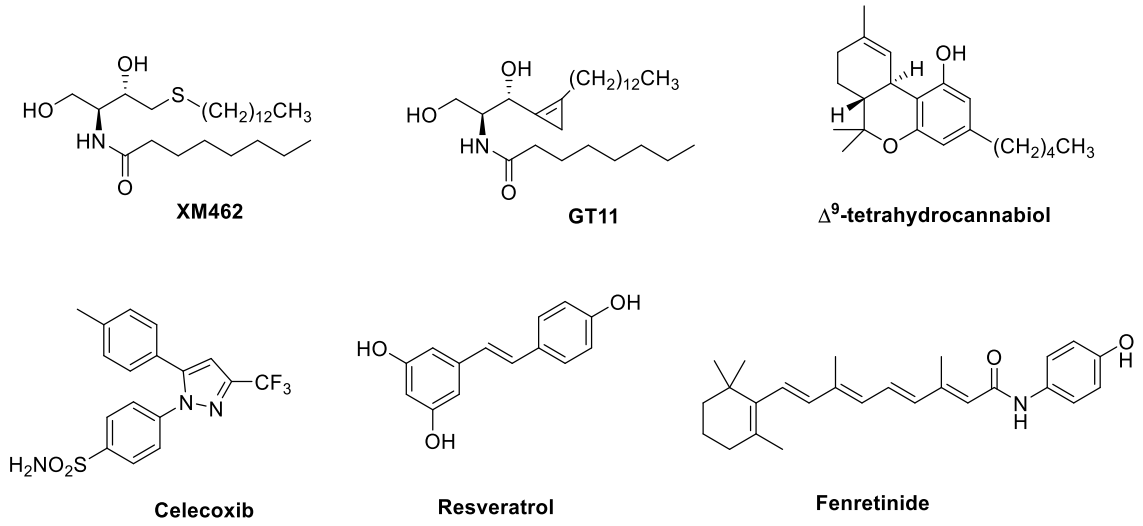

***Figura 7.4**. Inhibidors descrits de Des1.*

Apart del substrat fluorescent mencionat anteriorment (dhCerC_6NBD, Fig. 7.2) per monitoritzar l'activitat de l'enzim Des1, s'han descrit altres substrats no naturals. L'any 1997, Michael *et al.* va dissenyar un anàleg de dhCer radioactiu (*N*-[1- ^{14}C]octanoil-*D*-*erythro*-esfinganina) com a substrat de Des1 utilitzant NADH o NADPH com a co-substrat per monitoritzar l'activitat de la proteïna en microsomes intactes de fetge de rata.[17] Una altra alternativa va ser reportada per Geeraert *et al*. on utilitzava la *N*-hexanoil-[4,5-^{3}H]-D-*erythro*-esfinganina com a substrat i estudiava la conversió de dhCer a Cer en hepatòcits de rata, seguint la formació d'aigua tritiada després de l'addició del substrat tritiat.[18] L'activitat d'aquest enzim també pot ser determinada per l'ús de la *N*-octanoil-*D*-*erythro*-esfinganina com a substrat, i mesurant la formació de Cer per GC-MS dels derivats de trimetilsilil volàtils. [19]

Objectius

La idea i motivació principals de la present Tesi va ser el desenvolupament d'un assaig HTS per monitoritzar l'activitat de l'enzim Des1, un dels enzims de la biosíntesi *de novo* dels SLs. L'expansió de mètodes per a la quantificació del enzims dels SLs i l'ús de proves específiques per determinar la seva localització i tràfic intracel·lular està guanyant importància en l'actualitat de la química biomèdica i del disseny de fàrmacs. A més a més, el descobriment de nous inhibidors de Des1 es veuria accelerat amb l'ajut d'un assaig HTS eficient.

Basant-nos en les consideracions descrites anteriorment, l'objectiu principal d'aquest treball consisteix en el disseny de sondes químiques per a la seva implementació en assajos HTS fluorescents per tal de monitoritzar l'activitat de Des1. Seria ideal que aquest assaig fos adaptable a un format en microarray, utilitzant un substrat immobilitzat en un suport sòlid, seguit d'una derivatització del producte de reacció de Des1 amb un compost fluorescent. Amb aquesta finalitat, es consideraran dues opcions:

1) En primer lloc, s'avaluarà l'ús d'un derivat de la dhCer ancorat a un suport sòlid, com a substitut del substrat natural de Des1 (Fig. 7.5A). En aquest cas, la resultant Δ^4-Cer formada com a producte de la reacció enzimàtica podria ser atrapada per mitjà d'una reacció de Alder-ene amb un enòfil fluorescent adequat, així poder quantificar l'adducte format.
2) D'altra banda, es considerarà l'opció d'utilitzar com a substrat una Δ^6-dhCer no natural ancorada en un suport sòlid (Fig. 7.5B). Després de la reacció enzimàtica, la $\Delta^{4,6}$-Cer podria reaccionar amb un dienòfil fluorescent per mitjà d'una reacció de Diels Alder, per la seva posterior detecció i quantificació.

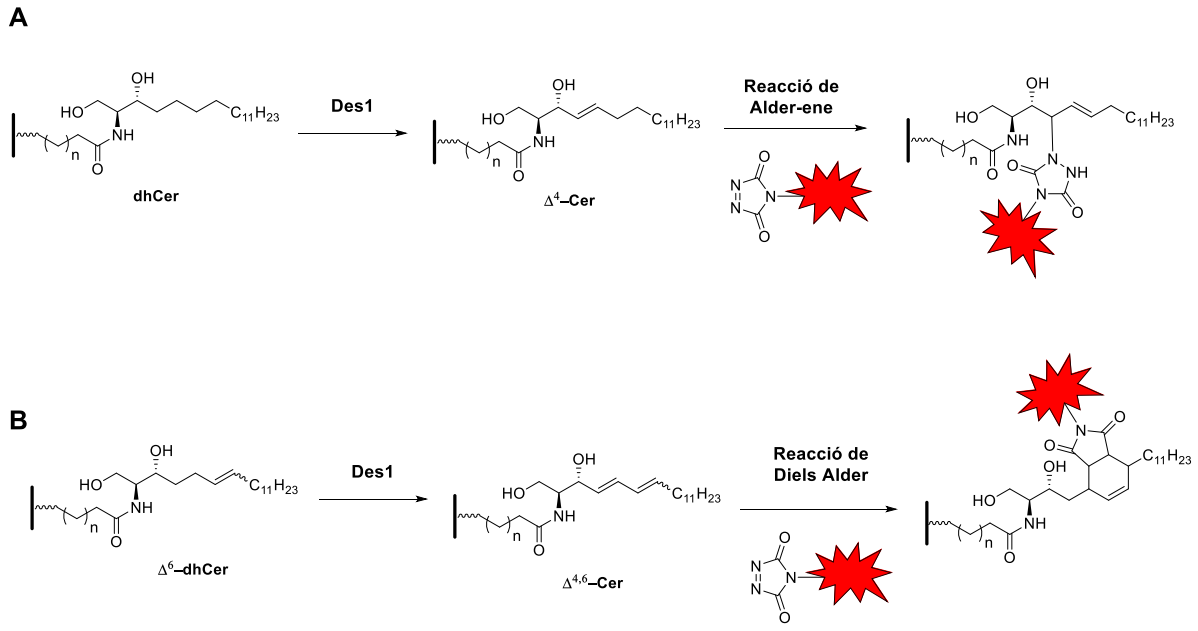

Figura 7.5. A. *Disseny d'un assaig HTS fent servir una dhCer natural ancorada a un suport sòlid. El producte de reacció pot reaccionar amb un enòfil fluorescent per mitjà d'una reacció de Alder-ene.* ***B.*** *Disseny d'un assaig HTS utilitzant un anàleg Δ^6-dhCer immobilitzat. El producte de reacció podria reaccionar amb un dienòfil fluorescent (com derivats del TAD) per mitjà d'una reacció de Diels Alder.*

Curiosament, la reactivitat dels derivats de les triazolindiones (TAD) són compatibles tant amb la reacció de Alder-ene com amb la reacció de Diels-Alder.[20,21] Per tant, el primer objectiu està adreçat a avaluar la reactivitat del TAD amb la Δ^4-Cer natural en la reacció de Alder-ene (segons l'aproximació 1, Fig. 7.5A) o amb la $\Delta^{4,6}$-Cer en la reacció de Diels Alder, segons la segona aproximació (Fig. 7.5B). En ambdós casos es dissenyarà i sintetitzarà un derivat fluorescent del TAD com a possible reactiu adient.

Com a resultat dels estudis preliminars que es mencionaran en la secció de Resultats i Discussió, ens han donat lloc a escollir la segona aproximació com la més idònia. Per tant, això requerirà l'estudi tant de la *E* com la *Z*- Δ^6-dhCers com a substrats de Des1 en experiments *in vitro*.

Un cop optimitzades les condicions de reacció, es dissenyarà l'assaig HTS per tal de fer-lo possible en format microarray. Això requerirà de:

- La síntesis dels compostos derivats de Δ^6-dhCer i $\Delta^{4,6}$-Cer per a la seva posterior immobilització en suport sòlid.
- El desenvolupament d'un protocol per tal de monitoritzar l'activitat de Des1 en lisats cel·lulars utilitzant com a substrat una Δ^6-dhCer ancorada.
- L'optimització de l'assaig HTS en format microarray per tal de poder detectar el producte de la reacció enzimàtica unit a un reactiu fluorescent derivat del TAD.

Resultats i discussió

Aproximacions sintètiques pel desenvolupament d'un assaig HTS en un sistema de microarray

Assajos preliminars

Com s'ha indicat en els objectius (Fig. 7.5), es poden considerar dues aproximacions pel disseny de l'assaig HTS. Per tal d'avaluar ambdues propostes es van dur a terme assajos preliminars, on es va determinar quina de les dues opcions seria més factible.

En primer lloc, es va provar la reactivitat del derivat de Cer natural amb un reactiu de tipus TAD com a enòfil per tal de dur a terme la reacció de Alder-ene en solució (Fig. 7.6). En conseqüència, es va fer reaccionar la Δ^4-C_8Cer **RBM8-349** amb 10 equiv. de PTAD[22] en CH_2Cl_2 a temperatura ambient durant 24 h. Malauradament, no es va observar l'adducte tipus "ene" esperat tot i afegint successives quantitats de PTAD en intervals diferents durant el transcurs de la reacció. Donats aquests resultats, vam descartar aquesta via com a mètode d'assaig, ja que probablement no seria compatible amb les condicions d'assaig requerides.

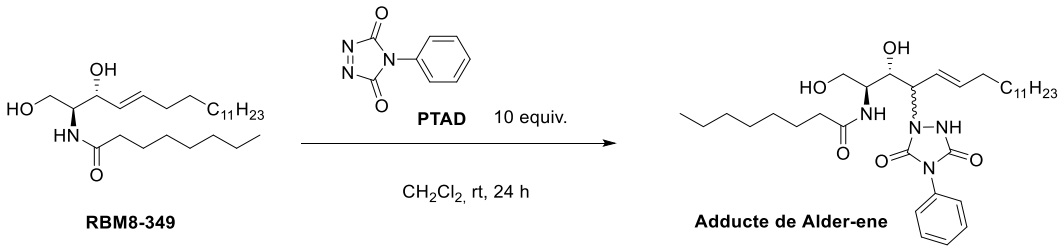

Figura 7.6. *Reactivitat de la Δ^4-C_8Cer **RBM8-349** amb el PTAD per mitjà d'una reacció de Alder-ene.*

En segon lloc, es va tenir en compte l'aproximació de la figura 7.5B, on l'ús d'un anàleg de Δ^6-dhCer com a substrat de Des1 seria una alternativa raonable per tal de mesurar l'activitat de Des1 si el dià-$\Delta^{4,6}$ resultant pogués donar lloc a una reacció de tipus Diels Alder amb un dienòfil adient. Per aquesta raó, es va optimitzar aquesta última reacció emprant com a model dienic el compost **RBM8-216** (Fig. 7.7) amb diferents dienòfils comercials. L'estereoquímica escollida d'aquest compost s'explicarà més endavant.

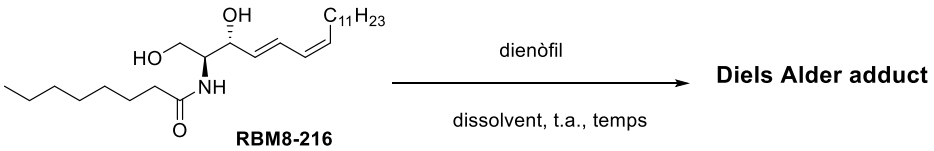

Figura 7.7. *Avaluació de la reacció de Diels Alder amb diferents dienòfils. Veure la taula 7.8 per als resultats obtinguts.*

Com es pot observar en la Taula 7.8, inicialment la reacció es va dur a terme amb la *N*-fenilmaleimida (entrada 1) com a dienòfil, però no es va observar adducte d'acoblament i es va poder aïllar només material de partida no reaccionat. Per tant, aquests fets evidencien la lenta reactivitat de diens interns a la reacció de Diels Alder sota condicions normals. També es va provar amb el PTAD com a dienòfil (entrada 2), emprant 5 equivalents d'aquest en una mescla de CH_2Cl_2/THF (1:1). Després de 16 h a temperatura ambient, es va poder aïllar un estereoisòmer de l'adducte de Diels Alder amb rendiments quantitatius.

Table 7.8. Reactivitat de RBM8-216 amb dienòfils comercials.

Entrada	Dienòfil	Dissolvent	Temps (h)	Rendiment (%)	Adducte de Diels Alder
1	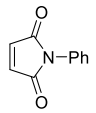	DMSO	3	–	–
2	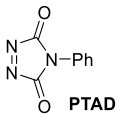 **PTAD**	THF/CH_2Cl_2	16	50	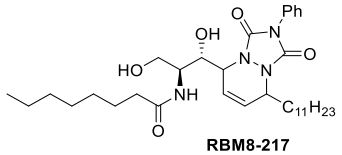 **RBM8-217**

Degut als resultats positius obtinguts en aquesta segona aproximació, es va considerar adient escollir la reacció de Diels Alder entre $\Delta^{4,6}$-Cers i dienòfils del tipus TAD com a estratègia per al desenvolupament de l'assaig de Des1.

Síntesis de d'anàlegs de Δ^6- dhCer i Δ^4-Cer per la monitorització de l'activitat de Des1 en solució

Estimulats pels resultats esmentats, seguidament es va procedir a la síntesi dels anàlegs de Δ^6-dhCer per determinar si algun d'ells seria adient com a substrat de Des1. A més a més, també es van sintetitzar les corresponents $\Delta^{4,6}$-Cers, que serien els productes de reacció esperats després de dur a terme la reacció enzimàtica. Tot i que els nostre principal objectiu del projecte era dur a terme l'assaig enzimàtic amb el substrat ancorat a un suport sòlid, primer es va provar l'assaig en dissolució per verificar si eren adients com a substrat de Des1.

D'entre tots els assajos descrits per determinar l'activitat de Des1, la dhCerC_6NBD ha estat utilitzada en el nostre grup com a substrat fluorescent de Des1.[23] Aquest assaig es basa en la conversió de la dhCerC_6NBD (Fig. 7.9) per formar la CerC_6NBD, que pot ser quantificada per HPLC acoblat a un detector de fluorescència (HPLC-FD).

S'han publicat diferents exemples d'àcids grassos monoènics *E* [24,25] i *Z* [26,27] acceptats per dessaturasses d'acil-CoA que proporcionen els diens conjugats corresponents per mitjà d'una addició d'un doble enllaç a la posició veïna. Per tal d'avaluar la estereoselectivitat de Des1 en

la dessaturació de les Δ^6-dhCer monoèniques no naturals, es van sintetitzar els compostos **RBM8-029** i **RBM8-126**, junts amb els diens isomèrics **RBM8-053** i **RBM8-138**, productes esperats en la reacció de Des1, i usats com a patrons analítics (Fig. 7.9). Aquests compostos contenen el grup fluorescent C_6NBD, essencial per a la monitorització de l'activitat de Des1 en lisats cel·lulars per HPLC-FD. A més a més, també es van sintetitzar les corresponents Δ^6-dhCers *E* i *Z*-monoèniques (**RBM2-085** i **RBM8-202**, respectivament) per tal d'estudiar la seva activitat en cèl·lules intactes (Fig. 7.9). Això també va requerir la síntesi les (*E,E*)- i (*E,Z*)-$\Delta^{4,6}$-Cers (**RBM2-076** i **RBM8-216**, respectivament) com a patrons analítics per l'anàlisi per UPLC-TOF dels extractes lipídics.

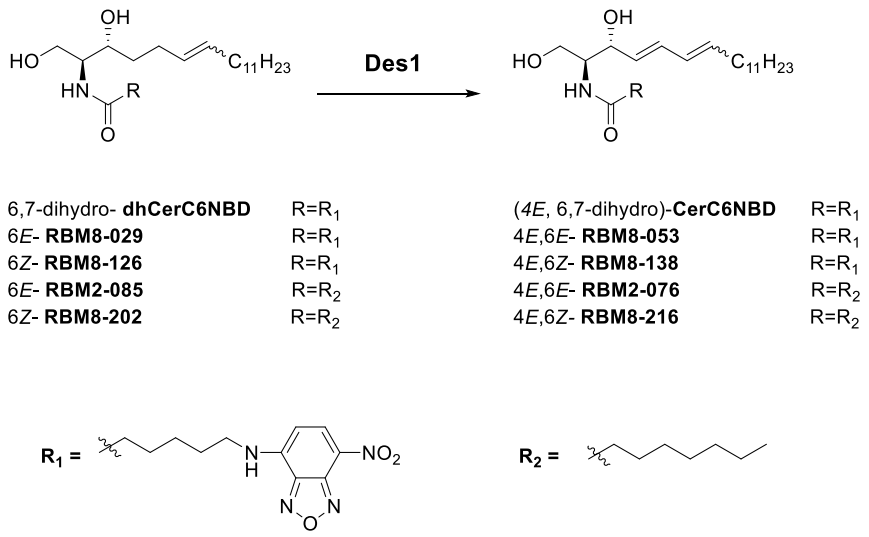

Figura 7.9. *Anàlegs de dhCer i Cer per dur a terme l'assaig enzimàtic en solució i quantificar la reacció per mitjà de HPLC-FD o per anàlisi per UPLC-TOF.*

La síntesi dels *E*- Δ^6-monoèns **RBM2-085** i **RBM8-029** es van dur a terme per acilació de les corresponents bases esfingoides insaturades, a partir de l'aldehid de Garner,[28,29] com indica en la Figura 7.10. Amb aquesta finalitat, vam utilitzar una metàtesi creuada entre la olefina **RBM8-009** i 1-tridecè amb la presència del catalitzador de Grubbs de 2a generació com a pas clau de la ruta sintètica. Aquest procés ens va permetre obtenir l'intermedi **RBM8-027** com a mescla isomèrica *E/Z* 6:1 amb un rendiment del 53%. L'isòmer *E* pur es va poder separar en el transcurs de la reacció d'eliminació del grup MPA, just en el següent pas.

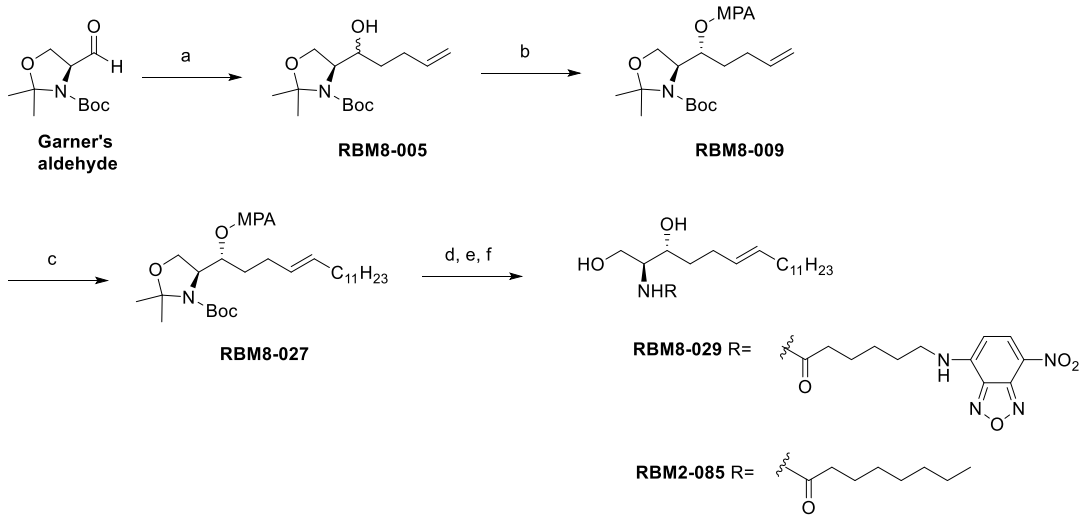

Figura 7.10. *Condicions i reactius. (a) 3-butenilMgBr, THF, 76%. (b) (R)-MPA, EDC, DMAP, CH_2Cl_2, d.r (S,S,R:S,R,R): 4/1, 57%. (c) n-tridecè, Grubbs II, d.r (E,Z): 6/1, 53%. (d) K_2CO_3, MeOH, 75%, (e) AcCl, MeOH. (f) àcid C_6NBD per* ***RBM8-029*** *o àcid n-octanoic per* ***RBM2-085****, HOBt, EDC, CH_2Cl_2, 32% rendiment en els passos (e) i (f) per* ***RBM8-029*** *i 36% rendiment per* ***RBM2-085****.*

La ruta sintètica s'inicià per addició del bromur de butenil magnesi a l'aldehid de Garner en THF a -78 ˚C, donant lloc a una mescla inseparable d'alquenols amb una relació *erythro/threo* 4:1, on posteriorment van ser separats per derivatització amb (*R*)-MPA. Curiosament, aquest darrer pas també ens va permetre l'assignació de la configuració del nou estereocentre de **RBM8-009** seguint la metodologia del Riguera.[30] Seguidament es va procedir a la metàtesi creuada ja esmentada anteriorment per formar **RBM8-027**. La següent desprotecció del MPA, seguit de la simultània desprotecció de la oxazolidina i del *N*-Boc sota condicions àcides, i la subseqüent *N*-acilació amb àcid octanoic o àcid C_6NBD en presència de EDC i HOBt com a agents d'acoblament, va permetre obtenir **RBM2-085** i **RBM8-029** amb rendiments acceptables.

La síntesi dels (*Z*)-Δ^6-monoèns **RBM8-202** i **RBM8-126** (Fig. 7.11) es van dur a terme per mitjà d'una reacció de Wittig estereocontrolada com a pas clau. La síntesi començà amb l'addició de l'alcohol OTBS-propargílic **RBM8-090** a l'aldehid de Garner (Fig. 7.11) per mitjà d'una alquinilació diastereoselectiva[31], donant lloc a relació diastereomèrica *erythro*/*threo* 36:1, passant per un estat de transició de Felkin-Anh.[29] En el següent pas, el compost **RBM8-095** es va obtenir quantitativament per hidrogenació del triple enllaç del material de partida amb el catalitzador de rodi.

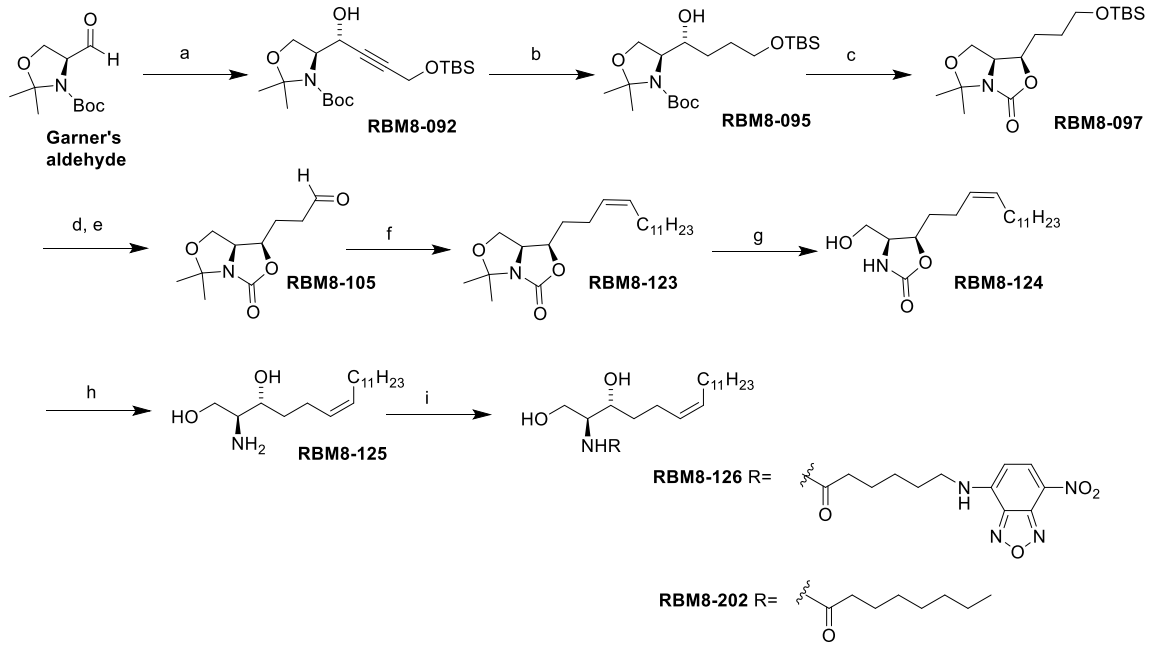

Figura 7.11. *Condicions i reactius. (a) alcohol propargilic TBS* ***RBM8-090****, BuLi, THF, -78˚C, d.r. (erythro/threo): 36/1, 89%. (b)* H_2*, Rh cat, MeOH, 99% (c) NaH, THF, 50˚C, 85%. (d) TBAF, THF, 0˚C to rt, 86%. (e) IBX, EtOAc, 85˚C, 87%. (f)* $BrPh_3PC_{12}H_{25}$*, BuLi, HMPA, THF, d.r.(E/Z):1/30, 64%. (g) pTsOH,* H_2O*, MeOH, 84%. (h) NaOH, EtOH, 103˚C, 70%. (i) àcid* C_6NBD *àcid per* ***RBM8-126*** *I àcid n-octanoic per* ***RBM8-202****, HOBt, EDC,* CH_2Cl_2*, 80% i 87%, respectivament.*

La posterior protecció de l'alcohol secundari de **RBM8-095** per formar el bicicle de oxazol[3,4-*c*]oxazolona **RBM8-097** sorgí a partir del desplaçament intramolecular del grup Boc obtingut pel tractament **de RBM8-095** amb NaH. La desprotecció de l'alcohol primari amb TBAF,[32] seguit de l'oxidació amb IBX[33] va donar lloc a l'aldehid **RBM8-105**. La olefina amb configuració *Z* **RBM8-123** va ser obtinguda amb un 64% de rendiment I una relació diastereomèrica *E/Z* 1:30 a partir d'una reacció de Wittig diastereocontrolada amb bromur de *n*-dodecilfosfoni. Les consecutives hidròlisis de l'isopropilidè I l'oxazolidina, seguit de la *N*-acilació amb l'àcid C_6NBD de la resultant base esfingoide **RBM8-125** va donar lloc a la corresponent (*Z*)-Δ^6-dhCer **RBM8-126** amb un rendiment bo. De manera similar, el derivat octanoic **RBM8-202** es va obtenir a partir de la *N*-acilació de **RBM8-125** amb l'àcid octanoic sota les mateixes condicions de reacció.

La síntesi de les Cers que contenen el $\Delta^{4,6}$-diè es basà en una ruta convergent donant lloc a una 6,4-enina on l'estereoquímica *E* del Δ^4 s'obtenia a partir d'una reducció diastereoselectiva del triple enllaç en el C4. Com s'observa en la Figura 7.12, l'acetilè **RBM8-031** va ser el "building block" comú requerit per a la construcció dels esquelets (*E,E*) i (*E,Z*)-$\Delta^{4,6}$-Cer per mitjà d'un acoblament de Sonogashira.[34] La preparació de **RBM8-031** parteix de l'addició del etinil trimetilsililacetilur de liti a l'aldehid de Garner a -78˚C en THF i HMPA com a co-solvent.[35] La següent desililació de l'alquinol resultant en K_2CO_3 metanòlic va donar lloc a l'alquí terminal **RBM8-031** amb un rendiment del 73% en dos passos i una diastereoselectivitat molt elevada.

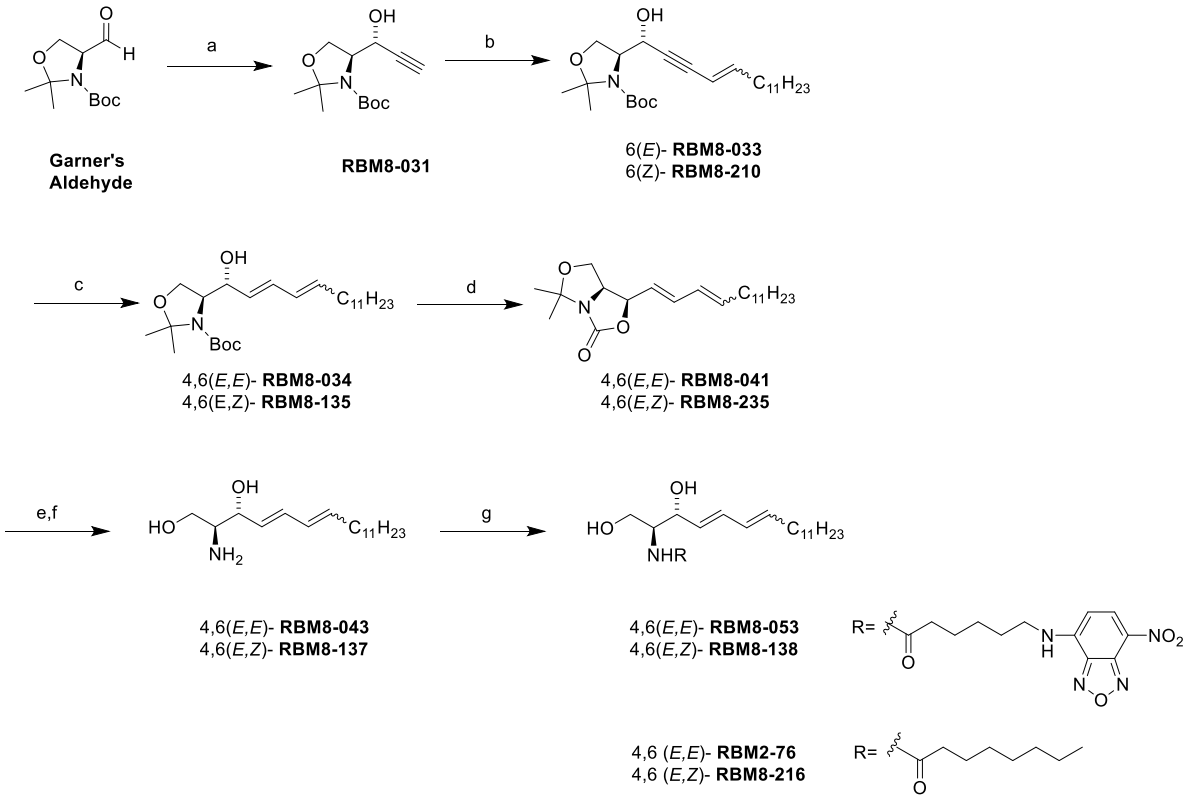

Figura 7.12. *Condicions i reactius. (a) 1. ethynyl-TMS, BuLi, HMPA, THF, 2. K_2CO_3, MeOH, 73% en dues etapes. (b) (E) or (Z)-iodotridecè (**RBM8-032** o **RBM8-209**), Pd(PPh$_3$)$_4$, CuI, piperidina, (E) 42% and (Z) 72%. (c) Red-Al, THF, 0 ˚C, (E,E) 85% i (E,Z) 95% (d) NaH, THF, 50 ˚C, (E,E) 70% i (E,Z) 80% (e) pTsOH, MeOH, (E,E) 82% i (E,Z) 85%. (f) NaOH, EtOH, reflux, (E,E) 82% i (E,Z) 98%. (g) àcid C_6NBD per **RBM8-053** i **RBM8-138**,àcid n-octanoic per **RBM2-076 i RBM8-216**, HOBt, EDC, CH_2Cl_2.*

La síntesi dels enines **RBM8-033** i **RBM8-210** (Fig. 7.12) es van obtenir per mitjà d'un acoplament de Sonogashira amb les iodurs de vinil *E* i *Z* **RBM8-032** i **RBM8-209**, respectivament. Com es mostra en la Figura 7.13, la hidrozirconació amb 1-tridecí utilitzant el reactiu de Schwartz,[36] seguit d'una iodació, va permetre obtenir del iodur vinílic (*E*)- **RBM8-032** amb un rendiment alt i una completa diastereoselectivitat. D'altra banda, la síntesi del iodur vinílic (*Z*) **RBM8-209** va tenir lloc per una reducció del iodotridecí[37] amb azodicarboxilat de potassi[38] i àcid acètic.

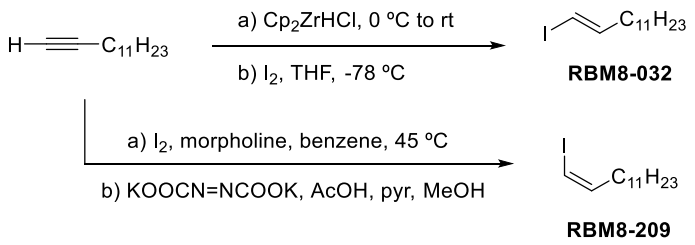

Figura 7.13*. Preparació de les iodurs vinílics E i Z **RBM8-032** i **RBM8-209**, respectivament.*

Així doncs, amb els corresponents "building blocks" necessaris per realitzar l'acoblament de Sonogashira, l'alquí **RBM8-031** es va fer reaccionar amb els respectius halurs d'alquil *E* i *Z* **RBM8-032** i **RBM8-209**, respectivament, en presència del catalitzador de pal·ladi Pd(Ph$_3$P)$_4$ i

sals de Cu (I). Els enins **RBM8-033** i **RBM8-210** (Fig. 7.12) van ser reduïts estereoselectivament amb Red-Al[26] als corresponents diens conjugats (*E,E*) i (*E,Z*) **RBM8-034** i **RBM8-135**, respectivament, i seguidament es va considerar la desprotecció seqüencial d'ambdós compostos via les ozazolidinones **RBM8-041** i **RBM8-235** per formar els amino diols (*E,E*)-**RBM8-043** i (*E,Z*)**-RBM8-137** corresponents en condicions bàsiques. Finalment, les Cers fluorescents **RBM8-053** i **RBM8-138**, així com els derivats de *N*-octanoil **RBM2-076** i **RBM8-216** es van obtenir per *N*-acilació de les corresponents bases esfingoides amb l'àcid C_6NBD o l'àcid *n*-octanoic, respectivament.

Validació dels anàlegs de Δ^6- dhCer

La capacitat de les (*E*) i (*Z*)-Δ^6-dhCers com a substrats de Des1 es va avaluar amb els anàlegs fluorescents **RBM8-029** i **RBM8-126** (Fig. 7.11 i 7.12), respectivament, en lisats cel·lulars d'una línia cel·lular de càncer gàstric (HGC 27) i en presència de NADH com a cofactor enzimàtic. La conversió d'aquests anàlegs a les corresponents Cers dièniques (*E,E*) i (*E,Z*) **RBM8-053** i **RBM8-138**, respectivament, va ser monitoritzat per HPLC-FD, seguint el protocol optimitzat pel nostre grup.[39]

Com es mostra en la figura 7.14A, els resultats en l'anàlisi per HPLC-FD evidencien que el (*E*)-Δ^6-monoè **RBM8-029** va donar lloc al (*E*,*E*)-$\Delta^{4,6}$-diè **RBM8-053**, comparant-lo amb l'autèntic diè utilitzat com a patró, encara que la conversió va ser molt baixa. Contràriament, els resultats obtinguts per a la incubació del (*Z*)-Δ^6-monoè **RBM8-126** van ser més favorables, donant lloc al (*E*,*Z*)-$\Delta^{4,6}$-diè **RBM8-138** a nivells similars als observats en el control positiu de l'activitat de Des1 utilitzant la dhCerC_6NBD com a substrat.[23] Com en el cas anterior, aquest diè va ser identificat per comparació amb el patró sintetitzat.

Així doncs, els resultats evidencien que el (*Z*)-Δ^6-monoè **RBM8-126** pot ser un substrat adequat per mesurar l'activitat de Des1, mentre que l'isòmer *E* no ho és.

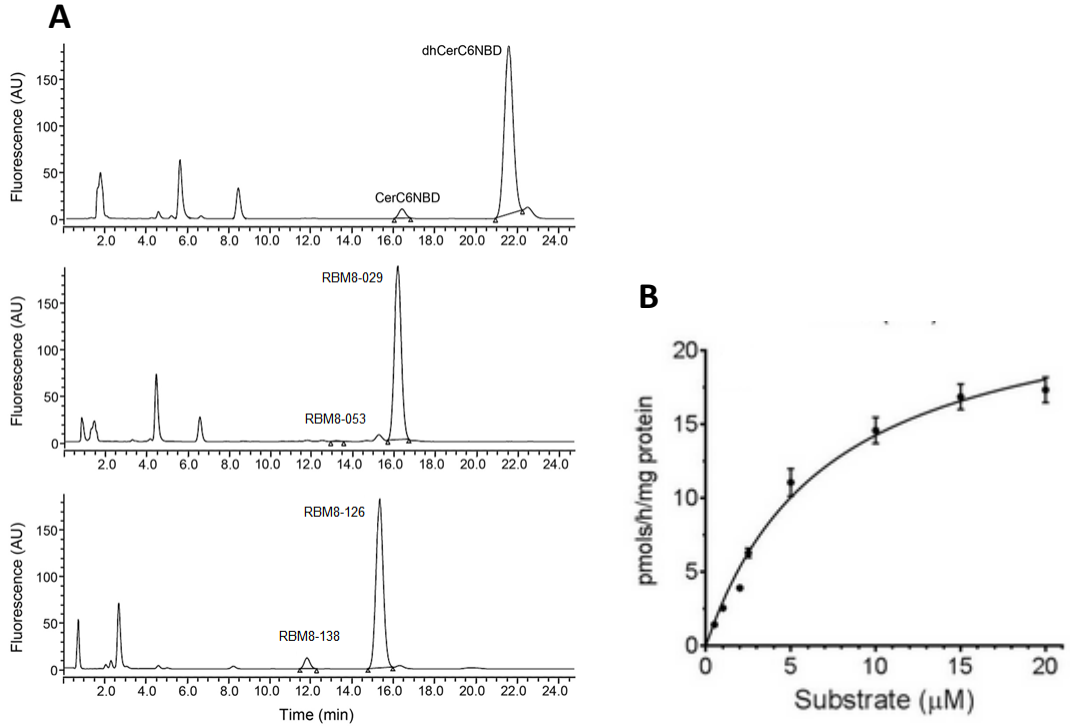

***Figura 7.14. A**. Perfils representatius de HPLC-FD dels substrats i productes fluorescents detectats en els lisats cel·lulars incubats amb **RBM8-029** i **RBM8-126**, i utilitzant com a control positiu la dhCerC$_6$NBD. **B.** Efecte de l'activitat de Des emprant **RBM8-126** a diferents concentracions (mitjana ± SD de dos experiments per triplicat).*

Per tal de determinar els paràmetres cinètics de **RBM8-126** com a substrat (Fig. 7.14B), es va dur a terme l'assaig a diferents concentracions d'aquest. Els anàlisis cinètics indiquen que **RBM8-126** va ser dessaturat amb un valors de $K_{m(app)}$ i $V_{max(app)}$ de 7.6 μM(±1.0) μM i 23.03 (±1.5) pmol/h/mg, respectivament. Aquestes constants són similar a les obtingudes utilitzant l'anàleg saturat dhCerC$_6$NBD ($K_{m(app)}$= 7.7 μM; $V_{max(app)}$= 19.3 pmol/h/mg).

Per tal de confirmar que el (*Z*)-Δ^6-monoè era un bon substrat de Des1, es van incubar cèl·lules intactes de glioblastoma T98G I U87MG amb els derivats *N*-octanoics dels monoens *E* i *Z* **RBM2-085** i **RBM8-202**, respectivament. Es van avaluar els efectes d'aquests compostos en l'esfingolipidòmica, incubant-los a una concentració de 10 μM (concentració que no afecta a la viabilitat cel·lular) durant 2 i 24 h, i comparant-lo amb un experiment de control (tractament amb EtOH). Els lípids es van extreure i es van analitzar per UPLC-TOF MS. Com a resultat, es va mostrar que **RBM2-85** i **RBM8-202** eren convertits ens les corresponents Cers **RBM2-76** i **RBM8-216**, respectivament, i que posteriorment eren metabolitzades al C1-OH per formar els anàlegs d'esfingomielina (derivats de la fosfocolina: PC en la figura 7.15A), amb nivells negligibles dels derivats glicosilats.

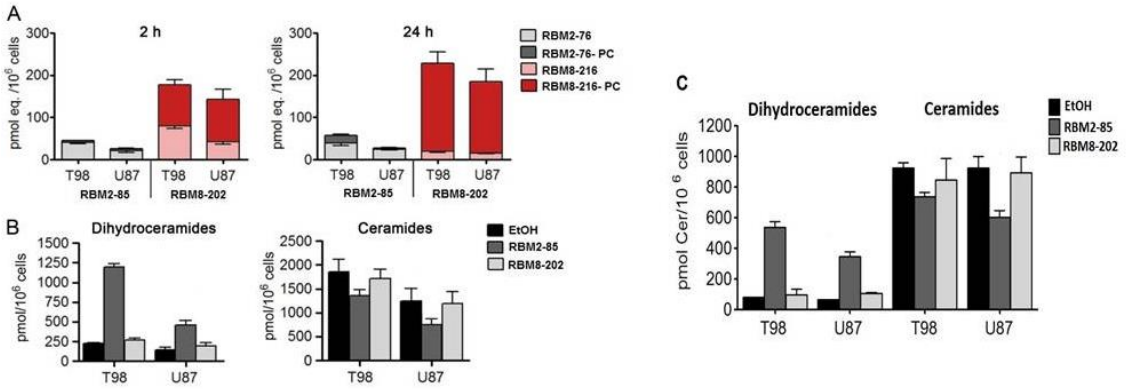

Figura 7.15. *Activitat de Des1 en presència dels compostos* ***RBM2-085*** *i* ***RBM8-202****.* ***A****. Quantitats de Cer dièniques i anàlegs de esfingomielina formades a partir de RBM2-085 i RBM8-202.* ***RBM2-076-PC*** *i* ***RBM8-216-PC*** *són els derivats de fosfocolina de RBM2-085 i RBM8-202, respectivament.* ***B****. Efecte de* ***RBM2-085*** *i* ***RBM8-202*** *en el tractament després de 2 h.* ***C.*** *Efecte de* ***RBM2-085*** *i* ***RBM8-202*** *en el tractament a les 24 h en la producció de dhCer i Cers. Els anàlisis de* ***A****,* ***B*** *i* ***C*** *van ser enregistrats per UPLC-TOF MS en extractes de cèl·lules tractades amb o sense els compostos en els temps indicats. Els resultats són la mitja ± SD de dos experiments independents amb triplicats i estan normalitzats en funció del número de cèl·lules extretes.*

Curiosament, els anàlisis de la composició d'SLs després del tractament mostraren que **RBM2-085**, però no **RBM8-202**, produïen un augment dels nivells de dhCer de 3 a 5 vegades més, fet que s'evidenciava ja després de les 2 h de tractament (Fig. 7.15B) i perdurava inclús després de les 24 h (Fig. 7.15C). Aquests resultats ens van suggerir que l'isòmer *E* (**RBM2-085**), però no l'isòmer *Z* (**RBM8-202**) dels Δ^6-monoèns de dhCer inhibia l'activitat de Des1. Encara que l'acumulació de dhCers a les 2 h suggereixen una inhibició de Des1 més forta en les cèl·lules T98 que en les U87, aquesta aparent discrepància pot ser explicada considerant que els nivells de Cer també són més alts en les cèl·lules T98 que en les U87 (Fig. 7.15B i 7.15C), tot i que la relació entre dhCer/Cer són similars en presència de **RBM2-085**.

Per tal de confirmar la inhibició de Des1 produïda per **RBM2-085**, es va dur a terme un assaig *in vitro* incubant lisats cel·lular amb la dhCerC_6NBD (10 µM) com a substrat i en presència de diferents concentracions de **RBM2-085**. La determinació de l'activitat-concentració mostren que **RBM2-085** inhibeix Des1 amb una IC_{50} de 155.4 nM (Fig. 7.16A). Així doncs, posteriorment es van investigar els paràmetres cinètics de **RBM2-085**. Amb aquesta finalitat, els lisats cel·lulars es van incubar amb el compost a diferents concentracions i a diferents quantitats del substrat (dhCerC_6NBD) durant 4 h. Els resultats van mostrar una inhibició depenent de la concentració en tots els casos. A més a més, mentre la $K_{m(app)}$ no es veia afectada, la $V_{max(app)}$ disminuïa al augmentar la concentració de **RBM2-085** (Fig. 7.16B), fet que ens indica que la inhibició és no competitiva. Mitjançant l'ús d'una representació de Lineweaver-Burk, es va calcular una Ki de 111.4 nM pel compost **RBM2-085** (Fig. 7.16C).

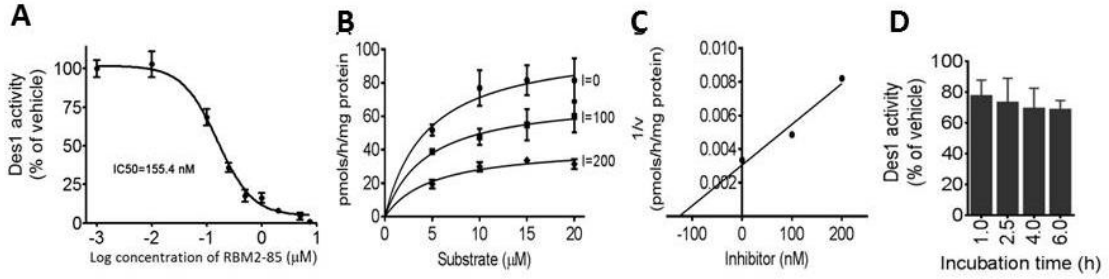

***Figura 7.16. A**. Efecte resposta de **RBM2-085** en l'activitat de Des1. **B.** Inhibició de Des1 amb el compost **RBM2-085** a diferents concentracions de substrat. La quantitat de proteïna va ser de 140 µg en tots els casos. **C.** Figura de la $V_{max(app)}$ recíproca a la concentració de l'inhibidor. **D.** Dependència amb el temps de la inhibició de Des1 amb **RBM2-085.** La concentració de substrat (dhCerC$_6$NBD) va ser de 10 µM i la concentració d'inhibidor de 150 nM.*

Finalment, es va realitzar un assaig d'inhibició depenent del temps per tal de confirmar el tipus d'inhibició. Com es mostra en la Figura 7.16D, la inhibició no va canviar en el transcurs del temps, fet que explica que RBM2-085 és un inhibidor reversible.

Amb els resultats esmentats anteriorment, podem concloure que el compost **RBM2-085** és un inhibidor 13 vegades més potent que XM462, un inhibidor mixt de Des1 (Ki = 2 µM).[23] No obstant, la potència inhibidora de **RBM2-085** és de 3 a 5 vegades menys que el compost GT11,[40] un inhibidor competitiu de Des1, que proporciona un valor de IC_{50} de 52 nM en el mateix assaig utilitzat anteriorment i una Ki de 22 nM.[41]

Disseny d'un assaig HTS per monitoritzar l'activitat de Des1 en suport sòlid

Introducció al capítol

Les 1,2,4-triazolin-3,5-diones (TADs) són sistemes heterocíclics que contenen un grup azo conectat a dos grups carbonils.[42] Degut a la simetria en el seu sistema electrònic, tenen una reactivitat semblant a la de l'oxígen[20], els quals són molt reactius però a la vegada inestables i tenen temps de vida molt curts. Per aquest motiu, s'ha vist que afavoreixen la reacció de Diels Alder, la reacció de Alder-ene (Fig. 7.17), i les cicloaddicions [2+2] per a una gamma de substrats similar (ric en electrons o olefines no polaritzades).

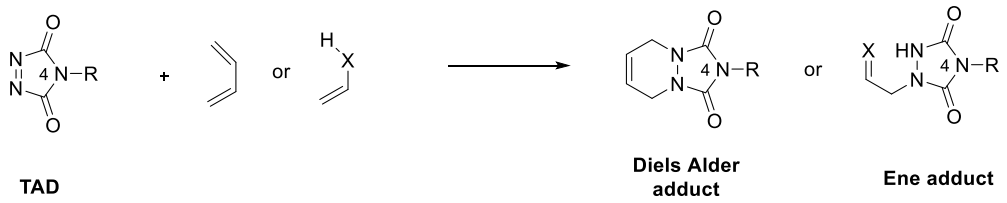

***Figura 7.17**. Adductes de Diels Alder i Ene formats per reactius de tipus TAD.*

Tot i que en aquest treball només es tractarà de la reactivitat d'aquests compostos enfront de la reaccions de Diels Alder i Alder-ene, es coneix que els TADs participen en un gran nombre de reaccions i s'han establert com a eina sintètica per un gran nombre d'aplicacions, com per exemple en la química "click".[43]

Pel que fa a la reacció de Diels Alder, l'ús dels TADs com a dienòfils no es va establir fins l'any 1960, quan Cookson *et al.* va obtenir per primer cop la 4-fenil-1,2,4-triazolin-3,5-diona (PTAD) de forma cristal·lina pura.[44] Des de llavors, la reactivitat d'aquests compostos s'ha estudiat extensament en els camps de la síntesi orgànica, en aplicacions farmacèutiques, i en l'etiquetatge de pèptids. A més a més, tenen la reputació de ser els dienòfils més ràpids que poden ser aïllats.[22] La reactivitat excepcional dels TADs es pot apreciar pel fet de que les seves reaccions són quasi instantànies i acostumen a ser quantitatives, inclús a baixes temperatures i utilitzant diens de baixa reactivitat.

En relació a la reacció de Alder-ene, que consisteix en una reacció pericíclica formada per un alquè o enol i un enòfil que actua de nucelòfil, s'ha vist que els TADs poden actuar com a enòfils d'aquest tipus de reacció, tot i que no són reaccions tant favorables com les de Diels Alder.

Els compostos de tipus TAD també els podem considerar-se com una eina eficient per tal d'introduir enllaços covalents entre dues espècies. Aquest tipus de reaccions se les coneix com a reaccions de tipus "click". Fins a dia d'avui s'han sintetitzat una sèrie de compostos del tipus TAD que contenen un grup azida terminal, susceptible a poder ser reaccionat amb altres grups funcionals (com per exemple un triple enllaç), per mitjà d'una reacció de click. Així doncs, aquests compostos tenen un ventall força ampli per diverses aplicacions, com per exemple la bioconjugació de pèptids i proteïnes,[45] la derivatització de metabòlits de lípids en mostres biològiques,[46] i també com a eines en la síntesi de llibreries químiques,[47] entre d'altres.[43]

Aproximacions pel disseny d'una plataforma de microarray per a mesurar l'activitat de Des1

Els microarrays són estructures miniaturitzades de molècules organitzades a través d'una superfície plana. Són molt utilitzats per a la miniaturització d'assajos biològics per tal d'augmentar el seu rendiment i reduir costos, de manera que s'utilitza com a mètode HTS. Com bé s'ha dit en la part dels Objectius d'aquest treball, la idea fonamental del projecte és desenvolupar un assaig enzimàtic de tipus HTS, i per tant, el fet de poder disposar d'una tècnica com és la del microarray, ens podria facilitar el desenvolupament de l'assaig.

En el capítol anterior hem pogut trobar un anàleg fluorescent de Δ^6-dhCer (**RBM8-126**) per tal de monitoritzar l'activitat de Des1 en solució (Fig. 7.18A). No obstant, com que aquest mètode no és adequat com a format HTS, aquest capítol anirà adreçat al desenvolupament d'un nou assaig fluorescent utilitzant la tècnica del microarray com a format HTS. Per aquest motiu, s'haurà de modificar el substrat fluorescent **RBM8-126** per un altre substrat Δ^6-(*Z*)-monoènic immobilitzat (Fig. 7.18B), on el producte $\Delta^{4,6}$-(*E,Z*)-diènic resultant podria ser atrapat per un derivat del tipus TAD fluorescent per mitjà d'una reacció de Diels Alder.

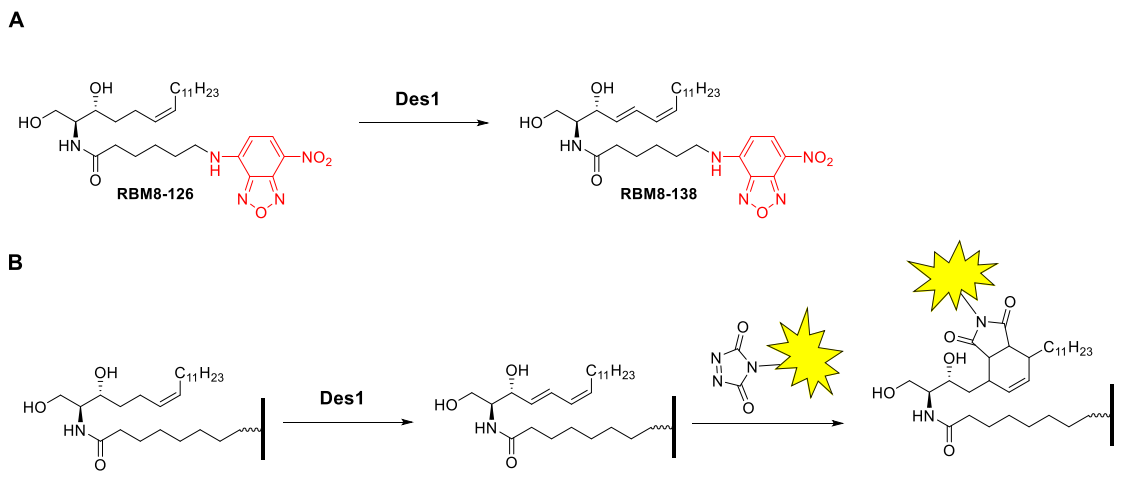

Figura 7.18. *Mètodes desenvolupats per tal de monitoritzar l'activitat de Des1.* ***A.*** *Assaig de Des1 en solució, utilitzant l'anàleg fluorescent* ***RBM8-126. B.*** *Assaig de Des1 dissenyat per a usar un substrat immobilitzat en suport sòlid i la subseqüent derivatització del producte de reacció amb un dienòfil fluorescent.*

En primer lloc s'haurà de reemplaçar la Δ^6-dhCer fluorescent **RBM8-126** per un altre anàleg no fluorescent adequat per a la immobilització en suport sòlid. Seguidament, s'haurà de confirmar que el monoè ancorat és substrat de Des1, i que el diè format en la reacció enzimàtica pot reaccionar amb un reactiu fluorescent del tipus TAD per a la posterior quantificació. Arribats a aquest punt, s'hauran d'optimitzar les condicions de reacció de cada pas en el format de microarray per tal de millorar la sensibilitat en la mesura.

Disseny d'un derivat de TAD fluorescent

Per tal d'escollir un dienòfil fluorescent del tipus TAD per poder-lo fer reaccionar amb el diè format després de la reacció enzimàtica, inicialment es va considerar adient l'ús del DMEQ-TAD.[48] Tot i poder corroborar que aquest derivat reaccionava amb el $\Delta^{4,6}$-(*E,Z*)-dienic **RBM8-216** en dissolució per mitjà d'una reacció de Diels Alder, la longitud d'ona d'emissió del DMEQ-TAD (λ_{em}=440 nm)[49] no entrava dins del rang espectral requerit per a l'escàner que utilitzaríem en la lectura del microarray (entre 543 i 633 nm). Per aquesta raó, es va dissenyar un dienòfil fluorescent compost per dos passos; en primer lloc el diè reaccionaria amb la triazolindiona **RBM8-254** (Fig.7.19), que provenia d'una oxidació *in situ* del derivat d'urazole "TAD-Azide", seguit d'una reacció de cicloaddició (SPAAC)[50] amb el DBCO-PEG$_4$-TAMRA. En aquest cas, les longituds d'excitació i emissió de l'agent fluorescent (TAMRA) sí que entraven dins del rang espectral requerit (λ_{exc}=545 nm, λ_{em}=567 nm).

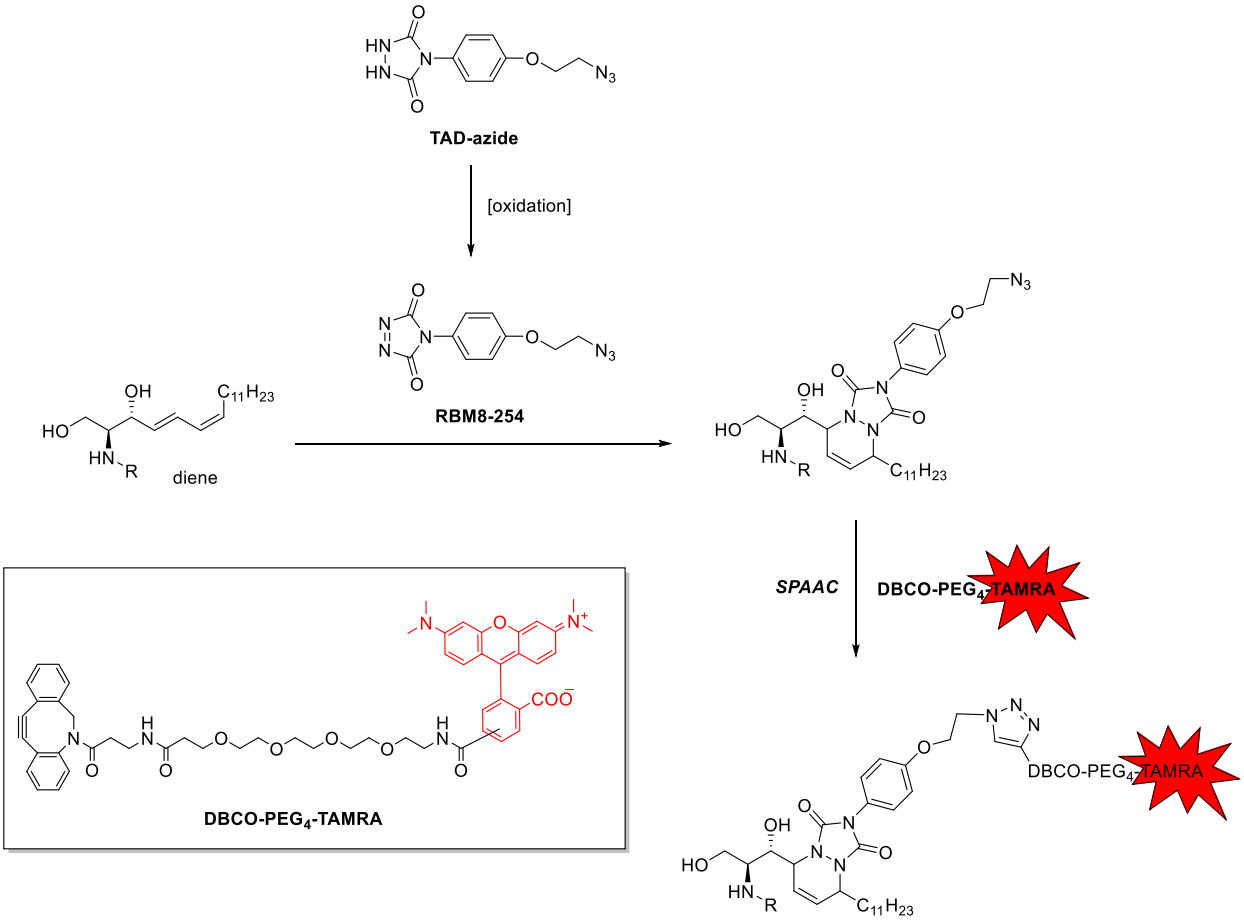

Figura 7.19. *Agent fluorescent basat en la reacció de cicloaddició SPAAC entre* ***RBM8-254*** *i DBCO-PEG$_4$-TAMRA.*

Tot i que el TAD-Azide és comercial, el compost es va sintetitzar seguint el procediment de Barbas i col·laboradors.[45] El mètode d'oxidació per tal d'obtenir **RBM8-254** es va optimitzar, escollint com a millor agent oxidant el DABCO-Br,[50] un complex tetramèric no soluble en dissolvents orgànics, fet que facilitava poder aïllar el producte d'oxidació **RBM8-254** sense necessitat d'un pas de purificació.

Síntesis, immobilització i estudi d'anàlegs de Δ^6-dhCer com a substrat de Des1

La modificació de l'anàleg fluorescent **RBM8-126** com a substrat de Des1 per un altre anàleg que pogués immobilitzar-se en un suport sòlid es va iniciar amb la síntesi del compost **RBM8-251** (Fig. 7.20A). Seguidament, es va immobilitzar aquest compost per tal d'avaluar l'activitat de Des1 en format de microarray. La seqüència de passos requerits es mostra en la Figura 7.20A.

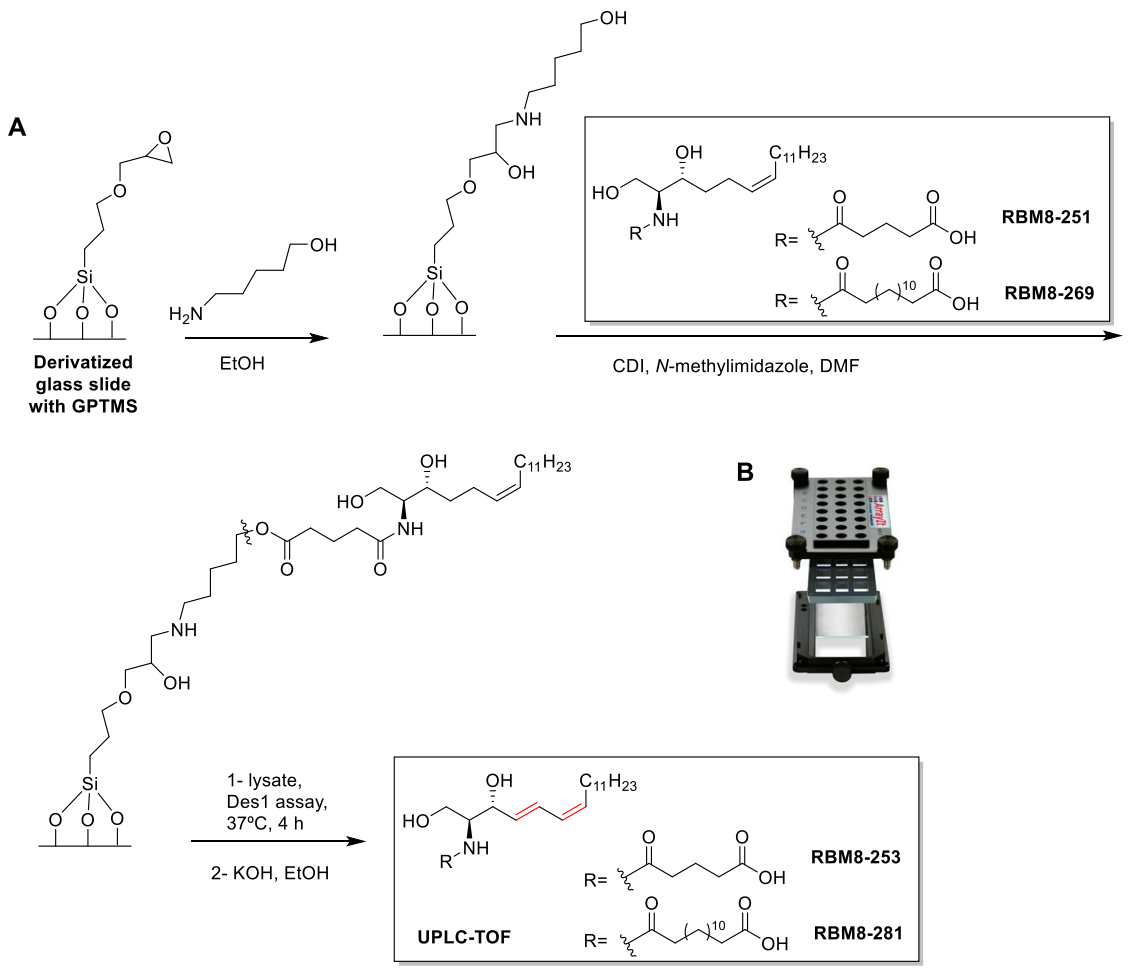

***Figura 7.20**. **A**. Descripció dels passos de reacció per a l'avaluació de **RBM8-251** i **RBM8-269** com a substrats de Des1 en format de microarray. **B**. Microplate microarray Arrayit hardware system. Adaptador amb junta de silicona que divideix el vidre en 24 pous.*

El pas inicial va ser la reacció del 5-aminopentanol amb el vidre derivatitzat amb glicidilpropil trimetilsilà (GPTMS). Seguidament, es va immobilitzar l'alquè **RBM8-251** en el suport sòlid via esterificació del grup carboxilat terminal amb els hidroxils lliures del suport. El vidre funcionalitzat es va incubar amb lisats cel·lulars per dur a terme la reacció enzimàtica. L'últim pas de reacció consistia en la hidròlisi del grup ester en condicions bàsiques i el posterior anàlisi dels extractes lipídics per UPLC-TOF MS. Tots els passos de reacció es van dur a terme amb l'adaptador descrit en la Figura 7.20B, que dividia el suport en 24 pous. Els resultats obtinguts van ser negatius, ja que en els extractes lipídics no es va observar senyal del diè esperat **RBM8-253**.

Enfront dels resultats negatius, que es van atribuir a que la naturalesa del linker de **RBM8-251** era massa curta (només 3 àtoms de C) per permetre un accés eficient del substrat al centre actiu de l'enzim, es va procedir a la síntesi d'un nou anàleg de (*Z*)-Δ^6-dhCer amb una cadena *N*-acil més llarga (**RBM8-269**). Seguidament es va procedir al mateix procediment experimental que amb l'anàleg **RBM8-251** (Fig. 7.20), i, en aquest cas, els extractes lipídics sí que van proporcionar un bon resultat, amb obtenció del diè $\Delta^{4,6}$-ceramide **RBM8-281** amb conversions d'entre 1 i 5 %, resultats similars als obtingut en l'assaig enzimàtic en solució esmentat en el capítol anterior.

Optimització de les condicions d'assaig en format de microarray per a l'avaluació de l'activitat de Des1

Un cop dissenyat l'anàleg de (*Z*)-Δ^6-dhCer (**RBM8-269**) adequat per a la seva immobilització i posterior assaig enzimàtic en format de microarray, es va procedir a modificar el mètode d'ancoratge d'aquest, per tal d'immobilitzar-lo per mitjà d'un enllaç no hidrolitzable, ja que la finalitat inicial de que el compost **RBM8-269** tingués un àcid carboxílic terminal en la cadena de *N*-acil per tal d'ancorar-lo via esterificació només ens servia per poder trencar aquest enllaç i corroborar per UPLC-TOF MS que el compost s'havia immobilitzat i que la reacció enzimàtica havia funcionat. Així doncs, es va dissenyar un nou substrat (**RBM8-324**, Fig. 7.21), reemplaçant l'enllaç ester per un enllaç amida.

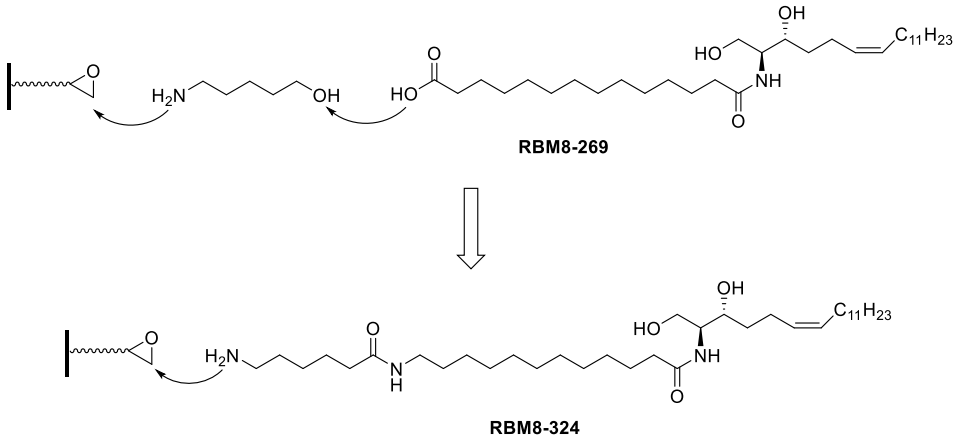

Figura 7.21. *Modificació de la cadena de N-acil del substrat per una immobilització covalent no hidrolitzable.*

A més, es va sintetitzar també el producte esperat (**RBM8-313**) de la reacció enzimàtica utilitzant com a anàleg de (*Z*)-Δ^6-dhCer el compost **RBM8-324** (Fig. 7.22) per tal d'immobilitzar-lo i utilitzar-lo com a patró per a la posterior optimització de la reacció de Diels Alder amb el derivat del TAD **RBM8-254** i la subseqüent derivatització d'aquest amb DBCO-PEG_4-TAMRA (Fig. 7.22).

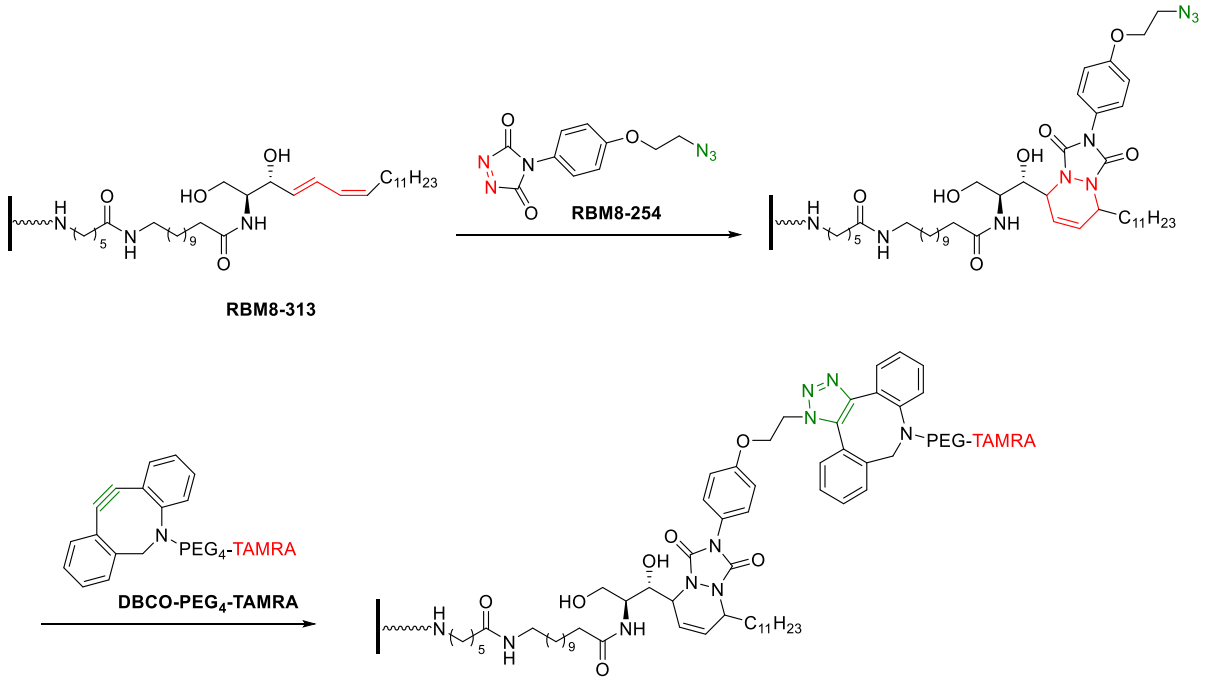

Figura 7.22. *Immobilització del producte de reacció esperat (**RBM8-313**). Les successives reaccions de Diels Alder amb **RBM8-254**, seguit d'una reacció de click sense Cu amb DBCO-PEG$_4$-TAMRA s'optimitzaren per tal de trobar les millors condicions de l'assaig HTS.*

El procés d'optimització requeria d'una etapa inicial d'immobilització de l'esfingolípid **RBM8-313** per mitjà de nano gotes ("spots") en el suport derivatitzat amb GPTMS. El vidre es va dividir en 24 pouets, i cada pouet contenia una matriu de 3x3 (9 spots) de l'esfingolípid **RBM8-313**. A continuació, per tal de reproduir l'assaig el més pròxim possible a les condicions d'assaig reals, es va incloure un pas d'incubació (però en aquest cas sense lisat cel·lular, només amb el tampó fosfat que s'utilitzaria en l'assaig real) amb el temps de reacció requerit. Arribats a aquest punt, es van utilitzar diferents agents blocants per tal de disminuir les adsorcions inespecífiques del background. Seguidament, el vidre es va submergir en una solució recent preparada del dienòfil **RBM8-254**, es va netejar el suport, i seguidament s'afegí el DBCO-PEG$_4$-TAMRA. Després d'una etapa de rentat, el vidre es va llegir a l'escàner.

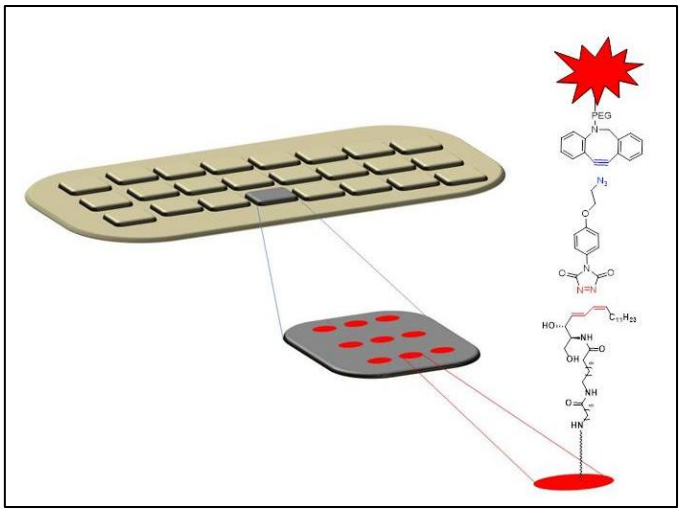

Figura 7.23. *Imatge representativa per al procés d'optimització en el disseny de l'assaig, amb el compost* ***RBM8-313*** *immobilitzat.*

Per tal d'obtenir les millors condicions d'assaig, es van optimitzar cadascun dels passos de reacció pertinents, tant les concentracions dels reactius, com els dissolvents emprats, les etapes de rentat, els temps de reacció, els agents blocadors per disminuir les adsorcions inespecífiques, o la morfologia dels "spots". En la Taula 7.24 es mostren els paràmetres obtinguts un cop optimitzades les condiciones descrites anteriorment.

Taula 7.24. Paràmetres importants a tenir en compte pel desenvolupament de l'assaig en microarray.

Mètode d'immobilització	covalent
Temperatura i humitat	60 % i 20˚C
Dissolvent d'immobilitzatió/concentració de RBM8-313	DMF/ 10 mg mL^{-1} to 0 $mg.mL^{-1}$
Agent bloquejant	PVP 2% en PBS
Tampó per a la reacció enzimàtica /Temps d'incubació	Tampó fosfat pH 7.4/ 4h, 37˚C
Dissolvent/concentració/temps de reacció de RBM8-254	MeOH/ 1 mg mL^{-1}/ 1 h
Dissolvent/concentració/temps de reacció de DBCO-PEG_4-TAMRA	MeOH/ 1 µg mL^{-1}/ 1 h
Etapa de rentat final	MeOH/ MilliQ H_2O

Un cop obtingudes les millors condicions d'assaig, es van realitzar corbes de calibrat a diferents concentracions d'analit **RBM8-313**, obtenint un límit de detecció final (LOD) de 3.32 µg/mL del producte de reacció enzimàtic (Fig. 7.25).

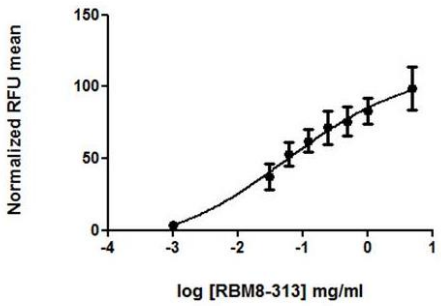

	RBM8-313
Norm. RFU max	102,44 ± 5,44
Norm. RFU min	-0,11 ± 2,80
Slope	0,84 ± 0,22
IC_{50} (µg/mL)	70,75 ± 38,60
LOD (µg/mL)	3,32 ± 1,97
LOQ (µg/mL)	17,16 ± 7,19
r^2	0,98 ± 0,02

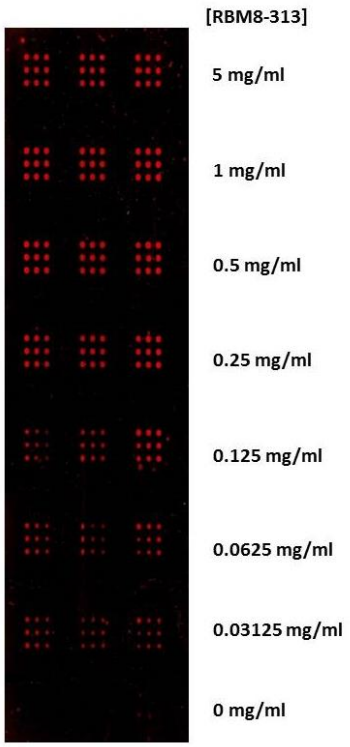

Figura 7.25. *Corba de calibrat per a la detecció de RBM8-313 i els paràmetres que defineixen aquesta corba. Els experiments es va realitzar per triplicat (3 columnes) i en 3 dies diferents. La imatge correspon a un experiment. RFU :Relative Fluorescence Units. LOD: Limit of detection. LOQ: Limit of Quantification.*

Cap a un assaig enzimàtic complet per a l'avaluació de l'activitat de Des1

Un cop optimitzada la determinació quantitativa del diè **RBM8-313**, es va procedir a realitzar l'assaig de Des1 en format microarray, utilitzant com a substrat el monoè **RBM8-324** ancorat, i la posterior incubació amb lisats cel·lulars de cèl·lules HGC 27 (Fig. 7.26).

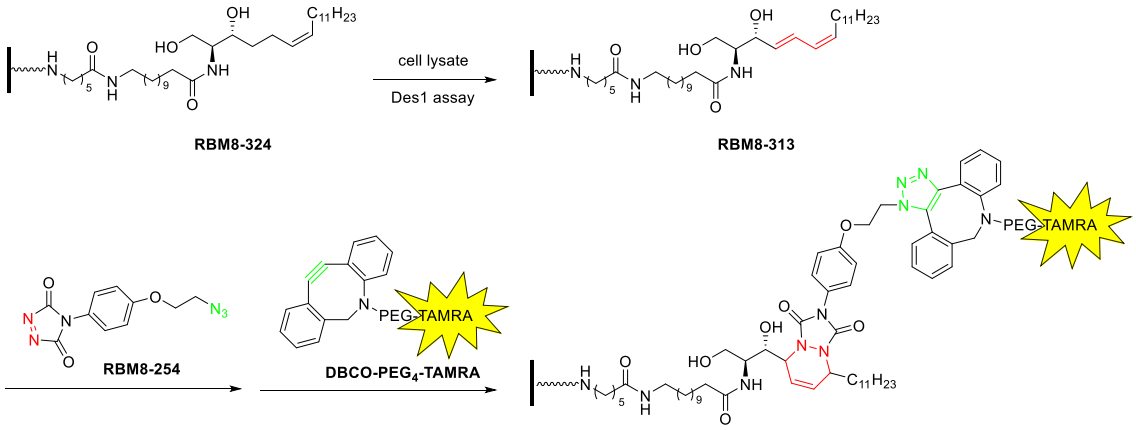

Figura 7.26. *Representació esquemàtica de les reaccions involucrades en l'assaig HTS per monitoritzar l'activitat de Des1 en format de microarray.*

L'experiment consistia en dipositar en el suport sòlid el substrat **RBM8-324** a una concentració de 5 mg/mL en DMF, seguit de la incubació d'una suspensió de 10^6cel·lules/mL en cadascun dels pous durant 4 h. El diè resultant (**RBM8-313**) format en la reacció enzimàtica seria atrapat amb el dienòfil **RBM8-254** per a la següent reacció de click sense coure amb el reactiu fluorescent **DBCO-PEG$_4$-TAMRA**.

Els resultats obtinguts en l'experiment van ser força curiosos, obtenint una senyal del blanc molt elevada quan s'immobilitzava el substrat **RBM8-324** sense cèl·lules. Tot i així, aquesta senyal no superava la de l'assaig real amb cèl·lules, senyal que provenia del producte de la reacció enzimàtica **RBM8-313**. Per tal d'investigar a què era deguda la senyal del blanc del substrat, es va procedir a fer diversos assajos d'immobilització tant del substrat **RBM8-324** com del producte **RBM8-313** per poder comparar ambdues senyals sense tenir en compte l'assaig enzimàtic, només fent-lo reaccionar amb els passos posteriors a aquest. Primerament es pensava que la senyal provenia d'adsorcions inespecífiques i que trobaríem la manera de disminuir-la, o, fins i tot, anul·lar-la, però això no va ser possible. Es va fer ús d'un altre fluoròfor, substituint el TAMRA per un Cy3, també es va modificar el grup DBCO de la reacció de click sense coure per un alquí senzill en presència de coure, es van modificar les concentracions d'analits en tots els passos de reacció, i fins i tot, es va fer ús de diferents blocadors per tal de disminuir aquesta senyal no desitjada. La persistent senyal del substrat **RBM8-324** tot i modificant totes les condicions esmentades anteriorment, ens van fer pensar que la fluorescència no era deguda a adsorcions inespecífiques, sinó a un enllaç covalent entre el substrat monoènic **RBM8-324** i el TAD **RBM8-254**.

Avaluació de la reacció de Alder-ene usant RBM8-125 com a model

En la discussió dels assajos preliminars d'aquest treball per al desenvolupament de l'assaig HTS es va descartar l'ús d'un derivat de la dhCer natural com a substrat de Des1 ja que el producte esperat Δ^4-monoènic no reaccionava amb un enòfil de tipus TAD en solució com el PTAD (Fig. 7.5A pel plantejament d'assaig, Fig. 7.6 per la reacció en dissolució). Així doncs, es va assumir que els derivats de la Δ^6-dhCer tampoc reaccionarien per mitjà d'una reacció de Alder-ene, i per tant, podríem aprofitar l'avinentesa d'utilitzar aquest com a substrat i el producte dènic format després de la reacció enzimàtica podria reaccionar per mitjà d'una reacció de Diels Alder. Tot i així, la forta senyal de fluorescència obtinguda en els assajos en microarray del substrat Δ^6–monoènic indicaven que s'estava donant lloc una reacció covalent específica.

Per tal de corroborar la reactivitat del Δ^6-monoè enfront del derivat del TAD **RBM8-254**, es va fer reaccionar la base esfingoide **RBM8-125** com a model Δ^6-monoènic enfront de **RBM8-254** com a enòfil (Fig. 7.27).

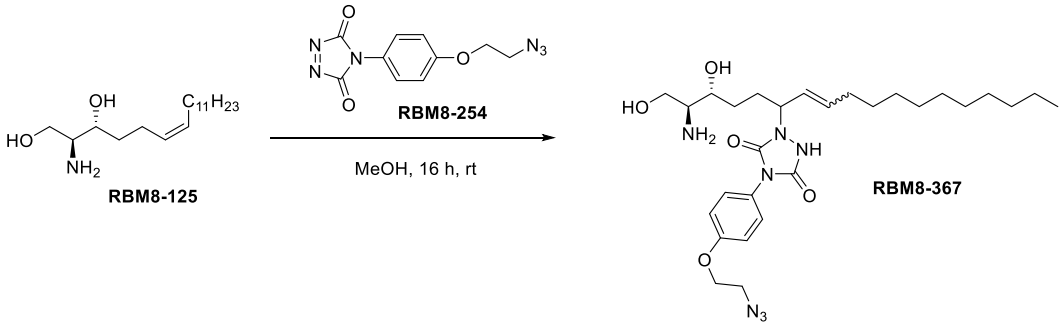

Figura 7.27. *Reacció de Δ^6-**RBM8-125** amb el **RBM8-254** com a enòfil en la reacció de Alder-ene en solució.*

Malauradament, el compost **RBM8-125** va donar lloc a l'adducte de Alder-ene, com s'evidencia en els espectres de RMN i de MS, coincidint amb el compost **RBM8-367** (Fig. 7.27).

Amb la finalitat de confirmar els resultats esmentats, es va dur a terme un últim experiment basat en la immobilització dels compostos descrits en la figura 7.28. En primer lloc es van sintetitzar els compostos **RBM8-337** i **RBM8-351**, que correspondrien als derivats de dhCer i Δ^4-Cer, respectivament per dur a terme l'assaig en condicions de Alder-ene amb el dienòfil **RBM8-254**. D'altra banda, també es van tenir en compte la Δ^6-dhCer i la $\Delta^{4,6}$-Cer **RBM8-324** i **RBM8-313**, respectivament, com a patrons de fluorescència i per tal de poder comparar els 4 senyals de fluorescència a la vegada.

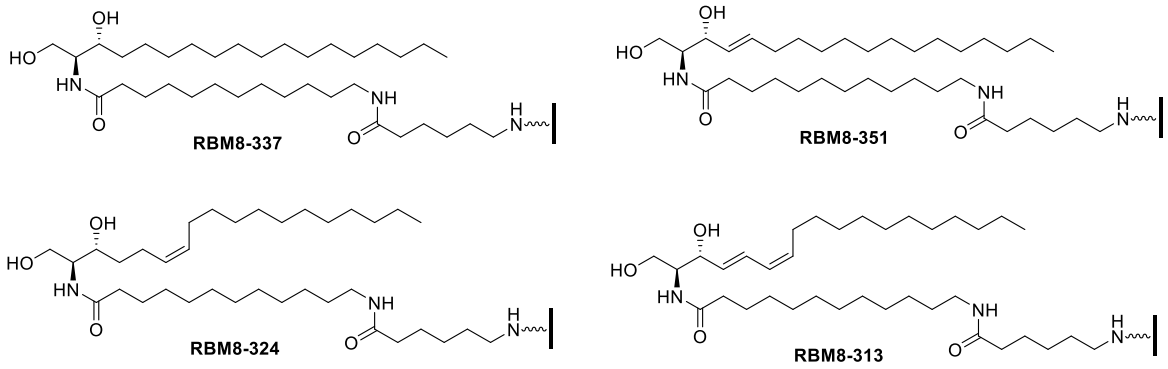

Figura 7.28*. Estructures químiques dels compostos immobilitzats per tal d'avaluar la seva senyal de fluorescència utilitzats com a blancs, sense assaig enzimàtic.*

Com s'esperava, la Figura 7.29 mostra la fluorescència dels 4 compostos per separat, obtenint una senyal de fluorescència pels compostos Δ^6-**RBM8-324** i $\Delta^{4,6}$-**RBM8-313**, degudes a la reacció de Alder-ene i de Diels Alder amb el TAD **RBM8-254**, respectivament, com ja havíem corroborat anteriorment.

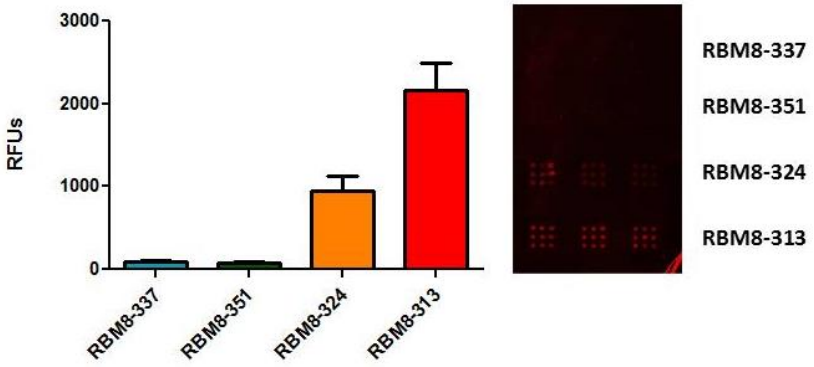

Figura 7.29. *Senyal de fluorescència dels compostos* ***RBM8-337****,* ***RBM8-351****,* ***RBM8-324*** *i* ***RBM8-313****.Les barres corresponen a la mitjana i la desviació estàndard de les senyals enregistrades de 9 punts x 3 files x duplicats en cada compost (54 punts per cadascun). La imatge és representativa de cada compost.*

En canvi, tot i que ja sabíem que la reactivitat de Δ^4-Cer enfront de la reacció de Alder-ene en solució era negligible, vam provar-ho amb el substrat ancorat Δ^4-**RBM8-351**, per corroborar que les nostres hipòtesis estaven ben formulades, i com es pot veure en la Figura 7.29, no s'observà cap tipus de senyal. Per tant, mentre la Δ^6-dhCer és reactiva tant en solució com en suport de microarray, la Δ^4-Cer isomèrica és inerta en les mateixes condicions. La naturalesa del doble enllaç en la posició 4 podria ser la responsable de la baixa reactivitat. No obstant, aquesta assumpció requeriria d'experiments addicionals que estan fora de les possibilitats d'aquest treball.

Conclusions generals

Les conclusions generals més significatives d'aquesta Tesi es mostren a continuació:

1) Els resultats preliminars positius per tal de dur a terme un assaig HTS per monitoritzar l'activitat de Des1 utilitzant com a substrat una Δ^6-dhCer, ja que es va poder observar que la Cer $\Delta^{4,6}$-diènica reaccionava amb un derivat del TAD per mitjà d'una reacció de Diels Alder, ens van permetre escollir aquesta estratègia per realitzar el desenvolupament de l'assaig de Des1.
2) S'han sintetitzat els derivats d'anàlegs de *Z* i *E*- Δ^6-dhCer **RBM8-029** i **RBM8-126**, respectivament, per dur a terme l'assaig enzimàtic en solució. També s'han sintetitzat els isòmers diènics **RBM8-053** i **RBM8-138** com a patrons analítics, ja que són els productes enzimàtics esperats. A més a més, s'han sintetitzat els isòmers *N*-octanoics dels substrats *E* i *Z* Δ^6-dhCer **RBM2-085** i **RBM8-216**, respectivament, per tractar-los amb cèl·lules intactes.
3) Amb els resultats de 2) s'ha pogut observar que la introducció d'un doble enllaç en la posició 6 de la dhCer té finalitats diferents depenent de la geometria del doble enllaç; mentre l'isòmer *Z* **RBM8-126** és dessaturat per Des1 per formar el diè conjugat conjugated $\Delta^{4,6}$, amb una $K_{m(app)}$ i $V_{max(app}$ de 7.6 µM(±1.0) µM i 23.03 (±1.5) pmol/h/mg,

respectivament. L'isòmer *E* **RBM2-085** resultà ser un inhibidor no competitiu de Des1 amb un valor de Ki de 111.4 nM, utilitzant la dhCerC_6NBD com a substrat.

4) S'ha intentat dissenyar un assaig HTS per tal de monitoritzar l'activitat de Des1 en suport sòlid. Amb aquesta finalitat, s'ha demostrat que l'enzim Des1 és capaç de dessaturar l'anàleg de *Z*-Δ^6-dhCer **RBM8-269** immobilitzat en un vidre de tipus suport sòlid que conté una cadena de *N*-acil de llargada determinada.
5) S'ha dissenyat un dienòfil fluorescent basat en un sistema que conté dos passos de reacció: la síntesi de la triazolindiona **RBM8-254** (que s'obté de la prèvia oxidació *in situ* del derivat TAD-azida) seguit d'una reacció de click sense coure amb el DBCO-PEG_4-TAMRA.
6) S'han optimitzat les condicions de detecció, immobilitzant el producte enzimàtic (*E,Z*)-$\Delta^{4,6}$-Cer **RBM8-313**, modificant les concentracions dels reactius, els dissolvents, la morfologia dels "spots", i la utilització de diversos agents blocants, obtenint un límit de detecció del compost **RBM8-313** de 3.32 µg/mL.
7) Pel que fa al disseny de l'assaig complet per avaluar l'activitat de Des1, s'ha immobilitzat el substrat **RBM8-324** obtenint una senyal de fluorescència del blanc molt elevada. Intents de trobar la causa del problema ens han donat lloc a no descartar que el sistema (*Z*)-Δ^6-dhCer **RBM8-324** podria experimentar una reacció de tipus de Alder-ene. L'avaluació d'aquesta reacció s'ha dut a terme amb el model olefínic (*Z*)-Δ^6-**RBM8-125** en presència del enòfil **RBM8-254**, obtenint l'adducte de Alder-ene **RBM8-367**.
8) Encara que els resultats preliminars d'aquest treball ens van fer descartar la possibilitat d'utilitzar un derivat de la dhCer natural com a substrat de Des1 degut a que la Δ^4-Cer (producte de reacció) no era reactiva enfront de derivats del TAD, vam considerar la possibilitat de dur a terme la reacció en format de microarray immobilitzant el compost Δ^4-Cer **RBM8-351** i la dhCer **RBM8-337** per tal de comparar les senyals de fluorescència amb els compostos Δ^6-dhCer **RBM8-324** i $\Delta^{4,6}$-Cer **RBM8-313**. Els resultats evidencien que la reacció de Alder-ene no es pot dur a terme amb Δ^4-monoèns, tot i que amb Δ^6-monoèns sí. Aquests últims resultats han impedit poder desenvolupar el cribratge massiu, tot i que tots els objectius inicials s'han aconseguit per a la seva finalització.

Referències

(1) Head, B. P.; Patel, H. H.; Insel, P. A. Interaction of Membrane/lipid Rafts with the Cytoskeleton: Impact on Signaling and Function: Membrane/lipid Rafts, Mediators of Cytoskeletal Arrangement and Cell Signaling. *Biochim. Biophys. Acta - Biomembr.* **2014**, *1838* (2), 532–545.

(2) Futerman, A. H.; Hannun, Y. A. The Complex Life of Simple Sphingolipids. *EMBO Rep.* **2004**, *5* (8), 777–782.

(3) Bartke, N.; Hannun, Y. A. Bioactive Sphingolipids: Metabolism and Function. *J. Lipid Res.* **2009**, *50 Suppl* (Supplement), S91-6.

(4) Hannun, Y. A.; Luberto, C.; Mao, C.; Obeid, L. M. *Bioactive Sphingolipids in Cancer Biology and Therapy*; 2015.

(5) Merril, A. H.; Sandhoff, K. *Sphingolipids: Metabolism and Cell Signalling*; Elsevier Masson SAS, 2002; Vol. 31.

(6) Kim, H. J.; Qiao, Q.; Toop, H. D.; Morris, J. C.; Don, A. S. A Fluorescent Assay for Ceramide Synthase Activity. *J. Lipid Res.* **2012**, *53* (8), 1701–1707.

(7) Nikolova-Karakashian, M.; Morgan, E. T.; Alexander, C.; Liotta, D. C.; Merrill, A. H. Bimodal Regulation of Ceramidase by Interleukin-1β. Implications for the Regulation of Cytochrome P450 2C11 (CYP2C11). *J. Biol. Chem.* **1997**, *272* (30), 18718–18724.

(8) Casasampere, M.; Ordoñez, Y. F.; Pou, A.; Casas, J. Inhibitors of Dihydroceramide Desaturase 1: Therapeutic Agents and Pharmacological Tools to Decipher the Role of Dihydroceramides in Cell Biology. *Chem. Phys. Lipids* **2016**, *197*, 33–44.

(9) Rodriguez-Cuenca, S.; Barbarroja, N.; Vidal-Puig, a. Dihydroceramide Desaturase 1, the Gatekeeper of Ceramide Induced Lipotoxicity. *Biochim. Biophys. Acta - Mol. Cell Biol. Lipids* **2015**, *1851* (1), 40–50.

(10) Bielawska, A.; Crane, H. M.; Liotta, D.; Obeid, L. M.; Hannun, Y. A. Selectivity of Ceramide-Mediated Biology: Lack of Activity of Erythro-Dihydroceramide. *J. Biol. Chem.* **1993**, *268* (35), 26226–26232.

(11) Kraveka, J. M.; Li, L.; Szulc, Z. M.; Bielawski, J.; Ogretmen, B.; Hannun, Y. A.; Obeid, L. M.; Bielawska, A. Involvement of Dihydroceramide Desaturase in Cell Cycle Progression in Human Neuroblastoma Cells. *J. Biol. Chem.* **2007**, *282* (23), 16718–16728.

(12) Camacho, L.; Simbari, F.; Garrido, M.; Abad, J. L.; Casas, J.; Delgado, A.; Fabriàs, G. 3-Deoxy-3,4-Dehydro Analogs of XM462. Preparation and Activity on Sphingolipid Metabolism and Cell Fate. *Bioorganic Med. Chem.* **2012**, *20* (10), 3173–3179.

(13) Zheng, W.; Kollmeyer, J.; Symolon, H.; Momin, A.; Munter, E.; Wang, E.; Kelly, S.; Allegood, J. C.; Liu, Y.; Peng, Q.; Ramaraju, H.; Sullards, M. C.; Cabot, M.; Merrill, A. H. Ceramides and Other Bioactive Sphingolipid Backbones in Health and Disease: Lipidomic Analysis, Metabolism and Roles in Membrane Structure, Dynamics, Signaling and Autophagy. *Biochim. Biophys. Acta - Biomembr.* **2006**, *1758* (12), 1864–1884.

(14) Pervaiz, S.; Holme, A. L. Resveratrol: Its Biological Targets and Functional Activity. *Antioxid Redox Signal* **2009**, *11* (11).

(15) Kartal, M.; Saydam, G.; Sahin, F.; Baran, Y. Resveratrol Triggers Apoptosis Through Regulating Ceramide Metabolizing Genes in Human K562 Chronic Myeloid Leukemia Cells. *Nutr. Cancer* **2011**, *634* (4), 637–644.

(16) Cakir, Z.; Saydam, G.; Sahin, F.; Baran, Y. The Roles of Bioactive Sphingolipids in Resveratrol-Induced Apoptosis in HL60 Acute Myeloid Leukemia Cells. *J. Cancer Res. Clin. Oncol.* **2011**, *137* (2), 279–286.

(17) Michel, C.; van Echten-Deckert, G.; Rother, J.; Sandhoff, K.; Wang, E.; Merrill, A. H. Characterization of Ceramide Synthesis. *J. Biol. Chem.* **1997**, *272* (36), 22432–22437.

(18) Geeraert, L.; Mannaerts, G. P.; van Veldhoven, P. P. Conversion of Dihydroceramide into Ceramide: Involvement of a Desaturase. *Biochem. J.* **1997**, *327 (Pt 1*, 125–132.

(19) Raith, K.; , Jorg Darius, R. H. H. N. Ceramide Analysis Utilizing Gas Chromatography – Mass Spectrometry. *J. Chromatogr.* **2000**, *876*, 229–233.

(20) Leach, A. G.; Houk, K. N. Diels–Alder and Ene Reactions of Singlet Oxygen, Nitroso Compounds and Triazolinediones: Transition States and Mechanisms from Contemporary Theory. *Chem. Commun.* **2002**, No. 12, 1243–1255.

(21) Roling, O.; De Bruycker, K.; Vonhören, B.; Stricker, L.; Körsgen, M.; Arlinghaus, H. F.; Ravoo, B. J.; Du Prez, F. E. Rewritable Polymer Brush Micropatterns Grafted by Triazolinedione Click Chemistry. *Angew. Chemie -International Ed.* **2015**, *54* (44), 13126–13129.

(22) Radl, S. 1,2,4-Triazoline-3,5-Diones. *Adv. Heterocycl. Chem.* **1996**, *67* (30), 119–205.

(23) Munoz-Olaya, J. M.; Matabosch, X.; Bedia, C.; Egido-Gabás, M.; Casas, J.; Llebaria, A.; Delgado, A.; Fabriàs, G. Synthesis and Biological Activity of a Novel Inhibitor of Dihydroceramide Desaturase. *ChemMedChem* **2008**, *3* (6), 946–953.

(24) Rodríguez, S.; Hao, G.; Liu, W.; Piña, B.; Rooney, A. P.; Camps, F.; Roelofs, W. L.; Fabriàs, G. Expression and Evolution of Δ9 and Δ11 Desaturase Genes in the Moth Spodoptera Littoralis. *Insect Biochem. Mol. Biol.* **2004**, *34* (12), 1315–1328.

(25) Liu, W.; Jiao, H.; Murray, N. C.; O'Connor, M.; Roelofs, W. L. Gene Characterized for Membrane Desaturase That Produces (E)-11 Isomers of Mono- and Diunsaturated Fatty Acids. *Proc. Natl. Acad. Sci. U. S. A.* **2002**, *99* (2), 620–624.

(26) Abad, J. L.; Camps, F.; Fabriàs, G. Substrate-Dependent Stereochemical Course of the (Z)-13-Desaturation Catalyzed by the Processionary Moth Multifunctional Desaturase. *J. Am. Abad, J. L.; Camps, F.; Fabriàs, G. Substrate-Dependent Stereochem. Course (Z)-13-Desaturation Catalyzed by Process. Moth Multifunct. Desaturase. J. Am. Chem. Soc. 2007, 129 (48), 15007–15012. Chem. Soc* **2007**, *129* (48), 15007–15012.

(27) Liénard, M. A.; Strandh, M.; Hedenström, E.; Johansson, T.; Löfstedt, C. Key Biosynthetic Gene Subfamily Recruited for Pheromone Production prior to the Extensive Radiation of Lepidoptera. *BMC Evol. Biol.* **2008**, *8*, 270.

(28) Garner, P. Stereocontrolled Addition to a Penaldic Acid Equivalent: An Asymmetric of Threo-β-Hydroxy-L-Glutamic Acid. *Tetrahedron Lett.* **1984**, *25* (51), 5855–5858.

(29) Passiniemi, M.; Koskinen, A. M. P. Garner's Aldehyde as a Versatile Intermediate in the Synthesis of Enantiopure Natural Products. *Beilstein J. Org. Chem.* **2013**, *9*, 2641–2659.

(30) Seco, J. M.; Quioá, E.; Riguera, R. A Practical Guide for the Assignment of the Absolute Configuration of Alcohols, Amines and Carboxylic Acids by NMR. *Tetrahedron Asymmetry* **2001**, *12* (21), 2915–2925.

(31) Gruza, H.; Kiciak, K.; Krasiński, A.; Jurczak, J. The Highly Diastereocontrolled Addition of the Lithium Derivative of Tert Butyldimethylsilyl Propargyl Ether to N-Boc-N,O-Isopropylidene-L-Serinal. *Tetrahedron Asymmetry* **1997**, *8* (15), 2627–2631.

(32) Collington, E. W.; Finch, H.; Smith, I. J. Selective Deprotection of Alcoholic and Phenolic Silyl Ethers. *Tetrahedron Lett.* **1985**, *26* (5), 681–684.

(33) Bartlett, S. L.; Beaudry, C. M. High-Yielding Oxidation of β-Hydroxyketones to β-Diketones Using O-Iodoxybenzoic Acid. *J. Org. Chem.* **2011**, *76* (23), 9852–9855.

(34) Chinchilla, R.; Najera, C. The Sonogashira Reaction: A Booming Methodology in Synthetic Organic Chemistry. *Chem. Rev.* **2007**, *107* (3), 874–922.

(35) Herold, P. Synthesis of D-Erythro and D-Threo Sphingsosine. *Helv. Chim. Acta* **1988**, *71* (2), 354–362.

(36) Hart, D. W.; Schwartz, J. Hydrozirconation. Organic Synthesis via Organozirconium Intermediates. Synthesis and Rearrangement of Alkylzirconium (IV) Complexes and Their Reaction with. *J. Am. Chem. Soc.* **1974**, *199* (1972), 8115.

(37) Corey, E. J.; Barton, A. Synthesis of Three Potential Inhibitors of the Biosynthesis of Leukotrienes A–E. *Tetrahedron Lett.* **1980**, *21* (44), 4243–4246.

(38) C. Luethy, Peter Konstantin, K. G. U. Total Synthesis of Dl-19-Hydroxyprostaglandin E1 and Dl-13-Cis-15-Epi-19-Hydroxyprostaglandin E1. *J. Am. Chem. Soc.* **1978**, *100* (19), 6211–6217.

(39) Cingolani, F.; Casasampere, M.; Sanllehí, P.; Casas, J.; Bujons, J.; Fabrias, G. Inhibition of Dihydroceramide Desaturase Activity by the Sphingosine Kinase Inhibitor SKI II. *J. Lipid Res.* **2014**, *55* (8), 1711–1720.

(40) Triola, G.; Fabriàs, G.; Casas, J.; Llebaria, A. Synthesis of Cyclopropene Analogues of Ceramide and Their Effect on Dihydroceramide Desaturase. *J. Org. Chem.* **2003**, *68* (26), 9924–9932.

(41) Cer, R. Z.; Mudunuri, U.; Stephens, R.; Lebeda, F. J. IC50-to-Ki: A Web-Based Tool for Converting IC50 to Ki Values for Inhibitors of Enzyme Activity and Ligand Binding. *Nucleic Acids Res.* **2009**, *37* (SUPPL. 2), 441–445.

(42) Cookson, R. C. 4-Phenyl-1,2,4-Triazolin-3,5-Dione: A Powerful Dienophile. *Tetrahedron Lett.* **1962**, *1* (14), 615–618.

(43) De Bruycker, K.; Billiet, S.; Houck, H. A.; Chattopadhyay, S.; Winne, J. M.; Du Prez, F. E. Triazolinediones as Highly Enabling Synthetic Tools. *Chem. Rev.* **2016**, *116* (6), 3919–3974.

(44) Korobitsyna, I. K.; Khalikova, A. V.; Rodina, L. L.; Shusherina, N. P. 4-Phenyl-I, 2,4-Triazoline-3,5-Dione in Organic Synthesis. *Khimiya Geterotsiklicheskikh Soedin.* **1983**, No. 2, 117–136.

(45) Ban, H.; Nagano, M.; Gavrilyuk, J.; Hakamata, W.; Inokuma, T.; Barbas, C. F. Facile and

Stabile Linkages through Tyrosine: Bioconjugation Strategies with the Tyrosine-Click Reaction. *Bioconjug. Chem.* **2013**, *24* (4), 520–532.

(46) Murao, N.; Ishigai, M.; Sekiguchi, N.; Takahashi, T.; Aso, Y. Ferrocene-Based Diels-Alder Derivatization for the Determination of 1-Hydroxyvitamin D3 in Rat Plasma by High-Performance Liquid Chromatography-Electrospray Tandem Mass Spectrometry. *Anal. Biochem.* **2005**, *346* (1), 158–166.

(47) Tasdelen, M. A. Diels–Alder "click" Reactions: Recent Applications in Polymer and Material Science. *Polym. Chem.* **2011**, *2* (10), 2133.

(48) Higashi, T.; Awada, D.; Shimada, K. Simultaneous Determination of 25-Hydroxyvitamin D2 and 25-Hydroxyvitamin D3 in Human Plasma by Liquid Chromatography-Tandem Mass Spectrometry Employing Derivatization with a Cookson-Type Reagent. *Biol. Pharm. Bull.* **2001**, *24* (7), 738–743.

(49) Yasumoto, T.; Takizawa, A. Fluorometric Measurement of Yessotoxins in Shellfish by High-Pressure Liquid Chromatography. *Biosci. Biotechnol. Biochem.* **1997**, *61* (10), 1775–1777.

(50) Xiao, L.; Chen, Y.; Zhang, K. Efficient Metal-Free "grafting Onto" method for Bottlebrush Polymers by Combining RAFT and Triazolinedione-Diene Click Reaction. *Macromolecules* **2016**, *49* (12), 4452–4461.

8. SUPPORTING INFORMATION

Supplementary data related to the present doctoral thesis can be found in the attached CD. The following material is included:

- NMR spectral data of:

1. Compounds (*E*)-Δ^6-dhCer (**RBM8-029**) and derivatives.
2. Compounds (*Z*)-Δ^6-dhCer (**RBM8-126**) and derivatives
3. Compound (*E,E*)-$\Delta^{4,6}$-dhCer (**RBM8-053**)
4. Compound (*Z,E*)-$\Delta^{4,6}$-dhCer (**RBM8-138**) and derivatives
5. Compound **RBM8-311**
6. Compound **RBM8-337**
7. Compounds of sphingosine derivatives
8. Triazolinedione (**RBM8-254**)
9. Diels Alder adducts
10. Ene-Alder adducts

- PDF file of doctoral thesis